

สำนักงานกองทุนสนับสนุนการวิจัย THE THAILAND RESEARCH FUND

รายงานวิจัยฉบับสมบูรณ์

เครือข่ายวิจัยนานาชาติ " เครือข่ายวิจัยการค้นหาและพัฒนายาจากสารธรรมชาติ" (Natural product-based drug discovery and development)

โปรแกรม "การค้นหา ปรับเปลี่ยนโครงสร้าง และศึกษากลไกการออกฤทธ์ของสาร ธรรมชาติจากจุลินทรีย์ในทะเล และจากพืชสมุนไพรในการรักษาโรคในผู้สูงอายุ" (Discovery, Modification and Mechanistic studies of the Active Natural Products from Chinese Marine Microbes and Thai Medicinal Plants For treatment of Age-related Diseases)

โดย

ศ. ดร. ภาวิณี ปิยะจตุรวัฒน์ และตณะ
ภาควิชาสรีรวิทยา คณะวิทยาศาสตร์
มหาวิทยาลัยมหิดล

พ.ศ. 2564

รายงานวิจัยฉบับสมบูรณ์

เครือข่ายวิจัยนานาชาติ " เครือข่ายวิจัยการค้นหาและพัฒนายาจากสารธรรมชาติ" (Natural product-based drug discovery and development)

โปรแกรม "การค้นหา ปรับเปลี่ยนโครงสร้าง และศึกษากลไกการออกฤทธ์ ของสารธรรมชาติจากจุลินทรีย์ในทะเล และจากพืชสมุนไพรในการรักษาโรคในผู้สูงอายุ" (Discovery, Modification and Mechanistic studies of the Active Natural Products from Chinese Marine Microbes and Thai Medicinal Plants for treatment of Age-related Diseases)

คณะผู้วิจัย	สังกัด
1. ศ.ดร.ภาวิณี ปิยะจตุรวัฒน์	มหาวิทยาลัยมหิดล
2. ศ.ดร.ปทุมรัตน์ ตู้จินดา	มหาวิทยาลัยมหิดล
3. รศ.ดร.อาทิตย์ ไชยร้องเดื่อ	มหาวิทยาลัยมหิดล
4. รศ.ดร.จิตติมา วีระชยาภรณ์	มหาวิทยาลัยมหิดล
5. ผศ.ดร.วิชชุดา แสงสว่าง	มหาวิทยาลัยมหิดล
6. ศ.ดร.ปราณีต โอปณะโสภิต	มหาวิทยาลัยศิลปากร
7. ศ.ดร.อภิชาต สุขสำราญ	มหาวิทยาลัยรามคำแหง

สนับสนุนโดยสำนักงานกองทุนสนับสนุนการวิจัย

(ความเห็นในรายงานนี้เป็นของผู้วิจัย สกว. ไม่จำเป็นต้องเห็นด้วยเสมอไป)

Executive summary

Over the past two decades, growth of elderly population has rapidly increased worldwide including Thailand. Aging is primarily a change in bodily functions which is associated with a number of physiological changes. This population is generally more susceptible to multiple chronic diseases as well as non-communicable diseases (NCDs), which are a wide range of chronic illness conditions including cancer, diabetes, cardiovascular disease, hypertension, as well as Alzheimer's disease, dementia and other neurodegenerative diseases. The natural products play a dominant role in the discovery of leads for the development of drugs for the treatment of human diseases. Therefore, in this international research network project, we have established a multi-institutional collaborative research with members from three institutes in Thailand together with the international collaborators in China and the United States. We focused on the natural product-based drug discovery and development of pharmaceutical products from natural resources including those from terrestrial tropical plants and marine microorganisms for prevention and treatment of age-related NCDs diseases. To fulfill the goal of research and to produce high quality Ph.D. graduates for sustainable development of human resources and to increase international visibility and research capability through overseas research collaboration and dissemination of advance research results, multidisciplinary research members were recruited including chemists, biologists, pharmacologist and pharmacists and the research activities consisted of 5 sub-projects research activities.

From the first sub-project, the Thai chemists had compiled 725 samples of natural, modified and synthetic compounds, while the Chinese chemists had provided more than 200 compounds from marine microorganisms with quite marked structures for evaluation of cytotoxic activity in several mammalian cancer cell lines. The non-cytotoxic compounds were further evaluated for anti-diabetic, anti-obesity and anti-Alzheimer activity. Some bioactive compounds with potent activity were selected as leads, which were further modified structurally to obtain more potent/less toxic analogues. Some of them were selected as candidates for investigating mechanisms of actions.

The second sub-project was aimed to search for anticancer activities. From our screening, a number of compounds from both Thailand and China were found to have promising anticancer activities against several types of cancers including gastric cancer, colorectal cancer and cholangiocarcinoma. The underlying anticancer mechanisms and intracellular targets of these compounds were also elucidated. The outputs from this collaboration among Thai and Chinese scientists are high impact international publications

and the highly potent anticancer candidates with potential and promising to be developed as anticancer drugs in the future. Nanoparticles of these compounds for delivery to their intracellular targets were further developed in subproject -6.

The sub-project-3 was aimed to find a new SGLT2 inhibitor from natural for diabetic treatment. Sodium glucose cotransporter (SGLT) 2 inhibition has been found to be anti-diabetic drug target for type 2 diabetes. Compounds from natural sources including plant and marine were tested for SGLT2 inhibition. Interestingly, the extracts from Kaempferia parviflora, and Boesenbergia pandurata showed an inhibitory effect on glucose transport in renal proximal tubular cells. Oral administration of the extracts of *Kaempferia parviflora*, and *Boesenbergia pandurata* to the diabetic rat -Goto Kakizaki (GK) rat reduced plasma glucose without changing plasma insulin indicating the therapeutic potential for type 2 DM treatment. In addition to the therapeutic potential application of *Boesenbergia pandurate* on diabetes, compounds from this plant panduratin A and pinostrobin showed protective effect of nephrotoxicity induced by drug including cisplatin, anti-cancer, and antibiotic drug, colistin.

Subproject-4 aimed to screen various natural compounds for PPAR α agonists and PPAR γ antagonist in vitro system. We found that andrographolide and phytoestrogen diarylheptanoid from *C. comosa* (DPHD) have promising effect for suppressing PPAR γ and activate PPAR α . Treatments with E2, DPHD or *C. comosa* extract in OVX rats prevented an increase in adiposity, down-regulated lipogenic genes and proteins with marked increases in the protein levels of AMPK- α and PPAR- α , supporting the use of this plant for health promotion in the post-menopausal women. In addition, DPHD also inhibited adipocyte differentiation of human bone marrow-derived mesenchymal stem cells (hBMSCs) by suppressing the expression of genes involved in adipogenesis through the activation of ER and Wnt/ β catenin signaling pathways. This finding suggests the potential role of DPHD in preventing bone marrow adiposity which is one of major factor that exacerbates osteoporosis in post-menopause.

In subproject-5, we have tested several natural product derived compounds and modified compounds for their ability to prevent neurons from damages and death caused by both oxidative stress and factors known to induce neurodegeneration. We found that several plant-derived compounds and modified compounds showed high scavenging property and can protect neurons from oxidative stress induced cell damage and death. In addition, we discovered a novel methodology for neuronal differentiation, which will be useful for further investigation of potential compounds with neuroprotective effects.

Subproject 6 aimed to develop effective novel nanocarriers containing anticancer drugs with high potency against cancer cells by using colorectal cancer (CRC), and with low toxicity to normal cells. We have developed semi-synthetic andrographolide, namely 3A.1 analog that has been investigated thoroughly for its potent and promising antitumor activity against colorectal cancer (CRC) was selected. It is a hydrophobic drug for colorectal cancer treatment. The results showed that 3A.1 was successful incorporated into self-assembled polymeric nanoparticles based on amphiphilic chitosan derivatives. These nanoparticles were formed by self-assembly in an aqueous solution and their hydrophobic part helped to solubilize the hydrophobic drug within the nanoparticles. The 3A.1-loaded NSCS nanoparticles with 40 wt% drug added prepared by a dropping method revealed the highest drug loading capacity and good physical stability in a refrigerator. Moreover, the 3A.1-loaded nanoparticles also inhibited cell migration of oral cancer HN-22 cells, suggesting it's potential to be nanocarriers for oral intestine/colon drug delivery. Furthermore, compared with the non-conjugated polymers, the folate-conjugated NSCS polymers showed much more anticancer activity and highly potent apoptotic induction, suggesting that the folateconjugated were active-targeting drug nanocarriers for colon tumor therapy via folate mediation.

In conclusion, we have achieved the goal in establishing the international research network to collaborate conducting the project and published 37 international peered publications. We produced Ph.D. students with outstanding intellectual abilities and a strong commitment to research. The promising drug candidates obtained from this project will lead their future research and development of such drugs.

กิตติกรรมประกาศ (Acknowledgement)

คณะวิจัย ขอขอบคุณสำนักงานกองทุนสนับสนุนการวิจัย (The Thailand Research Fund) ที่ได้ จัดสรรงบ ให้การสนับสนุนการวิจัยโครงการเครือข่ายวิจัยนานาชาติ "เครือข่ายวิจัยการค้นหาและพัฒนายา จากสารธรรมชาติ (Natural product-based drug discovery and development)" ในโปรแกรมวิจัย เรื่อง "การค้นหา ปรับเปลี่ยน โครงสร้าง และศึกษากลไกการออกฤทธ์ของสารธรรมชาติ จากจุลินทรีในทะเล และจากพืชสมุนไพรในการรักษาโรคในผู้สูงอายุ (Discovery, Modification and Mechanistic Study of the Active Natural Products for treatments of Age-related Diseases from Chinese Marine Microbes and Thai Medicinal Plants" สัญญาเลขที่ IRN58W0004 ประจำปี 2558-2564

คณะผู้วิจัย กรกฎาคม 2564

สารบัญ

หัวข้อ	เนื้อเรื่อง	หน้า
	e summary (สรุปผลการดำเนินงาน)	i
กิตติกรรมา	ประกาศ	Vİ
ส่วนที่ 1 จ้	ข้อมูลโครงการ	1
ส่วนที่ 2. ร	รายงานการสร้างและพัฒนาเครือข่ายวิจัยนานาชาติ	2
•	ความร่วมมือระหว่างนักวิจัย	
•	ความร่วมมือระหว่างสถาบัน/องค์กร	
	 ความร่วมมือระหว่างเครือข่ายในประเทศ 	
_	• ความร่วมมือระหว่างเครือข่ายระหว่างประเทศ	4
	กิจกรรมที่สนับสนุนการพัฒนาความร่วมมือและงานวิจัยของเครือข่าย ข้อมูลด้านจำนวนและงบประมาณ	4
	ข้อมูลการสนับสนุนทุนผู้ช่วยวิจัยระดับปริญญาเอก	6 6
	ปัญหาและอุปสรรค/ความเห็นและข้อเสนอแนะ	7
	·	_
	ายงานเนื้อหาของโครงการวิจัยภายใต้เครือข่าย	8
	ภัตถุประสงค์ของโครงการ อยที่ 1: สกัดแยกสาร ดัดแปลงโครงสร้าง และสังเคราะห์สาร เพื่อใช้เป็น compound library	10
•	บทคัดย่อ	11
•	compound library	12
โครงการย่	อยที่ 2: พิษต่อเซลล์ ฤทธิ์และกลไกการออกฤทธิ์ต้านมะเร็งที่ เป้าหมาย ระดับโมเลกุล	67
•	บทคัดย่อ	67
•	วัตถุประสงค์ของโครงการ	71
•	พิษของสารจากพืชไทยต่อเซลล์มะเร็ง	72
•	พิษของสารจากmarine microbes ต่อเซลล์มะเร็ง	73
•	ทดสอบฤทธิ์ของสาร HD ZWM 978 จาก marine microbes ในการยับยั้ง การเจริญเติบโต หรือฆ่าเซลล์มะเร็งกระเพาะอาหาร	78
•	ศึกษากลไกการออกฤทธิ์ของสาร Andrographolide analogue ต่อ Apoptosis, DNA damage and inhibition of Wnt target gene	85
โครงการย่	อยที่ 3: ฤทธิ์ต้านเบาหวาน (Anti-diabetes)	100
•	บทคัดย่อ	100
•	วัตถุประสงค์ ทดสอบฤทธิ์ของสารบริสุทธิ์ที่แยกได้จากพืชและสารดัดแปลงจากจีนต่อการ	102
•	พดสอบฤพธของสารบรสุทธพแยกเดงากพชและสารตดแบลงจากจนต่อการ ยับยั้งการทำงานของตัวขนส่งกลูโคส SGLT2, GLUT2 ในเซลล์	104

	หัวข้อ	เนื้อเรื่อง	หน้า	หน้า
•		รบริสุทธิ์ที่แยกได้จากพืชและสารดัดแปลของไทยต่อการยับยั้ง นส่งกลูโคส SGLT2 ในเซลล์	106	
โครงก	ารย่อยที่ 4 ถทธิ์ลดไ	ขมัน และลดความอ้วน Anti-adipogenesis/obesity	109	
•	บทคัดย่อ		109	
•	วัตถุประสงค์		112	
•		่ฤทธิ์ลดภาวะดื้อต่อฮอร์โมนอินซูลิน โดยเน้นฤทธิ์ต่อ lipid	115	
•	ศึกษาฤทธิ์ต่อการยั	ายังการ Adipogenic Differentiation of Human Bone Mesenchymal Stem Cells by DPHD	124	
โครงกา	ารย่อยที่ 5: ฤทธิ์ในกา	ารป้องกันการเสื่อมของเซลล์ประสาท	134	
	บทคัดย่อ วัตถุประสงค์		135	
	การทดสอบฤทธิ์ของ	n marine microbes ในการป้องกันซลล์ประสาทจากการถูก phosphorylated Tau-induced neurodegeneration	137	
•		มอนุมูลอิสระของสารและป้องกันการตายของเซลล์ประสาท	140	
•	การทดสอบความปล ต่อเซลล์ประสาท	าอดภัยของสารดัดแปลง lipoic acid และ organoselenium	142	
โครงก	ารย่อยที่ 6: การพัฒเ	มาระบบนำส่งตัวยาต้านมะเร็งไปยังเป้าหมาย		
•	บทคัดย่อ		151	
	ตถุประสงค์	2	156	
•		มินอนุพันธ์ใคโตซาน และ ศึกษาผลและกลไกของไคโตซาน ตซานต่อการทำงานของตัวขนส่งยาประจุบวก	159	
กิจกรร	มที่วางแผนและที่ดำเ	นินการ		
ผลผลิต	ที่ได้จากการวิจัย (Ou	tput)		
	ผลงานวิจัยตีพิมพ์ใน		192	
•	ผลงานวิชาการอื่นๆ	d. s	197	
	นักศึกษษที่ผลิตได้แ		199	
	ล การดำเนินงานของโ เวก – แยกเล่ม Reprir	ครงการโดยย่อ nt ผลงานวิจัยที่ตีพิมพ์	200	

สัญญาเลขที่ IRN58W0004

โครงการเครือข่ายวิจัยนานาชาติ "เครือข่ายวิจัยการค้นหาและพัฒนายาจากสารธรรมชาติ (Natural product-based drug discovery and development)"

ส่วนที่ 1 ข้อมูลโครงการ

ชื่อเครือข่ายวิจัยเครือข่ายวิจัยการค้นหาและพัฒนายาจากสารธรรมชาติ

ชื่อโปรแกรมวิจัย การค้นหา ปรับเปลี่ยนโครงสร้าง และการศึกษากลไกการออกฤทธิ์ของสารธรรมชาติ

จากจุลินทรีย์ในทะเล และจากพืชสมุนไพรในการรักษาโรคในผู้สูงอายุ

สัญญาเลขที่ RN58W0004 ระยะเวลาโครงการ 3 ปี วันเริ่มโครงการ 1 กันยายน 2558

รายงานโครงการ โครงการหลัก ระหว่างวันที่ 1 กันยายน 2560 ถึง 31 สิงหาคม 2561

ชื่อหัวหน้าเครือข่ายวิจัยผู้รับทุน นางภาวิณี ปิยะจตุรวัฒน์

สังกัด ภาควิชาสรีรวิทยา คณะวิทยาศาสตร์ มหาวิทยาลัยมหิดล

รายชื่อผู้วิจัยร่วมหลักฝ่ายไทยและสังกัด

Collaborative Institute-1 Faculty of Science, Mahidol University

- 1. Pawinee Piyachaturawat, Professor, Ph.D., Department of Physiology
- 2. Arthit Chairongdua, Ph. D., Associate Professor Department of Physiology
- 3. Sunhapas Soodvilai, Ph.D., Associate Professor Department of Physiology
- 4. Jittima Weerachayaphorn, Ph.D., Assistant Professor, Department of Physiology
- 5. Witchuda Saengsawang, Ph.D., Assistant Professor, Department of Physiology
- 6. Patoomratana Tuchinda, Professor, Ph.D., Department of Chemistry

Collaborative Institute-2 Faculty of Pharmacy, Silpakorn University (Department of Pharmaceutic)

Praneet Opanasopit, Ph.D., Professor,

Collaborative Institute-3 Faculty of Science, Ramkhamhaeng University (Department of Chemistry)

Apichart Suksamrarn, Ph.D., Professor,

รายชื่อผู้วิจัยร่วมหลักฝ่ายต่างประเทศและสังกัด

Chinese Collaborators: (Marine microbes-based drug discovery)

- 1. Weiming Zhu, Professor, Ph.D., (PI) Vice Director of the Key Laboratory of Marine Drugs, Ocean University of China, Ministry of Education of China and hiscolleagues: Prof. Dr. Li, WenLi; Prof. Wan, Sheng Biao, Assoc. Prof. Dr. Li, HuaYue, Miss Liu, PeiPei
- 2. Chunhong Dong, Professor, Ph.D., Jiaozuo University, China

USA. Collaborators

- 1. Tianxin Yang, Professor, Ph.D., University of Utah, USA
- 2. Harry Blair, Professor, Ph.D., University of Pittsburgh School of Medicine, USA
- 3. Micheal J Caplan Professor, Ph.D., Yale University School of Medicine, USA
- 4. Erik W. Dent, Associate Professor, Ph.D., University of Wisconsin-Madison, USA

ส่วนที่ 2 รายงานการสร้างและพัฒนาเครือข่ายวิจัยนานาชาติ

1. ได้สร้างและพัฒนาเครือข่ายวิจัยนานาชาติ โดยสมาชิกนักวิจัยของเครือข่าย มีทั้งจากสถาบันในประเทศ และต่างประเทศ กิจกรรมการวิจัยอยู่ในแนวทางของการศึกษาค้นคว้าหาตัวยาใหม่จากธรรมชาติ เพื่อการพัฒนาไปใช้เป็นยาในอนาคต โดยเน้นฤทธิ์ต่อประกอบด้วยการค้นหาสารออกฤทธิ์จากธรรมชาติ ปรับเปลี่ยนโครงสร้างทางเคมี ศึกษาฤทธิ์ทางชีววิทยาและเภสัชวิทยาเพื่อให้ได้สารที่มีฤทธิ์ดีเด่น ใช้เป็น candidate lead compounds ที่มีฤทธิ์ทางยา พัฒนาระบบนำส่งยา เพื่อการพัฒนาสารเป็นผลิตภัณฑ์ ที่ออกฤทธิ์ได้ดีที่เป้าหมายต่อไป การดำเนินงานวิจัยมีการรับช่วงต่อกัน ดังนี้

1.1 ด้านความร่วมมือระหว่างนักวิจัย

- 1.1.1 กลุ่มนักวิจัยเคมี ได้ส่งสารที่แยกได้จากพืชสมุนไพรให้กลุ่มวิจัยในเครือข่ายเพื่อทดสอบฤทธิ์ทาง ชีวภาพ และเภสัชวิทยา เบื้องต้นดังต่อไปนี้
 - 1.1.2. กลุ่มนักวิจัยศึกษาฤทธิ์ทางชีวภาพ และเภสัชวิทยา ได้แก่
 - ฤทธิ์ cytotoxic and anticancer activities
 - ฤทธิ์ anti-diabetic activity และ ฤทธิ์ต่อเซลล์ไขมัน anti-adiposity activity
 - ฤทธิ์ antioxidant activity และ ฤทธิ์ป้องกันความเสื่อมของเซลล์ประสาท
- 1.1.3 กลุ่มนักวิจัยศึกษา ร่วมมือกับนักวิจัยสาขาเทคโนโลยีเภสัชกรรมเพื่อพัฒนาระบบนำส่งตัว ยาที่ออกฤทธิ์สำคัญได้

1.2 ด้านความร่วมมือระหว่างสถาบัน/องค์กร

<u>ความร่วมมือระหว่างเครือข่ายในประเทศ</u>

ได้มีความร่วมมืออย่างใกล้ชิดกับนักวิจัยในโครงการทั้งในสถาบันและต่างสถาบันดังข้อมูลผลงานวิจัยข้างต้น โดยศ.ดร.อภิชาต สุขสำราญ มหาวิทยาลัยรามคำแหง และผศ.ดร.รุ่งนภา แช่เอ็งมหาวิทยาลัยบูรพา เป็นผู้ สกัดสารจากพืช และดัดแปลงโครงสร้างของสารเคมี มาใช้ในการวิจัยศึกษาหาฤทธิ์ทางชีวภาพ โดยเฉพาะ ฤทธิ์เกี่ยวข้องกับไขมัน

ศ.ดร.ปราณีต โอปณะโสภิต คณะเภสัชศาสตร์ มหาวิทยาลัยศิลปากร ได้นำสารที่ผ่านการศึกษาว่ามีฤทธิ์ ฆ่ามะเร็งได้ดีเด่น แต่มีความเป็นพิษต่อเซลล์สูงไปพัฒนาระบบนำส่งยาด้วย chitosan-base polymeric micelles และ liposomes และติด ligand เพื่อนำส่งยาสู่เป้าหมายเซลล์มะเร็ง เพื่อลดความเป็นพิษ ของยาต่อเซลล์ปกติเมื่อเข้าสู่ร่างกาย

ความร่วมมือระหว่างเครือข่ายต่างประเทศดังนี้

สาธารณรัฐประชาชนจีน เป็นการสร้างความร่วมมือใหม่กับนักวิจัยชาวจีน เน้นการค้นหาสารจากเชื้อ จุลชีพในทะเลเป็นหลัก โดยได้ร่วมมือกับ

- 1. Weiming Zhu, Professor, Ph.D., Vice Director of the Key Laboratory of Marine Drugs, Ocean University of China, Ministry of Education of China
- 2. Chunhong Dong, Professor, Ph.D., Jiaozuo University, China

ประเทศสหรัฐอเมริกา เป็นการต่อยอดความร่วมมือวิจัยที่มีอยู่ให้เข้มแข็ง โดยได้ร่วมมือกับ

- Professor Dr. Harry Blair, University of Pittsburgh, Department of Pathology, Section of Laboratory Medicine รัฐ Pennsylvania ประเทศสหรัฐอเมริกา
- 2. Assoc. Prof Dr. Erik W. Dent,. University of Wisconsin-Madison, Department of Neuroscience รัฐ Wisconsinประเทศสหรัฐอเมริกา
- 3. Professor Tianxin Yang University of Utah ประเทศสหรัฐอเมริกา

จากการดำเนินงานของโครงการเครือข่ายวิจัยที่ผ่าน มีความร่วมมือกันเป็นอย่างดีของนักวิจัยทั้งจาก เครือข่ายภายในประเทศไทยเอง และจากต่างประเทศ การวิจัยของเครือข่ายกับต่างประเทศ ได้เน้นการสร้าง ความร่วมมือใหม่กับนักวิจัยจากสาธารณรัฐประชาชนจีนของกลุ่ม Prof. Dr. Zhu, WeiMing จาก School of Medicine and Pharmacy, Ocean University of China, จังหวัด Qingdao มณฑล Shandong เป็นหลัก ซึ่ง มีความเชี่ยวชาญในการแยกสารเคมีจากจุลลินทรีย์ในทะเล และยังมีความร่วมมือกับนักวิจัยในประเทศ สหรัฐอเมริกาที่มีมาก่อน ผ่านทุนความร่วมมืออื่น เป็นการสร้างความเข้มแข็งในการวิจัยให้กับนักวิจัย นักศึกษา บุคคลากร และสถาบันในประเทศ โดยในระยะเวลา 3 ปี Output –Outcome ถึงปัจจุบัน โครงการมีผลงานวิจัย ตีพิมพ์ในวารสารนานาชาติรวมทั้งสิ้น 37 ชิ้น ตามเอกสารแนบ list of Publications มีบัณฑิตระดับปริญญาเอกที่ เป็นผลผลิตโดยตรงจากโครงการ 2 คนและที่มีส่วนร่วมอีก 9 คน ซึ่งกลุ่มนักศึกษาทั้งหมดในกลุ่มวิจัยมีกิจจกรรม ทางวิชาการและวิจัยร่วมกันตลอดระยะเวลาของโครงการ

1.3 กิจกรรมที่สนับสนุนการพัฒนาความร่วมมือ และงานวิจัยของเครือข่าย

1. จัดประชุมกลุ่มวิจัยประจำ (ทุก 2 เดือน) เพื่อติดตามความก้าวหน้าในการดำเนินงานกับเครือข่ายกลุ่ม วิจัยในประเทศ

	รมของสมาชิกในเครือข่ายที่สนับสนุนการพัฒนาความร่วมมือ และงานวิจัยของเครือข่ายมีดังนี้
20-24	มีการจัดประชุมสรุปผลการดำเนินงานและวางแผนความร่วมมือในโครงการวิจัยกับเครือข่าย
กรกฎาคม	นักวิจัยในต่างประเทศ กลุ่มนักวิจัยชาวจีนโดยการนำของ Prof. Weiming Zhu และทีมนักวิจัย
2559	อีก 4 ท่านจาก Ocean University of China, Ministry of Education of China ได้เดินทางมา
	ประเทศไทย และไปเยี่ยมชมสถาบันในเครือข่าย ได้แก่ คณะเภสัชศาสตร์ มหาวิทยาลัยศิลปากร
	จังหวัดนครปฐม
16-20	สมาชิกกลุ่มวิจัยเข้าร่วมประชุม The 6th China-Thailand Joint Workshop on Natural
ตุลาคม	Products and Drug Discovery ที่โรงแรม Aonang Cliff Beach Resort จังหวัดกระบี่ จัดโดย
2559	ฝ่ายวิชาการ สกว. ได้พบปะกับนักวิจัยทางเคมีสมุนไพรของประเทศ และประเทศจีนจาก
	มหาวิทยาลัยต่างๆ รวมถึง Prof. Weiming Zhu และสมาชิกของกลุ่ม ได้นำเสนอผลงานทั้งใน
	รูปแบบของการนำเสนอปากเปล่าและแบบโพสเตอร์
1 ตุลาคม	น.ส. สมฤดี เรียบร้อย นักศึกษาปริญญาเอก คปก. หลักสูตรสรีรวิทยา ได้เดินทากลับจากการวิจัย
2559	ต่อยอดงานวิทยานิพนธ์ที่เกี่ยวข้องกับผลของสารจากสมุนไพรต่อการลุกลามของเซลล์มะเร็งกับ
	Assoc. Prof. Erik W. Dent, Department of Neuroscience, University of Wisconsin-
	Madison, รัฐ Wisconsin ประเทศสหรัฐอเมริกา โดย เป็นเวลา 9 เดือน
31 ตุลาคม	นส. นรีรัตน์ สุจริต นักศึกษาปริญญาเอกทุนโครงการพัฒนากำลังคนทางด้านวิทยาศาสตร์
2559	หลักสูตรพิษวิทยา ได้เดินทางกลับจากไปทำงานวิจัยกับ Professor Harry Blair, University of
	Pittsburgh, Department of Pathology, Section of Laboratory Medicine গুঁবু
	Pennsylvania ประเทศสหรัฐอเมริกา โดยต่อยอดงานที่เกี่ยวข้องกับผลของสารจากสมุนไพรต่อ
	เซลล์ไขมันเป็นเวลา 1 ปี
4 สิงหาคม	จัดประชุมเครือข่ายวิจัยและสัมมนาทางวิชาการในประทศ ณ มหาวิทยาลัยศิลปากร จังหวัด
2560	นครปฐม เพื่อให้สมาชิกกลุ่มวิจัยได้นำเสนอผลงานวิจัย และประชุมหารือเกี่ยวกับความก้าวหน้า
	และแผนการทำงานร่วมกันของเครือข่ายวิจัย
เมษายน	ผศ.ดร. วิชชุดา แสงสว่าง เข้าร่วมประชุมและนำเสนอผลงานวิจัยในการประชุมระดับ นานาชาติ EB
2560	meeting ณ เมือง Chicago, รัฐ Illinois ประเทศสหรัฐอเมริกา และได้เดินทางต่อ ไปหารือความ
	ร่วมมือและปฏิบัติงานวิจัยกับนักวิจัยในเครือข่าย Assoc. Prof. Erik W. Dent, Department of
	Neuroscience, University of Wisconsin-Madison, รัฐ Wisconsin ประเทศสหรัฐอเมริกาเป็น
F 0	เวลา 2 เดือน (28 เมษายน -7 กรกฎาคม 2560)
5-9 กันยายน	Prof. Harry Blair จาก University of Pittsburgh, Department of Pathology, Section of
กนยายน 2560	Laboratory Medicine รัฐ Pennsylvania ประเทศสหรัฐอเมริกา เดินทางมาประเทศไทยเพื่อ
2300	ติดตามความก้าวหน้าของงานวิจัยที่ทำร่วมกัน ให้สัมมนาพิเศษ ณ ภาควิชาสรีรวิทยา คณะ
	วิทยาศาสตร์มหาวิทยาลัยมหิดล

2. กิจกร	รมของสมาชิกในเครือข่ายที่สนับสนุนการพัฒนาความร่วมมือ และงานวิจัยของเครือข่ายมีดังนี้
20-24	กลุ่มนักวิจัยไทยได้เดินทางไปประเทศจีน เพื่อเยี่ยมเยือน นำเสนอความก้าวหน้าของงานวิจัยใน
ตุลาคม	โครงการ ประชุมปรึกษาหารือวางแผนงานวิจัยร่วมกัน และทำความรู้จักกับสถาบัน และเครือข่าย
2560	วิจัยของ Prof. Dr. Zhu, WeiMing และคณะที่ School of Medicine and Pharmacy,
	Ocean University of China ซึ่งเป็นThe Key Laboratory of Marine Drugs, Ocean
	University of China, Ministry of Education of China
6-8	น.ส. สมฤดี เรียบร้อย นักศึกษาในกลุ่มวิจัยนำเสนอผลงานวิจัยที่ได้จากโครงการในที่ประชุม
ธันวาคม	ระดับชาติ เรื่อง An andrographolide analogue suppresses the proliferation and
2560	Wnt/ eta -catenin signaling pathway in colorectal cancer cells ที่งานประชุม The 45 $^{ ext{th}}$
	Physiology Society of Thailand Annual Meeting 2017, 6-8 December 2017,
	Khonkaen University Thailand และได้รับรางวัล Excellent Oral Presentation for Ph.D.
	Student Award
6-8	น.ส.นรีรัตน์ สุจริต นักศึกษาในกลุ่มวิจัยนำเสนอผลงานวิจัยที่ได้จากโครงการในที่ประชุม
ธันวาคม	ระดับชาติ เรื่อง Modulating effect of Wan-Chak motluk in adipose tissues of
2560	ovariectomized (OVX) rats ที่งานประชุม The 45 th Physiology Society of Thailand
	Annual Meeting 2017, 6-8 December 2017, Khonkaen University Thailand
24	Professor Katherine Kalil, Ph,D., Department of Neuroscience, University of
มกราคม	Madison-isconsin, USA เดินทางมาให้สัมนาพิเศษเรื่อง The role of the microtubule
2561	associated protein tau in regulating the growth cone cytoskeleton พร้อมกับให้
	คำปรึกษางานวิจัยแก่ทีมนักวิจัย
24 มีนาคม	Prof. Erik W. Dent จาก Department of Neuroscience, University of Wisconsin-
2561	Madison รัฐ Wisconsinประเทศสหรัฐอเมริกามีกำหนดการจะเดินทางมาประเทศไทยวันที่ 24
	มีนาคม 2561 เพื่อติดตามความก้าวหน้าของงานวิจัยที่ทำร่วมกัน ให้สัมมนาพิเศษณภาควิชา
	สรีรวิทยาคณะวิทยาศาสตร์มหาวิทยาลัยมหิดลและประชุมหารือความร่วมมือ
27-28	นายธีรทัศน์ กันโสม นักศึกษาในกลุ่มวิจัยนำเสนอผลงานวิจัยที่ได้จากโครงการในที่ประชุมระดับ
มีนาคม	นานาชาติ เรื่อง Effect of semi-synthetic andrographolide analogue-loaded
2561	polymeric micelles on HN22 cell migration ที่งานประชุม The 10thWalailak Research
	National Conference, 27-28 March 2018, Walailak University Thailand.
14-18	รศ.ดร. อาทิตย์ ไชยร้องเดื่อ ได้เข้าร่วมประชุมวิชาการนานาชาติ Annual meeting of
เมษายน	American Association for Cancer Research (AACR) ณ เมือง Chicago รัฐ Illinois และได้
2561	เดินไปติดตามความก้าวหน้าของนักศึกษาและสร้างความร่วมมืองานวิจัยด้านโรคมะเร็งกับ
	Assistant Professor Dr. Andrea L. Kasinski ภาควิชา Biological Scicences, Purdue
	University เมือง West Lafayette รัฐ Indiana ประเทศสหรัฐอเมริกา ระหว่างวันที่ 18-25
	เมษายน 2561
เมษายน	รศ. ดร.สัณหภาส สุดวิไล เข้าร่วมประชุมวิชาการและนำผลงานวิจัยไปนำเสนอที่งานประชุม

2. กิจกร	2. กิจกรรมของสมาชิกในเครือข่ายที่สนับสนุนการพัฒนาความร่วมมือ และงานวิจัยของเครือข่ายมีดังนี้						
2561	2561 วิชาการนานาชาติ Experimental Biology 2018 ณ เมือง San Diego มลรัฐ California เ						
	ได้เดินทางไปปรึกษางานวิจัยกับนักวิจัยในเครือข่าย Professor Tianxin Yang University of						
	Utah ประเทศสหรัฐอเมริกาจนถึงเดือน มิถุนายน 2561						
7-12	Prof. Praneet Opanasopit มีแผนการเดินทางไปนำเสนอผลงานวิจัยที่ได้จากโครงการในที่						
กรกฎาคม	ประชุมระดับนานาชาติ ในงานประชุม The 43rd FEBS Congress, to be held during 7–12						
2561	July 2018 ที่ Prague						
18-20	ศ.ดร.ภาวิณี ปิยะจตุรวัฒน์ และ ศ.ดร.ปทุมรัตน์ ตู้จินดา จะเข้าร่วมประชุมวิชาการและนำเสนอ						
ตุลาคม	ผลงานวิจัยในการประชุม The 7th International Conference on Natural Product						
2561 (NATPRO7) ณ เมือง Gyeongju ประเทศเกาหลี							
4-7	- ศ.ดร.ภาวิณี ปิยะจตุรวัฒน์ ศ.ดร.ปราณีต โอปณะโสภิต และรศ.ดร.อาทิตย์ ไชยร้องเดื่อ จะ						
พฤศจิกายน	เดินทางกับนักวิจัยสกว. เข้าร่วมประชุม "The 7th Chinese-Thailand Workshop on						
2561	Natural Products and Drug Discovery" ณ. เมืองนานจิง						

1.4 ข้อมูลด้านจำนวนและงบประมาณ

- (1) จำนวนของหน่วยงานในประเทศที่เข้าร่วมในเครือข่ายและลักษณะของการร่วมสนับสนุน
 - จำนวนหน่วยงานต้นสังกัดของนักวิจัยในเครือข่ายจำนวน 3 แห่งที่เป็นทางการและ
 - จำนวนหน่วยงานอื่นๆ ที่สนับสนุนเครือข่ายจำนวนไม่มี
 - ลักษณะการร่วมมือหรือสนับสนุน/งบประมาณที่สนับสนุน (ถ้ามี)......
 - (2) จำนวนของหน่วยงานต่างประเทศที่เข้าร่วมในเครือข่ายและลักษณะของการร่วมสนับสนุน
 - จำนวนหน่วยงานต้นสังกัดของนักวิจัยในเครือข่ายจำนวน 1 แห่ง (จากสาธารณะรัฐประชาชนจีน-ไม่มี MOU)
 - จำนวนหน่วยงานอื่นๆ ที่สนับสนุนเครือข่ายจำนวน 3 แห่งจาก USA.
 - ลักษณะการร่วมมือหรือสนับสนุน/งบประมาณที่สนับสนุน (ถ้ามี)......
- (3) จำนวนรวมของหน่วยงานในต่างประเทศที่เข้าร่วมในเครือข่าย....4....แห่ง
 - หน่วยงานต้นสังกัดของนักวิจัยในเครือข่ายจำนวน....3....แห่ง และ
 - หน่วยงานอื่นๆ ที่สนับสนุนเครือข่ายจำนวน.....แห่ง
 - * อยู่ระหว่างการพัฒนาความร่วมมือเพิ่มเติม โดยเป็นอาจารย์ที่ปรึกษาร่วมในต่างประเทศของนักศึกษา
- 3. ข้อมูลการสนับสนุนทุนผู้ช่วยวิจัยระดับปริญญาเอกและ/หรือทุนนักวิจัยหลังปริญญาเอก
 - 🗌 ได้รับทุนผู้ช่วยวิจัยระดับปริญญาเอกด้วยทุนของ
 - โครงการ IRN จำนวน 2 ทุน เป็นเงิน 3,384,000บาท คือ
 - 1. นายเกียรติดำรงค์ จันทร์พิพัฒน์กุล ภายใต้การดูแลของ รศ.ดร.อาทิตย์ ไชยร้องเดื่อ

2. นางสาวเพ็ญใจ ทองนวลจันทร์ ภายใต้การดูแลของ รศ.ดร. สัณหภาส สุดวิลัย

• โครงการอื่นๆ ได้แก่

ก. โครงการ คปก.

- 1. นักศึกษา คปก. ชื่อ น.ส. สมฤดี เรียบร้อย นักศึกษาหลักสูตรสรีรวิทยา
- 2. นักศึกษา คปก. ชื่อน.ส.นิตยา บุญหมื่นนักศึกษาหลักสูตรสรีรวิทยา
- 3. นักศึกษา คปก. ชื่อ น.ส.ศรัญญา กิจดำรงธรรม นักศึกษาหลักสูตรพิษวิทยา
- 4. นักศึกษา คปก. ชื่อ นางศิริมา สุดวิลัย นักศึกษาหลักสูตรเทคโนโลยีเภสัชกรรม
- 5. นักศึกษาคปก. ชื่อ นายธีรทัศน์ กันโสม นักศึกษาหลักสูตรเทคโนโลยีเภสัชกรรม

ข. โครงการพัฒนากำลังคนด้านวิทยาศาสตร์

- 1. นางสาวนรีรัตน์ สุจริต นักศึกษาปริญญาเอก หลักสูตรพิษวิทยา
- 2. นางสาวขวัญชนก อุปการะ นักศึกษาปริญญาเอก หลักสูตรพิษวิทยา
- 3. นายเอกพจน์ คงกล้า นักศึกษาปริญญาเอก หลักสูตรสรีรวิทยา

ค. โครงการศรีตรั้งทอง

1. นายจาตุรนต์ ขวัญทองดี นักศึกษาปริญญาเอก หลักสูตรสรีรวิทยา

รวมนักศึกษาได้รับทุนผู้ช่วยวิจัยระดับปริญญาเอกที่เกี่ยวข้องกับโครงการ 11 คน

ได้รับทุนนักวิจัยหลังปริญญาเอกจำนวน	ทุน ด้ว	เยทุนของ	
Oโครงการ IRN จำนวน ทุน เป็นเงิน	งบาท		
🔾 โครงการ (โปรดระบุ)	จำนวน	ทุน เป็นเงิน	 บาท
ได้รับทุนอื่น (หากมี) โปรดระบุ			

4. ปัญหาและอุปสรรค/ความเห็นและข้อเสนอแนะ

ด้วยโครงการเครือข่ายวิจัยนานาชาตินี้ ระยะเวลาการรับทุน 3 ปี การสนับสนุนเงินทุนประกอบด้วย 2 ส่วน คือส่วนที่เกี่ยวข้องกับการวิจัย และส่วนที่เกี่ยวข้องกับการศึกษาของนักศึกษาระดับปริญญาเอก 2 คน ใน ส่วนของการวิจัย ไม่มีอุปสรรค สามารถดำเนินงานให้สำเร็จลุล่วงได้ตามเป้าหมายในเวลา 3 ปีที่ทุนกำหนด ถึงแม้ ความร่วมมือกับนักวิจัยจากสาธารณะรัฐประชาชนจีน จะเป็นการเริ่มต้นใหม่ ด้วยประสบการณ์วิจัย และความ ชำนาญ ของนักวิจัยหลักทั้ง 2 ฝ่ายเสริมกันและกัน (จีนเน้นการแยกสาร- ไทยเน้นการ screen และวิจัยต่อยอด และพัฒนา) จากความมุ่งมั่น เข้มแข็งของนักวิจัยจีนได้ทำการเพาะเลี้ยง marine microbes ซึ่งมีปรีมาณน้อย

มาก สกัดแยกสาร และส่งสารมายังประทศไทยเพื่อทำการตรวจสอบฤทธิ์ ทำการวิจัยได้อย่างต่อเนื่อง รวมถึง การส่งสารมาต่อยอดศึกษากลไกการทำงาน ทำให้ได้ผลงานร่วมกับนักวิจัยจีนเป็นจำนวนมาก

อุปสรรคหลักที่พบในโครงการ คือระยะเวลา 3 ปี ไม่เพียงพอกับการศึกษาระดับปริญญาเอกของ นักศึกษาในหลักสูตรที่มี course works และการสอบประเมินคุณภาพขึ้นเป็น Ph.D.-candidate นอกจากนี้ใน ระยะท้ายของการวิจัยมีอุปสรรคจากการระบาดของ Virus Covid-19 มาตลอด 2 ปี มหาวิทยาลัยและคณะฯ ได้มี มาตรการจำกัดบุคคลเข้าออก การเข้าทำงาน ทำให้งานล่าซ้าออกไป ประกอบกับในปัจจุบัน การตีพิมพ์ผลงาน วิจัยในวารสารนานาชาติที่เป็นที่ยอมรับ จะยากขึ้นมาก มีการคัดกรอง เสนอแนะให้ทำงานเพิ่ม ซึ่งการเข้าทำงาน และการสั่งของล้วนมีอุปสรรค หลังจากทำงานเพิ่มแล้ว ยังถูกปฏิเสธการรับตีพิมพ์ ซึ่งจะต้องเริ่มต้นใหม่ ทุก กระบวนการล้วนใช้เวลาทั้งสิ้น ทำให้โครงการหลักที่เสร็จสิ้นแล้ว ไม่สามารถปิดโครงการได้ในเวลาที่กำหนด ต้อง รอผลงานจากโครงการย่อยของนักศึกษา.ให้เสร็จสิ้น

โครงการวิจัยเครือข่ายนี้เป็นโครงการที่ดีมาก ทำให้สามารถดึงนักวิจัยจากสาขาที่แตกต่างกันในประเทศ มาร่วมมือกัน ทำงานเป็นเครือข่าย รับช่วงการทำงานกันในแนวทางของการค้นหาและพัฒนายาใหม่ (Modern drug development) ถึงแม้ผลงานวิจัยมีระดับTRL 3-4 ยังไม่ถึงจุดที่จะใช้งานได้ก็ตาม ผลงานที่ได้เป็นผลงาน ขั้นพื้นฐานที่สำคัญ นักวิจัยสามารดำเนินการต่อยอดได้ต่อไปหลังจากนี้ เนื่องจากนักวิจัยหลักแต่ละท่านมี ความร่วมมือกับนักวิจัยในต่างประเทศอยู่แล้ว โดยเฉพาะในประเทศสหรัฐอเมริกาผ่านนักศึกษา ทั้งจาก โครงการคปก. และโครงการพัฒนากำลังคนด้านวิทยาศาสตร์ของทบวงมหาวิทยาลัย โครงการวิจัยเครือข่ายนี้ยัง เปิดโอกาสให้นักวิจัยสามารถทำงานต่อยอดกับเครือข่ายวิจัยที่มีอยู่แล้ว ในต่างประเทศ เป็นการสร้างความเข้มแข็ง ของเครือข่ายวิจัย ต่อยอดงานวิจัยให้มีคุณภาพมากขึ้น

ในโครงการนอกจากนักศึกษาระดับปริญญาเอกที่รับทุนโดยตรงจากโครงการ ยังมีนักศึกษาระดับ ปริญญาเอกที่รับทุนจากโครงการอื่นอีก 9 คนเข้าร่วมวิจัย นับว่าเป็นการร่วมผลิตและพัฒนานักวิจัยรุ่นใหม่ที่มี คุณภาพได้เป้นจำนวนมาก เป็นการช่วยลดปัญหาการขาดแคลนนักวิจัยที่มีความรู้ความสารมารถของประเทศ และปัจจุบันนักศึกษาเหล่านั้นได้รับการบรรจุเข้าทำงานเกือบหมดแล้ว

ส่วนที่ 3 รายงานเนื้อหาของโครงการวิจัยภายใต้เครือข่าย

1. การดำเนิเ	มงาน ความก้าวหน้าของโครงการ100 ของโครงการหลัก
	ได้ดำเนินงานตามแผนที่วางในส่วนของโครงการหลัก
$\overline{\checkmark}$	ได้ดำเนินงานล่าช้ากว่าแผนที่วางไว้ ในส่วนของโครงการย่อยของนักศึกษา
	ได้เปลี่ยนแผนงานที่วางไว้ดังนี้

2. รายละเอียดผลการดำเนินงานของโครงการ

Backgrounds and the Significance of the research project:

Over the past two decades, growth of elderly population has rapidly increased

worldwide including Thailand. The increase in advance aged population has profound effects on the health care systems as the elderly has faced to various chronic diseases that require ongoing treatments and a long-term medical care. The direct costs of medical care for the elderly patients are high and become a real burden for health care systems of the country. Aging is primarily a change in bodily functions which is associated with a number of physiological changes. Thus, aging population is generally more susceptible to non-communicable diseases (NCDs), which are a wide range of chronic illness conditions including cancer, diabetes, cardiovascular disease, hypertension, as well as Alzheimer's disease, dementia and other neurodegenerative diseases.

Many natural product-derived compounds are promising sources for treatment of many diseases. Thailand is located in the tropical rainforest area that contains an amazing abundance of plant life. The exciting to scientist, particularly in non-rainforest community, is the great structural variety and the medicinal qualities of plant compounds in this rich environment. The healing power of compounds from rainforest herbs is unique. Almost half of the prescribed drugs that are used in the USA come from rainforest plants. In addition to the rainforest, the ocean is considered as the 'mother of origin of life' that contains highly ecological, chemical and biological diversity starting from microorganisms to vertebrates. Marine has been the resource of unique chemical compounds, which held great pharmaceutical prospective. Recently, a number of bioactive compounds extracted from a range of marine animals are reported as potent anti-cancers. Natural product compounds have substantially structural diversity and frequently afford new mechanisms of biological activity. Thus they are the main sources for developing new drugs by the pharmaceutical industries around the world.

Thailand and China have their own indigenous medicines with a long history of using natural products for both prevention and treatment of several diseases, especially among local people and it becomes the mainstay in health care system in some parts of the countries. With tremendous sources of natural products in Thailand and China and the collaboration between multidiscipline scientists, consisting of chemists, biologists, physiologists and pharmacists from both countries, new biologically active compounds for prevention/treatment of age-related diseases could be extensively developed, which will have a strong positive impact on Thailand health care systems and economy.

One cause of the social and economic weakness of Thailand is the severe shortage of highly qualified human resources especially in the field of science and technology as compared to our neighboring countries. Thousands of high quality Ph.D. graduates with the international standard are needed to provide academic staffs with great potential for both newly and well established universities and research institutes. Research collaborations and network formation

among Thai and oversea scientists could be a strategy to achieve this goal.

The project is focused on the natural product-based drug discovery and development of pharmaceutical product from national resources including those from marine microorganisms, and terrestrial tropical plants for prevention and treatment of age-related diseases including diabetes mellitus, obesity, cancer and neurodegenerative diseases.

1. Objectives of the project:

- 6.1. To establish and strengthen both national and international research networks
- 6.2. To discover and develop novel active compounds for prevention/treatment of age-related diseases from Thai and Chinese medicinal natural products
- 6.3. To produce high quality Ph.D. graduates for sustainable development of human resources
- 6.4. To increase international visibility and research capability through overseas research collaboration and dissemination of advance research results to user/practical applications

To fulfill the objectives, a multi-institutional collaborative research project from three institutes in Thailand together with international collaborators in China and the United States is formed to search for new biologically active compounds from national resources including those from marine microorganisms, and terrestrial tropical plants and development for prevention and treatment of age-related diseases. Two Ph.D. students participating in the projects are supported.

Scope of Research

The project is divided into 5 sub-projects. The significance and scope of each research project are described below.

Sub-project 1: Extraction/isolation/structure elucidation of natural products

ABSTRACT

Our research group has compiled 725 samples of natural, modified and synthetic compounds, as well as fractions and extracts from our laboratory and tabulated as a list which contains information about types of the isolated compounds, plant sources, sample types, plant parts and bioassays. In addition three more plants have been chemically investigated. The structures of forty-nine pure compounds and a mixture of β -sitosterol/stigmasterol were established on the basis of spectroscopic methods.

Keywords: Flavonoids, terpenoids, lignans, phenolics, Styryllactones, iridoids, xanthones benzophenones

บทคัดย่อ

คณะวิจัยได้จัดรวบรวมข้อมูล ของสารธรรมชาติ สารดัดแปลง และสารสังเคราะห์ พร้อมทั้ง รายละเอียดต่าง ๆ เกี่ยวกับพืช ส่วนของพืช ชนิดของสารที่แยกได้ รวมทั้งฤทธิ์ทางชีวภาพที่ทำการทดสอบ โดยจัดทำเป็นรายการรวม ทั้งหมด 725 รายการ นอกจากนี้นักวิจัยยังได้ทำการศึกษาสารองค์ประกอบของพืชอีก 3 สปีชีส์ ได้แก่ ต้นกาญจนิการ์ หรือ แคดง (Santisukia pagetii) ต้นสบันงาป่า (Goniothalamus calvicarpus) และต้นหมากเหลี่ยม (Mallotus glomerulatus) ซึ่งสามารถแยกสารได้ 49 สาร และสารคู่ผสมของ β —sitosterol/stigmasterol ที่พบในพืชทั้ง 3 สปีชีส์ และได้ทำการวิเคราะห์โครงสร้างเคมีของสารที่แยกได้ด้วยวิธีทางสเปคโทรสโคปี

คำสำคัญ: ฟลาโวนอยด์ เทอปืน ลิกแนน ฟิโนลิก สไตริลแลกโตน อิริดอย แซนโทน เบนโซฟิโนน

1. สกัดแยกสาร ดัดแปลงโครงสร้างและสังเคราะห์สาร เพื่อใช้เป็น compound library นักวิจัยได้ดำเนินการวิจัยดังต่อไปนี้

The information covering the code of sample, natural (Nat) or modified (Mod) or synthetic (Syn) compound, type of compound, plant source, sample type, plant part and bioassay are tabulated (Table 1). A collection of 725 samples, including crude extracts (E), fractions (F) and pure compounds (P) are also categorized.

Table 1.1 Compound Library

No	CODE	Nat/Mod/Syn compound	Type of Compound	Plant Source	Extract (E)/ Fraction (F)/Pure (P)	Plant part	Assay
1	MUC-941	Nat	Phenolic	Mallotus glomerulatus	Р	PX	Cytotoxic
2	MUC-942	Nat	Flavanone	Mallotus glomerulatus	Р	PX	Cytotoxic
3	MUC-943	Nat	Diterpenoid	Mallotus glomerulatus	Р	PX	Cytotoxic
4	MUC-944	Nat	Flavone	Mallotus glomerulatus	Р	PX	Cytotoxic
5	MUC-1020	Mod	Modified triterpenoid	Gardenia collinsae	Р	LF+TW	Cytotoxic
6	MUC-1021	Mod	Modified triterpenoid	Gardenia collinsae	Р	LF+TW	Cytotoxic
7	MUC-1022	Mod	Modified triterpenoid	Gardenia collinsae	Р	LF+TW	Cytotoxic
8	MUC-1023	Nat	Triterpenoid	Gardenia collinsae	Р	LF+TW	Cytotoxic
9	MUC-1028	Mod	Cyclic ether	Polyalthia crassa	Р	LF+TW	Cytotoxic
10	MUC-1029	Mod	Styryl lactone	Polyalthia crassa	Р	LF+TW	Cytotoxic
11	MUC-1030	Mod	Styryl lactone	Polyalthia crassa	р	LF+TW	Cytotoxic
12	MUC-1031	Mod	Styryl lactone	Polyalthia crassa	р	LF+TW	Cytotoxic
13	MUC-1032	Nat	Styryl lactone	Polyalthia crassa	Р	LF+TW	Cytotoxic
14	MUC-1255	Syn	Halogenated flavone	-	Р	-	Cytotoxic
15	MUC-1261	Nat	Lignan glycoside	Mallotus glomerulatus	Р	LF+TW	Cytotoxic
16	MUC-1262	Nat	Diterpenoid	Mallotus glomerulatus	Р	LF+TW	Cytotoxic
17	MUC-1263	Nat	Diterpenoid	Mallotus glomerulatus	Р	LF+TW	Cytotoxic
18	MUC-896	Nat	Flavone	Gardenia sessiliflora	Р	LF+TW	Anti-diabetic

No	CODE	Nat/Mod/Syn	Type of Compound	Plant Source	Extract (E)/ Fraction (F)/Pure (P)	Plant part	Assay
INO	CODL	compound	Type of Compound	rtailt Source	Fraction (F)/Pure (P)	Ftant part	Assay
19	MUC-897	Nat	Flavone	Gardenia sessiliflora	Р	LF+TW	Anti-diabetic
20	MUC-898	Nat	Flavone	Gardenia sessiliflora	Р	LF+TW	Anti-diabetic
21	MUC-899	Nat	Flavone	Gardenia carinata	Р	LF+TW	Anti-diabetic
22	MUC-900	Nat	Flavone	Gardenia sessiliflora	Р	LF+TW	Anti-diabetic
23	MUC-901	Nat	Flavone	Gardenia sessiliflora	Р	LF+TW	Anti-diabetic
24	MUC-902	Nat	Flavone	Gardenia sessiliflora	Р	LF+TW	Anti-diabetic
25	MUC-903	Nat	Flavanone	Gardenia sessiliflora	Р	LF+TW	Anti-diabetic
26	MUC-904	Nat	Flavanone	Gardenia sessiliflora	Р	LF+TW	Anti-diabetic
27	MUC-905	Nat	Flavanone	Gardenia sessiliflora	Р	LF+TW	Anti-diabetic
28	MUC-906	Nat	Flavone	Gardenia sessiliflora	Р	LF+TW	Anti-diabetic
29	MUC-907	Nat	Flavone	Gardenia carinata	Р	LF+TW	Anti-diabetic
30	MUC-908	Nat	Flavone	Gardenia carinata	Р	LF+TW	Anti-diabetic
31	MUC-909	Nat	Flavone	Gardenia sessiliflora	Р	LF+TW	Anti-diabetic
32	MUC-910	Nat	Flavone	Mallotus glomerulatus	Р	PX	Anti-diabetic
33	MUC-911	Nat	Flavonol	Zingiber maekongense	Р	RT	Anti-diabetic
34	MUC-912	Nat	Flavonol	Zingiber maekongense	Р	RT	Anti-diabetic
35	MUC-913	Nat	Flavone	Gardenia carinata	Р	LF+TW	Anti-diabetic
36	MUC-914	Nat	Flavanone	Mallotus glomerulatus	Р	PX	Anti-diabetic

No	CODE	Nat/Mod/Syn compound	Type of Compound	Plant Source	Extract (E)/ Fraction (F)/Pure (P)	Plant part	Assay
37	MUC-915	Nat	Flavanone	Goniothalamus calvicarpus	Р	LF+TW	Anti-diabetic
38	MUC-916	Nat	Flavone	Mallotus glomerulatus	Р	PX	Anti-diabetic
39	MUC-1013	Nat	Diterpenoid glycoside	Stevia rebaudiana	Р	LF	Anti-diabetic
40	MUC-1014	Nat	Diterpenoid glycoside	Stevia rebaudiana	Р	LF	Anti-diabetic
41	MUC-1015	Mod	Diterpenoid glycoside	Stevia rebaudiana	Р	LF	Anti-diabetic
42	MUC-1016	Mod	Diterpenoid glycoside	Stevia rebaudiana	Р	LF	Anti-diabetic
43	MUC-1017	Mod	Diterpenoid	Stevia rebaudiana	Р	LF	Anti-diabetic
44	MUC-1018	Mod	Diterpenoid glycoside	Stevia rebaudiana	Р	LF	Anti-diabetic
45	MUC-1019	Mod	Diterpenoid glycoside	Stevia rebaudiana	Р	LF	Anti-diabetic
46	MUC-1024	Mod	Triterpenoid	Gardenia collinsae	Р	LF+TW	Anti-diabetic
47	MUC-1025	Mod	Triterpenoid	Gardenia collinsae	Р	LF+TW	Anti-diabetic
48	MUC-1026	Mod	Triterpenoid	Gardenia collinsae	Р	LF+TW	Anti-diabetic
49	MUC-1027	Mod	Triterpenoid	Gardenia collinsae	Р	LF+TW	Anti-diabetic
50	MUC-1256	Mod	Triterpenoid	Gardenia collinsae	Р	LF+TW	Anti-diabetic
51	MUC-1257	Mod	Triterpenoid	Gardenia collinsae	Р	LF+TW	Anti-diabetic
52	MUC-1258	Nat	Triterpenoid	Gardenia sessiliflora	Р	LF+TW	Anti-diabetic
53	MUC-1259	Nat	Triterpenoid	Gardenia sessiliflora	Р	LF+TW	Anti-diabetic
54	MUC-1260	Nat	Triterpenoid	Gardenia sessiliflora	Р	LF+TW	Anti-diabetic

No	CODE	Nat/Mod/Syn	Type of Compound	Plant Source	Extract (E)/	Dlant part	Access
INO	CODE	compound	Type of Compound	Plant Source	Fraction (F)/Pure (P)	Plant part	Assay
55	MUC-631	Nat	Flavone	Gardenia carinata	Р	LF+TW	Anti-diabetic
56	MUC-632	Nat	Triterpenoid	Gardenia carinata	Р	LF+TW	Anti-diabetic
57	MUC-633	Nat	Triterpenoid	Gardenia carinata	Р	LF+TW	Anti-diabetic
58	MUC733	Nat	Triterpenoid	Gardenia carinata	Р	LF+TW	Anti-diabetic
59	MUC734	Nat	Triterpenoid	Gardenia carinata	Р	LF+TW	Anti-diabetic
60	MUC735	Nat	Triterpenoid	Gardenia carinata	Р	LF+TW	Anti-diabetic
61	MUC736	Nat	Triterpenoid	Gardenia carinata	Р	LF+TW	Anti-diabetic
62	MUC737	Nat	Triterpenoid	Gardenia carinata	Р	LF+TW	Anti-diabetic
63	MUC738	Nat	Triterpenoid	Gardenia carinata	Р	LF+TW	Anti-diabetic
64	MUC739	Nat	Triterpenoid	Gardenia carinata	Р	LF+TW	Anti-diabetic
65	MUC740	Nat	Triterpenoid	Gardenia carinata	Р	LF+TW	Anti-diabetic
66	MUC741	Nat	Triterpenoid	Gardenia carinata	Р	LF+TW	Anti-diabetic
67	MUC742	Nat	Flavone	Gardenia carinata	Р	LF+TW	Anti-diabetic
68	MUC743	Nat	Triterpenoid	Gardenia carinata	Р	LF+TW	Anti-diabetic
69	MUC744	Nat	Triterpenoid	Gardenia carinata	Р	LF+TW	Anti-diabetic
70	MUC745	Nat	Sugar	Gardenia carinata	Р	LF+TW	Anti-diabetic
71	MUC746	Nat	Phenolic	Gardenia carinata	Р	LF+TW	Anti-diabetic
72	MUC747	Nat	Triterpenoid	Gardenia carinata	Р	LF+TW	Anti-diabetic

No	CODE	Nat/Mod/Syn compound	Type of Compound	Plant Source	Extract (E)/ Fraction (F)/Pure (P)	Plant part	Assay
73	MUC748	Nat	Coumarin	Gardenia carinata	Р	LF+TW	Anti-diabetic
74	MUC749	Nat	Phenolic	Gardenia carinata	Р	LF+TW	Anti-diabetic
75	MUC750	Nat	Triterpenoid glycoside	Gardenia carinata	Р	LF+TW	Anti-diabetic
76	MUC751	Nat	Triterpenoid	Gardenia carinata	Р	LF+TW	Anti-diabetic
77	MUC752	Nat	Flavone	Gardenia carinata	Р	LF+TW	Anti-diabetic
78	MUC753	Nat	Flavone	Gardenia carinata	Р	LF+TW	Anti-diabetic
79	MUC754	Nat	Flavone	Gardenia carinata	Р	LF+TW	Anti-diabetic
80	MUC755	Nat	Flavone	Gardenia carinata	Р	LF+TW	Anti-diabetic
81	MUC756	Nat	Flavone	Gardenia carinata	Р	LF+TW	Anti-diabetic
82	MUC757	Nat	Alkaloid	Polyalthia suberosa	Р	ST	Anti-diabetic
83	MUC758	Nat	Alkaloid	Polyalthia suberosa	Р	ST	Anti-diabetic
84	PT-382-SS	Nat	Flavonol	Gardenia obtusifolia	Р	LF+TW	Anti-diabetic
85	PT-383-SS	Nat	Flavonol	Gardenia obtusifolia	Р	LF+TW	Anti-diabetic
86	PT-384-SS	Nat	Flavonol	Gardenia obtusifolia	Р	LF+TW	Anti-diabetic
87	PT-385-SS	Nat	Flavone	Gardenia collinsae	Р	LF+TW	Anti-diabetic
88	PT-386-SS	Nat	Flavone	Gardenia obtusifolia	Р	LF+TW	Anti-diabetic
87	PT-387-SS	Nat	triterpenoid	Gardenia obtusifolia	Р	LF+TW	Anti-diabetic
88	PT-388-SS	Nat	triterpenoid	Gardenia obtusifolia	Р	LF+TW	Anti-diabetic

No	CODE	Nat/Mod/Syn compound	Type of Compound	Plant Source	Extract (E)/ Fraction (F)/Pure (P)	Plant part	Assay
89	PT-389-SS	Nat	Flavone	Gardenia thailandica	P	LF+TW	Anti-diabetic
90	PT-390-SS	Nat	Flavone	Gardenia thailandica	Р	LF+TW	Anti-diabetic
91	PT-391-SS	Nat	Triterpenoid	Gardenia thailandica	Р	LF+TW	Anti-diabetic
92	PT-392-SS	Nat	Triterpenoid	Gardenia thailandica	Р	LF+TW	Anti-diabetic
93	PT-393-SS	Nat	Alkaloid	Phyllanthus acutissima	Р	PX	Anti-diabetic
94	PT-394-SS	Nat	Alkaloid	Phyllanthus acutissima	Р	PX	Anti-diabetic
95	PT-395-SS	Nat	Triterpenoid	Phyllanthus acutissima	Р	PX	Anti-diabetic
96	PT-396-SS	Nat	Triterpenoid	Phyllanthus acutissima	Р	PX	Anti-diabetic
97	PT-397-SS	Nat	Triterpenoid	Phyllanthus acutissima	Р	PX	Anti-diabetic
98	PT-398-SS	Nat	Lignan	Phyllanthus acutissima	Р	PX	Anti-diabetic
99	PT-399-SS	Nat	Cyclic amide	Polyalthia suberosa	Р	ST	Anti-diabetic
100	PT-400-SS	Nat	Alkaloid	Polyalthia suberosa	Р	ST	Anti-diabetic
101	PT-401-SS	Nat	Conjugated amide	Polyalthia suberosa	Р	ST	Anti-diabetic
102	PT-402-SS	Nat	Conjugated amide	Polyalthia suberosa	Р	ST	Anti-diabetic
103	PT-403-SS	Nat	Alkaloid	Polyalthia suberosa	Р	ST	Anti-diabetic
104	PT-404-SS	Nat	Alkaloid	Polyalthia suberosa	Р	ST	Anti-diabetic
105	PT-405-SS	Nat	Alkaloid	Polyalthia suberosa	Р	ST	Anti-diabetic
106	PT-406-SS	Nat	Styryl lactone	Polyalthia crassa	Р	LF+TW	Anti-diabetic

No	CODE	Nat/Mod/Syn compound	Type of Compound	Plant Source	Extract (E)/ Fraction (F)/Pure (P)	Plant part	Assay
107	PT-407-SS	Nat	Alkaloid	Polyalthia crassa	P	LF+TW	Anti-diabetic
108	PT-408-SS	Nat	Styryl lactone	Polyalthia crassa	Р	LF+TW	Anti-diabetic
109	PT-409-SS	Nat	Styryl lactone	Polyalthia crassa	Р	LF+TW	Anti-diabetic
110	PT-410-SS	Nat	Diterpenoid	Polyalthia sclerophylla	Р	LF+TW	Anti-diabetic
111	PT-411-SS	Nat	Diterpenoid	Polyalthia sclerophylla	Р	LF+TW	Anti-diabetic
112	PT-412-SS	Nat	Diterpenoid	Polyalthia sclerophylla	Р	LF+TW	Anti-diabetic
113	PT-413-SS	Nat	Diterpenoid	Polyalthia sclerophylla	Р	LF+TW	Anti-diabetic
114	PT-414-SS	Nat	Flavonol glycodide	Polyalthia sclerophylla	Р	LF+TW	Anti-diabetic
115	PT-415-SS	Nat	Flavonol	Polyalthia sclerophylla	Р	LF+TW	Anti-diabetic
120	PT-416-SS	Nat	Diterpenoid	Polyalthia sclerophylla	Р	LF+TW	Anti-diabetic
121	PT-417-SS	Nat	Triiterpenoid	Phyllanthus taxodiifolius	Р	PX	Anti-diabetic
122	PT-418-SS	Nat	Lignan glycoside	Phyllanthus taxodiifolius	Р	PX	Anti-diabetic
123	PT-419-SS	Nat	Dipeptide	Phyllanthus taxodiifolius	Р	PX	Anti-diabetic
124	PT-420-SS	Nat	Lignan glycoside	Phyllanthus taxodiifolius	Р	PX	Anti-diabetic
125	MUC-57	Mod	Lignan glycoside	Phyllanthus taxodiifolius	Р	PX	Cytotoxic
126	MUC-58	Mod	Lignan glycoside	Phyllanthus taxodiifolius	Р	PX	Cytotoxic
127	MUC-59	Mod	Lignan glycoside	Phyllanthus taxodiifolius	Р	PX	Cytotoxic
128	MUC-60	Mod	Lignan glycoside	Phyllanthus taxodiifolius	Р	PX	Cytotoxic

No	CODE	Nat/Mod/Syn compound	Type of Compound	Plant Source	Extract (E)/ Fraction (F)/Pure (P)	Plant part	Assay
129	MUC-61	Mod	Lignan glycoside	Phyllanthus taxodiifolius	Р	PX	Cytotoxic
130	MUC-62	Mod	Lignan glycoside	Phyllanthus taxodiifolius	Р	PX	Cytotoxic
131	MUC-63	Mod	Lignan glycoside	Phyllanthus taxodiifolius	Р	PX	Cytotoxic
132	MUC-65	Mod	Lignan glycoside	Phyllanthus taxodiifolius	Р	PX	Cytotoxic
133	MUC-66	Mod	Lignan glycoside	Phyllanthus taxodiifolius	Р	PX	Cytotoxic
134	MUC-67	Mod	Lignan glycoside	Phyllanthus taxodiifolius	Р	PX	Cytotoxic
135	MUC-68	Mod	Lignan glycoside	Phyllanthus taxodiifolius	Р	PX	Cytotoxic
136	MUC-69	Mod	Lignan glycoside	Phyllanthus taxodiifolius	Р	PX	Cytotoxic
137	MUC-222	Mod	Lignan glycoside	Phyllanthus taxodiifolius	Р	PX	Cytotoxic
138	MUC-223	Mod	Lignan glycoside	Phyllanthus taxodiifolius	Р	PX	Cytotoxic
139	MUC-225	Mod	Lignan glycoside	Phyllanthus taxodiifolius	Р	PX	Cytotoxic
140	MUC-274	Mod	Lignan glycoside	Phyllanthus taxodiifolius	Р	PX	Cytotoxic
141	MUC-275	Mod	Lignan glycoside	Phyllanthus taxodiifolius	Р	PX	Cytotoxic
142	MUC-967	Nat	Flavanone	Gloniothalamus aurantiacus	Р	LF+TW	Neuroprotective
143	MUC-968	Nat	Flavanone	Gloniothalamus aurantiacus	Р	LF+TW	Neuroprotective
144	MUC-969	Nat	Flavone	Gardinia carinata	Р	LF+TW	Neuroprotective
145	MUC-970	Nat	Flavone	Gardinia carinata	Р	LF+TW	Neuroprotective
146	MUC-971	Nat	Flavonol	Zingiber maekongense	Р	RT	Neuroprotective

No	CODE	Nat/Mod/Syn compound	Type of Compound	Plant Source	Extract (E)/ Fraction (F)/Pure (P)	Plant part	Assay
147	MUC-972	Nat	Flavonol	Zingiber maekongense	P	RT	Neuroprotective
147	10100-912	INGL	Flavoriol	Zingioei maekongense	r	ΝI	Neuroprotective
148	MUC-973	Nat	Flavone	Gardenia sessiliflora	Р	LF+TW	Neuroprotective
149	MUC-974	Nat	Flavone	Gardenia sessiliflora	Р	LF+TW	Neuroprotective
150	MUC-975	Nat	Flavanone	Gardenia sessiliflora	Р	LF+TW	Neuroprotective
151	MUC-976	Nat	Flavone	Gardenia sessiliflora	Р	LF+TW	Neuroprotective
152	MUC-977	Nat	Flavone	Gardenia sessiliflora	Р	LF+TW	Neuroprotective
153	MUC-978	Nat	Flavanone	Gardenia sessiliflora	Р	LF+TW	Neuroprotective
154	MUC-979	Nat	Flavone	Gardenia sessiliflora	Р	LF+TW	Neuroprotective
155	MUC-980	Nat	Flavone	Gardenia sessiliflora	Р	LF+TW	Neuroprotective
156	MUC-981	Nat	Flavone	Gardenia sessiliflora	Р	LF+TW	Neuroprotective
157	MUC-982	Nat	Flavone	Gardenia sessiliflora	Р	LF+TW	Neuroprotective
158	MUC-983	Nat	Flavone	Gardenia sessiliflora	Р	LF+TW	Neuroprotective
159	MUC-984	Nat	Flavone	Gardenia sessiliflora	Р	LF+TW	Neuroprotective
160	MUC-1024	Mod	Triterpenoid	Gardenia collinsae	Р	LF+TW	Anti-diabetic
161	MUC-1025	Mod	Triterpenoid	Gardenia collinsae	Р	LF+TW	Anti-diabetic
162	MUC-1026	Mod	Triterpenoid	Gardenia collinsae	Р	LF+TW	Anti-diabetic
163	MUC-1027	Nat	Triterpenoid	Gardenia collinsae	Р	LF+TW	Anti-diabetic
164	MUC-1284	Nat	Styryl lactone	Goniothalamus calvicarpus	Р	ST	Cytotoxic

No	CODE	Nat/Mod/Syn compound	Type of Compound	Plant Source	Extract (E)/ Fraction (F)/Pure (P)	Plant part	Assay
165	MUC-1285	Nat	Styryl lactone	Goniothalamus calvicarpus	Р	ST	Cytotoxic
166	MUC-1286	Nat	Flavanone	Goniothalamus calvicarpus	Р	ST	Cytotoxic
167	MUC-1405	Nat	Triterpenoid	Santisukia pagetii	Р	LF+TW	Cytotoxic
168	MUC-1406	Nat	Triterpenoid	Santisukia pagetii	Р	LF+TW	Anti-diabetic
169	MUC-1407	Nat	Iridoid glycoside	Santisukia pagetii	Р	LF+TW	Cytotoxic
170	MUC-1208	Nat	Iridoid glycosides	Santisukia pagetii	Р	LF+TW	Cytotoxic
171	MUC-1020	Mod	Triterpenoid	Gardenia collinsae	Р	LF+TW	Cytotoxic
172	MUC-1021	Mod	Triterpenoid	Gardenia collinsae	Р	LF+TW	Cytotoxic
173	MUC-1022	Mod	Triterpenoid	Gardenia collinsae	Р	LF+TW	Cytotoxic
174	MUC-1023	Nat	Triterpenoid	Gardenia collinsae	Р	LF+TW	Cytotoxic
175	MUC-1028	Mod	Lactone	Polyalthia crassa	Р	LF+TW	Cytotoxic
176	MUC-1029	Mod	Styryllactone	Polyalthia crassa	Р	LF+TW	Cytotoxic
177	MUC-1030	Mod	Styryllactone	Polyalthia crassa	Р	LF+TW	Cytotoxic
178	MUC-1031	Mod	Styryllactone	Polyalthia crassa	Р	LF+TW	Cytotoxic
179	MUC-1032	Mod	Styryllactone	Polyalthia crassa	Р	LF+TW	Cytotoxic
180	MUC-1264	Nat	C ₆ C ₂ compound	Boesenbergia thorelii	Р	RZ	Cytotoxic
181	MUC-1265	Nat	C ₆ C ₂ compound	Boesenbergia thorelii	Р	RZ	Cytotoxic
182	MUC-1277	Nat	C_6C_2 compound	Boesenbergia thorelii	Р	RZ	Anti-diabetic

No	CODE	Nat/Mod/Syn compound	Type of Compound	Plant Source	Extract (E)/ Fraction (F)/Pure (P)	Plant part	Assay
183	MUC-1278	Nat	C ₆ C ₂ compound	Boesenbergia thorelii	Р	RZ	Anti-diabetic
184	MUC-1279	Nat	C ₆ C ₂ compound	Boesenbergia thorelii	Р	RZ	Anti-diabetic
185	MUC-1280	Nat	Lignan	Boesenbergia thorelii	Р	RZ	Anti-diabetic
186	MUC-1281	Nat	C ₆ C ₃ compound	Boesenbergia thorelii	Р	RZ	Anti-diabetic
187	MUC-1282	Nat	C ₆ C ₃ compound	Boesenbergia thorelii	Р	RZ	Anti-diabetic
188	MUC-1283	Nat	Benzoic acid derivative	Boesenbergia thorelii	Р	RZ	Anti-diabetic
189	MUC-1284	Nat	Styryllactone	Goniothalamus calvicarpus	Р	ST	Cytotoxic
190	MUC-1285	Nat	Styryllactone	Goniothalamus calvicarpus	Р	ST	Cytotoxic
191	MUC-1286	Nat	Flavanone	Goniothalamus calvicarpus	Р	ST	Cytotoxic
192	MUC-1287	Nat	Styryllactone	Goniothalamus calvicarpus	Р	ST	Cytotoxic
193	MUC-1303	Nat	Triterpenoid	Mallotus glomerulatus	Р	PX	Anti-diabetic
194	MUC-1304	Nat	Triterpenoid	Mallotus glomerulatus	Р	PX	Anti-diabetic
195	MUC-1305	Nat	Diterpenoid	Mallotus glomerulatus	Р	PX	Anti-diabetic
196	MUC-1306	Nat	Flavanone	Mallotus glomerulatus	Р	PX	Anti-diabetic
197	MUC-1307	Nat	Diterpenoid	Mallotus glomerulatus	Р	PX	Anti-diabetic
198	MUC-1308	Nat	Flavanone	Mallotus glomerulatus	Р	PX	Anti-diabetic
199	MUC-1309	Nat	Flavanone	Mallotus glomerulatus	Р	PX	Anti-diabetic
200	MUC-1310	Nat	Aromatic compound	Mallotus glomerulatus	Р	PX	Anti-diabetic

No	CODE	Nat/Mod/Syn compound	Type of Compound	Plant Source	Extract (E)/ Fraction (F)/Pure (P)	Plant part	Assay
201	MUC-1311	Nat	Diterpenoid	Mallotus glomerulatus	Р	PX	Anti-diabetic
202	MUC-1312	Nat	Lignan glycoside	Mallotus glomerulatus	Р	PX	Anti-diabetic
203	MUC-1313	Nat	Flavone	Mallotus glomerulatus	Р	PX	Anti-diabetic
204	MUC-1314	Nat	Xanthone	Mallotus glomerulatus	Р	PX	Anti-diabetic
205	MUC-1323	Nat	Styryllactone	Goniothalamus calvicarpus	Р	ST	Anti-diabetic
206	MUC-1324	Nat	Styryllactone	Goniothalamus calvicarpus	Р	ST	Anti-diabetic
207	MUC-1325	Nat	Styryllactone	Goniothalamus calvicarpus	Р	ST	Anti-diabetic
208	MUC-1326	Nat	Styryllactone	Goniothalamus calvicarpus	Р	ST	Anti-diabetic
209	MUC-1327	Nat	Flavanone	Goniothalamus calvicarpus	Р	ST	Anti-diabetic
210	MUC-1328	Nat	Styryllactone	Goniothalamus calvicarpus	Р	ST	Anti-diabetic
211	MUC-1329	Nat	alkaloid	Goniothalamus calvicarpus	Р	ST	Anti-diabetic
212	MUC-1330	Nat	Flavone	Gardenia sessiliflora	Р	LF+TW	Cytotoxic
213	MUC-1331	Nat	Flavone	Gardenia sessiliflora	Р	LF+TW	Cytotoxic
214	MUC-1332	Nat	Flavanone	Gardenia sessiliflora	Р	LF+TW	Cytotoxic
215	MUC-1333	Nat	Flavone	Gardenia sessiliflora	Р	LF+TW	Cytotoxic
216	MUC-1334	Nat	Flavone	Gardenia sessiliflora	Р	LF+TW	Cytotoxic
217	MUC-1335	Nat	Flavanone	Gardenia sessiliflora	Р	LF+TW	Cytotoxic
218	MUC-1336	Nat	Flavone	Gardenia sessiliflora	Р	LF+TW	Cytotoxic

No	CODE	Nat/Mod/Syn compound	Type of Compound	Plant Source	Extract (E)/ Fraction (F)/Pure (P)	Plant part	Assay
219	MUC-1337	Nat	Triterpenoid	Gardenia sessiliflora	Р	LF+TW	Cytotoxic
220	MUC-1338	Nat	Triterpenoid	Gardenia sessiliflora	Р	LF+TW	Cytotoxic
221	MUC-1339	Nat	Triterpenoid	Gardenia sessiliflora	Р	LF+TW	Cytotoxic
222	MUC-1340	Nat	Triterpenoid	Gardenia sessiliflora	Р	LF+TW	Cytotoxic
223	MUC-1341	Nat	Triterpenoid	Gardenia sessiliflora	Р	LF+TW	Cytotoxic
224	MUC-1342	Nat	Triterpenoid	Gardenia sessiliflora	Р	LF+TW	Cytotoxic
225	MUC-1343	Nat	Triterpenoid	Gardenia sessiliflora	Р	LF+TW	Cytotoxic
226	MUC-1344	Nat	Triterpenoid	Gardenia sessiliflora	Р	LF+TW	Cytotoxic
227	MUC-1345	Nat	Flavanone	Gardenia sessiliflora	Р	LF+TW	Cytotoxic
228	MUC-1346	Nat	Triterpenoid	Gardenia sessiliflora	Р	LF+TW	Cytotoxic
229	MUC-1347	Nat	Triterpenoid	Gardenia sessiliflora	Р	LF+TW	Cytotoxic
230	MUC-1348	Nat	Triterpenoid	Gardenia sessiliflora	Р	LF+TW	Cytotoxic
231	MUC-1349	Nat	Flavone	Gardenia sessiliflora	Р	LF+TW	Cytotoxic
232	MUC-1350	Nat	Triterpenoid	Gardenia sessiliflora	Р	LF+TW	Cytotoxic
233	MUC-1351	Nat	Flavone	Gardenia sessiliflora	Р	LF+TW	Cytotoxic
234	MUC-1352	Nat	Flavone	Gardenia sessiliflora	Р	LF+TW	Cytotoxic
235	MUC-1353	Nat	Triterpenoid	Gardenia sessiliflora	Р	LF+TW	Cytotoxic
236	MUC-1354	Nat	Flavanone	Gardenia sessiliflora	Р	LF+TW	Cytotoxic

		Nat/Mod/Syn			Extract (E)/		
No	CODE	compound	Type of Compound	Plant Source	Fraction (F)/Pure (P)	Plant part	Assay
237	MUC-1409	Nat	Aromatic Aldehyde	Boesenbergia thorelii	Р	RZ	Anti-diabetic
238	MUC-1411	Syn	Tertiary Amine	-	Р	-	Cytotoxic
239	MUC-1412	Syn	Tertiary Amine	-	Р	-	Cytotoxic
240	MUC-1413	Syn	Tertiary Amine	-	Р	-	Cytotoxic
241	MUC-1414	Syn	Tertiary Amine	-	Р	-	Cytotoxic
242	MUC-1415	Syn	Tertiary Amine	-	Р	-	Cytotoxic
243	MUC-1416	Syn	Tertiary Amine	-	Р	-	Cytotoxic
244	MUC-1417	Syn	Tertiary Amine	-	Р	-	Cytotoxic
245	MUC-1418	Syn	Tertiary Amine	-	Р	-	Anti-diabetic
246	MUC-1419	Syn	Tertiary Amine	-	Р	-	Anti-diabetic
247	MUC-1420	Syn	Tertiary Amine	-	Р	-	Anti-diabetic
248	MUC-1421	Syn	Tertiary Amine	-	Р	-	Anti-diabetic
249	MUC-1422	Syn	Tertiary Amine	-	Р	-	Anti-diabetic
250	MUC-1423	Syn	Tertiary Amine	-	Р	-	Anti-diabetic
251	MUC-1424	Syn	Tertiary Amine	-	Р	-	Anti-diabetic
252	MUC-1491	Nat	Triterpenoid	Santisukia pagetii	Р	LF+TW	Cytotoxic
253	MUC-1492	Nat	Triterpenoid	Santisukia pagetii	Р	LF+TW	Cytotoxic
254	MUC-1493	Nat	iridoid glycoside	Santisukia pagetii	Р	LF+TW	Cytotoxic

No	CODE	Nat/Mod/Syn compound	Type of Compound	Plant Source	Extract (E)/ Fraction (F)/Pure (P)	Plant part	Assay
255	MUC-1633	Syn	Sulfide	-	Р	-	Cytotoxic
256	MUC-1634	Syn	Sulfide	-	Р	-	Cytotoxic
257	MUC-1635	Syn	Sulfide	-	Р	-	Cytotoxic
258	MUC-1644	Nat	Styryllactone	Goniothalamus calvicarpus	Р	ST	Cytotoxic
259	MUC-1653	Nat	C_6C_3 compound	Boesenbergia thorelii	Р	RZ	Cytotoxic
260	MUC-1654	Nat	C_6C_3 compound	Boesenbergia thorelii	Р	RZ	Cytotoxic
261	MUC-1655	Nat	C_6C_3 compound	Boesenbergia thorelii	Р	RZ	Cytotoxic
262	MUC-1656	Nat	C_6C_3 compound	Boesenbergia thorelii	Р	RZ	Cytotoxic
263	MUC-1674	Nat	Triterpenoid	Santisukia pagetii	р	LF+TW	Anti-diabetic
264	MUC-1675	Nat	Triterpenoid	Santisukia pagetii	р	LF+TW	Anti-diabetic
265	MUC-1676	Nat	Iridoid glycoside	Santisukia pagetii	Р	LF+TW	Anti-diabetic
266	MUC-1677	Nat	Iridoid glycoside	Santisukia pagetii	Р	LF+TW	Anti-diabetic
267	MUC-1678	Nat	Monoterpenoid	Santisukia pagetii	Р	LF+TW	Anti-diabetic
268	MUC-1679	Nat	Iridoid glycoside	Santisukia pagetii	Р	LF+TW	Anti-diabetic
269	MUC-1680	Nat	C6C3 compound	Santisukia pagetii	Р	LF+TW	Anti-diabetic
270	MUC-1681	Nat	C6C3 compound	Santisukia pagetii	Р	LF+TW	Anti-diabetic
271	MUC-1682	Nat	Flavonoid glycoside	Santisukia pagetii	Р	LF+TW	Anti-diabetic
272	MUC-1683	Nat	Flavonoid glycoside	Santisukia pagetii	Р	LF+TW	Anti-diabetic

No	CODE	Nat/Mod/Syn compound	Type of Compound	Plant Source	Extract (E)/ Fraction (F)/Pure (P)	Plant part	Assay
273	MUC-1684	Nat	Triterpenoid	Santisukia pagetii	Р	LF+TW	Anti-diabetic
274	MUC-1685	Nat	Triterpenoid	Santisukia pagetii	Р	LF+TW	Anti-diabetic
275	MUC-1686	Nat	Styryllactone	Goniothalamus aurantiacus	Р	LF+TW	Cytotoxic
276	MUC-1694	Nat	Styryllactone	Goniothalamus aurantiacus	Р	LF+TW	Cytotoxic
277	MUC-1619	Nat	-	Paris polyphylla	E	RZ	Cytotoxic
278	MUC-1620	Nat	-	Paris polyphylla	F	RZ	Cytotoxic
279	MUC-1621	Nat	-	Paris polyphylla	F	RZ	Cytotoxic
280	MUC-1622	Nat	-	Paris polyphylla	F	RZ	Cytotoxic
281	MUC-1623	Nat	-	Paris polyphylla	F	RZ	Cytotoxic
282	MUC-1624	Nat	-	Paris polyphylla	F	RZ	Cytotoxic
283	MUC-1625	Nat	-	Paris polyphylla	F	RZ	Cytotoxic
284	MUC-1626	Nat	-	Paris polyphylla	E	RZ	Anti-diabetic
285	MUC-1627	Nat	-	Paris polyphylla	F	RZ	Anti-diabetic
286	MUC-1628	Nat	-	Paris polyphylla	F	RZ	Anti-diabetic
287	MUC-1629	Nat	-	Paris polyphylla	F	RZ	Anti-diabetic
288	MUC-1630	Nat	-	Paris polyphylla	F	RZ	Anti-diabetic
289	MUC-1631	Nat	-	Paris polyphylla	F	RZ	Anti-diabetic
290	MUC-1632	Nat	-	Paris polyphylla	F	RZ	Anti-diabetic

No	CODE	Nat/Mod/Syn compound	Type of Compound	Plant Source	Extract (E)/ Fraction (F)/Pure (P)	Plant part	Assay
291	MUC-1695	Nat	-	Paris polyphylla	F	RZ	Cytotoxic
292	MUC-1696	Nat	-	Paris polyphylla	F	RZ	Cytotoxic
293	MUC-1697	Nat	-	Paris polyphylla	F	RZ	Cytotoxic
294	MUC-1698	Nat	-	Paris polyphylla	F	RZ	Cytotoxic
295	MUC-1699	Nat	-	Paris polyphylla	F	RZ	Cytotoxic
296	MUC-1700	Nat	-	Paris polyphylla	F	RZ	Cytotoxic
297	MUC-1701	Nat	-	Paris polyphylla	F	RZ	Cytotoxic
298	MUC-1702	Nat	-	Paris polyphylla	F	RZ	Cytotoxic
299	MUC-1703	Nat	-	Paris polyphylla	F	RZ	Cytotoxic
300	MUC-1704	Nat	-	Paris polyphylla	F	RZ	Anti-diabetic
301	MUC-1705	Nat	-	Paris polyphylla	F	RZ	Anti-diabetic
302	MUC-1706	Nat	-	Paris polyphylla	F	RZ	Anti-diabetic
303	MUC-1707	Nat	-	Paris polyphylla	F	RZ	Anti-diabetic
304	MUC-1708	Nat	-	Paris polyphylla	F	RZ	Anti-diabetic
305	MUC-1709	Nat	-	Paris polyphylla	F	RZ	Anti-diabetic
306	MUC-1710	Nat	-	Paris polyphylla	F	RZ	Anti-diabetic
307	MUC-1711	Nat	-	Paris polyphylla	F	RZ	Anti-diabetic
308	MUC-1712	Nat	-	Paris polyphylla	F	RZ	Anti-diabetic

No	CODE	Nat/Mod/Syn compound	Type of Compound	Plant Source	Extract (E)/ Fraction (F)/Pure (P)	Plant part	Assay
309	MUC-1713	Nat	Flavone	Gardenia sessiliflora	P	LF+TW	Drug transporter for chemotherapy
310	MUC-1714	Nat	Flavone	Gardenia sessiliflora	Р	LF+TW	Drug transporter for chemotherapy
311	MUC-1715	Nat	Flavone	Gardenia sessiliflora	Р	LF+TW	Drug transporter for chemotherapy
312	MUC-1716	Nat	Flavanone	Gardenia sessiliflora	Р	LF+TW	Drug transporter for chemotherapy
313	MUC-1717	Nat	Flavone	Gardenia sessiliflora	Р	LF+TW	Drug transporter for chemotherapy
314	MUC-1718	Nat	Flavanone	Gardenia sessiliflora	Р	LF+TW	Drug transporter for chemotherapy
315	MUC-1719	Nat	Triterpenoid	Santisukia pagetii	Р	LF+TW	Drug transporter for chemotherapy
316	MUC-1720	Nat	Iridoid glycoside	Santisukia pagetii	Р	LF+TW	Drug transporter for chemotherapy
317	MUC-1721	Nat	Iridoid glycoside	Santisukia pagetii	Р	LF+TW	Drug transporter for chemotherapy
318	MUC-1722	Nat	Monoterpenoid	Santisukia pagetii	Р	LF+TW	Drug transporter for chemotherapy
319	MUC-1723	Nat	Iridoid glycoside	Santisukia pagetii	Р	LF+TW	Drug transporter for chemotherapy
320	MUC-1724	Nat	Flavonoid glycoside	Santisukia pagetii	Р	LF+TW	Drug transporter for chemotherapy
321	MUC-1725	Nat	C_6C_2 compound	Boesenbergia thorelii	Р	RZ	Drug transporter for chemotherapy
322	MUC-1726	Nat	C_6C_2 compound	Boesenbergia thorelii	Р	RZ	Drug transporter for chemotherapy
323	MUC-1727	Nat	C ₆ C₃ compound	Boesenbergia thorelii	Р	RZ	Drug transporter for chemotherapy
324	MUC-1728	Nat	Aromatic aldehyde	Boesenbergia thorelii	Р	RZ	Drug transporter for

No	CODE	Nat/Mod/Syn compound	Type of Compound	Plant Source	Extract (E)/ Fraction (F)/Pure (P)	Plant part	Assay
			,			•	chemotherapy
325	MUC-1729	Nat	C₀C₃ compound	Boesenbergia thorelii	Р	RZ	Drug transporter for chemotherapy
326	MUC-1730	Nat	C ₆ C₃ compound	Boesenbergia thorelii	Р	RZ	Drug transporter for chemotherapy
327	MUC-1731	Nat	C ₆ C₃ compound	Boesenbergia thorelii	Р	RZ	Drug transporter for chemotherapy
328	MUC-1732	Nat	lignan	Boesenbergia thorelii	Р	RZ	Drug transporter for chemotherapy
329	MUC-1733	Nat	Flavone	Gardenia collinsae	Р	LF+TW	Drug transporter for chemotherapy
330	MUC-1734	Nat	Flavone	Gardenia thailandica	Р	LF+TW	Drug transporter for chemotherapy
331	MUC-1735	Nat	Flavone	Gardenia thailandica	Р	LF+TW	Drug transporter for chemotherapy
332	MUC-1736	Nat	Triterpenoid	Gardenia thailandica	Р	LF+TW	Drug transporter for chemotherapy
333	MUC-1737	Nat	Triterpenoid	Gardenia thailandica	Р	LF+TW	Drug transporter for chemotherapy
334	MUC-1737	Nat	Flavone	Gardenia collinsae	Р	LF+TW	Drug transporter for chemotherapy
335	MUC-1776	Nat	Triterpenoid	Gardenia sessiliflora	Р	LF+TW	Drug transporter for chemotherapy
336	MUC-1777	Nat	Triterpenoid	Gardenia sessiliflora	Р	LF+TW	Drug transporter for chemotherapy
337	MUC-1778	Nat	Triterpenoid	Gardenia sessiliflora	Р	LF+TW	Drug transporter for chemotherapy
338	MUC-1779	Nat	Triterpenoid	Gardenia sessiliflora	Р	LF+TW	Drug transporter for chemotherapy
339	MUC-1780	Nat	Triterpenoid	Gardenia sessiliflora	Р	LF+TW	Drug transporter for chemotherapy

No	CODE	Nat/Mod/Syn compound	Type of Compound	Plant Source	Extract (E)/ Fraction (F)/Pure (P)	Plant part	Assay
		compound	.) Po ex composition	1 10.110 0 0 11 0 0	Traction (1)/1 are (1)		Proliferation of cancer
340	MUC-1672	Nat	Triterpenoid	Phyllanthus taxodiifolius	Р	PX	cells
			'				Proliferation of cancer
341	MUC-1672	Nat	Triterpenoid	Phyllanthus taxodiifolius	Р	PX	cells
							Proliferation of cancer
340	MUC-1807	Nat	Lignan glycoside	Phyllanthus taxodiifolius	Р	PX	cells
							Proliferation of cancer
341	MUC-1808	Nat	Lignan glycoside	Phyllanthus taxodiifolius	Р	PX	cells
							Mechanistic study of
342	MUC-535 (1)	Mod	Lignan glycoside	Phyllanthus taxodiifolius	Р	PX	anti-cancer effect
							Mechanistic study of
343	MUC-535 (2)	Mod	Lignan glycoside	Phyllanthus taxodiifolius	Р	PX	anti-cancer effect
							Mechanistic study of
344	MUC-535 (3)	Mod	Lignan glycoside	Phyllanthus taxodiifolius	Р	PX	anti-cancer effect
							Mechanistic study of
345	MUC-536 (1)	Mod	Lignan glycoside	Phyllanthus taxodiifolius	Р	PX	anti-cancer effect
							Mechanistic study of
346	MUC-536 (2)	Mod	Lignan glycoside	Phyllanthus taxodiifolius	Р	PX	anti-cancer effect
							Mechanistic study of
347	MUC-536 (3)	Mod	Lignan glycoside	Phyllanthus taxodiifolius	Р	PX	anti-cancer effect
							Mechanistic study of
348	MUC-536 (4)	Mod	Lignan glycoside	Phyllanthus taxodiifolius	Р	PX	anti-cancer effect
							Mechanistic study of
349	MUC-536 (5)	Mod	Lignan glycoside	Phyllanthus taxodiifolius	Р	PX	anti-cancer effect
							Mechanistic study of
350	MUC-537 (1)	Mod	Lignan glycoside	Phyllanthus taxodiifolius	Р	PX	anti-cancer effect
					_		Mechanistic study of
351	MUC-537 (2)	Mod	Lignan glycoside	Phyllanthus taxodiifolius	Р	PX	anti-cancer effect
				2/ // // // // // // // // // // // // /		5) (Mechanistic study of
352	MUC-537 (3)	Mod	Lignan glycoside	Phyllanthus taxodiifolius	Р	PX	anti-cancer effect
353	MUC-537 (4)	Mod	Lignan glycoside	Phyllanthus taxodiifolius	Р	PX	Mechanistic study of

		Nat/Mod/Syn			Extract (E)/		
No	CODE	compound	Type of Compound	Plant Source	Fraction (F)/Pure (P)	Plant part	Assay
							anti-cancer effect
							Mechanistic study of
354	MUC-538 (1)	Mod	Lignan glycoside	Phyllanthus taxodiifolius	Р	PX	anti-cancer effect
0.5.5	A 41 (C F20 (O)			DI II I	6	D) (Mechanistic study of
355	MUC-538 (2)	Mod	Lignan glycoside	Phyllanthus taxodiifolius	Р	PX	anti-cancer effect
356	MUC-1503	Mod	Flavanone derivative	Boesenbergia rotunda	Р	RZ	Anti-diabetic
357	MUC-1504	Mod	Flavanone derivative	Boesenbergia rotunda	Р	RZ	Anti-diabetic
358	MUC-1505	Mod	Flavanone derivative	Boesenbergia rotunda	Р	RZ	Anti-diabetic
359	MUC-1506	Mod	Flavanone derivative	Boesenbergia rotunda	Р	RZ	Anti-diabetic
360	MUC-1507	Nat	Flavanone derivative	Boesenbergia rotunda	Р	RZ	Anti-diabetic
361	MUC-1669	Nat	Styryllactone	Goniothalamus aurantiacus	Р	ST	Cytotoxic
362	MUC-1670	Nat	Styryllactone	Goniothalamus aurantiacus	Р	ST	Cytotoxic
363	MUC-1671	Nat	Styryllactone	Goniothalamus aurantiacus	Р	ST	Cytotoxic
							Proliferation of
364	MUC-1672	Nat	triterpenoid	Phyllanthus taxodiifolius	Р	PX	cancer cells
							Proliferation of
365	MUC-1673	Nat	triterpenoid	Phyllanthus taxodiifolius	Р	PX	cancer cells
366	MUC-1809	Nat	Alkaloid	Goniothalamus calvicarpus	Р	ST	Cytotoxic
367	MUC-1810	Nat	Styryllactone	Goniothalamus calvicarpus	Р	ST	Cytotoxic
368	MUC-1811	Nat	Alkaloid	Goniothalamus calvicarpus	Р	ST	Cytotoxic
369	MUC-1812	Nat	Alkaloid	Goniothalamus calvicarpus	Р	ST	Cytotoxic

		Nat/Mod/Syn			Extract (E)/		
No	CODE	compound	Type of Compound	Plant Source	Fraction (F)/Pure (P)	Plant part	Assay
370	MUC-1813	Nat	Lactone	Goniothalamus calvicarpus	Р	ST	Cytotoxic
371	MUC-1814	Nat	Alkaloid	Goniothalamus calvicarpus	Р	ST	Cytotoxic
372	MUC-1815	Nat	Conjugated amide	Goniothalamus calvicarpus	Р	ST	Cytotoxic
373	MUC-1816	Nat	Styryllactone	Goniothalamus calvicarpus	Р	ST	Cytotoxic
374	MUC-1817	Nat	Conjugated ester	Goniothalamus calvicarpus	Р	ST	Cytotoxic
375	MUC-1818	Nat	Styryllactone	Goniothalamus calvicarpus	Р	ST	Cytotoxic
376	MUC-1819	Nat	Styryllactone	Goniothalamus calvicarpus	Р	ST	Cytotoxic
377	MUC-1832	Nat	-	Phyllanthus taxodiifolius	F	PX	Mechanistic study of anti-cancer effect
378	MUC-1833	Nat	-	Phyllanthus taxodiifolius	F	PX	Mechanistic study of anti-cancer effect
379	MUC-1834	Nat	-	Phyllanthus taxodiifolius	F	PX	Mechanistic study of anti-cancer effect
380	MUC-1835	Nat	-	Phyllanthus taxodiifolius	F	PX	Mechanistic study of anti-cancer effect
381	MUC-1836	Nat	-	Phyllanthus taxodiifolius	F	PX	Mechanistic study of anti-cancer effect
382	MUC-1837	Nat	C₀C₃ compound	Boesenbergia thorelii	Р	RZ	Cytotoxic
383	MUC-1838	Nat	Lignan	Boesenbergia thorelii	Р	RZ	Cytotoxic
384	MUC-1839	Nat	C₀C₃ compound	Boesenbergia thorelii	Р	RZ	Cytotoxic
385	MUC-1840	Nat	C₀C₃ compound	Boesenbergia thorelii	Р	RZ	Cytotoxic
386	MUC-1841	Nat	Benzoic acid derivative	Boesenbergia thorelii	Р	RZ	Cytotoxic

No	CODE	Nat/Mod/Syn compound	Type of Compound	Plant Source	Extract (E)/ Fraction (F)/Pure (P)	Plant part	Assay
387	MUC-1842	Nat	Lignan	Boesenbergia thorelii	P P	RZ	Cytotoxic
388	MUC-1843	Nat	Benzaldehyde derivative	Boesenbergia thorelii	Р	RZ	Cytotoxic
389	MUC-1844	Nat	Benzene derivative	Boesenbergia thorelii	Р	RZ	Cytotoxic
390	MUC-1845	Nat	Benzoic acid derivative	Boesenbergia thorelii	Р	RZ	Cytotoxic
391	MUC-1864	Nat	C ₆ C ₃ compound	Boesenbergia thorelii	Р	RZ	Cytotoxic
392	MUC-1865	Nat	Lignan	Boesenbergia thorelii	Р	RZ	Anti-diabetic
393	MUC-1866	Nat	C ₆ C ₃ compound	Boesenbergia thorelii	Р	RZ	Anti-diabetic
394	MUC-1867	Nat	C ₆ C ₃ compound	Boesenbergia thorelii	Р	RZ	Anti-diabetic
395	MUC-1868	Nat	Benzoic acid derivative	Boesenbergia thorelii	Р	RZ	Anti-diabetic
396	MUC-1869	Nat	Lignan	Boesenbergia thorelii	Р	RZ	Anti-diabetic
397	MUC-1870	Nat	Benzaldehyde derivative	Boesenbergia thorelii	Р	RZ	Anti-diabetic
398	MUC-1871	Nat	Benzene derivative	Boesenbergia thorelii	Р	RZ	Anti-diabetic
399	MUC-1872	Nat	Benzaldehyde derivative	Boesenbergia thorelii	Р	RZ	Anti-diabetic
400	MUC-1873	Nat	Iridoid glycoside	Santisukia pagetii	Р	LF+TW	Anti-oxidant
401	MUC-1874	Nat	Iridoid glycoside	Santisukia pagetii	Р	LF+TW	Anti-oxidant
402	MUC-1875	Nat	Iridoid glycoside	Santisukia pagetii	Р	LF+TW	Anti-oxidant
403	MUC-1876	Mod	Iridoid glycoside	Santisukia pagetii	Р	LF+TW	Anti-oxidant
404	MUC-1877	Nat	-	Garcinia succifolia	E	ST	Cytotoxic

No	CODE	Nat/Mod/Syn compound	Type of Compound	Plant Source	Extract (E)/ Fraction (F)/Pure (P)	Plant part	Assay
405	MUC-1878	Nat	-	Garcinia succifolia	F	ST	Cytotoxic
406	MUC-1879	Nat	-	Garcinia succifolia	F	ST	Cytotoxic
407	MUC-1881	Mod	Iridoid glycoside	Santisukia pagetii	Р	LF+TW	Anti-oxidant
408	MUC-1882	Mod	Iridoid glycoside	Santisukia pagetii	Р	LF+TW	Anti-oxidant
409	MUC-1883	Nat	-	Phyllanthus taxodiifolius	F	PX	Mechanistic study of anti-cancer effect
410	MUC-1884	Nat	-	Phyllanthus taxodiifolius	F	PX	Mechanistic study of anti-cancer effect
411	MUC-1185	Nat	-	Phyllanthus taxodiifolius	F	PX	Mechanistic study of anti-cancer effect
412	MUC-1186	Nat	-	Phyllanthus taxodiifolius	F	PX	Mechanistic study of anti-cancer effect
413	MUC-1187	Nat	-	Phyllanthus taxodiifolius	F	PX	Mechanistic study of anti-cancer effect
414	MUC-1189	Nat	-	Phyllanthus taxodiifolius	F	PX	Mechanistic study of anti-cancer effect
415	MUC-1890	Nat	-	Phyllanthus taxodiifolius	F	PX	Mechanistic study of anti-cancer effect
416	MUC-1891	Nat	-	Phyllanthus taxodiifolius	F	PX	Mechanistic study of anti-cancer effect
417	MUC-1892	Nat	-	Phyllanthus taxodiifolius	F	PX	Mechanistic study of anti-cancer effect
418	MUC-1893	Nat	-	Phyllanthus taxodiifolius	F	PX	Mechanistic study of anti-cancer effect
419	MUC-1894	Mod	Chalcone derivative	Boesenbergia rotunda	Р	RZ	Anti-diabetic
420	MUC-1895	Mod	Chalcone derivative	Boesenbergia rotunda	Р	RZ	Anti-diabetic

No	CODE	Nat/Mod/Syn compound	Type of Compound	Plant Source	Extract (E)/ Fraction (F)/Pure (P)	Plant part	Assay
421	MUC-1896	Mod	Chalcone derivative	Boesenbergia rotunda	Р	RZ	Anti-diabetic
422	MUC-1897	Nat	Triterpenoid	Garcinia succifolia	Р	ST	Cytotoxic
423	MUC-1898	Nat	Triterpenoid	Garcinia succifolia	Р	ST	Cytotoxic
424	MUC-1899	Nat	Xanthone	Garcinia succifolia	Р	ST	Cytotoxic
425	MUC-1900	Nat	Xanthone	Garcinia succifolia	Р	ST	Cytotoxic
426	MUC-1901	Nat	Xanthone	Garcinia succifolia	Р	ST	Cytotoxic
427	MUC-1912	Nat	-	Phyllanthus taxodiifolius	F	PX	Mechanistic study of anti-cancer effect
428	MUC-1913	Nat	-	Phyllanthus taxodiifolius	F	PX	Mechanistic study of anti-cancer effect
429	MUC-1914	Nat	-	Phyllanthus taxodiifolius	F	PX	Mechanistic study of anti-cancer effect
430	MUC-1916	Nat	-	Phyllanthus taxodiifolius	F	PX	Mechanistic study of anti-cancer effect
431	MUC-1917	Nat	-	Clitoria ternatea	E	Fl	Anti-diabetic
432	MUC-1918	Nat	Xanthone	Garcinia succifolia	Р	ST	Cytotoxic
433	MUC-1919	Nat	Xanthone	Garcinia succifolia	Р	ST	Cytotoxic
434	MUC-1920	Nat	Xanthone	Garcinia succifolia	Р	ST	Cytotoxic
435	MUC-1921	Nat	Benzoic derivative	Garcinia succifolia	Р	ST	Cytotoxic
436	MUC -102	Nat	Sesquiterpenoid	Goniothalamus aurantiacus	Р	LF+TW	Cytotoxic
437	MUC-105	Nat	Flavanone derivative	Goniothalamus aurantiacus	Р	LF+TW	Cytotoxic

No	CODE	Nat/Mod/Syn compound	Type of Compound	Plant Source	Extract (E)/ Fraction (F)/Pure (P)	Plant part	Assay
438	MUC-108	Nat	Styryllactone	Goniothalamus aurantiacus	Р	LF+TW	Cytotoxic
439	MUC-111	Nat	Styryllactone	Goniothalamus aurantiacus	Р	LF+TW	Cytotoxic
440	MUC-114	Nat	Conjugated amide	Goniothalamus aurantiacus	Р	LF+TW	Cytotoxic
441	MUC-117	Nat	Styryllactone	Goniothalamus aurantiacus	Р	LF+TW	Cytotoxic
442	MUC-121	Nat	Styryllactone	Goniothalamus aurantiacus	Р	LF+TW	Cytotoxic
443	MUC-124	Nat	Styryllactone	Goniothalamus aurantiacus	Р	LF+TW	Cytotoxic
444	MUC-127	Nat	Styryllactone	Goniothalamus aurantiacus	Р	LF+TW	Cytotoxic
445	MUC-130	Nat	Styryllactone	Goniothalamus aurantiacus	Р	LF+TW	Cytotoxic
446	MUC-133	Nat	Triterpenoid	Gardenia carinata	Р	LF+TW	Cytotoxic
447	MUC-136	Nat	Sugar	Gardenia carinata	Р	LF+TW	Cytotoxic
448	MUC-202	Mod	Lignan glycosides	Phyllanthus taxodiifolius	Р	PX	Cytotoxic
449	MUC-203	Mod	Lignan glycosides	Phyllanthus taxodiifolius	Р	PX	Cytotoxic
450	MUC-207	Nat	Xanthones	Garcinia succifolia	Р	LF+TW	CYtotoxic
451	MUC-210	Nat	Xanthones	Garcinia succifolia	Р	LF+TW	CYtotoxic
452	MUC-213	Nat	Triterpenoid	Garcinia succifolia	Р	LF+TW	CYtotoxic
453	MUC-216	Nat	Xanthone	Garcinia succifolia	Р	LF+TW	CYtotoxic
454	MUC-219	Nat	Benzophenone derivative	Garcinia succifolia	Р	LF+TW	CYtotoxic
455	MUC-256	Nat	-	Mallotus glomerulatus	E	LF+TW	Cytotoxic

No	CODE	Nat/Mod/Syn compound	Type of Compound	Plant Source	Extract (E)/ Fraction (F)/Pure (P)	Plant part	Assay
456	MUC-257	Nat	-	Mallotus glomerulatus	F	LF+TW	Cytotoxic
457	MUC-258	Nat	-	Mallotus glomerulatus	F	LF+TW	Cytotoxic
458	MUC-259	Nat	-	Mallotus glomerulatus	F	LF+TW	Cytotoxic
459	MUC-260	Nat	-	Mallotus glomerulatus	F	LF+TW	Cytotoxic
460	MUC-261	Nat	-	Mallotus glomerulatus	F	LF+TW	Cytotoxic
461	MUC-262	Nat	-	Mallotus glomerulatus	F	LF+TW	Cytotoxic
462	MUC-263	Nat	-	Mallotus glomerulatus	F	LF+TW	Cytotoxic
463	MUC-265	Nat	-	Mallotus glomerulatus	F	LF+TW	Cytotoxic
464	MUC-266	Nat	-	Mallotus glomerulatus	F	LF+TW	Cytotoxic
465	MUC-268	Mod	Styryllatone derivative	Goniothalamus aurantiacus	Р	LF+TW	Cytotoxic
466	MUC-269	Mod	Styryllatone derivative	Goniothalamus aurantiacus	Р	LF+TW	Cytotoxic
467	MUC-270	Mod	Styryllatones derivative	Goniothalamus aurantiacus	Р	LF+TW	Cytotoxic
468	MUC-276	Mod	Styryllatones derivative	Goniothalamus aurantiacus	Р	LF+TW	Cytotoxic
469	MUC-277	Nat	-	Cleistanthus myrianthus	E	LF+TW	Cytotoxic
470	MUC-278	Nat	-	Cleistanthus myrianthus	F	LF+TW	Cytotoxic
471	MUC-279	Nat	-	Cleistanthus myrianthus	F	LF+TW	Cytotoxic
472	MUC-280	Nat	-	Cleistanthus myrianthus	F	LF+TW	Cytotoxic
473	MUC-281	Nat	-	Cleistanthus myrianthus	F	LF+TW	Cytotoxic

No	CODE	Nat/Mod/Syn compound	Type of Compound	Plant Source	Extract (E)/ Fraction (F)/Pure (P)	Plant part	Assay
474	MUC-282	Nat	-	Cleistanthus myrianthus	F	LF+TW	Cytotoxic
475	MUC-283	Nat	-	Cleistanthus myrianthus	F	LF+TW	Cytotoxic
476	MUC-284	Nat	-	Cleistanthus myrianthus	F	LF+TW	Cytotoxic
477	MUC-285	Nat	-	Cleistanthus myrianthus	F	LF+TW	Cytotoxic
478	MUC-286	Nat	-	Cleistanthus myrianthus	F	LF+TW	Cytotoxic
479	MUC-287	Nat	-	Cleistanthus myrianthus	F	LF+TW	Cytotoxic
480	MUC-288	Nat	-	Cleistanthus myrianthus	F	LF+TW	Cytotoxic
481	MUC-313	Nat	-	Cleistanthus hirsutulus	Е	LF+TW	Cytotoxic
482	MUC-314	Nat	-	Cleistanthus denudatus	F	LF+TW	Cytotoxic
483	MUC-315	Nat	-	Cleistanthus denudatus	F	LF+TW	Cytotoxic
484	MUC-316	Nat	-	Cleistanthus denudatus	F	LF+TW	Cytotoxic
485	MUC-325	Nat	-	Bauhinia ordata	F	PX	Cytotoxic
486	MUC-326	Nat	-	Bauhinia ordata	F	PX	Cytotoxic
487	MUC-327	Nat	-	Bauhinia ordata	F	PX	Cytotoxic
488	MUC-328	Nat	-	Bauhinia ordata	F	PX	Cytotoxic
489	MUC-329	Nat	-	Bauhinia ordata	F	PX	Cytotoxic
490	MUC-330	Nat	-	Bauhinia ordata	F	PX	Cytotoxic
491	MUC-331	Nat	-	Bauhinia ordata	F	PX	Cytotoxic

		Nat/Mod/Syn			Extract (E)/		
No	CODE	compound	Type of Compound	Plant Source	Fraction (F)/Pure (P)	Plant part	Assay
492	MUC-332	Nat	-	Bauhinia ordata	F	PX	Cytotoxic
493	MUC-349	Nat	Flavanone	Goniothalamus calvicapus	Р	LF+TW	Cytotoxic
494	MUC-350	Nat	Styryllatone	Goniothalamus calvicapus	Р	LF+TW	Cytotoxic
495	MUC-351	Nat	Styryllatone	Goniothalamus calvicapus	Р	LF+TW	Cytotoxic
496	MUC-352	Nat	Styryllatones	Goniothalamus calvicapus	Р	LF+TW	Cytotoxic
497	MUC-353	Nat	Styryllatones	Goniothalamus calvicapus	Р	LF+TW	Cytotoxic
498	MUC-354	Nat	Styryllatone	Goniothalamus calvicapus	Р	LF+TW	Cytotoxic
499	MUC-355	Nat	Triterpenoid	Goniothalamus calvicapus	Р	LF+TW	Cytotoxic
500	MUC-356	Nat	Triterpenoid	Goniothalamus calvicapus	Р	LF+TW	Cytotoxic
501	MUC-373	Nat	-	Cleistanthus denudatus	F	LF+TW	Cytotoxic
502	MUC-374	Nat	-	Cleistanthus denudatus	F	LF+TW	Cytotoxic
503	MUC375	Nat	-	Cleistanthus denudatus	F	LF+TW	Cytotoxic
504	MUC-376	Nat	-	Cleistanthus denudatus	F	LF+TW	Cytotoxic
505	MUC-377	Nat	-	Cleistanthus denudatus	F	LF+TW	Cytotoxic
<u>506</u>	<u>MUC-378</u>	<u>Nat</u>	Ē	<u>Cleistanthus denudatus</u>	<u>E</u>	<u>LF+TW</u>	<u>Cytotoxic</u>
507	MUC-379	Nat	-	Cleistanthus denudatus	F	LF+TW	Cytotoxic
508	MUC-380	Nat	-	Cleistanthus denudatus	F	LF+TW	Cytotoxic
509	MUC-397	Mod	Lignan glycoside	Phyllanthus taxodiifolius	Р	PX	Cytotoxic

No	CODE	Nat/Mod/Syn compound	Type of Compound	Plant Source	Extract (E)/ Fraction (F)/Pure (P)	Plant part	Assay
510	MUC-398 (1)	Nat	Lignan glycoside	Phyllanthus taxodiifolius	Р	PX	Cytotoxic
511	MUC-398 (2)	Nat	Lignan glycoside	Phyllanthus taxodiifolius	Р	PX	Cytotoxic
512	MUC-398 (3)	Nat	Lignan glycoside	Phyllanthus taxodiifolius	Р	PX	Cytotoxic
513	MUC-398 (4)	Nat	Lignan glycoside	Phyllanthus taxodiifolius	Р	PX	Cytotoxic
514	MUC-398 (5)	Nat	Lignan glycoside	Phyllanthus taxodiifolius	Р	PX	Cytotoxic
515	MUC-399 (1)	Nat	Lignan glycoside	Phyllanthus taxodiifolius	Р	PX	Cytotoxic
516	MUC-399 (2)	Nat	Lignan glycoside	Phyllanthus taxodiifolius	Р	PX	Cytotoxic
517	MUC-399 (3)	Nat	Lignan glycoside	Phyllanthus taxodiifolius	Р	PX	Cytotoxic
518	MUC-399 (4)	Nat	Lignan glycoside	Phyllanthus taxodiifolius	Р	PX	Cytotoxic
519	MUC-399 (5)	Nat	Lignan glycoside	Phyllanthus taxodiifolius	Р	PX	Cytotoxic
520	MUC-400	Mod	Styryllactone derivative	Goniothalamus aurantiacus	Р	LF+TW	Cytotoxic
521	MUC-404	Nat	-	Cleistanthus hirsutulus	F	LF+TW	Cytotoxic
522	MUC-405	Nat	-	Cleistanthus hirsutulus	F	LF+TW	Cytotoxic
523	MUC-406	Nat	-	Cleistanthus hirsutulus	F	LF+TW	Cytotoxic
524	MUC-407	Nat	-	Cleistanthus hirsutulus	F	LF+TW	Cytotoxic
525	MUC-408	Nat	-	Cleistanthus hirsutulus	F	LF+TW	Cytotoxic
526	MUC-409	Nat	-	Cleistanthus hirsutulus	F	LF+TW	Cytotoxic
527	MUC-410	Nat	-	Cleistanthus hirsutulus	F	LF+TW	Cytotoxic

No	CODE	Nat/Mod/Syn compound	Type of Compound	Plant Source	Extract (E)/ Fraction (F)/Pure (P)	Plant part	Assay
528	MUC-411	Nat	-	Cleistanthus hirsutulus	F	LF+TW	Cytotoxic
529	MUC-412	Nat	-	Cleistanthus hirsutulus	F	LF+TW	Cytotoxic
530	MUC-413	Nat	-	Cleistanthus hirsutulus	F	LF+TW	Cytotoxic
531	MUC-434	Nat	-	Gardenia sessiliflora	Е	LF+TW	Cytotoxic
532	MUC-435	Nat	-	Gardenia sessiliflora	F	LF+TW	Cytotoxic
533	MUC-436	Nat	-	Gardenia sessiliflora	F	LF+TW	Cytotoxic
534	MUC-437	Nat	-	Gardenia sessiliflora	F	LF+TW	Cytotoxic
535	MUC-438	Nat	-	Gardenia sessiliflora	F	LF+TW	Cytotoxic
536	MUC-439	Nat	-	Gardenia sessiliflora	F	LF+TW	Cytotoxic
537	MUC-440	Nat	-	Gardenia sessiliflora	F	LF+TW	Cytotoxic
538	MUC-441	Nat	-	Gardenia sessiliflora	F	LF+TW	Cytotoxic
539	MUC-442	Nat	-	Gardenia sessiliflora	F	LF+TW	Cytotoxic
540	MUC-443	Nat	-	Gardenia sessiliflora	F	LF+TW	Cytotoxic
541	MUC-496 (1)	Mod	Lignan glycoside	Phyllanthus taxodiifolius	Р	PX	Cytotoxic
542	MUC-496 (2)	Mod	Lignan glycoside	Phyllanthus taxodiifolius	Р	PX	Cytotoxic
543	MUC-496 (3)	Mod	Lignan glycoside	Phyllanthus taxodiifolius	Р	PX	Cytotoxic
544	MUC-507	Nat	-	Bauhinia harmsiana	E	LF	Cytotoxic
545	MUC-508	Nat	-	Bauhinia harmsiana	F	LF	Cytotoxic

No	CODE	Nat/Mod/Syn compound	Type of Compound	Plant Source	Extract (E)/ Fraction (F)/Pure (P)	Plant part	Assay
546	MUC-509	Nat	-	Bauhinia harmsiana	F	LF	Cytotoxic
547	MUC-510	Nat	-	Bauhinia harmsiana	F	LF	Cytotoxic
548	MUC-511	Nat	-	Bauhinia harmsiana	F	LF	Cytotoxic
549	MUC-512	Nat	-	Bauhinia harmsiana	F	LF	Cytotoxic
550	MUC-513	Nat	-	Bauhinia harmsiana	F	LF	Cytotoxic
551	MUC-514	Nat	-	Bauhinia harmsiana	F	LF	Cytotoxic
552	MUC-515	Nat	-	Bauhinia harmsiana	F	LF	Cytotoxic
553	MUC-539	Nat	Triterpenoid	Mallotus glomerulatus	Р	LF+TW	Cytotoxic
554	MUC-540	Nat	Flavone	Mallotus glomerulatus	Р	LF+TW	Cytotoxic
555	MUC-541	Nat	Xanthone	Mallotus glomerulatus	Р	LF+TW	Cytotoxic
556	MUC-542	Nat	Flavanone	Mallotus glomerulatus	Р	LF+TW	Cytotoxic
557	MUC-543	Nat	Chalcone	Mallotus glomerulatus	Р	LF+TW	Cytotoxic
558	MUC-544	Nat	Lignan	Polyaltha glauca	Р	LF+TW	Cytotoxic
559	MUC-545	Nat	Lignan	Polyaltha glauca	Р	LF+TW	Cytotoxic
560	MUC-546	Mod	Lignan	Polyaltha glauca	F	LF+TW	Cytotoxic
561	MUC-568 (1)	Mod	Lignan glycoside	Phyllanthus taxodiifolius	Р	PX	Cytotoxic
562	MUC-568 (2)	Mod	Lignan glycoside	Phyllanthus taxodiifolius	Р	PX	Cytotoxic
563	MUC-569 (1)	Mod	Lignan glycoside	Phyllanthus taxodiifolius	Р	PX	Cytotoxic

No	CODE	Nat/Mod/Syn	Type of Compound	Plant Source	Extract (E)/	Plant part	Assay
110	CODE	compound	Type of Compound	rtant source	Fraction (F)/Pure (P)	rtant part	Assay
564	MUC-569 (2)	Mod	Lignan glycoside	Phyllanthus taxodiifolius	Р	PX	Cytotoxic
565	MUC-570 (1)	Mod	Lignan glycoside	Phyllanthus taxodiifolius	Р	PX	Cytotoxic
566	MUC-570 (2)	Mod	Lignan glycoside	Phyllanthus taxodiifolius	Р	PX	Cytotoxic
567	MUC-571 (1)	Mod	Lignan glycoside	Phyllanthus taxodiifolius	Р	PX	Cytotoxic
568	MUC-571 (2)	Mod	Lignan glycoside	Phyllanthus taxodiifolius	Р	PX	Cytotoxic
569	MUC-572 (1)	Mod	Lignan glycoside	Phyllanthus taxodiifolius	Р	PX	Cytotoxic
570	MUC-572 (2)	Mod	Lignan glycoside	Phyllanthus taxodiifolius	Р	PX	Cytotoxic
571	MUC-573 (1)	Mod	Lignan glycoside	Phyllanthus taxodiifolius	Р	PX	Cytotoxic
572	MUC-573 (2)	Mod	Lignan glycoside	Phyllanthus taxodiifolius	Р	PX	Cytotoxic
573	MUC-584	Mod	Styryllactone derivqtive	Gardenia carinata	Р	LF+TW	Cytotoxic
574	MUC-585 (1)	Mod	Lignan glycoside	Phyllanthus taxodiifolius	Р	PX	Cytotoxic
575	MUC-585 (2)	Mod	Lignan glycoside	Phyllanthus taxodiifolius	Р	PX	Cytotoxic
576	MUC-586	Mod	Lignan glycoside	Phyllanthus taxodiifolius	Р	PX	Cytotoxic
577	MUC-587	Mod	Lignan glycoside	Phyllanthus taxodiifolius	Р	PX	Cytotoxic
578	MUC-599	Nat	Lignan glycoside	Phyllanthus taxodiifolius	Р	PX	Cytotoxic
579	MUC-600	Mod	Lignan	Phyllanthus taxodiifolius	Р	PX	Cytotoxic
580	MUC-601	Mod	Lignan glycoside	Phyllanthus taxodiifolius	Р	PX	Cytotoxic
581	MUC-602	Mod	Lignan glycoside	Phyllanthus taxodiifolius	Р	PX	Cytotoxic

No	CODE	Nat/Mod/Syn compound	Type of Compound	Plant Source	Extract (E)/ Fraction (F)/Pure (P)	Plant part	Assay
582	MUC-603 (1)	Mod	Lignan glycoside	Phyllanthus taxodiifolius	Р	PX	Cytotoxic
583	MUC-603 (2)	Mod	Lignan glycoside	Phyllanthus taxodiifolius	Р	PX	Drug delivery
584	MUC-604	Nat	-	Garcinia succifolia	E	ST	Cytotoxic
585	MUC-605	Nat	-	Garcinia succifolia	F	ST	Cytotoxic
586	MUC-606	Nat	-	Garcinia succifolia	F	ST	Cytotoxic
587	MUC-607	Nat	-	Garcinia succifolia	F	ST	Cytotoxic
588	MUC-608	Nat	-	Garcinia succifolia	F	ST	Cytotoxic
589	MUC-609	Nat	-	Garcinia succifolia	F	ST	Cytotoxic
590	MUC-625	Nat	-	Nauclea orientalis	E	LF+TW	Anti-diabetic
591	MUC-626	Nat	-	Nauclea orientalis	E	LF+TW	Anti-diabetic
592	MUC-627	Nat	-	Nauclea orientalis	E	LF+TW	Anti-diabetic
593	MUC-651	Nat	Styryllactone	Goniothalamus calvicapus	Р	LF+TW	Cytotoxic
594	MUC-652	Nat	Alkaloid	Goniothalamus calvicapus	Р	LF+TW	Cytotoxic
595	MUC-653	Nat	Alkaloid	Goniothalamus calvicapus	Р	LF+TW	Cytotoxic
596	MUC-654	Nat	Conjugated amide	Goniothalamus calvicapus	Р	LF+TW	Cytotoxic
597	MUC-655	Nat	Flavanone	Goniothalamus calvicapus	Р	LF+TW	Cytotoxic
598	MUC-656	Nat	Styryllactone	Goniothalamus calvicapus	Р	LF+TW	Cytotoxic
599	MUC-657	Nat	Styryllactone	Goniothalamus calvicapus	Р	LF+TW	Cytotoxic

No	CODE	Nat/Mod/Syn compound	Type of Compound	Plant Source	Extract (E)/ Fraction (F)/Pure (P)	Plant part	Assay
600	MUC-658	Nat	Styryllactone	Goniothalamus calvicapus	P	LF+TW	Cytotoxic
601	MUC-659	Nat	Styryllactone	Goniothalamus calvicapus	Р	LF+TW	Cytotoxic
602	MUC-660	Nat	Styryllactone	Goniothalamus calvicapus	Р	LF+TW	Cytotoxic
603	MUC-661	Nat	Triterpenoid	Goniothalamus calvicapus	Р	LF+TW	Cytotoxic
604	MUC-662	Nat	Triterpenoid	Goniothalamus calvicapus	Р	LF+TW	Cytotoxic
605	MUC-663	Nat	Styryllactone	Goniothalamus calvicapus	Р	LF+TW	Cytotoxic
606	MUC-664	Nat	Alkaloid	Goniothalamus calvicapus	Р	LF+TW	Cytotoxic
607	MUC-665	Nat	Alkaloid	Goniothalamus calvicapus	Р	LF+TW	Cytotoxic
608	MUC-666	Nat	Conjugated amide	Goniothalamus calvicapus	Р	LF+TW	Cytotoxic
609	MUC-667	Nat	Xanthone	Garcinia succifolia	Р	LF+TW	Cytotoxic
610	MUC-668	Nat	Xanthone	Garcinia succifolia	Р	LF+TW	Cytotoxic
611	MUC-669	Nat	Triterpenoid	Garcinia succifolia	Р	LF+TW	Cytotoxic
612	MUC-670	Nat	Xanthone	Garcinia succifolia	Р	LF+TW	Cytotoxic
613	MUC-671	Nat	Xanthone	Garcinia succifolia	Р	LF+TW	Cytotoxic
614	MUC-672	Nat	Xanthone	Garcinia succifolia	Р	LF+TW	Cytotoxic
615	MUC-673	Nat	Benzophenone derivative	Garcinia succifolia	Р	LF+TW	Cytotoxic
616	MUC-674	Nat	triterpenoid	Garcinia succifolia	Р	LF+TW	Cytotoxic
617	MUC-675	Nat	Xanthone	Garcinia succifolia	Р	LF+TW	Cytotoxic

		Nat/Mod/Syn			Extract (E)/		
No	CODE	compound	Type of Compound	Plant Source	Fraction (F)/Pure (P)	Plant part	Assay
618	MUC-676	Nat	Xanthone	Garcinia succifolia	Р	LF+TW	Cytotoxic
619	MUC-677	Nat	Xanthone	Garcinia succifolia	Р	LF+TW	Cytotoxic
620	MUC-678	Nat	Xanthone	Garcinia succifolia	Р	LF+TW	Cytotoxic
621	MUC-679	Nat	Xanthone	Garcinia succifolia	Р	LF+TW	Cytotoxic
622	MUC-680	Nat	Xanthone	Garcinia succifolia	Р	LF+TW	Cytotoxic
623	MUC-681	Nat	Xanthone	Garcinia succifolia	Р	LF+TW	Cytotoxic
624	MUC-682	Nat	Xanthone	Garcinia succifolia	Р	LF+TW	Cytotoxic
625	MUC-683	Nat	Xanthone	Garcinia succifolia	Р	LF+TW	Cytotoxic
626	MUC-701	Nat	-	Memecylon geddesianum	E	LF+TW	Cytotoxic
627	MUC-702	Nat	-	Memecylon geddesianum	F	LF+TW	Cytotoxic
628	MUC-703	Nat	-	Memecylon geddesianum	F	LF+TW	Cytotoxic
629	MUC-704	Nat	-	Memecylon geddesianum	F	LF+TW	Cytotoxic
630	MUC-705	Nat	-	Memecylon geddesianum	F	LF+TW	Cytotoxic
631	MUC-706	Nat	-	Memecylon geddesianum	F	LF+TW	Cytotoxic
632	MUC-707	Nat	-	Memecylon geddesianum	F	LF+TW	Cytotoxic
633	MUC-722	Mod	Lignan glycoside	Phyllanthus taxodiifolius	Р	PX	Cytotoxic
634	MUC-723	Mod	Lignan glycoside	Phyllanthus taxodiifolius	Р	PX	Cytotoxic
635	MUC-724	Mod	Styryllactone derivative	Goniothalamus aurantiacus	Р	LF+TW	Cytotoxic

No	CODE	Nat/Mod/Syn	Type of Compound	Plant Source	Extract (E)/	Plant part	Assay
INO	CODE	compound	Type of Compound	Flant Source	Fraction (F)/Pure (P)	Plant part	Assay
636	MUC-725	Mod	Styryllactone derivative	Goniothalamus aurantiacus	Р	LF+TW	Cytotoxic
637	MUC-726	Mod	Styryllactone derivative	Goniothalamus aurantiacus	Р	LF+TW	Cytotoxic
638	MUC-727	Mod	Styryllactone derivative	Goniothalamus aurantiacus	Р	LF+TW	Cytotoxic
639	MUC-732	Nat	Flavonol	Zingiber maekongense	Р	RT	Anti-oxidant
640	MUC-759	Nat	Styryllactone	Polyalthia crassa	Р	LF+TW	Anti-inflammatory
641	MUC-760	Nat	Styryllactone	Polyalthia crassa	Р	LF+TW	Anti-inflammatory
642	MUC-761	Nat	Xanthone	Garcinia succifolia	Р	LF+TW	Anti-inflammatory
643	MUC-762	Nat	Xanthone	Garcinia succifolia	Р	LF+TW	Anti-inflammatory
644	MUC-763	Nat	Xanthone	Garcinia succifolia	Р	LF+TW	Anti-inflammatory
645	MUC-764	Nat	Benzophenone derivative	Garcinia succifolia	Р	LF+TW	Anti-inflammatory
646	MUC-765	Nat	Benzophenone derivative	Garcinia succifolia	Р	LF+TW	Anti-inflammatory
647	MUC-778	Nat	-	Santisukia pagetii	E	LF+TW	Cytotoxic
648	MUC-779	Nat	-	Santisukia pagetii	F	LF+TW	Cytotoxic
649	MUC-780	Nat	-	Santisukia pagetii	F	LF+TW	Cytotoxic
650	MUC-781	Nat	-	Santisukia pagetii	F	LF+TW	Cytotoxic
651	MUC-782	Nat	-	Santisukia pagetii	F	LF+TW	Cytotoxic
652	MUC-783	Nat	-	Santisukia pagetii	F	LF+TW	Cytotoxic
653	MUC-784	Nat	-	Santisukia pagetii	F	LF+TW	Cytotoxic

No	CODE	Nat/Mod/Syn compound	Type of Compound	Plant Source	Extract (E)/ Fraction (F)/Pure (P)	Plant part	Assay
654	MUC-785	Nat	-	Santisukia pagetii	F	LF+TW	Cytotoxic
655	MUC-786	Nat	-	Santisukia pagetii	F	LF+TW	Cytotoxic
656	MUC-787	Nat	-	Santisukia pagetii	F	LF+TW	Cytotoxic
657	MUC-808	Nat	-	Goniothalamus calvicarpus	E	ST	Cytotoxic
658	MUC-809	Nat	-	Goniothalamus calvicarpus	F	ST	Cytotoxic
659	MUC-810	Nat	-	Goniothalamus calvicarpus	F	ST	Cytotoxic
660	MUC-811	Nat	-	Goniothalamus calvicarpus	F	ST	Cytotoxic
661	MUC-812	Nat	-	Goniothalamus calvicarpus	F	ST	Cytotoxic
662	MUC-813	Nat	-	Goniothalamus calvicarpus	F	ST	Cytotoxic
663	MUC-814	Nat	-	Goniothalamus calvicarpus	F	ST	Cytotoxic
664	MUC-815	Nat	-	Goniothalamus calvicarpus	F	ST	Cytotoxic
665	MUC-843	Mod	Styryllactone	Goniothalamus aurantiacus	Р	LF+TW	Anti-inflammatory
666	MUC-844	Mod	Lignan glycoside	Phyllanthus taxodiifolius	Р	PX	Cytotoxic in stem cells
667	MUC-845	Mod	Lignan glycoside	Phyllanthus taxodiifolius	Р	PX	Cytotoxic in stem cells
668	MUC-846	Mod	Lignan glycoside	Phyllanthus taxodiifolius	Р	PX	Cytotoxic in stem cells
669	MUC-847	Mod	Lignan glycoside	Phyllanthus taxodiifolius	Р	PX	Cytotoxic in stem cells
670	MUC-848	Mod	Lignan glycoside	Phyllanthus taxodiifolius	Р	PX	Cytotoxic in stem cells
671	MUC-849	Mod	Lignan glycoside	Phyllanthus taxodiifolius	Р	PX	Cytotoxic in stem cells

No	CODE	Nat/Mod/Syn compound	Type of Compound	Plant Source	Extract (E)/ Fraction (F)/Pure (P)	Plant part	Assay
672	MUC-850	Mod	Lignan glycoside	Phyllanthus taxodiifolius	Р	PX	Cytotoxic in stem cells
673	MUC-851	Mod	Lignan glycoside	Phyllanthus taxodiifolius	Р	PX	Cytotoxic in stem cells
674	MUC-852	Mod	Lignan glycoside	Phyllanthus taxodiifolius	Р	PX	Cytotoxic in stem cells
675	MUC-853	Mod	Lignan glycoside	Phyllanthus taxodiifolius	Р	PX	Cytotoxic in stem cells
676	MUC-854	Mod	Lignan glycoside	Phyllanthus taxodiifolius	Р	PX	Cytotoxic in stem cells
677	MUC-856	Mod	Lignan glycoside	Phyllanthus taxodiifolius	Р	PX	Cytotoxic in stem cells
678	MUC-857	Mod	Lignan glycoside	Phyllanthus taxodiifolius	Р	PX	Cytotoxic in stem cells
679	MUC-858	Mod	Lignan glycoside	Phyllanthus taxodiifolius	Р	PX	Cytotoxic in stem cells
680	MUC-859	Mod	Lignan glycoside	Phyllanthus taxodiifolius	Р	PX	Cytotoxic in stem cells
681	MUC-860	Mod	Lignan glycoside	Phyllanthus taxodiifolius	Р	PX	Cytotoxic in stem cells
682	MUC-862	Nat	-	Curcuma sp.	E	RZ	Cytotoxic
683	MUC-873	Nat	-	Boesenbergia thorelii	E	RZ	Cytotoxic
684	MUC-884	Nat	Stryllactone	Goniothalamus calvicarpus	Р	ST	Cytotoxic
685	MUC-885	Nat	Flavanone	Goniothalamus calvicarpus	Р	ST	Cytotoxic
686	MUC-886	Nat	Alkaloid	Goniothalamus calvicarpus	Р	ST	Cytotoxic
687	MUC-887	Nat	Stryllactone	Goniothalamus calvicarpus	Р	ST	Cytotoxic
688	MUC-888	Nat	Flavanone	Goniothalamus calvicarpus	Р	ST	Cytotoxic
689	MUC-889 (1)	Mod	Flavanone	Goniothalamus calvicarpus	Р	ST	Cytotoxic

No	CODE	Nat/Mod/Syn compound	Type of Compound	Plant Source	Extract (E)/ Fraction (F)/Pure (P)	Plant part	Assay
690	MUC-889 (2)	Mod	Stryllactone	Goniothalamus calvicarpus	Р	ST	Cytotoxic
691	MUC-889 (3)	Mod	Stryllactone	Goniothalamus calvicarpus	Р	ST	Cytotoxic
692	MUC-890	Mod	Stryllactone	Goniothalamus aurantiacus	Р	LF+TW	Cytotoxic
693	MUC-891	Mod	Stryllactone	Goniothalamus aurantiacus	Р	LF+TW	Cytotoxic
694	MUC-892	Mod	Stryllactone	Goniothalamus aurantiacus	Р	LF+TW	Cytotoxic
695	MUC-893	Mod	Stryllactone	Goniothalamus aurantiacus	Р	LF+TW	Cytotoxic
696	MUC-894	Mod	Stryllactone	Goniothalamus aurantiacus	Р	LF+TW	Cytotoxic
697	MUC-895	Mod	Stryllactone	Goniothalamus aurantiacuss	Р	LF+TW	Cytotoxic
698	MUC-917	Nat	-	Boesenbergia thorelii	E	RZ	Cytotoxic
699	MUC-918	Nat	-	Boesenbergia thorelii	F	RZ	Cytotoxic
700	MUC-919	Nat	-	Boesenbergia thorelii	F	RZ	Cytotoxic
701	MUC-920	Nat	-	Boesenbergia thorelii	F	RZ	Cytotoxic
702	MUC-921	Nat	-	Boesenbergia thorelii	F	RZ	Cytotoxic
703	MUC-922	Nat	-	Boesenbergia thorelii	F	RZ	Cytotoxic
704	MUC-923	Nat	-	Boesenbergia thorelii	F	RZ	Cytotoxic
705	MUC-924	Nat	-	Boesenbergia thorelii	F	RZ	Cytotoxic
706	MUC-941	Nat	Acetophenone derivative	Mallotus glomerulatus	Р	PX	Cytotoxic
707	MUC-942	Nat	Flavanone	Mallotus glomerulatus	Р	PX	Cytotoxic

No	CODE	Nat/Mod/Syn compound	Type of Compound	Plant Source	Extract (E)/ Fraction (F)/Pure (P)	Plant part	Assay
708	MUC-943	Nat	Diterpenoid	Mallotus glomerulatus	Р	PX	Cytotoxic
709	MUC-944	Nat	Flavone	Mallotus glomerulatus	Р	PX	Cytotoxic
710	MUC-945	Nat	-	Curcuma sp.	F	RZ	Cytotoxic
711	MUC-946	Nat	-	Curcuma sp.	F	RZ	Cytotoxic
712	MUC-947	Nat	-	Curcuma sp.	F	RZ	Cytotoxic
713	MUC-948	Nat	-	Curcuma sp.	F	RZ	Cytotoxic
714	MUC-949	Nat	-	Curcuma sp.	F	RZ	Cytotoxic
715	MUC-950	Nat	-	Curcuma sp.	F	RZ	Cytotoxic
716	MUC-951	Nat	-	Curcuma sp.	F	RZ	Cytotoxic
717	MUC-966 (1)	Nat	Lignan glycoside	Phyllanthus taxodiifolius	Р	PX	Cytotoxic
718	MUC-966 (2)	Nat	Lignan glycoside	Phyllanthus taxodiifolius	Р	PX	Cytotoxic
719	MUC-985	Nat	-	Zingiber junceum	E	RZ	Cytotoxic
720	MUC-986	Nat	-	Zingiber junceum	F	RZ	Cytotoxic
721	MUC-987	Nat	-	Zingiber junceum	F	RZ	Cytotoxic
722	MUC-988	Nat	-	Zingiber junceum	F	RZ	Cytotoxic
723	MUC-989	Nat	-	Zingiber junceum	F	RZ	Cytotoxic
724	MUC-1010	Nat	-	Paris polyphylla	E	RZ	Cytotoxic
725	MUC-1011	Nat	C ₆ C ₃ compound	Zingiber junceum	Р	RZ	Anti-oxidant

Nat = Natural compound, Mod = Modified compound, Syn = Synthetic compound; E = extract, F = fraction, P = Pure compound; PX = Aerial parts, Fl = Flowers, LF+TW = Leaves and twigs, LF = Leaves, ST = Stems, RT = Roots, RZ = Rhizomes

2. Isolation of bioactive compounds from leaves and twigs of Santisukia pagetii

Santisukia pagetii, known in Thai as 'Kanchanika' or 'Kaedong', is a plant in Bignoniaceae family. The plant material was collected from Kanchanaburi province of Thailand.

Dried leaves and twigs of *Santisukia pagetii* were pulverized to yield powdered material (3.1 kg.). Extraction was performed in methanol (7L x 5 times). A crude methanol extract (429.4 g) was obtained after evaporation to dryness. The methanol extract was dissolved in EtOAc: MeOH (1:1) and MeOH respectively. After evaporation to dryness, EtOAc:MeOH (1:1) fraction (277.8 g), MeOH fraction (39.3 g) and residue (54.5 g) were obtained, respectively.

The crude methanol extract and fractions were submitted for cytotoxic activity testing (in collaboration with Dr. Artit Chairoungdua) and anti-HIV-1 activity in RT assay (in collaboration with Dr. Radeekorn Akkarawongsapat). The testing results indicated that all extracts and the residue showed no significant cytotoxic activity in most of cancer cell lines (see Table 1). For anti-HIV-1 activity, the EtOAc-MeOH (1:1) extract was found to be very active in HIV-1-RT assay as shown in Table 2.

The EtOAc-MeOH (1:1) fraction (272.4 g) was further separated by vacuum chromatography, eluting hexanes, EtOAc-hexane, EtOAc, EtOAc-MeOH and finally with MeOH. All fractions were combined on the basis of TLC behavior to provide 6 fractions (F1-F6). The results indicated that fractions F2-F4 exhibited cytotoxic activity in some of cancer cell lines as shown in Table 1.2.

Table 1.2. Cytotoxic activities from extract and fractions of leaves and twigs of Santisukia pagetii

	ED ₅₀ (μ g/mL)									
Extracts/Fractions		Cell lines								
	P-388	KB	HT-29	MCF-7	A549	ASK	Hek 293			
Ellip	0.37	0.46	0.51	0.47	0.46	0.57	0.51			
MeOH Ext.	>20	>20	>20	>20	>20	>20	>20			
EtOAc:MeOH (1:1)	>20	>20	>20	>20	>20	>20	>20			
MeOH	>20	>20	>20	>20	>20	>20	>20			
Residue	>20	>20	>20	>20	>20	>20	>20			
F1	>20	>20	>20	>20	>20	>20	>20			
F2	7.06	18.30	>20	>20	>20	>20	>20			
F3	7.16	>20	>20	>20	>20	>20	>20			
F4	13.14	>20	15.78	12.68	19.68	>20	>20			
F5	>20	>20	>20	>20	>20	>20	>20			
F6	>20	>20	>20	>20	>20	>20	>20			

Results are expressed at ED₅₀ value (μ g/mL); ED₅₀ <20 μ g/mL is considered active.

P-388 = murine lymphocytic leukemia, KB = human nasopharyngeal carcinoma, HT-29 = human colon cancer, MCF-7 = Michigan cancer foundation, human breast cancer, A 549 = human lung cancer, ASK = cell line from rat glioma cell, Hek-293 = human kidney cell

In case of anti-HIV-1 assay, only fraction F4 was found very active as shown in Table 1.3.

Table 1.3 Anti-HIV-1-RT activities from extract and fractions of leaves and twigs of Santisukia pagetii

Extract	Anti-HIV-1-RT					
LAttact	% Inhibition	Activity				
MeOH Ext.	60.43	М				
EtOAc-MeOH (1:1)	72.66	VA				
MeOH	26.49					
Residue	41.57	W				
F1	41.02	W				
F2	43.19	W				
F3	7.86	I				
F4	100.10	VA				
F5	64.40	М				
F6	21.57	inactive				

RT assay: activity > 70% inhibition = very active (VA); >50-70% inhibition = moderately active (M); < 30% inhibition = inactive (I).

Further separation by column chromatography of each fraction was performed as follows:

Fraction F1, eluted by 0-10% EtOAc-hexane, contained mainly fat, therefore it was not further investigated.

Fraction F2, eluted by 15-25% EtOAc-hexane, was further separated by repeated column chromatography to afford triterpenoids, namely pomolic acid-3 β -acetate (1) ursolic acid (2) Line 3-O-acetylursolic acid (3) and a mixture of β -sitosterol/stigmasterol (4a/4b)

Fraction F3, eluted by 30-50% EtOAc-hexane, was further separated by repeated column chromatography to give ursolic acid (2) and a monoterpenoid, which was identified as menthiafolic acid (5) By comparison of the optical rotation value of 5, $[\alpha]_{589}^{26.6}$ +43.7 (c 0.47, CHCl₃) with that in the literature, Lit. $[\alpha]_{589}^{14}$ 18.2 (c 0.22, CHCl₃), the absolute configuration at carbon connected to the hydroxyl group was proved to be *S*. Beside compounds 2 and 5, another triterpenoid, siaresinolic acid (6) was also obtained.

- 1. Yoshikawa K, Satou Y, Tokunaga Y, Tanaka M, Arihara S, Nigam S.K. Four Acylated Triterpenoid Saponins from Albizia procera. J Nat Prod. 1988; 61: 440-445.
- 2. Zou K, Tong W-Y, Liang H, Cui J-R, Tu G-Z, Zhao Y-Y, Zhang R-Y. Diastereoisomeric saponins from Albizia julibrissin. Carbohydrate Reasearch. 2005; 340: 1329-1334.

Fraction F4, eluted by 30-50% EtOAc-hexane, was further separated by repeated column chromatography to provide ursolic acid (2), (6*S*)-menthiafolic acid (5), *p*-coumaric acid (7), caffeic acid (8) and β -sitosterol 3-*O*- β -D-glucopyranoside (9).

Fraction F5, eluted by 80% EtOAc-hexane-30 % MeOH-EtOAc was separated by repeated column chromatography to afford caffeic acid (8), β -sitosterol 3-O- β -D-glucopyranoside (9), ambiguuside (10), specioside (11), verminoside (12), isoquercitrin (13), apigenin-7-neohesperidoside (14), luteolin-7-O-neohes-terioside (15), β -D-maltose (16) and Ω -D-glucose (17)

Fraction F6, eluted by 40% MeOH-EtOAc-100% MeOH, was separated by repeated column chromatography to give β -sitosterol 3-O- β -D-glucopyranoside (9), ambiguuside (10), specioside (11), verminoside (12), apigenin-7-neohesperidoside (14), luteolin-7-O-neohesterioside (15), β -D-maltose (16) and α -D-glucose (17).

All isolated compounds were submitted for biological testings, such as cytotoxic activity in cancer cell lines (in collaboration with Dr. Artit Chairoungdua) and anti-HIV-1 activity (in collaboration with Dr. Radeekorn Akkarawongsapat). The results indicated that no significant cytotoxic activity was observed, but some of the isolated compounds showed significant anti-HIV-1 activities in both syncytium and reverse transcriptase assays as illustrated in Table 1.4.

Table 1.4 Anti-HIV-1 activities of pure isolated compounds from leaves and twigs of *Santisukia pagetii*

		Syncytiu	m assay**		HIV-1	L RT assay***	
Compound	IC ₅₀ (μΜ)	EC ₅₀ (μ Μ)	ΤΊ	Activity	%Inhibition at 200 μ g/mL	Activity	IC ₅₀ (μΜ)
Pomolic acid 3β -acetate	222.24	34.29	6.48	Aa	63.73	М	ND
Ursolic acid	85.50	11.35	7.53	Aa	84.36	VA	318.7
3- <i>O</i> -Acetylursolic acid	39.89	13.42	2.97	Aa	87.19	VA	210.3
Siaresinolic acid	254.24	120.99	2.1	Aa	37.00	W	ND
Specioside	>246	136.97	>1.80	Aa	12.59	I	ND
Verminoside	153.89	124.66	1.23	Aa	27.34	1	ND
Ambiguuside	>237	61.21	3.87	Aa	3.49	1	ND
Luteolin-7 <i>-O-</i> neohesperidoside	40.85	53.23	0.77	Т	70.37	VA	1016.5*
Apigenin-7- <i>O</i> -neohesperidoside	>762	>762	-	la	3.70	ı	ND
Isoquercitrin	36.77	99.09	0.37	T	15.98	I	ND
<i>p</i> -Coumaric acid	>210	>210	-	la	60.89	М	ND
Caffeic acid	>216	123.48	>1.75	Aa	40.90	W	ND
(6S)-Menthiafolic acid	>269	201.17	>1.31	Aa	44.16	W	ND

^{**} Syncytium reduction assay: EC_{50} = dose of compound that reduced 50% syncytium formation by $^{\Delta Tat/Rev}$ MC99 virus in 1A2 cells. AZT, averaged from four experiments, EC50 1.87 x 10-8 μ M; Aa = active (TI >1), Ia = inactive, T= toxic (IC50 is less than the lowest concentration tested), TI = Therapeutic Index (TI = IC₅₀/EC₅₀)

A manuscript concerning this work has been accepted for publication in Natural Product Communications 2018.

3. Structure modification of iridoid glycosides: ambiguuside (10), specioside (11), verminoside (12)

The structures of ambiguuside (10), specioside (11), verminoside (12) were modified by conversion to their acetate derivatives 18-20 by the chemical reaction with acetic anhydride/DMAP at room temperature

^{***} RT assay: Compounds were prescreened at 200 μ g/mL. Only those that were very active at this concentration were further determined for IC50, the dose that inhibited 50% HIV-1 RT activity; VA= very active, M = moderately active, W = weakly active, I = inactive, ND = not determined. Positive controls, averaged from one experiments. IC50 nevirapine 9.21 μ M.

The natural compounds 10-12 and modified compounds 18-20 submitted for biological testings, i.e. anti-Alzheimer's and anti-oxidant activities (in collaboration with Dr. Wichuda Sangsawang).

4. Isolation of bioactive compounds from stems of Goniothalamus calvicarpus

Goniothalamus calvicarpus known in Thai as 'Sa-Ban-Nga-Pa', is a plant in Annonaceae family. The plant material was collected from Chiang Mai province of Thailand.

The dried stems of *Goniothalamus calvicarpus* were pulverized to give powdered material (6.9 kg). Extraction was performed in methanol (16L x 6 times). A crude methanol extract (319.6 g) was obtained after evaporation to dryness. The methanol extract was dissolved in EtOAc:MeOH (1:1) and MeOH respectively. After evaporation to dryness, EtOAc:MeOH (1:1) fraction (267.8 g), MeOH fraction (28.2 g) and residue (22.6 g) were obtained, respectively.

The dried extract and fractions were submitted for cytotoxic activity testing (in collaboration with Dr. Artit Chairoungdua) and anti-HIV-1 activity in RT assay (in collaboration with Dr. Radeekorn Akkarawongsapat). The testing results indicated that the EtOAc:MeOH (1:1) fraction was the most active in cytotoxic and HIV-1-RT assays as shown in Tables 1.4 and 1.5.

The EtOAc-MeOH (1:1) fraction (267.6 g) was further separated by vacuum chromatography, eluting hexanes, EtOAc-hexane, EtOAc, EtOAc-MeOH and finally with MeOH. All fractions were combined on the basis of TLC behavior to provide 6 fractions (F1-F5). The results indicated that fractions F2, F3 and -F5 exhibited cytotoxic activity in some of cancer cell lines as shown in Table 1.4. In case of HIV-1 RT assay, only F2 was found to be very active (see Table 1.5).

Table 1.5 Cytotoxic activities from extracts and fractions of the stems of *Goniothalamus* calvicarpus

Fraction	,	Cell line (ED ₅₀ µg/mg)							
Fraction	P-388	KB	HT29	MCF-7	A549	ASK	Hek 293		
Ellipticine	0.39	0.51	0.62	0.45	0.54	0.51	0.60		
EtOAc:MeOH (1:1)	<4	4.28	<4	<4	<4	8.16	<4		
MeOH	<4	14.03	5.97	8.84	3.93	12.11	3.35		
Residue	15.16	>20	>20	>20	>20	>20	13.01		
F1	>20	>20	>20	>20	>20	>20	>20		
F2	<4	12.74	11.92	10.80	5.68	10.83	10.20		
F3	<4	<4	<4	<4	<4	<4	<4		
F4	>20	>20	>20	>20	>20	>20	>20		
F5	4	0.94	3.46	3.82	3.49	9.88	1.39		

Results are expressed at ED $_{50}$ value (μ g/mL); ED $_{50}$ <20 μ g/mL is considered active.

P-388 = murine lymphocytic leukemia, KB = human nasopharyngeal carcinoma, HT-29 = human colon cancer, MCF-7 = Michigan cancer foundation, human breast cancer, A 549 = human lung cancer, ASK = cell line from rat glioma cell, Hek-293 = human kidney cell

Table 1.6 Anti-HIV-1-RT activities from the extracts and fractions of the stems of *Goniothalamus calvicarpus*

	Anti-HIV-1-RT (at 200 μ g/mL)					
Extract/Fraction	% Inhibition	Activity				
EtOAc:MeOH (1:1)	94.51	VA				
MeOH	32.96	W				
Residue	39.63	W				
F1	11.96	I				
F2	97.53	VA				
F3	42.31	W				
F4	-21.88	I				
F5	12.74	I				

RT assay: VA= very active (>70% inhibition), M = moderately active (>50% to 70% inhibition), W = weakly active (30% to 50% inhibition), W = moderately active (<30% inhibition)

Table 1.7 Anti-HIV 1 activities in the anti-syncytium assay from extract and fractions of the stems of *Goniothalamus calvicarpus*

Fraction	Fraction IC ₅₀	IC ₅₀ EC ₅₀	SI	A ctiv (it)	AZT			
Fraction	IC ₅₀	C_{50} C_{50} C_{50} C_{50}	Activity	IC ₅₀	EC ₅₀	SI		
EtOAc:MeOH (1:1)	16.13	<7.8	>2.07	А				
MeOH	219.38	44.49	4.93	А		1.75 × 10 ⁻⁹	> 5.71	
Residue	155.33	29.14	5.33	А	۰			
F1	111.16	30.90	3.6	А	> 10 ⁻⁸			
F2	-	-	-	Т				
F3	-	-	-	Ţ				
F4	233.98	79.62	2.94	А				
F5	-	-	-	Т				

Syncytium reduction assay: A = active, I = inactive, T= toxic, SI = Selectivity Index (SI = IC_{50}/EC_{50})

Further separation by column chromatography of each fraction was performed as follows:

Fraction F1, eluted by 10-20% EtOAc-hexanes, was further separated by repeated column chromatography to afford ethyl 4-methoxycinnamate (1)

Fraction A2, eluted by 30-50% EtOAc-hexanes, was separated by repeated column chromatography to provide ethyl 4-methoxycinnamate (1), (–)-pinocembrin (2), (–)-mellein (3), (+)-goniothalamin (4), (+)-goniopypyrone (5), (+)-altholactone (6) and a mixture of β -sitosterol)/stigmasterol (7a/7b).

MeO
$$OCH_2CH_3$$
 OCH_2CH_3 OCH_2CH_3

Fraction A3, eluted by 60-100% EtOAc-hexanes, was separated by repeated column chromatography to provide (–)-pinocembrin (2), (+)-goniopypyrone (5), (+)-altholactone (6), aristolactam AII (8) aristolactam BII (9), (+)-goniodiol-7-monoacetate (10), (+)-goniodiol (11), (+)-goniofufurone (12), (–)-naringenin (13), velutinam (14), (+)-eriodictyol (15), (+)-goniotriol (16), (+)-8-epi-goniofufurone (17), paprazine (18), aristolactam AIIIa (19) and (+)-cardiobutanolide (20).

Fraction A4, eluted by 5-30% MeOH-EtOAc, was further separated by repeated column chromatography to give (+)-altholactone (6), (+)-goniofufurone (12), (+)-cardiobutanolide (20) and lysicamine (21).

Fraction A5, eluted by 40-100% EtOAc, was separated by repeated column chromatography to afford (+)-goniofufurone (12).

All isolated compounds were submitted for biological testings, such as cytotoxic activity in cancer cell lines in collaboration with Dr. Artit Chairoungdua

Table 1.8 Cytotoxic activities of the pure isolated compounds from the stems of *Goniothalamus calvicarpus*

	Cell line (ED ₅₀ µg/mL)									
Compound	P-388 KB HT 29 MCF-7 A 549 ASK Hek 293 (
Ellipticine	0.53	0.63	0.41	0.62	0.46	0.70	0.83	-		
(+)-Altholactone	1.73	5.16	2.02	2.22	1.42	1.49	1.17	-		
Aristolactam AII	>4	1.34	>4	>4	>4	>4	>4	-		
(–)-Pinocembrin	>4	>4	>4	>4	>4	>4	>4	-		
(+)-Eriodictyol	>4	>4	>4	>4	>4	>4	>4	_		
(+)-Goniofufurone	>4	>4	>4	>4	>4	>4	>4	_		
Ellipticine	0.52	0.53	0.63	0.41	0.62	0.83	0.46	-		
(+)-Goniothalamin	0.34	2.14	2.12	0.42	0.48	0.75	0.56	_		
(+)-Goniodiol	0.73	2.10	2.75	3.16	2.10	2.70	2.31	_		
(+)-Goniotriol	0.29	>4	2.96	3.52	>4	>4	2.36	-		
(+)-Goniopypyrone	0.68	>4	>4	>4	>4	>4	3.67	-		
(–)-Naringenin	2.56	>4	>4	>4	>4	>4	3.67	-		
Ellipticine	0.42	0.47	0.52	0.46	0.46	0.47	_	0.49		
(+)-Goniodiol-7- monoacetate	2.89	>4	>4	>4	>4	>4	-	>4		
(+)-8-epi-Goniofufurone	>4	>4	>4	>4	>4	>4	-	>4		
(+)-Cardiobutanolide	>4	>4	>4	>4	>4	>4	-	>4		
Velutinam	1.97	2.45	>4	0.76	>4	>4	_	1.89		
Aristolactam BII	>4	>4	>4	<0.16	>4	>4	_	>4		
Aristolactam Allla	0.71	0.65	>4	3.04	2.98	2.72	-	0.64		
(-)-Mellein	>4	>4	>4	>4	>4	>4	-	>4		
Ethyl 4 methoxycinnamate	>4	>4	>4	>4	>4	>4	-	>4		
Lysicamine	1.92	>4	>4	3.98	>4	2.15	-	>4		
Paprazine	>4	>4	>4	>4	>4	>4	_	>4		

Results are expressed at ED₅₀ value (μ g/mL); ED₅₀ <4 μ g/mL is considered active.

P-388 = murine lymphocytic leukemia, KB = human nasopharyngeal carcinoma, HT-29 = human colon cancer, MCF-7 = Michigan cancer foundation, human breast cancer, A 549 = human lung cancer, ASK = cell line from rat glioma cell, Hek-293 = human kidney cell transformed with adenovirus 5 DNA (normal cell control), CL = normal liver

The preparation of a manuscript of the work on *Goniothalamus calvicarpus* is in progress.

5. Isolation of bioactive compounds from the aerial parts of Mallotus glomerulatus

Mallotus glomerulatus, known in Thai as 'Mak lium', is a plant of Euphorbiacea family. The plant material was collected from Nakhon Phanom province of Thailand.

Powdered aerial parts of M. glomerulatus (4.4 kg) were percolated with MeOH (5 \times 24 L) at room temperature to give a crude MeOH extract (317.8 g). After sequential dissolving in

MeOH:EtOAc (1:1, 6 L), MeOH (2 L), followed by solvent removal, the MeOH:EtOAc (1:1) fraction (167.9 g), MeOH fraction (75.8 g), and the residue (72.1 g) were obtained, respectively.

The dried extract and fractions were submitted for cytotoxic activity testings (in collaboration with Dr. Artit Chairoungdua. The results from cytotoxicity testings of the crude methanol extract, the EtOAc:MeOH (1:1) and the MeOH fractions are as shown in Table 1.7.

The EtOAc-MeOH (1:1) fraction (166.9 g) was further separated by vacuum chromatography, eluting hexanes, CH_2Cl_2 -hexanes gradient, CH_2Cl_2 and MeOH- CH_2Cl_2 gradient, and finally with MeOH. All fractions were combined on the basis of TLC behavior to provide 8 fractions (F1-F8). The results indicated that fractions F3-5 and F8 exhibited cytotoxic activity in some of cancer cell lines, but fractions F6 and F7 were active in all tested cancer cell lines as shown in Table 1.8.

Table 1.9 Cytotoxic activities from extract and fractions of the aerial parts of *Mallotus* glomerulatus

	Cell lines* (ED ₅₀ (µ g/mL))								
Extract/Fraction	P-388	KB	HT-29	MCF-7	A549	ASK	Hek293		
Ellipticine	0.14	0.49	0.64	0.32	0.44	0.12	0.43		
MeOH	<0.16	<0.16	0.5	0.34	0.74	2.82	0.44		
MeOH:EtOAc (1:1)	<0.16	<0.16	0.5	0.27	<0.70	2.76	0.43		
MeOH	0.32	0.46	2.43	1.09	3.16	12.79	1.72		
F_1	>20	>20	>20	>20	>20	>20	>20		
F ₂	>20	>20	>20	>20	>20	>20	>20		
F ₃	7.99	13.04	14	<4	>20	>20	10.86		
F ₄	12.45	>20	>20	7.07	>20	>20	19.73		
F ₅	10.78	>20	>20	7.28	>20	>20	11.63		
F ₆	<0.16	<0.16	0.5	0.19	0.79	3.01	0.47		
F ₇	<0.16	<0.16	<0.16	<0.16	<0.16	0.58	<0.16		
F ₈	0.45	1.67	3.45	2.38	4.79	14.31	2.68		
Ellipticine	0.14	0.49	0.64	0.32	0.44	0.12	0.43		

^{*}Results are expressed as ED_{50} (μ g/mL): ED_{50} < 20 μ g/mL is considered active. P-388 = murine lymphocytic leukemia, KB = human oral nasopharyngal carcinoma, HT29 = human colorectal adenocarcinoma, MCF-7 = human breast cancer, A549 = human lung carcinoma, ASK = rat glioma cell, Hek293 = normal human kidney cell.

Further separation by column chromatography of each fraction was performed as follows:

Fractions F1 (eluted by 0-25% CH_2Cl_2 -hexanes) and F2 (eluted by 30-35% CH_2Cl_2 -hexanes) contained mainly fat, therefore they were not further investigated.

Fraction F3, eluted by 40-45% CH₂Cl₂-hexanes, was further separated by repeated column chromatography to give a new compound glomerulatusin (1), together with the known anomaluone (3), pinocembrin (7), pinostrobin (8), and friedelin (10).

Fraction F4, eluted by 50-65% CH $_2$ Cl $_2$ -hexanes, was separated by repeated column chromatography to afford a mixture of β -sitosterol/stigmasterol (14a/14b)

Fraction F5, eluted by 70-90% CH_2Cl_2 -hexanes, was separated by repeated column chromatography to provide 3,6-phenanthrene-dione (2), 5-hydroxy-6,7,3',4',5'-pentamethoxyflavone (5), cleistanthin A (12) and 4-hydroxyacetophenone (13),

Fraction F6, eluted by 100% CH_2Cl_2 and 1-5% MeOH- CH_2Cl_2 , was further separated by repeated column chromatography to yield betulinic acid (11).

Fraction F7, eluted by 10-40% MeOH-CH $_2$ Cl $_2$, was separated by repeated column chromatography to give α -mangostin (4), 5,7-dihydroxyflavone (chrysin) (6), pinocembrin (7), pinostrobin (8), cardamonin (9) and cleistanthin A (12).

Fraction F8, eluted by 50-100% MeOH-CH $_2$ Cl $_2$ contained mainly sugars, therefore it was not further investigated.

All pure isolated compounds, except **6a/6b** were submitted for cytotoxic activity testings in a panel of cancer cell lines. The results are as shown in Table 1.10

Table 1.10 Cytotoxic activities of pure compounds **1–13**, isolated from the aerial parts of *M. glomerulatus*

	Storrestates									
Cananaund	Cell lines (ED $_{50}~\mu$ g/mL) a									
Compound	P-388	KB	HT-29	MCF-7	A-549	ASK	HEK293			
1	>4	>4	>4	>4	>4	>4	>4			
2	>4	>4	>4	>4	>4	>4	>4			
3	>4	>4	>4	>4	>4	>4	>4			
4	2.29	1.75	2.02	1.92	>4	2.72	2.27			
	(5.58 mM)	(4.26 mM)	(4.92 mM)	(4.68 mM)		(6.63 mM)	(5.53 mM)			
5	>4	>4	>4	>4	>4	>4	>4			
6	>4	>4	>4	>4	>4	>4	>4			
7	>4	>4	>4	>4	>4	>4	>4			
8	>4	>4	>4	>4	>4	>4	>4			
9	1.84	2.14	3.89	2.61	2.82	>4	2.56			
	(6.81 mM)	(7.92 mM)	(14.39 mM)	(9.66 mM)	(10.43 mM)		(9.47 mM)			
10	>4	>4	>4	>4	>4	>4	>4			
11	>4	>4	>4	>4	>4	>4	>4			
12	<0.05	<0.05	<0.05	<0.05	<0.05	<0.05	<0.05			
	(0.09 mM)	(0.09 mM)	(0.09 mM)	(0.09 mM)	(0.09 mM)	(0.09 mM)	(0.09 mM)			
13	>4	>4	>4	>4	>4	>4	>4			
Ellipticine	0.46	0.68	0.57	0.51	0.60	0.63	0.65			
	(1.87 mM)	(2.76 mM)	(2.31 mM)	(2.07 mM)	(2.44 mM)	(2.56 mM)	(2.64 mM)			

 $^{^{}a}$ Cytotoxic assay: ED $_{50}$ < 4 μ g/mL is considered active; P-388, murine lymphocytic leukemia; KB, human oral nasopharyngal carcinoma; HT29, human colorectal adenocarcinoma; MCF-7, human breast cancer; A549, human lung carcinoma, ASK, rat glioma cell; Hek293, cell line derived from human embryonic kidney cells. Ellipticine was used as positive control.

Sub-project 2: Cytotoxicity, Anticancer effects of natural derived compounds and their mechanism at molecular targets

Abstract

Cancer remains the leading cause of death and becomes a significant public health burden worldwide including in Thailand and China. Chemotherapy is the gold standard for aggressive and metastasis cancer, however, the satisfactory outcome is poor because of the limitations from their side effects. Therefore, searching for novel compounds with great anticancer activities is our challenge. Herein, under the collaboration between Thai and Chinese scientists, we discover promising compounds from natural resources with anticancer activities. First, we screened 151 compounds from marine-derived actinobacteria and their analogs using sulforhodamine B assay. We found that 90 out of 151 (69.6%) exhibited cytotoxic activity. Among them, 27 compounds showed the IC50 less than 10 mM against all 6 cancer cell lines. Next, we investigated the mechanisms related to the anticancer activity of compound HD ZWM 978 identified from the screening against gastric cancer cell lines, AGS, and MKN 45. HD ZWM 978 was potentially more cytotoxic than the clinically used etoposide, with IC50 values at 48 h of 1.7±0.2 mM and 4.3±1.0 mM in AGS and MKN 45 cells, respectively, whereas the IC50 values of etoposide were 8.6±2.4 mM and >20 mM in AGS and MKN 45 cells. Treatment with HD ZWM 978 markedly induced apoptotic cell death in AGS cells. Moreover, HD ZWM 978 significantly inhibited Topo IIlpha activity leading to DNA damage as demonstrated by an increase in γ -H2A.X expression, the DNA damage marker, in a dose-dependent manner. The anticancer mechanism of HD ZWM 978 was further investigated in the WNT/b-catenin pathway and found that HD ZWM 978 significantly reduced the expression of b-catenin protein and WNT target gene; c-MYC, and survivin. Our results indicate that HD ZWM 978 induces gastric cancer cell apoptosis partly through induction of DNA damage-mediated by topoisomerase $II \alpha$ enzyme inhibition and inhibition of the WNT/ β -catenin signaling pathway. In addition, we investigated the anticancer mechanism of two andrographolide analogs, analog 6 (19-triisopropyl-andrographolide) and analogs 3A.1 (19-tert-butyldiphenylsilyl-8,17-epoxy andrographolide) on gastric cancer and colorectal cell lines, respectively. analog 6 exhibited highly cytotoxic than parent Andrographolide or the clinical drug etoposide with IC50 values of 6.3±0.7 mM and 1.7±0.05 mM at 48 h for MKN 45 and AGS cells, respectively. Analogue 6 reduced the expression of Topo II enzyme, induced DNA damage, and activated PARP-1 and Caspase 3, leading to late apoptosis in AGS cells whereas treatment with the compound did not affect the expression of tumor suppressor p53. Similarly, analogs 3A.1 exhibited a significant cytotoxic effect against CRC cells and more potent than the parent compound. Mechanistically, analogs 3A.1 induced apoptotic cell death probably through inhibition of WNT/b-catenin signaling pathway-mediated DNA damages. Taken together, under the collaboration project between Thai and Chinese scientists, we able to discover the promising compounds that have the potential to be developed as novel anticancer compounds for cancer treatment.

Keywords: anticancer activity, medicinal plants, marine microbes, gastric cancer cells, colorectal cells

บทคัดย่อ

โรคมะเร็งเป็นสาเหตุการตายและเป็นปัญหาทางสาธารณสุขทั่วโลกรวมถึงประเทศไทยและประเทศจีน การรักษาด้วย ยาเคมีบำบัดถือเป็นวิธีการรักษามาตรฐานสำหรับมะเร็งที่มีการแพร่กระจาย แต่ผลสำเร็จของการรักษายังต่ำเนื่องจาก ดังนั้นการค้นหาตัวยาใหม่สำหรับการรักษาโรคมะเร็งจึงมีความสำคัญ ผลข้างเคียงของการใช้ยา วัตถุประสงค์เพื่อค้นหาสารที่ออกฤทธิ์ต้านมะเร็งจากธรรมชาติ ภายใต้ความร่วมมือกับนักวิทยา ศาสตร์ชาวจีน กลุ่ม วิจัยได้คัดกรองสารที่ออกฤทธิ์ต้านมะเร็งจากสารที่คัดแยกได้จากแบคทีเรียใต้ทะเลและสารดัดแปลงโครงสารจำนวน 151 ตัว พบว่า 90 จาก 151 ตัว คิดเป็น 69.6 เปอร์เซ็นต์ ออกฤทธิ์ฆ่าเซลล์มะเร็ง ในจำนวนนี้มีสาร 27 ตัวมีฤทธิ์ดีเด่น โดยมีค่า IC50 ต่ำกว่า 10 μ M ในเซลล์มะเร็งที่ใช้ทดสอบทั้งหมด 6 ชนิด กลุ่มวิจัยได้คัดเลือกสาร HD ZWM 978 มา ศึกษาฤทธิ์ต้านมะเร็งและกลไกที่เกี่ยวข้องในเซลล์มะเร็งกระเพาะอาหาร 2 ชนิด คือ MKN 45 และ AGS จากการ ทดสอบพบว่าสาร HD ZWM 978 ออกฤทธิ์ฆ่าเซลล์มะเร็งกระเพาะอาหารได้ดีกว่า etoposide ซึ่งเป็นยาที่ใช้รักษา ปัจจุบัน โดยมีค่า IC50 ที่ 48 ชั่วโมง เท่ากับ 1.7±0.2 μ M และ 4.3±1.0 μ M สำหรับเซลล์ AGS และ MKN 45 ตามลำดับ ในขณะที่ค่า IC50 ของ etoposide เท่ากับ 8.6±2.4 μ M และมากกว่า 20 μ M สำหรับเซลล์ AGS and MKN 45 ตามลำดับ สาร HD ZWM 978 ออกฤทธิ์เหนี่ยวนำให้เซลล์มะเร็งกระเพาะอาหารตายแบบ apoptosis การศึกษากลไกการออกฤทธิ์ในระดับโมเลกุลพบว่า สาร HD ZWM 978 ออกฤทธิ์ยับยั้งการทำงานของเอนไซม์ Topo แlpha โดยที่ความเข้มข้น 10 μ M สามารถยับยั้งฤทธิ์ของเอนไซม์ Topo แlpha ได้เกือบสมบูรณ์ นอกจากนี้ยังพบว่าสาร HD ZWM 978 สามารถเหนี่ยวนำให้เซลล์เกิดการแตกหักของสายดีเอ็นเอ ซึ่งประเมินได้จากการแสดงของตัวบ่งชี้ของ การแตกหักของสารดีเอ็นเอ คือ 🥎 H2A.X สาร เมื่อบ่มเซลล์ด้วยสาร HD ZWM 978 ยังพบว่าการแสดงออกของ โปรตีน eta-catenin และยืนเป้าหมายของกลไกสัญญาณ WNT/eta-catenin คือ c-MYC, and survivin ลดลง แสดงว่า สาร HD ZWM 978 ออกฤทธิ์ยับยั้งกลไกสัญญาณ WNT/eta-catenin ซึ่งเป็นกลไกสัญญาณที่สำคัญต่อพฤติกรรมความ รุ่นแรงของเซลล์มะเร็ง จากผลการทดลองนี้สรุปได้ว่าสาร HD ZWM 978 เหนี่ยวนำเซลล์มะเร็งกระเพาะอาหารให้เกิด การตายแบบ apoptosis โดยยับยั้งการทำงานของเอนไซม์ Topo IIlpha ซึ่งส่งผลให้เกิดการแตกหักของสายดีเอ็นเอและ ้ ยังออกฤทธิ์ยับยั้งกลไกสัญญาณ WNT/eta-catenin นอกจากนี้กลุ่มวิจัยยังได้ศึกษาฤทธิ์ต้านมะเร็งและกลไกที่เกี่ยวข้อง ของสารดัดแปลงโครงสร้างของ andrographolide 2 ขนิด คือ analogue 6 (19-triisopropyl-andrographolide) ในเซลล์มะเร็งกระเพาะอาหาร และ analogue 3A.1 (19-tert-butyldiphenylsilyl-8,17-epoxy andrographolide) ในเซลล์มะเร็งลำไส้ สาร analogue 6 ออกฤทธิ์ฆ่าเซลล์มะเร็งกระเพาะอาหารได้ดีกว่าสาร andrographolide และ etoposide โดยมีค่า IC50 ที่ 48 ชั่วโมง เท่ากับ 6.3±0.7 μ M และ 1.7±0.05 μ M สำหรับ เซลล์ AGS และ MKN 45 ตามลำดับ โดยสาร analogue 6 ออกฤทธิ์ยับยั้งเอนไซม์ Topo II ก่อให้เกิดการแตกหัก ของสายดีเอ็นเอ เกิดการตัดของโปรตีน PARP-1 และ Caspase 3 ซึ่งส่งผลให้เซลล์มะเร็งกระเพาะอาหารเกิดการตาย apoptosis ในทำนองเดียวกัน สาร analogue 3A.1 ออกฤทธิ์ฆ่าเซลล์มะเร็งลำไส้ได้ดีกว่าสารตั้งต้น andrographolide โดยยับยั้งการทำงานของกลไกสัญญาณ WNT/eta-catenin ส่งผลให้เกิดการตายของเซลล์มะเร็ง จากการทดลองทั้งหมดแสดงให้เห็นว่า ภายใต้โครงการความร่วมมือระหว่าง apoptosis นักวิทยาศาสตร์ชาวไทยและจีนนี้ ส่งเสริมให้มีการค้นพบสารสำคัญที่มีศักยภาพสามารถนำไปพัฒนาต่อยอดเป็นยาต้าน มะเร็งต่อไป

คำสำคัญ: ฤทธิ์ต้านมะเร็ง สมุนไพร เชื้อจากทะเล เซลล์มะเร็งกระเพาะอาหาร เซลล์มะเร็งลำไส้ใหญ่และทวารหนัก

Introduction to the research problem and its significance:

Cancer is one of the most common causes of death worldwide. Based on the latest world cancer statistical data (WHO), global cancer burden rises to 14.1 million new cases in 2012 and 8.2 million cancer-related deaths occurred in 2012. Aging is one major risk factor for cancer development. It has been shown that 60% of newly diagnosed malignancies were reported in persons over 65 year-old and accounting for 70% of all cancer deaths (Berger et al., 2006). Cellular senescence play a role in oncogenic stimuli like DNA damage leading to disruption of oncogene or tumor suppressor gene expression in aging person (Campisi, 2013). Due to the increase in ageing of the global population, it predicts a substantial increase to 19.3 million new cancer cases per year by 2025 (GLOBOCAN 2012). World Health Organization has been reported that the population in their elderly years is rapidly increase in Thailand and China. In Thailand the people with more than 60 year-old of age is increase from 8.7% in 2000 to 30% in the year of 2050. Cancer is also the first leading of death in Thailand and China for many years. The mortality rate in these two countries is continuously increased. China and Thailand share the most common types of cancers. Lung cancer is the most common cancer found in Chinese population, followed by stomach, liver, esophageal and colorectal cancers (Zhao et al., 2010) whereas lung, liver and bile duct, colon, stomach, esophagus, breast and cervix cancer are prevalence in Thailand (National Cancer Institute of Thailand, 2012). Not only the above cancer types, some of rare cancer case like pancreatic cancer which has low 5-year survival rate (6.7%) is also recognized as the significant public health burden in China and Thailand. At present, chemotherapy is one of the principal method for cancer treatment, however, the effectiveness of most of current anticancer drugs is limited by its adverse effect and development of drug resistance. The toxicity to normal cells accounting for the adverse effects linked to these drugs is unavoidable. Throughout these years, natural products remain the major source of new anticancer drugs or lead compounds such as paclitaxel, docetaxel, vincristine, vinblastine, irinotecan, etoposide and bleomycin (da Rocha et al., 2001). However, the cost of these drugs is high. Thailand and china have a long history of using herbal medicine for treatment variety of diseases including cancer. In Thailand, some indigenous medicinal herbal compounds are found to be effective for cancer treatment but the sensitivity is poor. The structural modification of these compounds have showed a great improvement on the biological activities (Nateewattana et al., 2014; Nateewattana et al., 2013; Sirion et al., 2012; Wanitchakool et al., 2012). Therefore, the discovery and development of new anticancer drugs or lead compounds from natural products either from plants, marine, soil or other special microbes are our challenging subjects for Thai and China scientists. Furthermore, one current approach to overcome the complicated regulating molecular mechanisms in cancer is the development of drug targeting system (DDS). Drug delivery is designed to administer pharmaceutical agents as an alternative choice in order to increase safety and efficacy with remained therapeutic levels. Several targeting systems have been suggested for anticancer drugs including bead delivery, controlled release, liposomal and nanoparticulate systems (Perez-Herrero and Fernandez-Medarde, 2015). The drug delivery with nanoparticles, in addition to have the capacity to transport the particular compounds to specific target cancer sites, it is also able to solve the problems of low solubility of water insoluble compounds (Puntawee et al., 2015). In this project, our group interests in many types of cancers that commonly found in Thai and Chinese population including cholangiocarcinoma, lung, colorectal cancer, breast cancer, head and neck cancer, ovarian cancer, bone cancer. The projects will cover from the candidate compound and target identification, structure optimization *in vitro* system to *in vivo* preclinical study as well as the development of drug targeting system.

Literature review:

Cancer is one of the most common causes of death worldwide. Based on the latest world cancer statistical data (WHO), global cancer burden rises to 14.1 million new cases in 2012 and 8.2 million cancer-related deaths occurred in 2012. Aging is one important risk factor for cancer development. It has been shown that 60% of newly diagnosed malignancies were reported in persons over 65 year-old and accounting for 70% of all cancer deaths (Berger et al., 2006). Cellular senescence play a role in oncogenic stimuli like DNA damage leading to disruption of oncogene or tumor suppressor gene expression in aging person (Campisi, 2013). World Health Organization has been reported that the population in their elderly years is rapidly increased in Thailand and China. In Thailand the people with more than 60 year-old of age is increase from 8.7% in 2000 to 30% in the year of 2050. Due to the increase in ageing of the global population, it predicts a substantial increase to 19.3 million new cancer cases per year by 2025 (GLOBOCAN 2012). At present, chemotherapy is one of the principal methods for cancer treatments; however, the effectiveness of most of current anticancer drugs is limited by its adverse effect and development of drug resistance. The natural products and their derivatives account for more than 50% of all drugs in clinical use of the world including for anticancer drugs. Plants and marine organisms are the important resources for the discovery of new anticancer drug. Doctetaxel and paclitaxel, two well-known examples of anticancer drugs were originally discovered from plants (da Rocha et al., 2001). In addition, anticancer drug discovery from marine natural products has been reported. Ecteinascidin-743 (ET-743/trabectedin), the first anticancer derived from Ecteinascidia turbinate was approved by the European Commission in July 2007. The Phase I and Phase II studies demonstrated the remarkable antitumor activity against solid tumors, in particular breast and renal carcinoma (Molinski et al., 2009). Up to date, several compounds have been extracted from marine products and shown antitumor activity that have been in

clinical trial studies. The different in chemical and biological diversity of marine organisms make them become an amazing resource for the discovery of new anticancer drug.

Drug resistance remains the main cause of cancer treatment failure. The major mechanism of drug resistance in cancer is related to the expression of multidrug resistance (MDR) proteins belonging to ATP-binding cassette (ABC) family of membrane transport ATPase (Kathawala et al., 2015). Upregulation of these membrane proteins, MDR1/ABCB1, MRP1/ABCC1 and BCRP/ABCG2 in many types of cancer have been reported to be associated with the resistance to many of recent chemotherapeutic drugs such as doxorubicin, vinblastine and methotrexate (Kathawala et al., 2015). Therefore, the identification of their inhibitors have been a major goal for cancer treatment. Indeed, many of MDR modulators have been discovered from the marine and natural compounds such as Ecteinascidin 743, Agosterol A, curcumin, nobiletin, ginsenoside Rg3, silymarin and glycyrrhetinic acid (Kathawala et al., 2015; Wang et al., 2010).

Targeting cancer-related cellular signaling pathway or component has held the interest of discovery the active anticancer drugs. Aberrant activation of Wnt signaling pathway is associated with cancer development such as colon cancer, breast cancer, melanoma, head & neck cancer, non-small-cell lung cancer, gastric cancer (Barker and Clevers, 2006). Wnt/ β -catenin signaling pathway is characterized by cytoplasmic accumulation of β -catenin, subsequent nuclear translocation and activates the cancer phenotype-related target gene expression (Gordon and Nusse, 2006). Therefore, wnt/ β -catenin signaling is interesting target for anticancer drug discovery. Indeed, natural products like flavonoids (flavonone, luteolin, apigenin, genistein, kaempferol, isoquercitrin) has potential to be develop as anticancer drugs through inhibition of several proteins in wnt/ β -catenin signaling (Amado et al., 2014)

DNA topoisomerase enzymes are also one of the promising cellular targets for developing anticancer drugs. DNA topoisomerase II (Top2) plays a critical role for ensuring the genomic integrity. It controls DNA replication, transcription and chromosome segregation (Nitiss, 2009). Alteration of its activity generates enzyme mediated DNA damage and is used as target for chemotherapeutic agents. The alteration of Top2 activity by natural products and it analogue has been report. Etoposide, a synthetic chemical compound from *Podophyllum peltatum* is used for treatment of lung and testicular tumor with a significant inhibition potency on Top2 activity (Nitiss, 2009). Recently our group reported the semi-synthetic andrographolide analogues mediated the inhibition of Top2 activity in cancer cell line (Nateewattana et al., 2013).

Objectives

1. Screening for cytotoxic activity of natural products from Chinese Marine Microbes and Thai Medicinal Plants.

2. Identification the molecular mechanisms and molecular target of the candidate compounds.

Results and Discussion

<u>Part I:</u> Screening for cytotoxic activity of natural products from Chinese Marine Microbes and Thai Medicinal Plants.

Compounds were kindly provided by **Prof. Patoomratana Tuchinda, Mahidol University and Prof. Weiming Zhu, Ocean University of China.** The effect of compound on cell viability was determined by using the colorimetric SRB assay. Briefly, cancer cell lines were seeded in a 96-well plates. Cells were cultured for 24 h and then treated with various concentrations of compounds 72 h. In the control group, the cells were cultured in medium containing equivalent amount of DMSO required to dissolve the compounds. At the end of every specific duration of incubation, cell viability was determined by using the colorimetric SRB assay. As shown in Table 1 and 2, several compounds from both sources exhibited the cytotoxic effect against cancer cell lines. Interestingly, we screened 151 compounds from marine-derived actinobacteria and their analogues (all from Prof. Weiming Zhu, Ocean University of China) using sulforhodamine B assay. We found that 90 out of 151 (69.6%) exhibited cytotoxic activity. Among them, 27 compounds showed the IC $_{50}$ less than 10 μ M against all 6 cancer cell lines. We found that 90 out of 151 (69.6%) exhibited cytotoxic activity. We therefore selected some of these compound for further mechanistic study in next experiment.

<u>Table 2.1.</u> IC₅₀ values of tested compounds against cancer cell lines (Compounds were obtained from Prof. Patoomratana Tuchinda, Mahidol University)

Compounds	IC ₅₀ (μΜ)									
Compounds	P-388	KB	HT-29	MCF-7	A549	ASK	HuCCA-1	HEK293		
Ellipticine	2.07	2.26	2.32	1.53	2.32	1.80	2.83	1.76		
MUC941	>100	>100	>100	>100	>100	>100	>100	>100		
MUC942	>100	92.87	>100	>100	>100	>100	>100	>100		
MUC943	>100	>100	>100	>100	>100	>100	>100	>100		
MUC944	>100	>100	>100	>100	>100	>100	>100	>100		
MUC1020	58.73	81.22	77.14	91.63	91.99	64.19	74.36	51.67		
MUC1021	>100	>100	>100	>100	>100	96.47	>100	73.99		
MUC1022	51.93	91.83	>100	>100	>100	72.03	>100	59.29		
MUC1023	54.07	>100	>100	>100	>100	80.18	>100	71.70		
MUC1028	68.30	>100	>100	>100	>100	>100	>100	91.86		

MUC1029	3.29	4.92	3.96	3.96	3.07	1.65	4.9	0.95
MUC1030	>100	>100	>100	>100	>100	>100	>100	>100
MUC1031	>100	>100	>100	>100	>100	>100	>100	>100
MUC1032	5.93	34.91	9.05	25.23	8.47	5.41		4.72
MUC1255	24.35	20.28	>50	22.40	27.99	41.56		18.60
MUC1261		< 0.1	<0.1	<0.1	< 0.1	<0.1		
MUC1262		>50	>50	>50	>50	>50		
MUC1263		>50	>50	>50	>50	>50		

<u>Table 2.2</u> IC₅₀ values of tested compounds against cancer cell lines (Compounds were obtained from Prof. Weiming Zhu, Ocean University of China)

		n Proi. Weim		C ₅₀ (μм)			
Compound	P-388	KB	HT-29	MCF-7	A 549	HEK 293	ASK
Ellipticine	2.24	2.33	2.43	2.14	2.55	2.05	1.65
552	47.58	> 50	> 50	> 50	> 50	> 50	> 50
553	16.57	6.66	27.99	20.5	28.67	27.71	27.09
801	> 50	> 50	> 50	> 50	> 50	> 50	> 50
802	> 50	> 50	> 50	> 50	> 50	> 50	> 50
803	> 50	> 50	> 50	> 50	> 50	> 50	> 50
804	> 50	> 50	> 50	> 50	> 50	> 50	> 50
805	> 50	> 50	> 50	> 50	> 50	> 50	> 50
806	> 50	> 50	> 50	> 50	> 50	> 50	> 50
807	> 50	> 50	> 50	> 50	> 50	> 50	> 50
808	> 50	> 50	> 50	> 50	> 50	> 50	> 50
809	> 50	> 50	> 50	> 50	> 50	> 50	> 50
810	> 50	> 50	> 50	> 50	> 50	> 50	> 50
811	> 50	> 50	> 50	> 50	> 50	> 50	> 50
812	> 50	> 50	> 50	> 50	> 50	> 50	> 50
813	> 50	> 50	> 50	> 50	> 50	> 50	> 50
814	> 50	> 50	> 50	> 50	> 50	> 50	> 50
815	> 50	> 50	> 50	> 50	> 50	> 50	> 50
816	> 50	> 50	> 50	> 50	> 50	> 50	> 50
877	6.26	7.16	29.78	19.72	19.32	20.67	25.64
878	> 50	> 50	> 50	> 50	> 50	> 50	> 50
879	33.18	30.69	> 50	> 50	29.14	> 50	32.80
888	> 50	> 50	> 50	> 50	> 50	> 50	> 50

C				IC ₅₀ (μΜ)			
Compound	P-388	KB	HT-29	MCF-7	A 549	HEK 293	ASK
889	> 50	> 50	> 50	> 50	> 50	> 50	> 50
890	> 50	> 50	> 50	> 50	> 50	> 50	> 50
891	> 50	> 50	> 50	> 50	> 50	> 50	> 50
892	> 50	> 50	> 50	> 50	> 50	> 50	> 50
909	> 50	> 50	> 50	> 50	> 50	> 50	> 50
910	> 50	> 50	> 50	> 50	> 50	> 50	> 50
911	> 50	> 50	> 50	> 50	> 50	> 50	> 50
912	> 50	> 50	> 50	> 50	> 50	> 50	> 50
913	> 50	> 50	> 50	> 50	> 50	> 50	> 50
954	0.58	0.81	0.83	0.65	0.70	0.63	0.67
960	2.31	5.61	15.88	9.17	8.46	14.73	7.52
961	12.74	34.99	> 50	> 50	> 50	> 50	> 50
962	28.82	5.11	29.61	33.92	25.37	24.77	31.91
963	> 50	> 50	> 50	> 50	> 50	> 50	> 50
817	> 50	> 50	> 50	> 50	45.3	> 50	> 50
818	> 50	> 50	> 50	> 50	39.2	> 50	44.9
819	> 50	> 50	> 50	> 50	> 50	> 50	> 50
820	> 50	> 50	> 50	> 50	> 50	> 50	> 50
821	> 50	> 50	> 50	> 50	> 50	> 50	> 50
822	> 50	> 50	> 50	> 50	> 50	> 50	> 50
823	> 50	> 50	> 50	> 50	> 50	> 50	> 50
824	> 50	> 50	> 50	> 50	> 50	> 50	> 50
825	> 50	> 50	> 50	> 50	> 50	> 50	> 50
965	5.30	5.80	8.26	7.85	5.53	5.58	6.99
966	> 50	> 50	> 50	> 50	> 50	> 50	> 50
968	> 50	> 50	> 50	> 50	> 50	> 50	> 50
969	> 50	> 50	> 50	> 50	> 50	> 50	> 50
970	> 50	> 50	> 50	> 50	> 50	> 50	> 50
978	4.77	5.06	6.71	6.06	0.91	5.81	3.23
1003	6.45	7.83	16.73	9.48	23.08	8.17	7.36
1004	4.62	5.57	6.29	5.19	4.63	5.35	4.99
1006	5.55	5.21	5.29	5.71	5.21	5.34	4.84
1007	0.66	5.10	6.23	5.29	5.58	6.69	5.26
1008	3.16	3.75	2.39	2.94	3.83	4.22	2.79
1011	> 50	> 50	> 50	> 50	> 50	> 50	> 50

C				IC ₅₀ (μΜ)			
Compound	P-388	KB	HT-29	MCF-7	A 549	HEK 293	ASK
1012	8.64	5.72	6.34	7.04	5.54	5.31	19.83
1014	40.54	> 50	> 50	> 50	> 50	> 50	> 50
1015	0.85	0.88	3.23	5.64	5.24	0.82	4.89
1016	18.49	5.98	6.31	6.82	6.82	7.09	9.84
1017	9.61	7.09	8.30	7.28	8.53	6.80	9.37
1020	> 50	> 50	> 50	> 50	> 50	> 50	> 50
1021	> 50	> 50	> 50	> 50	> 50	> 50	> 50
1024	> 50	> 50	> 50	> 50	> 50	> 50	> 50
1041	6.11	34.00	32.69	21.54	8.49	7.20	18.66
1061	37.58	> 50	> 50	> 50	> 50	45.56	43.81
1062	> 50	> 50	> 50	> 50	> 50	> 50	> 50
1065	31.35	> 50	44.15	44.24	10.07	32.89	15.64
1066	> 50	> 50	> 50	> 50	> 50	> 50	> 50
1067	> 50	> 50	> 50	> 50	> 50	> 50	> 50
1081	5.08	21.65	33.02	20.33	7.80	27.70	4.84
1083	5.35	27.61	> 50	22.74	8.62	> 50	5.13
1085	27.56	4.47	39.88	5.29	11.48	6.26	32.38
1086	5.20	2.92	9.38	4.35	4.58	4.12	21.70
1087	4.57	0.62	6.07	0.71	2.69	0.78	5.86
1088	4.98	0.64	6.13	0.79	2.98	0.83	6.14
1089	7.30	4.86	28.86	8.69	6.12	6.13	7.79
1090	> 50	> 50	> 50	41.92	> 50	> 50	> 50
1091	> 50	25.64	> 50	> 50	39.24	> 50	> 50
1092	> 50	> 50	> 50	> 50	> 50	> 50	> 50
1093	43.31	42.48	> 50	> 50	47.94	> 50	> 50
1094	> 50	> 50	> 50	> 50	> 50	> 50	> 50
1095	> 50	> 50	> 50	> 50	27.66	> 50	36.19
1097	> 50	47.22	> 50	> 50	30.34	32.68	> 50
1099	> 50	> 50	> 50	> 50	> 50	> 50	> 50
1100	> 50	> 50	> 50	> 50	> 50	> 50	> 50
1101	42.91	> 50	> 50	> 50	> 50	> 50	> 50
1102	> 50	27.46	> 50	> 50	> 50	> 50	> 50
1103	> 50	30.00	> 50	> 50	> 50	> 50	> 50
1104	3.43	7.38	8.80	7.73	8.73	6.21	7.35
1105	5.26	5.72	5.36	5.44	4.76	9.40	4.92

C				IC ₅₀ (μΜ)			
Compound	P-388	KB	HT-29	MCF-7	A 549	HEK 293	ASK
1106	7.06	18.05	22.11	27.48	4.20	43.12	5.13
1107	3.19	5.25	5.11	5.37	4.93	5.01	4.63
1108	3.71	4.96	5.06	4.72	4.65	4.96	4.68
1109	1.72	5.03	4.75	4.90	4.64	5.07	4.51
1110	3.62	5.04	4.66	4.77	5.08	5.04	4.67
1113	4.00	21.16	32.52	7.50	13.81	27.48	8.80
1114	4.66	4.94	5.31	5.21	4.94	5.07	4.65
1115	4.73	4.96	5.40	5.19	4.86	5.08	4.65
1116	0.99	6.62	19.54	5.49	6.83	20.98	5.93
1117	3.46	5.87	7.95	5.47	5.55	6.24	5.55
1118	0.83	14.15	44.14	9.99	23.17	36.77	9.81
1119	5.37	5.22	5.21	4.91	4.96	5.06	4.75
1120	> 50	> 50	> 50	> 50	> 50	> 50	> 50
1121	5.30	14.93	18.70	17.78	17.49	6.16	22.07
1122	5.33	23.98	22.24	22.70	25.25	27.51	23.55
1123	5.32	5.06	5.12	4.97	5.09	5.09	4.57
1124	4.09	4.98	4.89	4.68	5.02	5.11	4.54
1125	3.50	9.03	30.07	6.17	8.30	9.33	7.05
1126	5.69	27.20	32.57	9.14	19.51	> 50	18.80
1127	9.38	> 50	> 50	8.93	> 50	> 50	> 50
1137	> 50	> 50	> 50	> 50	> 50	> 50	> 50
1142	> 50	> 50	> 50	> 50	> 50	> 50	> 50
1143	> 50	> 50	> 50	> 50	> 50	> 50	> 50
1144	> 50	> 50	> 50	> 50	> 50	> 50	> 50
1145	40.24	> 50	47.32	> 50	> 50	> 50	> 50
1146	> 50	> 50	> 50	> 50	> 50	> 50	> 50
1147	> 50	> 50	> 50	> 50	> 50	> 50	> 50
1148	> 50	> 50	> 50	> 50	> 50	> 50	> 50
1149	20.87	33.78	41.19	29.96	> 50	29.22	33.82
1150	> 50	> 50	> 50	> 50	> 50	> 50	> 50
1151	> 50	> 50	> 50	> 50	> 50	> 50	> 50
1152	31.93	> 50	> 50	> 50	> 50	> 50	> 50
1153	> 50	> 50	> 50	> 50	> 50	> 50	> 50
1154	> 50	> 50	> 50	> 50	> 50	> 50	> 50
1155	> 50	> 50	> 50	> 50	> 50	> 50	> 50

Compound		IC ₅₀ (μM)								
Compound	P-388	KB	HT-29	MCF-7	A 549	HEK 293	ASK			
1156	> 50	> 50	> 50	> 50	> 50	> 50	> 50			
1157	> 50	> 50	> 50	> 50	> 50	> 50	> 50			
1158	> 50	> 50	> 50	> 50	> 50	> 50	> 50			
1159	> 50	> 50	> 50	> 50	> 50	> 50	> 50			
1160	34.00	> 50	> 50	> 50	> 50	> 50	> 50			
1161	5.61	5.50	5.22	4.64	20.01	4.97	5.08			
1162	35.97	> 50	> 50	> 50	> 50	> 50	> 50			
1163	> 50	> 50	> 50	> 50	> 50	> 50	> 50			
1164	> 50	> 50	> 50	> 50	> 50	> 50	> 50			
1165	> 50	> 50	> 50	> 50	> 50	> 50	> 50			
1166	> 50	> 50	> 50	> 50	> 50	> 50	> 50			
1167	> 50	> 50	> 50	> 50	> 50	> 50	> 50			
1168	3.55	5.03	5.78	7.16	4.91	4.61	5.31			
1169	5.75	7.40	6.01	5.86	5.59	3.87	5.70			
1170	0.40	5.29	5.47	0.99	0.86	0.57	0.82			
1171	> 50	> 50	> 50	> 50	> 50	> 50	> 50			
1172	> 50	> 50	> 50	> 50	> 50	> 50	> 50			
1173	26.81	> 50	> 50	> 50	> 50	> 50	> 50			
1174	> 50	> 50	> 50	> 50	27.95	> 50	> 50			
1175	17.19	28.93	42.31	31.47	27.97	21.56	28.26			
1176	> 50	> 50	> 50	> 50	> 50	> 50	> 50			
1177	> 50	> 50	> 50	> 50	> 50	> 50	> 50			
1178	> 50	> 50	> 50	> 50	> 50	> 50	> 50			
1179	> 50	> 50	> 50	> 50	> 50	> 50	> 50			

Cell lines: Murine lymphocytic leukemia (P-388), Human epidermoid carcinoma in the mouth (KB), Human colon cancer (HT-29), Human breast cancer (MCF-7), Human lung cancer (A-549), Rat glioma cell (ASK), Human embryonic kidney cell (HEK 293), Human breast cancer (MCF-7), Liver cancer (HepG2 and Hep3B), liver cell (Chang liver or CL), cholangiocarcinoma (HuCCA-1)

Part II: Identification the molecular mechanisms and molecular target of the candidate compounds.

2.1 Anticancer activities of Marine Actinobacterium secondary metabolite (HD ZWM

978) on gastric cancer cell lines. <u>HD ZWM 978 was kindly provided by Prof. Weiming Zhu, Ocean University of China</u>

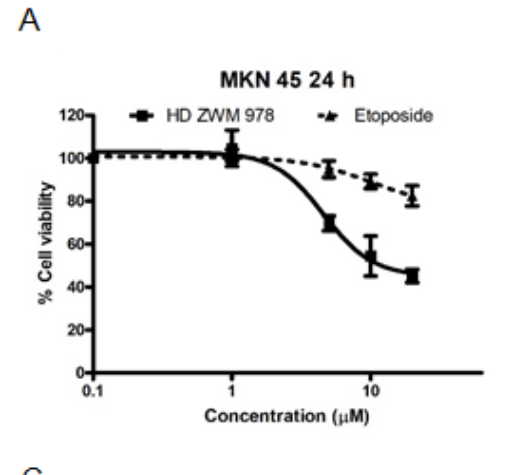
2.1.1 Cytotoxic effects of HD ZWM 978 on gastric cancer cells (MKN 45 and AGS cell lines)

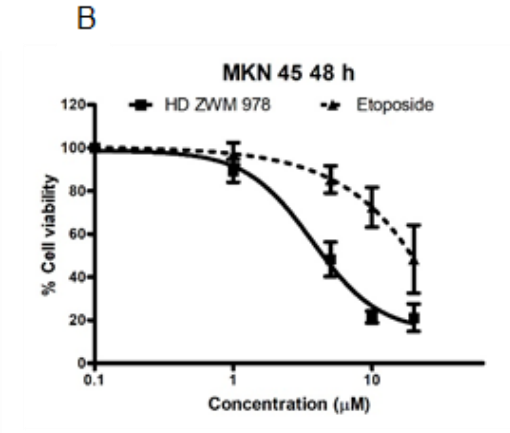
HD ZWM 978, a secondary metabolite from Marine *Actinobacterium* was investigated for its cytotoxic activities in MKN 45 gastric cancer cells at 24, 48 and 72 h using MTT assay. Etoposide, an anticancer drug, was used as a positive control. As shown in Fig. 2.1 and Table 3, the compound exhibits cytotoxic activities in a dose-related manner. The half maximal inhibitory concentration for cell survival (IC $_{50}$ value) of HD ZWM 978 was 14.2±1.8, 4.3±1.0 and 4.7±0.4 μ M after treatment for 24, 48 and 72 h, respectively. HD ZWM 978 was more potent than the clinically used anticancer drug, etoposide, having IC $_{50}$ of >20 μ M at 24, 48 h and 16±2.3 μ M at 72 h.

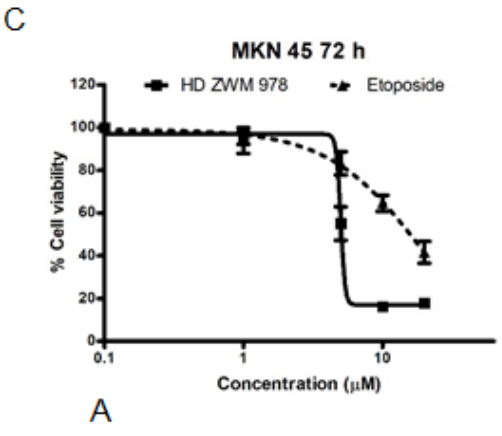
Similarly, HD ZWM 978 was also toxic to other gastric cancer cell line (AGS cells), as shown in Fig. 2.2 and Table 2.3. At 24 h, IC₅₀ values for HD ZWM 978 and etoposide are 4.9 \pm 1.3, and 19.6 \pm 0.9 μ M, respectively. The cytotoxic activity of HD ZWM 978 was substantially increased at 48 h and 72 h with IC₅₀ values of 1.7 \pm 0.2, and 2.1 \pm 0.3 μ M, respectively. More importantly, the cytotoxicity of HD ZWM 978 was greater than the clinically used etoposide. As AGS cells were more sensitive to HD ZWM 978, it was chosen for further investigation on the mechanisms of action in details.

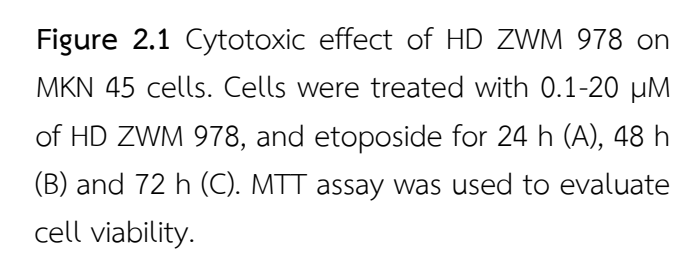
Table 2.3 IC₅₀ values of HD ZWM 978 gastric cancer cell lines Data are means \pm SEM of three independent experiments performed in triplicates.

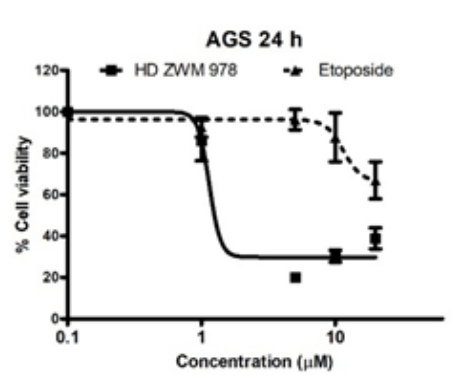
Cell lines	Incubation time (h)	IC ₅₀ (μM)	
		Etoposide	HD ZWM 978
	24	>20	14.2 ± 1.8
MKN 45	48	>20	4.3 ± 1.0
	72	16 ± 2.3	4.7 ± 0.4
	24	>20	4.9 ± 1.3
AGS	48	8.6 ± 2.4	1.7 ± 0.2
	72	2.9 ± 0.5	2.1 ± 0.3

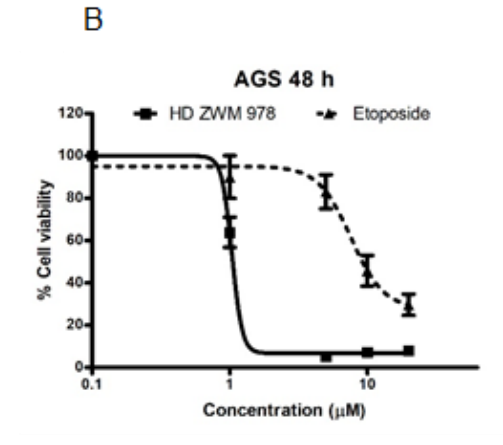












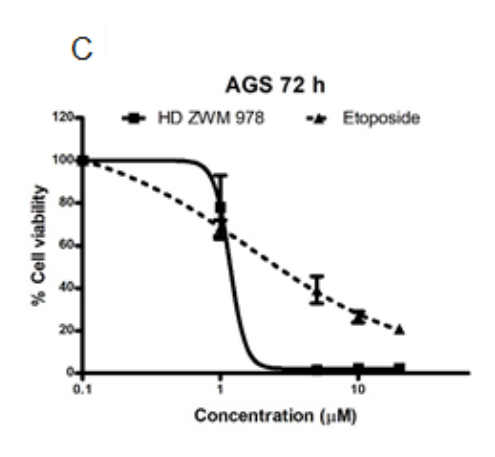


Figure 2.2 Cytotoxic effect of HD ZWM 978 on AGS cells. Cells were treated with 0.1-20 μ M of HD ZWM 978, and etoposide for 24 h (A), 48 h (B) and 72 h (C). MTT assay was used to evaluate cell viability.

2.1.2 Induction of cellular apoptosis by HD ZWM 978 in human gastric cancer cells

AGS cells were treated with HD ZWM 978 at 1, 2 and 5 μ M and etoposide at 10 μ M for 48 h. HD ZWM 978 induced early and late apoptosis in a dose related manner. Early apoptosis was respectively increased to 3.9±0.2%, 7.2±1.7% and 17.5±3.6% by HD ZWM 978 at 1, 2 and 5 μ M, respectively, as compared to DMSO control (2.3±0.7%). Etoposide induced the early apoptosis up to 11.2±3.8%. In addition, HD ZWM 978 at the concentration of 1, 2 and 5 μ M, induced the late apoptosis up to 8.6±0.8%, 19.0±4.3% and 35.3±4.0% as compared to DMSO control (7.3±3.0%). Likewise, etoposide at 10 μ M induced the late apoptosis significantly up to 27.5±3.0%. Of note HD ZWM 978 is more potent than etoposide in inducing apoptotic cell death process and it mediates cytotoxicity by causing apoptotic cell death mechanism.

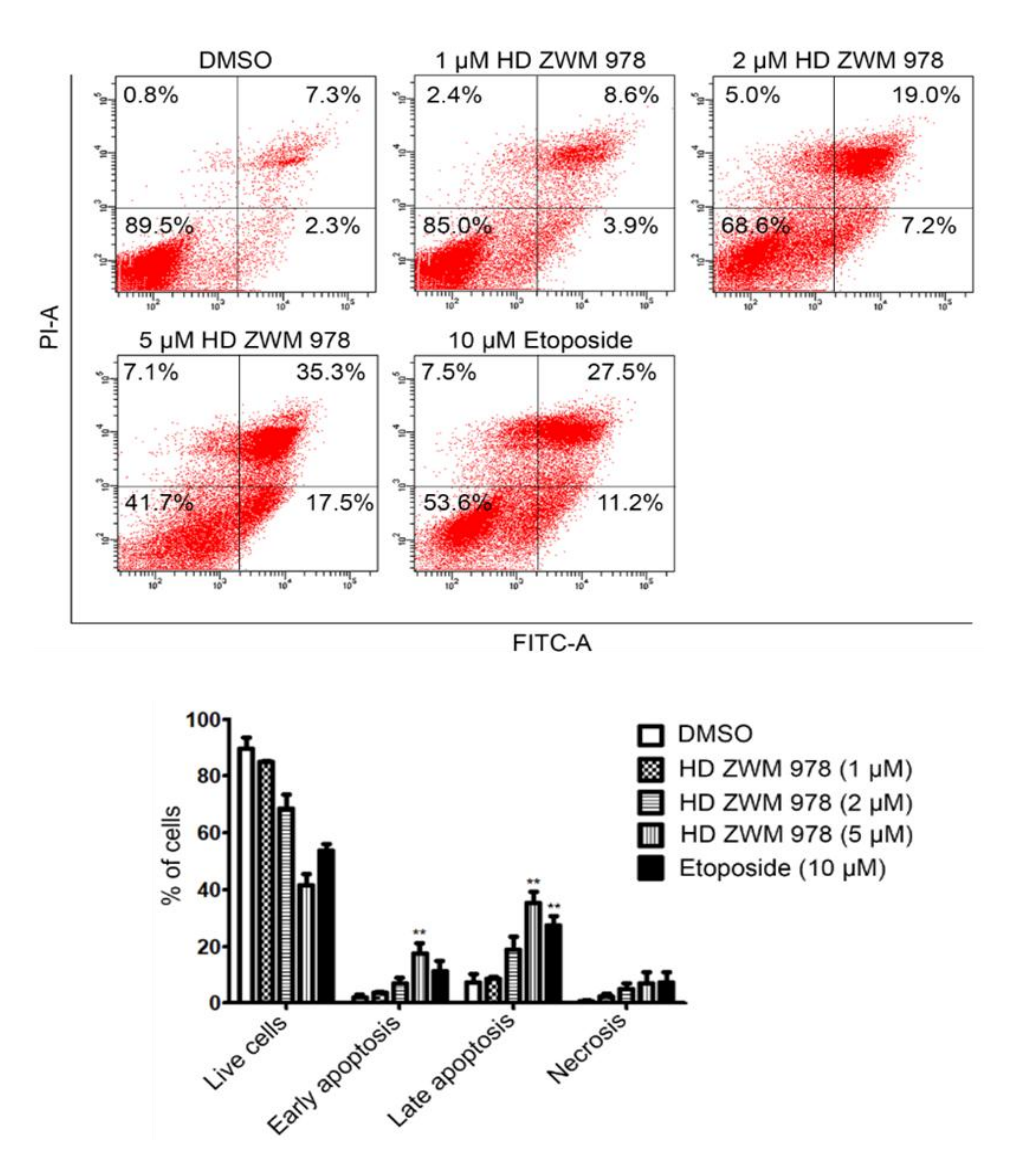


Figure 2.3 HD ZWM 978 induces apoptosis in AGS cells. (Upper) Cells were treated with HD

ZWM 978 and etoposide at the indicated concentrations for 48 h, stained by Annexin V-FITC and PI, and analyzed by flow cytometry. (Lower) Percentage of cell population in each conditions. Data are means \pm SEM of three independent experiments. **p<0.01 significantly different from vehicle control (Turkey's multiple comparison test)

2.1.3 Inhibition of human topoisomerase II α activity by HD ZWM 978

To investigate the underlying molecular mechanisms of HD ZWM 978 induced apoptosis, its inhibition on topoisomerase II α enzyme activity was conducted using supercoiled plasmid DNA relaxing assay. Etoposide (a first line topoisomerase II α poison drug) was used as a positive control. As shown in Fig. 2.4, lane 2 represents the supercoiled PBR322 DNA without Topo II enzyme. HD ZWM 978 and Etoposide inhibited the Topo II enzyme activity in a dose-related manner. HD ZWM 978 at 10 μ M fully inhibited the topoisomerase II α enzyme activity. Of note, etoposide at 10 μ M partially inhibited the enzyme activities. The topoisomerase II α activity was fully inhibited at the concentration as high as 50 μ M. This result suggests that HD ZWM 978 was acting as a Topo II inhibitor and it is more potent than etoposide. This finding was consistent with its cytotoxic and apoptotic effects that HD ZWM 978 exhibited greater effect than etoposide.

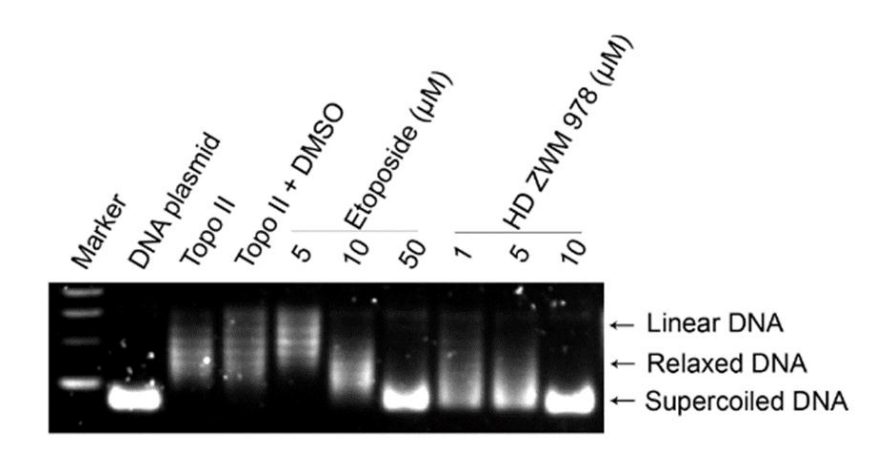


Figure 2.4 The inhibitory effects of HD ZWM 978 and etoposide on topoisomerase $II\alpha$ enzyme activity. Supercoiled pBR322 plasmid were incubated with human topoisomerase $II\alpha$ alpha enzyme at indicated concentrations of HD ZWM 978 and etoposide at 37° C for 1 h. The samples were electrophoresed using 1% agarose gel, stained with SYBR safe dye and photographed under gel documentation machine.

$\,$ 2.1.4 Effect of HD ZWM 978 on the induction of DNA damage by in human gastric cancer cells

Inhibition of topoisomerase II α activity results apoptosis cell death partly through DNA damage. We therefore investigated the effect of HD ZWM 978 on induction

DNA damage in human gastric cancer cell lines. The expression of γ -H2A.X, DNA damage marker, was determined by western blotting after treatment with various concentrations of HD ZWM 978 and etoposide. HD ZWM 978, and etoposide at the concentrations of 2, 4 and 8 μ M markedly increased the expression of γ -H2A.X in a dose-related manner in MKN45 cell line (Fig.2.5). Similarly, treatment with 2 μ M of HD ZWM 978 and etoposide increased the expression of γ -H2A.X protein in AGS cells. Of note, HD ZWM 978 was more potent in inducing DNA damage than the clinically used etoposide in both the gastric cancer cell lines. This finding correlates with the previous results and suggests that HD ZWM 978 induces apoptosis in GC cells partially through the inhibition of topoisomerase II α enzyme activity.

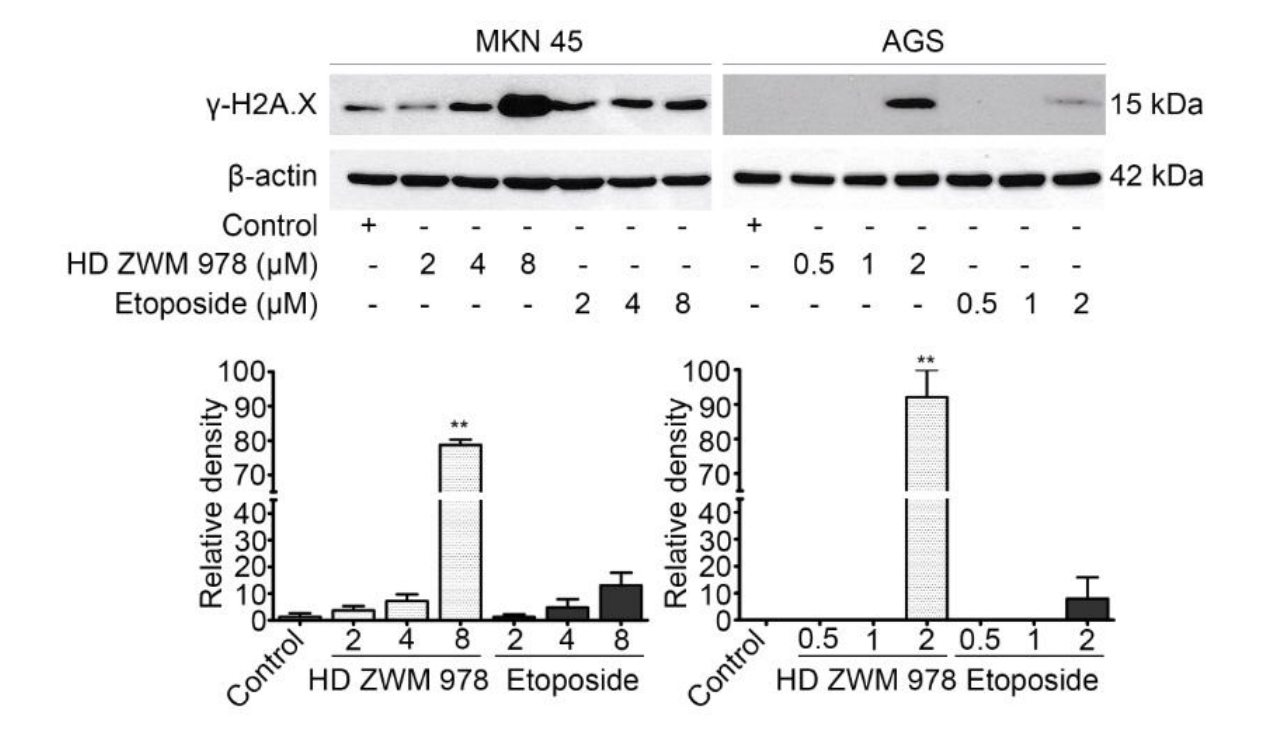


Figure 2.5 DNA damage induced by HD ZWM 978 and etoposide in gastric cancer cell lines (MKN 45 and AGS cells). Cells were treated with HD ZWM 978 and etoposide at indicated concentrations for 24 h. Levels of γ -H2A.X protein were detected from total protein lysates by western blotting. β-actin was used as the loading control. Bar graph represents the relative calculated density, normalized with β-actin. **p<0.01 significantly different from vehicle control (Turkey's multiple comparison test).

2.1.5 Inhibitory effect of HD ZWM 978 on WNT/ β -catenin signaling pathway in gastric cancer in gastric cancer cells

Aberrant activation of WNT/ β -catenin signaling pathway is one of major cause of gastric cancer development and progression. To investigate whether anticancer property of

HD ZWM 978 involvement with inhibition of WNT/ β -catenin signaling pathway, the effects of HD ZWM 978 on β -catenin proteins expression, transcriptional activity-mediated by β -catenin were investigated. The inhibitory effect of HD ZWM 978 on β -catenin protein expression was investigated by using western blotting in both AGS and MKN45 gastric cancer cells. As shown in Fig. 2.6, the expression of β -catenin protein was reduced slightly in MKN 45 cells whereas in AGS cells, treatment with 1 and 2 μ M of HD ZWM 978 significantly reduced the expression of β -catenin

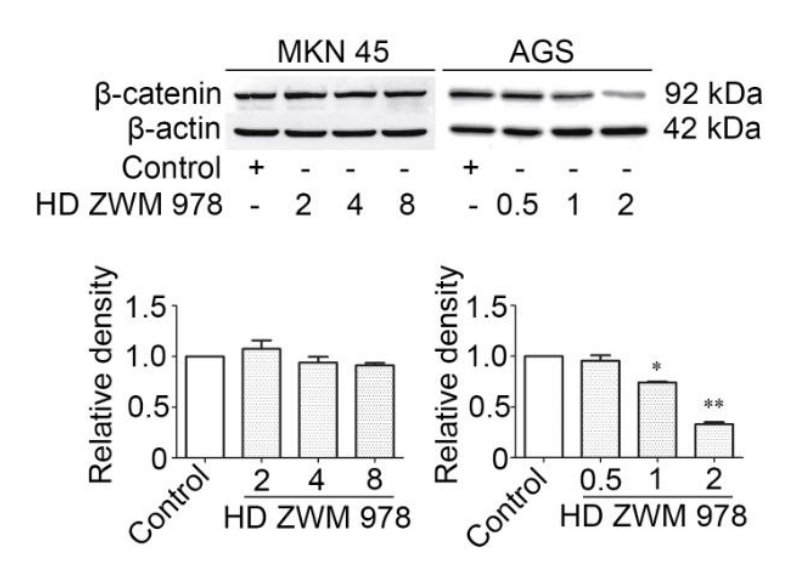


Figure 2.6 Effect of HD ZWM 978 on the expression of β-catenin protein in gastric cancer cells after treatment for 24 h. The expression of β-catenin was determined using western blotting. β-actin was used as the loading control. Three independent experiments yielded similar results. Bar graph represents the relative calculated density, normalized with β-actin. *P<0.05, **p<0.01 significantly different from vehicle control (Turkey's multiple comparison test).

To further investigate the inhibitory effect on WNT/ β -catenin signaling pathway by HD ZWM 978, the effects on c-MYC mRNA expression, a WNT/ β -catenin target gene, was determined using real time quantitative (Fig. 7). The expression of c-MYC mRNA was decreased after treatment with HD ZWM 978 at 4 and 8 μ M for MKN 45 cells; and 2 μ M for AGS cells. This result suggests that HD ZWM 978 has a modulating effect on the expression of WNT responsive gene and is consistent with the previous results in which the compound inhibits the expression of key WNT signaling molecule β -catenin.

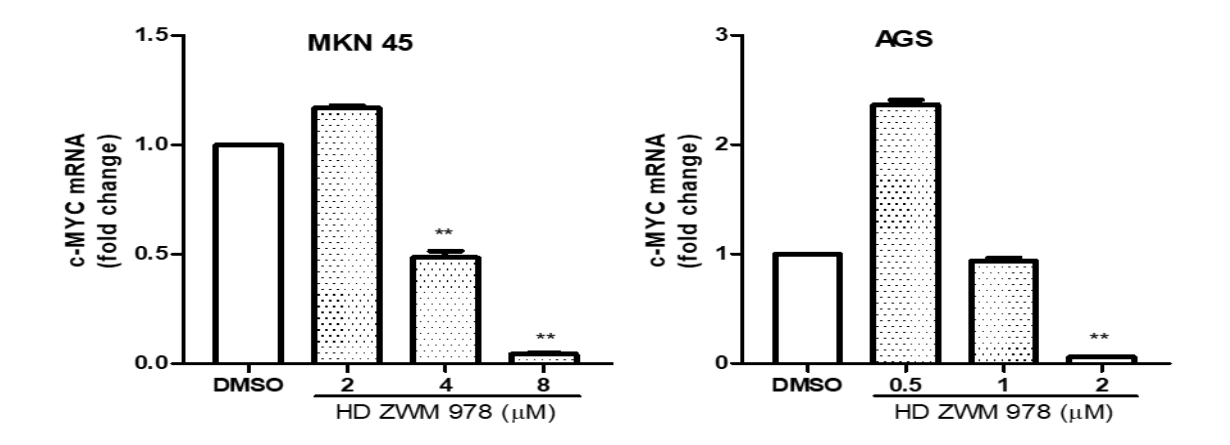


Figure 2.7 Effect of HD ZWM 978 on the expression of WNT/β-catenin target gene. MKN45 and AGS cells were treated with indicated concentration of HD ZWM 978 for 24 hours. Total RNAs were extracted and the expression of c-MYC was analyzed by real time quantitative PCR.

2.1.6 Effect on the expression of protein survivin by HD ZWM 978 in gastric cancer cells

Survivin, a member of inhibitor of apoptosis (IAP) protein family, is frequently found to be overexpressed in cancer that caused apoptosis resistance-induced by anticancer agents. To confirm the effect of tested compound on apoptosis induction, we next tested the effect of HD ZWM 978, and etoposide on the expression of survivin in gastric cancer cells (Fig. 2.4). MKN 45 cells were treated with HD ZWM 978 and etoposide at 2, 4 and 8 μ M for 24 h. HD ZWM 978, and etoposide significantly decreased survivin expression in a dose related manner. In addition, AGS cells, the more sensitive cells, were treated with lower concentrations of compounds, 0.5,1 and 2 μ M. Similar to MKN 45 cells, treatment with either HD ZWM 978 or etoposide significantly decreased survivin expression in a dose related manner. These results indicate that HD ZWM 978 inhibits the expression of survivin and thereby promotes apoptosis in gastric cancer cells. Survivin is also a WNT/ β -catenin target gene and inhibition of survivin expression might be a resulted from the consequence of inhibition of WNT signaling by HD ZWM 978 in both the AGS and MKN 45 gastric cancer cell lines.

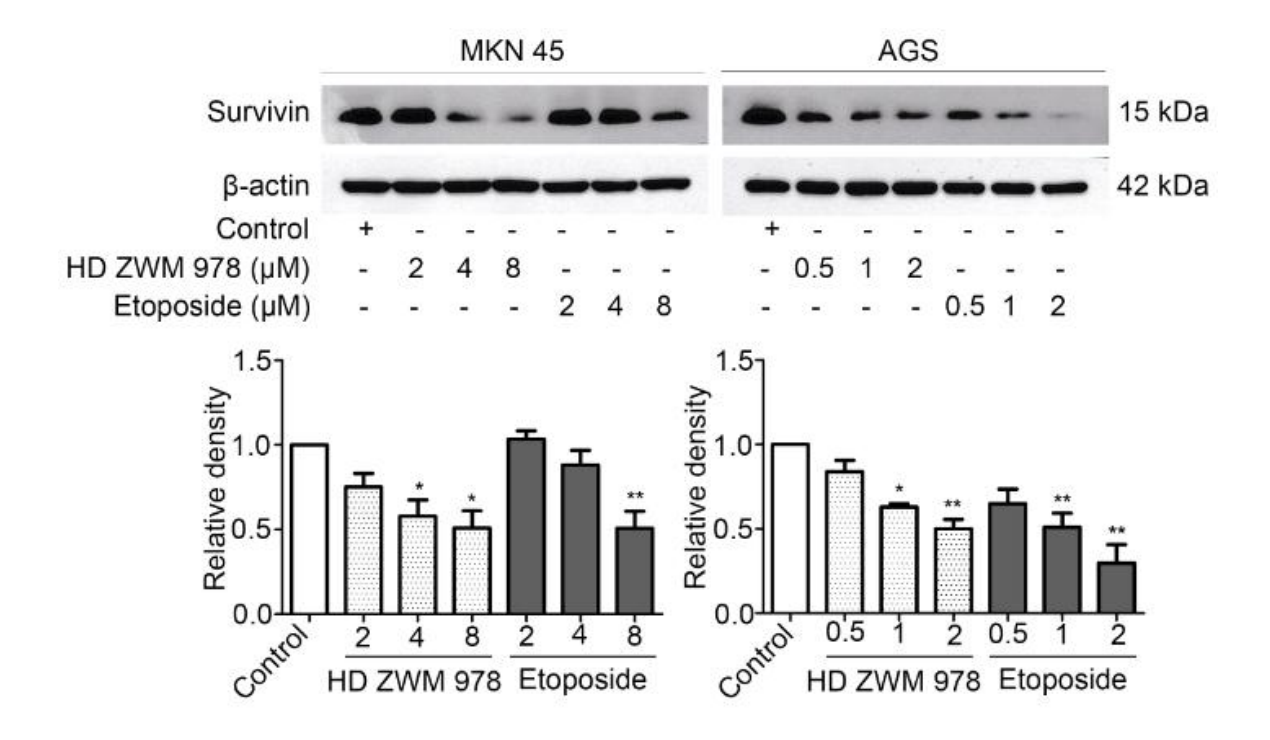


Figure 2.8 The effect of HD ZWM 978 and etoposide on the expression of survivin protein in gastric cancer cell lines; MKN 45 and AGS cells. After treatment with indicated concentrations for 24 h, total proteins were extracted and analyzed for survivin protein expression by western blotting. β-catenin was used as a loading control. Bar graph represents the relative calculated density, normalized with β-catenin. *p<0.05, **p<0.01 significantly different from vehicle control (Turkey's multiple comparison test).

2.2 Anticancer effects of Andrographolide analogue 6 on gastric cancer cell lines. (Andrographolide analogue 6 was kindly provided by Asst. Prof. Rungnapha Saeeng, Burapha University)

2.2.1 The cytotoxic effects of Andrographolide Analogue 6 on gastric cancer cell lines, MKN 45 and AGS

Andrographolide and its analogue 6 (19-triisopropyl-andrographolide) were investigated for their cytotoxic activities in MKN 45 gastric cancer cells. Both compounds exhibited cytotoxic activities in a dose- and time- related manner at 24, 48 and 72 h. The IC50 values of Analogue 6 were 8.8 \pm 2.2, 6.3 \pm 0.7 and 5.6 \pm 0.2 μ M at 24, 48 and 72 h, respectively (table 2.4) whereas that of the parent Andrographolide was >50 μ M at 24 and 48 h and 36.3 \pm 5.9 μ M at 72 h. Notably analogue 6 was more cytotoxic than the parent compound. IC50 values of etoposide, a positive control, at 24, 48 and 72 h were >50, 28.5 \pm 4.4 and 12.6 \pm 0.2 μ M, which was less potent than the Analogue 6. This results shows that Analogue 6 was more cytotoxic than the parent Andrographolide and etoposide. Similarly, the cytotoxic effect of Andrographolide, Analogue 6 and etoposide were also

investigated in AGS cell lines. These compounds exhibited dose dependent cytotoxic effects as shown in table 2.4. At 24 h, Andrographolide, Analogue 6 and etoposide were observed to be cytotoxic with IC₅₀ values of 21.5±6, 1.9±0.09 and 19.6±0.9 μ M respectively. The cytotoxic activities of these compounds increased at 48 hours with IC₅₀ values of 11.3±2.9, 1.7±0.05 and 4.0±0.5 μ M. At 72 h, their cytotoxicity further increased with IC₅₀ values of 13.3±1.4, 1.8±0.1 and 1.9±0.3 μ M. More importantly, the cytotoxicity of Analogue 6 was greater than the parent compound and clinically used etoposide. The molecular mechanism of Analogue 6 was further investigated in details.

Table 2.4 Cytotoxicity (IC₅₀ values) of Analogue 6 against gastric cancer cell lines. Data are means \pm SEM of three independent experiments performed in triplicates.

Cell lines	Incubation time	IC ₅₀ (μM)					
	(h)	Etoposide	Andrographolide	Analogue 6			
	24	19.6 ± 0.9	21.5 ± 6.0	1.9 ± 0.09			
MKN 45	48	4.08 ± 0.5	11.3 ± 2.9	1.7 ± 0.05			
	72	1.9 ± 0.3	13.3 ± 1.4	1.8 ± 0.1			
	24	>50	>50	8.8 ± 2.2			
AGS	48	28.5 ± 4.4	>50	6.3 ± 0.7			
	72	12.6 ± 0.2	36.3 ± 5.9	5.6 ± 0.2			

2.2.2 Analysis of induction of apoptosis by Andrographolide analogue 6 in human gastric cancer cell.

AGS cells are more sensitive to Analogue 6 and was chosen for further investigation. The effects of Andrographolide and Analogue 6 on apoptosis induction in AGS human gastric cancer cells were investigated by flow cytometry (Fig. 2.9). Analogue 6 at a concentration of 1, 2 and 5 μ M induced late apoptosis up to 10.7±0.5%, 28.2±4.6% and 60.4±6.5% as compared to DMSO control (9.0±3.2%), respectively. Conversely, the parent Andrographolide at 10 μ M induced up to 11.6±1.4% and etoposide (positive control) induced late apoptosis up to 34.7±0.5%. Taken together these results suggest that Analogue 6 mediated cytotoxicity is through apoptotic cell death mechanism.

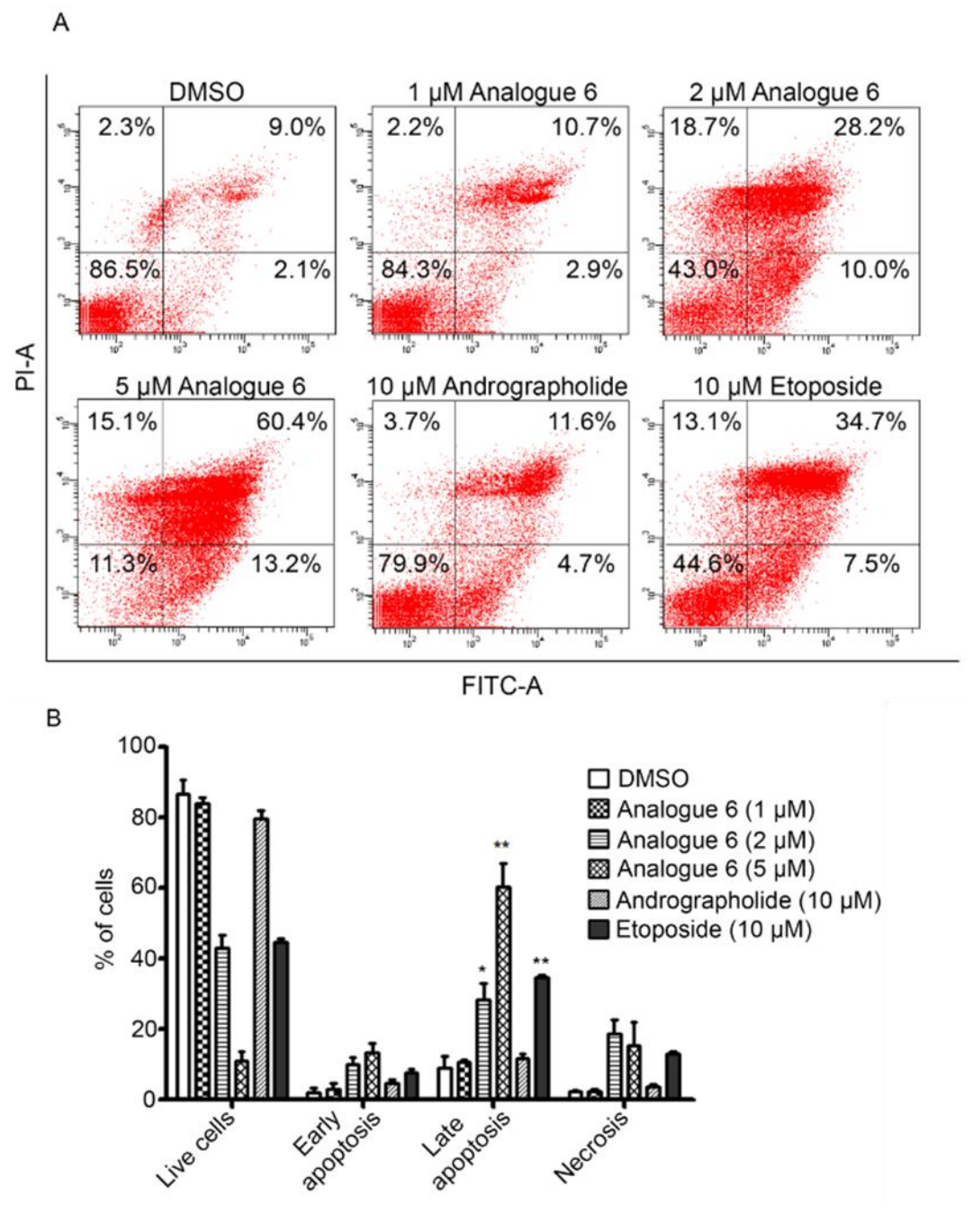


Figure 2.9 Analogue 6 induces apoptosis in AGS cells. (A) Cells were treated with indicated concentrations of Analogue 6, Andrographolide and etoposide for 48 h. (B) Percentage of cell population in each conditions. Data represents mean \pm SEM of three independent experiments. *p<0.05 and **p<0.01 are significantly different from vehicle control (Turkey's multiple comparison test).

2.2.3 The effects of Analogue 6 on DNA damage induction and inhibition of Topoisomerase II α enzyme expression in gastric cancer cells

To further investigate the underlying molecular mechanism involved in the induction of apoptosis by Analogue 6, western blotting was used to detect the expression of protein involved with DNA damage response (Fig. 2.10). Analogue 6 at the concentration of

1, 2 and 10 μ M induced DNA damage in a dose related manner in MKN 45 and AGS cells demonstrated by an increase in the expression of γ -H2A.X protein. Notably, the parent Andrographolide and etoposide at 10 μ M were less potent than that of Analogue 6. As Analogue 6 has previously been demonstrated to inhibit human topoisomerase II α activity in cell-free system (Nateewattana et al., 2013). We therefore examined the inhibitory effect of Analogue 6 on topoisomerase II α expression in the AGS gastric cancer cells. Analogue 6 at the concentration of 2 μ M and etoposide at 20 μ M markedly decreased the expression of topoisomerase II α at 4 h after the treatment as compared to the DMSO control (Fig. 2.11). The expression of topoisomerase II α was not decreased at 6, 12 and 24 h after exposure to andrographolide analogue 6. Collectively, these results suggest that GC apoptosis-induced by Analogue 6 is, at least, through Topo II mediated DNA damage.

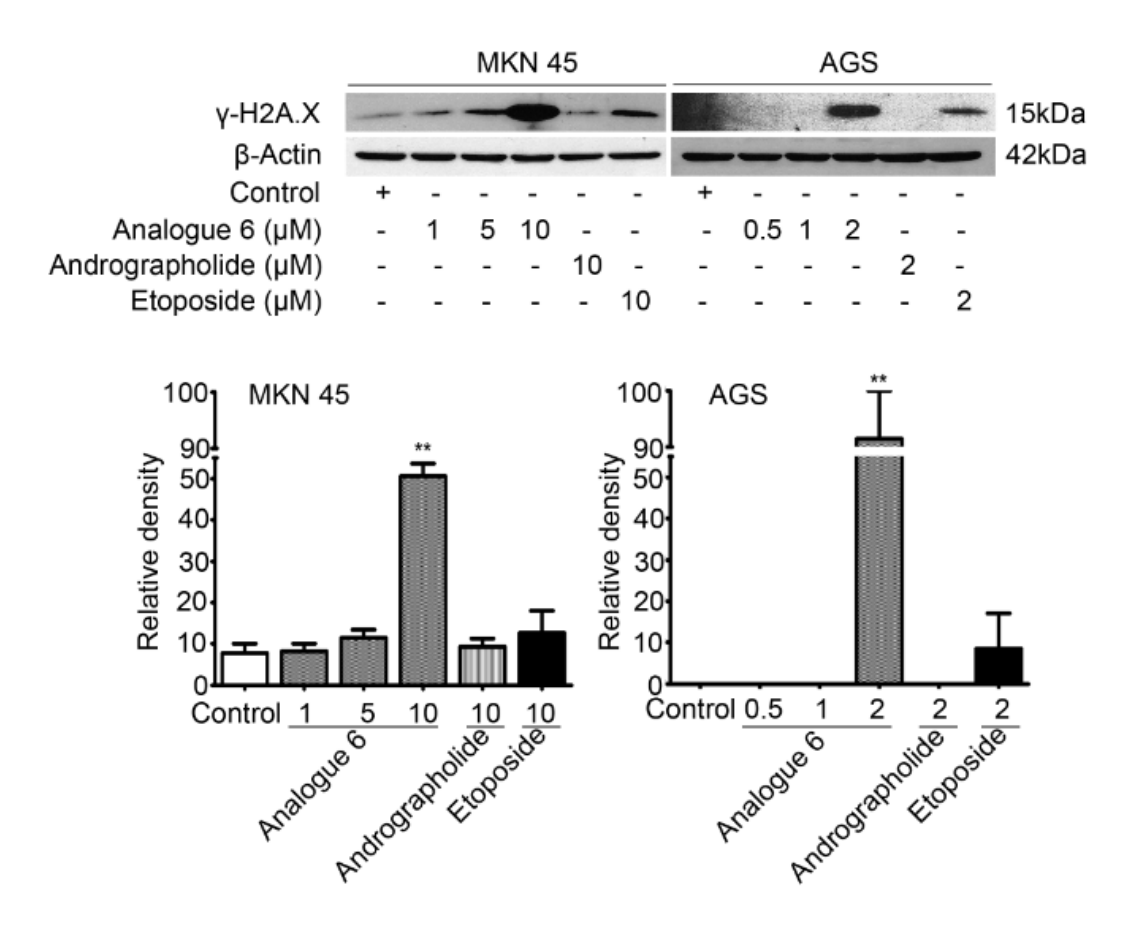
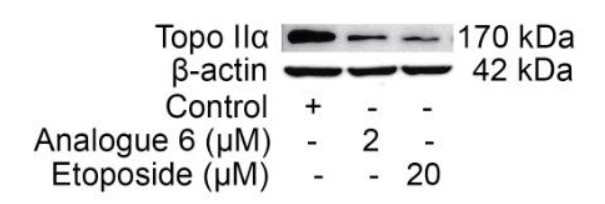


Figure 2.10 DNA damage induced by andrographolide analogue 6 in gastric cancer cell lines. MKN 45 and AGS cells were treated with indicated concentrations of Andrographolide, Analogue 6 and Etoposide for 24 h. Levels of γ -H2A.X were detected from total protein lysates by western blotting. β-actin was used as the loading control. Bar graph represents the relative calculated density, normalized with β-actin. Data are means ± SEM of three independent experiments. **p<0.01 indicates significantly different from vehicle control (Turkey's multiple comparison test).



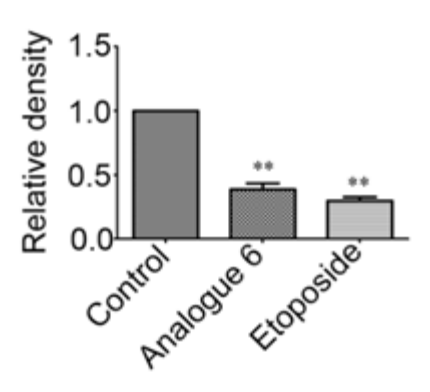


Figure 2.11 Inhibitory effect of Andrographolide analogue 6 on Topoisomerase II α expression in AGS cells after 4 h of treatment. β -actin was used as loading control. Bar graph represents the relative calculated density, normalized with β -actin. Data are means \pm SEM of three independent experiments. **p<0.01 indicates significantly different from vehicle control (Turkey's multiple comparison test).

2.2.4 The effects of Analogue 6 on proteins involved in apoptosis in human gastric cancer cells

Cleavage products of PARP-1 and caspase 3 actively participates in apoptosis pathway. We next investigated the effects of Analogue 6 on PARP-1 and caspase 3 cleavage. As shown in Fig. 2.12, treatment with 2 µM of Analogue 6 for 24 h markedly induced PARP-1 protein cleavage. Whereas the parent andrographolide and etoposide at 2 µM did not induced the PARP-1 cleavage. In addition, Caspase 3 protein cleavage was also increased in a dose related manner by treatment of indicated concentrations of Analogue 6. Andrographolide and etoposide were less effective in activation of caspase 3 protein. Moreover, Analogue 6 and parent andrographolide did not alter the expression of tumor suppressor protein p53 (Fig.2.13). While etoposide undoubtedly increased the expression of p53 as compared to the DMSO control. This results suggests that Analogue 6 induces AGS gastric cancer cells apoptosis via caspase 3-dependent and p53-independent pathway.

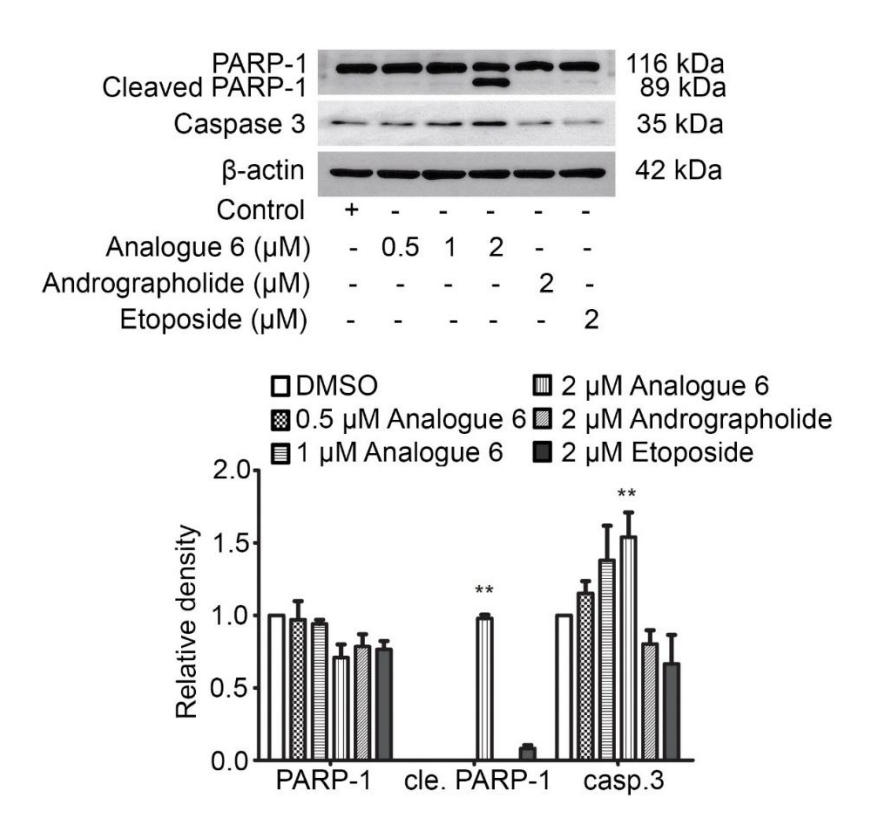


Figure 2.12 Effects of Andrographolide analogue 6 on the proteins involved in apoptosis pathway; PARP-1, cleaved PARP-1 (cle. PARP-1) and caspase 3 in AGS cells. Western blotting was used to detect the expression of apoptotic involved proteins. β-actin was used as a loading control. Bar graph represents the relative calculated density, normalized with β-actin. The results were obtained from three independent experiments. **p<0.01 indicates significantly different from vehicle control (Turkey's multiple comparison test).

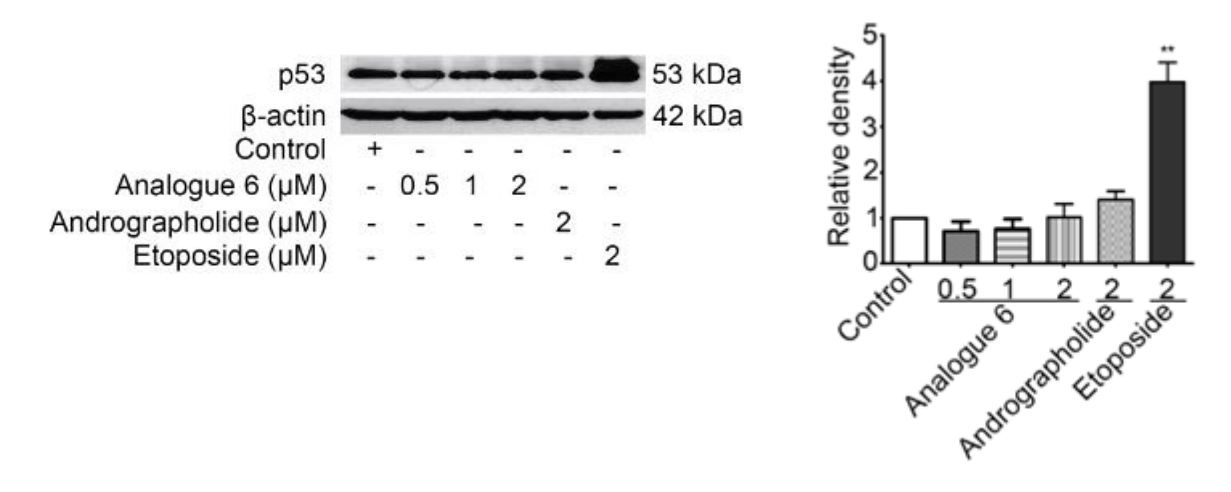


Figure 2.13 Effects of Andrographolide analogue 6 on the proteins involved in apoptosis pathway; tumor suppressor protein p53 in AGS cells. Various concentration of Analogue 6, parent Andrographolide, and Etoposide were used for treatment of the cells for 24 h and western blotting was used to detect the expression of p53. β -actin was used as a loading control and the results were obtained from three independent experiments. Bar graph

represents the relative calculated density, normalized with β -actin. **P<0.01 indicates significantly different from vehicle control (Turkey's multiple comparison test).

2.4 Anti-cancer effects of an andrographolide analogues, 3A.1 or 19-tert-butyldiphenylsilyl-8,17-epoxy andrographolide kindly provided by Asst. Prof. Rungnapha Saeeng, Burapha University.

2.4.1 Cytotoxic potency of analogue 3A.1.

Cytotoxicity of analogue 3A.1 was investigated in three CRC cell lines; HT29, HCT116, and SW480. Doxorubicin was used as a positive control. Cells were treated with analogue 3A.1 at various concentrations for 24, 48 or 72 h. By using MTT viability assay, the most sensitive cell line to analogue 3A.1 is HT29 with an IC50 value of 11.10 \pm 1.37 μM at 24 h of treatment, whereas those of HCT116, and SW480 cells are 16.10 \pm 2.10 and 18.18 \pm 2.91 μM , respectively (Table 5). IC50 values of analogue 3A.1, parent andrographolide and doxorubicin in HT29 cells at various time points are demonstrated in Table 6. The results show that analogue 3A.1 decreases cellular viability in dose, and time-related manners, which its cytotoxicity is much more potent than that of the parent andrographolide (IC50 = 46.12 \pm 2.89 μM at 24 h). These results indicate a potent anti-cancer activity of analogue 3A.1 in CRC cells.

Table 2.5 Cytotoxicity (IC $_{50}$ values) of analogue 3A.1 against colorectal cancer cell lines. Data are means \pm SEM of three independent experiments.

CRC cell lines	IC ₅₀ (μM)						
	24 h	48 h	72 h				
HT29	11.10 ± 1.37	4.66 <u>+</u> 0.67	3.21 <u>+</u> 0.33				
HCT116	16.10 <u>+</u> 2.10	4.78 <u>+</u> 1.22	4.32 <u>+</u> 1.28				
SW480	18.18 <u>+</u> 2.91	4.97 <u>+</u> 0.99	3.36 <u>+</u> 1.43				

Table 2.6 Comparison the IC_{50} values (μ M) of analogue 3A.1 with andrographolide and doxorubicin in HT29 cells. Data are means \pm SEM from three independent experiments

Compounds	IC ₅₀ (μM)					
	24 h 48 h 72 h					
Analogue 3A.1	11.10 ± 1.37	4.66 ± 0.67	3.21 ± 0.33			
Andrographolide	46.12 ± 2.89	29.89 ± 3.53	24.45 ± 3.80			
Doxorubicin	26.15 ± 1.17	3.83 ± 0.65	1.59 ± 0.71			

2.4.2 Effect of analogue 3A.1 on the induction of cellular apoptosis

The involvement of anti-cancer effects of analogue 3A.1 with induction of apoptotic cell death was evaluated by using flow cytometry. Doxorubicin was used as a positive control. As shown in Fig. 2.14, analogue 3A.1 at 10 μ M induced apoptotic cell death significantly in HT29 cells after 24 h of treatment. Cells treated with a positive control, doxorubicin, at 10 μ M obviously induced more number of necrotic cells death. This finding suggests that anti-cancer activity of analogue 3A.1 is involved with the induction of HT29 cell death via apoptosis mechanism.

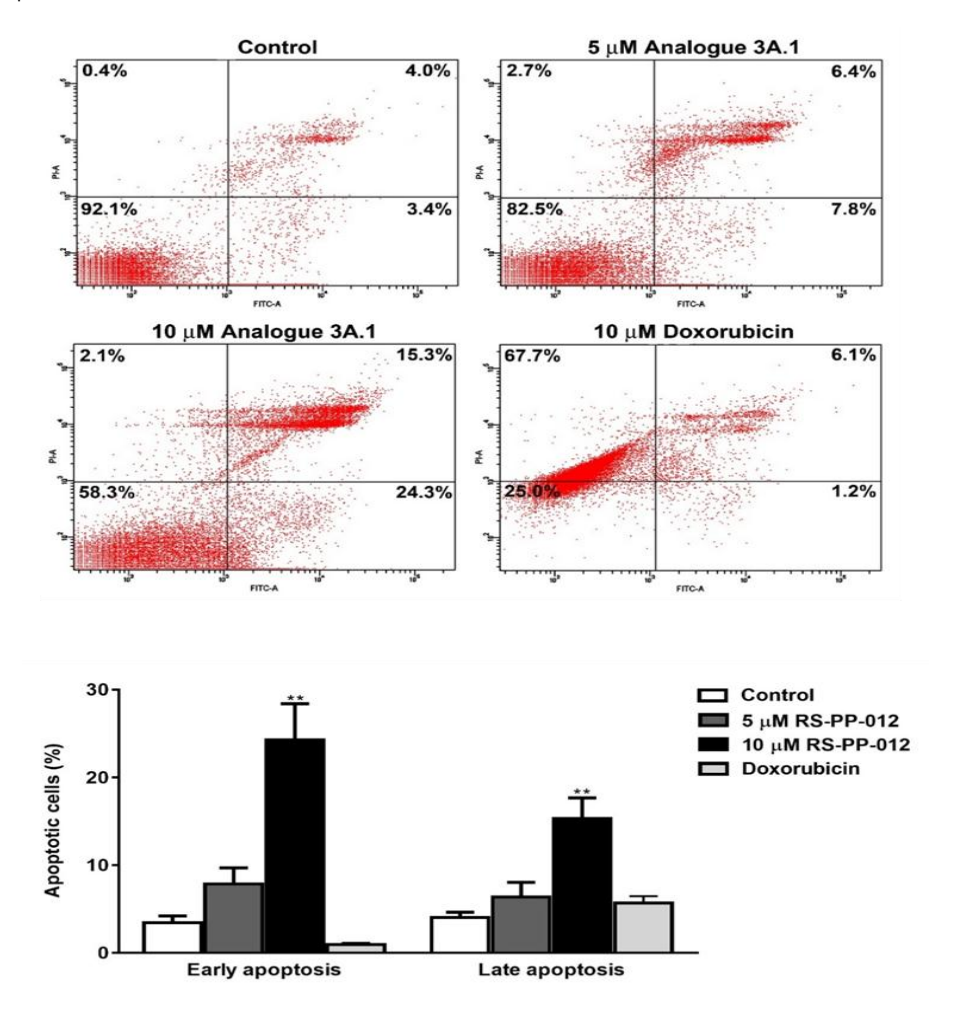


Figure 2.14 Effect of analogue 3A.1 on HT29 cell apoptosis. Cells were treated with analogue 3A.1 (5, and 10 μ M), or doxorubicin (10 μ M), stained with Annexin V-FITC, and PI before analyzing by flow cytometry. Bar graph represents percentage of apoptotic cells in each conditions. Data are means \pm SEM (n=3). **p<0.01 indicates significantly different compared with the vehicle control.

Proteins that are activated by DNA strand breaks upon the cellular apoptosis were investigated. A nuclear enzyme poly (ADP-ribose) polymerase-1 (PARP-1) catalyzes

repairing process single-strand DNA breaks was examined. Corresponding to the results from flow cytometry, analogue 3A.1 at concentrations of 2.5, 5, and 10 μ M increase levels of cleaved PARP-1 in HT29-treated cells in a dose-dependent manner (Fig. 2.15 A-C). Moreover, a marker of DNA damage, the phosphorylated H2AX (ser139) or γ -H2AX was up-regulated at 24 h of post-treatment with analogue 3A.1 (Fig.2.15 A and D). These results indicate that analogue 3A.1 essentially induced apoptotic cell death with profound increases in markers of DNA damage.

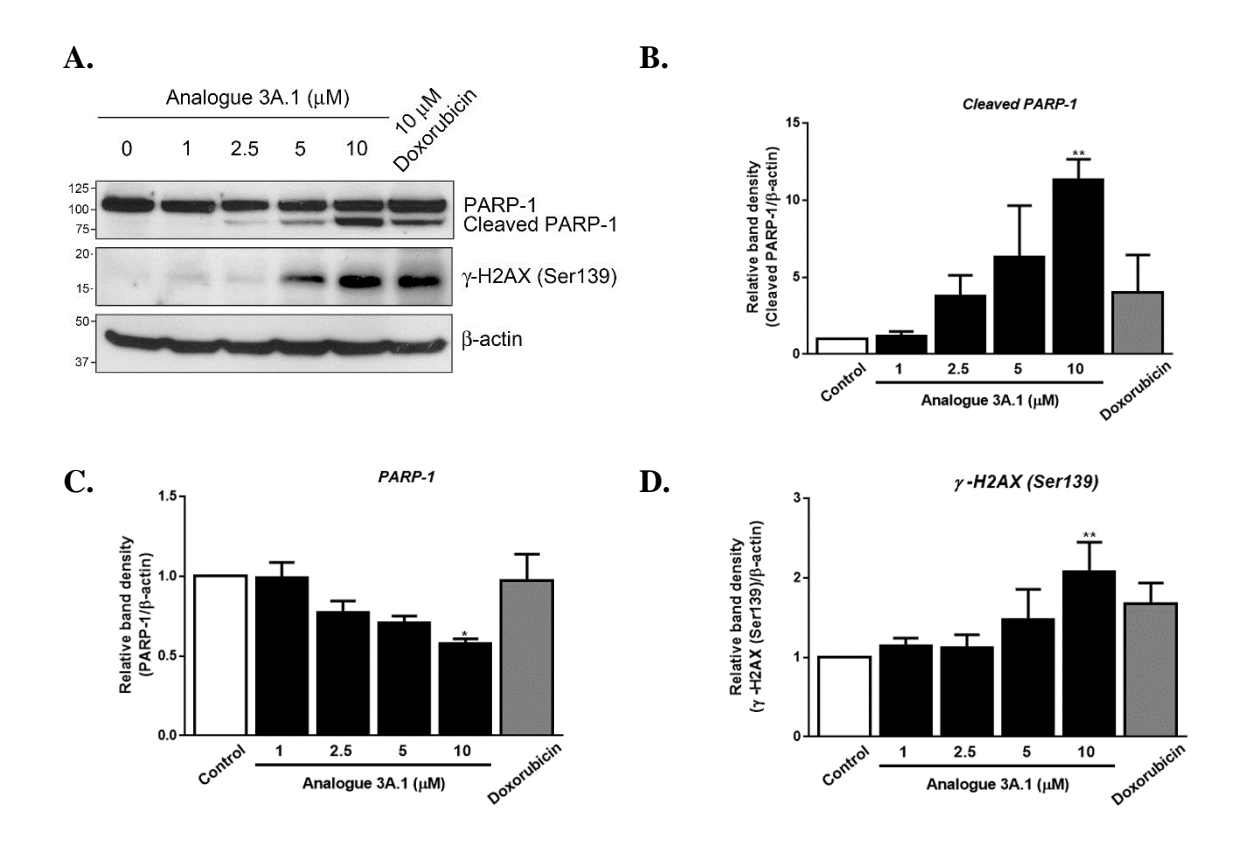


Figure 2.15 Effect of analogue 3A.1 on the expression of proteins related to DNA damage in cell death. (A) HT29 cells were treated with various concentrations of analogue 3A.1 or doxorubicin (10 μM) for 24 h. Total cell lysates were extracted and subjected to western blotting with anti-PARP-1 and anti-γ-H2AX. β-actin serves as a loading control. (B-D) The normalized band intensities are shown as means \pm SEM (n=3). *p<0.05 and **p<0.01 indicate significantly different compared with the vehicle control.

2.4.3 Effect of analogue 3A.1 on the inhibition of Wnt/ β -catenin signaling

The effect of analogue 3A.1 on the transcriptional activity and protein expression of Wnt signaling were investigated. In Fig. 2.16, the TOPflash luciferase activity induced by β -catenin overexpression in HEK293T cells was markedly inhibited by analogue 3A.1 as compared with control. While the luciferase activity of FOPflash, a mutant of TCF/LEF

binding site for β -catenin, was not affected, suggesting the specific suppressive function of analogue 3A.1 on Wnt/ β -catenin activity. In addition, the effect on expression of Wnt-responsive genes which play the important roles in CRC progression were further determined. As shown in Fig. 2.17A-D, the mRNA expression levels of Wnt target genes, *c-Myc*, *CCDN1*, *SURVIVIN*, and *MMP7*, are decreased with increasing concentrations of analogue 3A.1 in HT29 cells. This finding indicates to the inhibitory activity of analogue 3A.1 in Wnt/ β -catenin signaling pathway at transcriptional level.

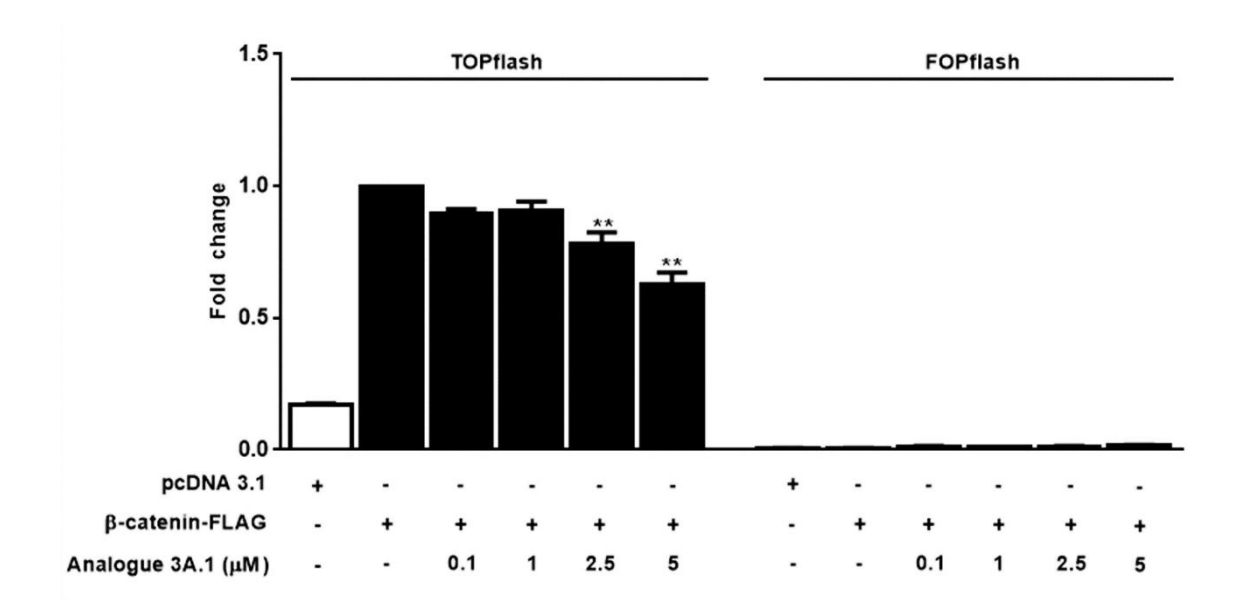


Figure 2.16 Effects of analogue 3A.1 on TCF/LEF reporter activity. HEK293T cells were transiently transfected with β-catenin-FLAG or pcDNA3.1, and TOPflash or FOPflash, and *Renilla* luciferase reporter plasmids. After transfection, cells were incubated with analogue 3A.1 for 24 h. The relative firefly luciferase activity units (RLUs) were then measured and normalized corresponding to *Renilla* luciferase activity. Bar graph is the fold change compared with β-catenin-FLAG-transfected cells and represented as means \pm S.E.M (n=3) (**p<0.01).

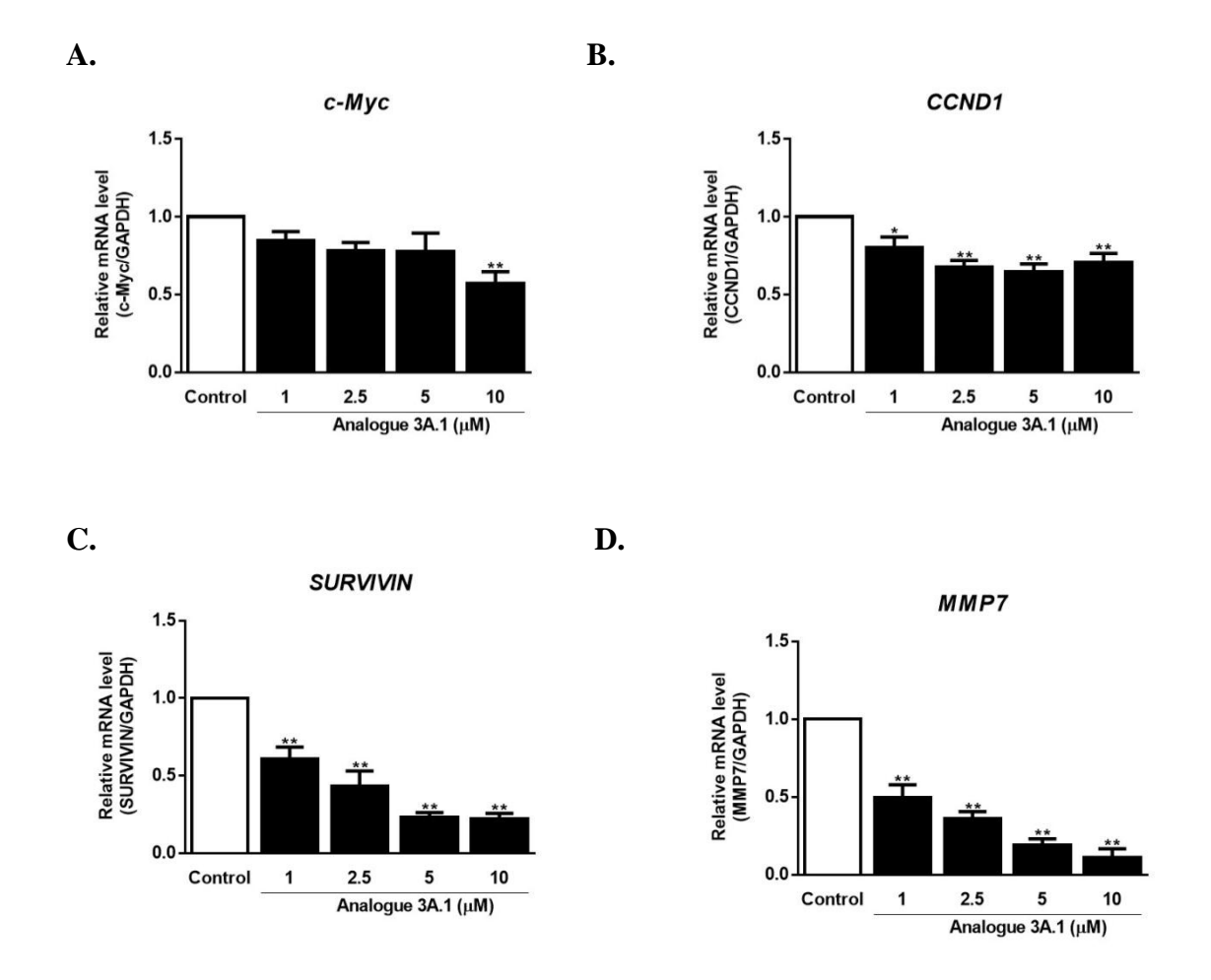


Figure 2.17 Effects of analogue 3A.1 on the expressions of downstream target genes of Wnt/β-catenin signaling pathway. Quantitative real-time PCR showing the concentration-dependent reduction in mRNA expression of Wnt target genes: (A) c-Myc, (B) CCDN1, (C) SURVIVIN, and (D) MMP7 in HT29 cells after treatment with analogue 3A.1 for 24 h. The relative mRNA expression was quantified and normalized with GAPDH. Data are means \pm S.E.M (n=3). *p<0.05 and **p<0.01 compared with the vehicle control.

Summary:

Part I: Screening for cytotoxic activity of natural products from Chinese Marine Microbes and Thai Medicinal Plants.

Under research corroboration through Thailand Research Fund (TRF) and Natural Science Foundation of China (NSFC), we obtained natural-derived compounds from Thai and Chinese scientist. The cytotoxic effects of these compounds were determined by using the colorimetric MTT assay against several cancer cell lines. We obtain several compounds with great cytotoxic effects against cancer cell lines and were selected for further mechanistic study in part II.

Part II: Identification the molecular mechanisms and molecular target of the candidate compounds.

The present study was to investigate the anticancer effects of the natural derived compounds, the marine Actinobacterium secondary metabolite HD ZWM 978 and an Andrographolide analogue 6, in gastric cancer cells.

HD ZWM 978 exhibited potent dose related cytotoxic effects on both the gastric cancer cell lines. Notably, the cytotoxicity of HD ZWM 978 was more potent than the clinically used Etoposide. Mechanically study, the cytotoxic effect of HD ZWM 978 in gastric cancer cells is via induction of apoptosis. Further investigations on the underlying molecular mechanism have found that HD ZWM 978 inhibited the activity of topoisomerase II α enzyme concomitant with the induction of DNA damage. Aberrant activation of WNT/ β -catenin signaling pathway is one of major cause of gastric cancer development and progression. To investigate whether anticancer property of HD ZWM 978 involvement with inhibition of WNT/ β -catenin signaling pathway, the effects of HD ZWM 978 on β -catenin proteins expression, transcriptional activity-mediated by β -catenin were investigated. We found that WNT/ β -catenin activity was inhibited by HD ZWM 978 treatment as demonstrated by the suppression of β -catenin protein and WNT/ β -catenin target gene (survivin and c-myc) expressions. Our results indicate that HD ZWM 978 induces gastric cancer cell apoptosis partly through (i) induction of DNA damage-mediated by topoisomerase II α enzyme inhibition and (ii) inhibition of WNT/ β -catenin signaling pathway (Fig. 2.18).

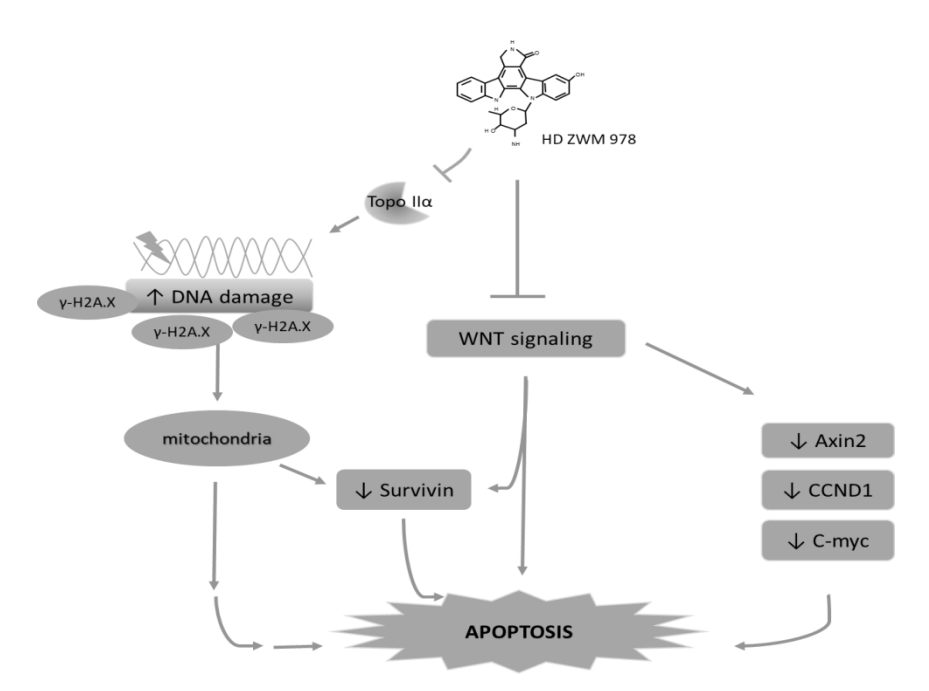


Figure 2-18 Diagramm showing the probable mechanistic action of HD ZWM 978 in gastric cancer cells.

Andrographolide analogue 6 showed the cytotoxic effects against two gastric cancer cells MKN45 and AGS. Interestingly, Analogue 6 was more potent than the parent Andrographolide compound as well as the clinically used etoposide. Mechanistically, Analogue 6 induced apoptosis in AGS gastric cancer cells as demonstrated by an increase in cleaved PARP-1 and caspase 3 products after treatment. Moreover, the apoptosis promoting of Andrographolide analogue 6 is probably through induction of DNA damage-induced by an inhibition of Topo II enzyme (Fig. 2.19).

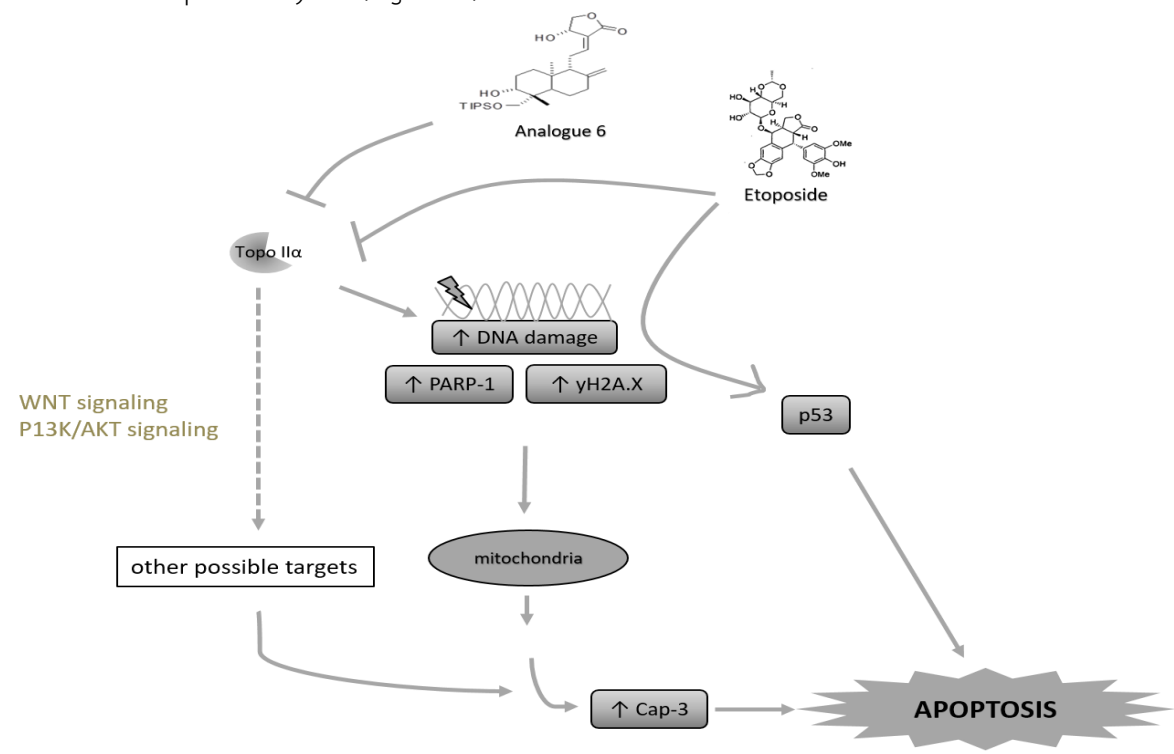


Figure 2.19 Diagram showing the potential mechanistic pathway of Analogue 6 in gastric cancer cells

In the present study, the anticancer effects and mechanisms of andrographolide analogue 3A.1 in colorectal cancers (CRC) were investigated. Analogue 3A.1 is highly toxic in three CRC cell lines; HT29, HCT116, and SW480 and they are more potent than that of parent compound (andrographolide). Analogue 3A.1 induced cell apoptosis and increased the expression of proteins related to DNA damage; PARP-1 and γ -H2AX. 3. Mechanistically, this analogue inhibited Wnt/ β -catenin signaling pathway demonstrated by suppressed TCF/LEF-mediated transcriptional activity of Wnt/ β -catenin signaling in HEK293T cells and suppression the expressions of Wnt target genes; *c-myc*, *CCDN1*, *SURVIVIN*, and *MMP7* in HT29 cells (Fig. 2.20). Thus, this compound has potential to be developed as the chemotherapeutic agents to target malignancies harboring hyperactivated Wnt/ β -catenin signaling.

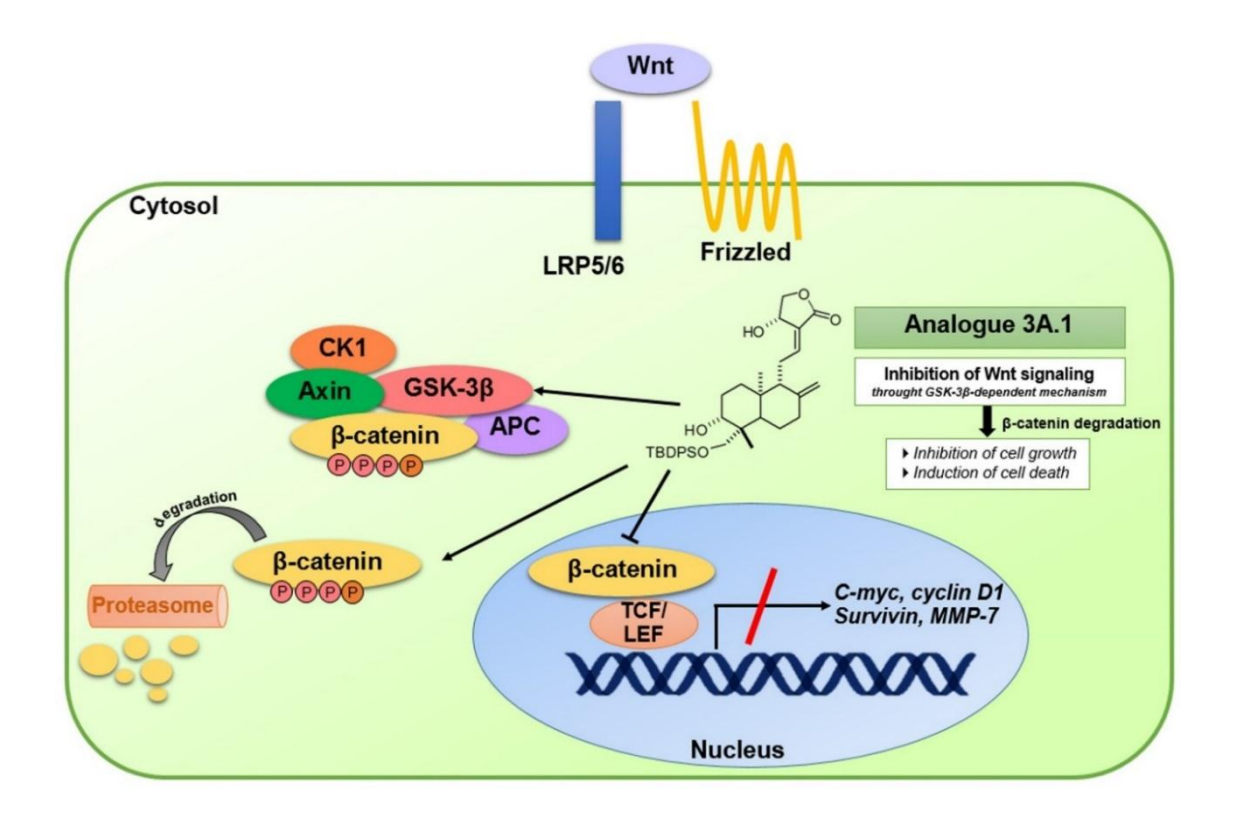


Figure 2.20 Schematic diagram representing the molecular mechanism of analogue 3A.1 on Wnt/ β -catenin signaling pathway in HT29 cells.

References:

- 1. Amado, N.G., Predes, D., Moreno, M.M., Carvalho, I.O., Mendes, F.A., and Abreu, J.G. (2014). Flavonoids and Wnt/beta-catenin signaling: potential role in colorectal cancer therapies. International journal of molecular sciences *15*, 12094-12106.
- 2. Barker, N., and Clevers, H. (2006). Mining the Wnt pathway for cancer therapeutics. Nature reviews Drug discovery *5*, 997-1014.
- 3. Berger, N.A., Savvides, P., Koroukian, S.M., Kahana, E.F., Deimling, G.T., Rose, J.H., Bowman, K.F., and Miller, R.H. (2006). Cancer in the elderly. Transactions of the American Clinical and Climatological Association *117*, 147-155; discussion 155-146.
- 4. Campisi, J. (2013). Aging, cellular senescence, and cancer. Annual review of physiology *75*, 685-705.
- 5. da Rocha, A.B., Lopes, R.M., and Schwartsmann, G. (2001). Natural products in anticancer therapy. Current opinion in pharmacology *1*, 364-369.
- 6. Gordon, M.D., and Nusse, R. (2006). Wnt signaling: multiple pathways, multiple receptors, and multiple transcription factors. The Journal of biological chemistry *281*, 22429-22433.
- 7. Kathawala, R.J., Gupta, P., Ashby, C.R., Jr., and Chen, Z.S. (2015). The modulation of ABC transporter-mediated multidrug resistance in cancer: a review of the past

- decade. Drug resistance updates : reviews and commentaries in antimicrobial and anticancer chemotherapy 18, 1-17.
- 8. Molinski, T.F., Dalisay, D.S., Lievens, S.L., and Saludes, J.P. (2009). Drug development from marine natural products. Nature reviews Drug discovery *8*, 69-85.
- 9. Nateewattana, J., Dutta, S., Reabroi, S., Saeeng, R., Kasemsook, S., Chairoungdua, A., Weerachayaphorn, J., Wongkham, S., and Piyachaturawat, P. (2014). Induction of apoptosis in cholangiocarcinoma by an andrographolide analogue is mediated through topoisomerase II alpha inhibition. European journal of pharmacology *723*, 148-155.
- 10. Nateewattana, J., Saeeng, R., Kasemsook, S., Suksen, K., Dutta, S., Jariyawat, S., Chairoungdua, A., Suksamrarn, A., and Piyachaturawat, P. (2013). Inhibition of topoisomerase II alpha activity and induction of apoptosis in mammalian cells by semi-synthetic andrographolide analogues. Investigational new drugs *31*, 320-332.
- 11. Nitiss, J.L. (2009). Targeting DNA topoisomerase II in cancer chemotherapy. Nature reviews Cancer *9*, 338-350.
- 12. Perez-Herrero, E., and Fernandez-Medarde, A. (2015). Advanced targeted therapies in cancer: Drug nanocarriers, the future of chemotherapy. European journal of pharmaceutics and biopharmaceutics: official journal of Arbeitsgemeinschaft fur Pharmazeutische Verfahrenstechnik eV.
- 13. Puntawee, S., Theerasilp, M., Reabroi, S., Saeeng, R., Piyachaturawat, P., Chairoungdua, A., and Nasongkla, N. (2015). Solubility enhancement and in vitro evaluation of PEG-b-PLA micelles as nanocarrier of semi-synthetic andrographolide analogue for cholan-giocarcinoma chemotherapy. Pharmaceutical development and technology, 1-8.
- 14. Sirion, U., Kasemsook, S., Suksen, K., Piyachaturawat, P., Suksamrarn, A., and Saeeng, R. (2012). New substituted C-19-andrographolide analogues with potent cytotoxic activities. Bioorganic & medicinal chemistry letters *22*, 49-52.
- 15. Wang, Z., Ravula, R., Cao, M., Chow, M., and Huang, Y. (2010). Transporter-mediated multidrug resistance and its modulation by Chinese medicines and other herbal products. Current drug discovery technologies *7*, 54-66.
- 16. Wanitchakool, P., Jariyawat, S., Suksen, K., Soorukram, D., Tuchinda, P., and Piyachaturawat, P. (2012). Cleistanthoside A tetraacetate-induced DNA damage leading to cell cycle arrest and apoptosis with the involvement of p53 in lung cancer cells. European journal of pharmacology *696*, 35-42.
- 17. Zhao, P., Dai, M., Chen, W., and Li, N. (2010). Cancer trends in China. Japanese journal of clinical oncology 40, 281-285.

Sub-project 3: Anti-diabetic effect of compounds

ABSTRACT

Kidney plays is one of the most important organ regulating blood glucose by reabsorption of filtered glucose from glomerulus via renal glucose transporters located at renal proximal tubular cells. Sodium glucose cotransporter (SGLT) 2 inhibition has been found to be anti-diabetic drug target for type 2 diabetes, all SGLT2 inhibitors have same core structure as same as phlorizin (first SGLT2 inhibitor). So, it is interesting to find a new SGLT2 inhibitor from natural for diabetic treatment. First, the inhibitory effect of 134 compounds was screened by uptake assay in human renal proximal cell line (HK-2 cell) using [3H]-2deoxy-d-glucose (2DG) as radioactive substrate. 3 marines (HD-ZWM-1081, HD-ZWM-1083, HD-ZWM-1084) inhibited SGLT2 in HK-2 cells with cytotoxicity effect. Kaempferia parviflora extract (KPE) and Boesenbergia pandurata extract (BPE) were found to inhibit SGLT2mediated $[^{3}H]$ -2DG uptake in HK-2 cell with IC₅₀ of 124 and 211 µg/ml, respectively. Moreover, effect of KPE and BPE on glucose transporter (GLUT) 2 inhibition was examined. KPE and BPE inhibited GLUT2-mediated [³H]-2DG uptake with IC₅₀ of 71.59 and 190.9 µg/ml, respectively. Selectivity of hit compounds was tested by examining effects of hit compounds on SGLT1 and GLUTs inhibition in enterocytes (Caco-2 cell). KPE did not inhibit SGLT1 while BPE significant inhibited SGLT1. Both KPE and BPE had no effect on GLUTs inhibition. The effect of KPE and BPE on anti-hyperglycemia was examined in diabetic rat (Goto Kakizaki (GK) rat). Orally administration of KPE and BPE reduce plasma glucose without changing plasma insulin indicating the therapeutic potential for type 2 DM treatment. In addition to the therapeutic potential application of *Boesenbergia pandurata* on diabetes, compounds from this plant panduratin A and pinostrobin showed protective effect of nephrotoxicity induced by drug including cisplatin, anti-cancer, and antibiotic drug, colistin. The protective effect of these compounds were mediated by decrease in ROS, pro-apoptotic proteins, ERK and caspases, and mitochondria damage. Collectively, panduratin A and pinostrobin have potential protective effect on nephrotoxicity induced by cisplatin and colistin.

Keywords: Diabetes; Sodium glucose co-transporter 2; flavonoids; kidney injury; *Boesenbergia pandurata*

บทคัดย่อ

ไตเป็นหนึ่งในอวัยวะที่สำคัญในการควบคุมระดับน้ำตาลกลูโคสในเลือด โดยการควบคุมการดูดกลับกลูโคสที่ ผ่านการกรองจากโกลเมอรูลัสโดยอาศัยการทำงานของตัวจนส่งกลูโคสที่เซลล์ของหลอดไตส่วนต้น การยับยั้ง การทำงานของตัวขนส่งตัวโคสชนิด Sodium glucose cotransporter (SGLT) 2 จึงเป็นหนึ่งเป้าหมายในการ ลดระดับน้ำตาลในเลือดเพื่อรักษาโรคเบาหวานชนิดที่ 2 ยารักษาโรคเบาหวานกลุ่ม SGLT2 inhibitors นั้นมี โครงสร้างพื้นฐานมาจากสาร phlorizin ซึ่งเป็น SGLT2 inhibitor ตัวแรก ดั้งนั้นจึงเป็นที่น่าสนใจที่จะค้นหา สารที่มีฤทธิ์ยับยั้ง SGLT2 ที่มีโครงสร้างอื่นๆจากสารธรรมชาติ โดยเริ่มทำการทดสอบฤทธิ์ของสาร 134 ตัว ใน การยับยั้ง SGLT2 โดยการวัดการขนส่ง [³H]-2-deoxy-d-elucose (2DG) ในเซลล์หลอดไตส่วนต้นของมนุษย์ ชนิด HK-2 cells ที่มีการแสดงออกของ SGLT2 จากการทดสอบพบว่าสารจากทะเล 3 ชนิด ได้แก่ HD-ZWM-1081, HD-ZWM-1083, HD-ZWM-1084 มีฤทธิ์ยับยั้งการขนส่งของ [3 H]-2DG เข้าสู่เซลล์ อย่างไรก็ ตามสารทั้ง 3 ชนิดมีความเป็นพิษต่อเซลล์ สารสกัดจากกระชายดำ Kaempferia parviflora และกระชาย Boesenbergia pandurate มีฤทธิ์ยับยั้ง SGLT โดยการยับยั้งการขนส่งสาร $[^3H]$ -2DG เข้าสู่เซลล์หลอดไต ส่วนต้น ด้วยค่า IC₅₀ ที่ 124 และ 211 µg/ml ตามลำดับ นอกจากนี้ยังพบว่าสารสกัดทั้ง 2 มีฤทธิ์ยับยั้งตัว ขนส่งกลูโคสชนิด GLUT2 ด้วยค่า IC₅₀ ที่ 71.59 และ 190.9 µg/ml ตามลำดับ เนื่องจากเซลล์ HK-2 มีการ แสดงอองทั้ง SGLT1 และ SGLT2 ดังนั้นจึงทำการทดสอบว่าสารสกัดทั้งสองมีฤทธิ์ต่อ SGLT1 หรือไม่ โดยทำ ทำการวัดการขนส่ง [³H]-2DG ในเซลล์ลำไส้ชนิด CaCo-2 ซึ่งมีการแสดงออกของ SGLT1 แต่ไม่พบการ แสดงออกของ SGLT2 จากผลพบว่าสารสกัดจากกระชายดำไม่มีฤทธิ์ยับยั้งการทำงานของ SGLT1 ขณะที่สาร สกัดจากกระชายมีฤทธิ์ยับยั้งการทำงานของ SGLT1 ด้วย อย่างไรก็ตามไม่พบฤทธิ์ของสารทั้งสองต่อการ ทำงานของ GLUT ของเซลล์ลำไส้ ฤทธิ์ลดระดับน้ำตาลในเลือดของสารสกัดกระชายดำและกระชายได้รับการ ทดสอบในหนูที่เป็นโรคเบาหวานชนิดที่ 2 พบว่าสารสกัดกระชายดำและกระชายมีฤทธิ์ลดระดับน้ำตาลใน เลือดโดยไม่มีผลเปลี่ยนแปลงระดับฮอร์โมนอินซูลิน ดังนั้นสารสกัดกระชายดำและกระชายอาจมีศักยภาพใน การรักษาโรคเบาหวานขนิดที่ 2 ได้ นอกเหนือจากฤทธิ์ต้านเบาหวานของสารสกัดจากกระชาย สารแพนดูรา ้ตินเอ และสารไพโนสโทรบิน ซึ่งเป็นสารที่แยกได้จากสารสกัดกระชายมีฤทธิ์ลดการเกิดความเป็นพิษต่อไตจาก การได้รับยาต้านมะเร็งซิสพลาตินและยาปฏิชีวนะโคลิสติน ฤทธิ์ต้านความเป็นพิษต่อไตของสารแพนดูราตินเอ และสารไพโนสโทรบิน เกิดจากการลดการเกิด ROS โปรตีนกระตุ้นการตายของเชลล์ ได้แก่ ERK และ caspases และการลดการทำลายไมโตคอนเดรีย ดังนั้นสารทั้งสองมีสักยภาพในการพัฒนาเพื่อเป็นสารสำหรับ ้ของกันความเป็นพิษต่อไตจากการใช้ยาต้านมะเร็งซิสพลาตินและยาปฏิชีวนะโคลิสติน

คำสำคัญ โรคเบาหวาน ตัวขนส่งกลูโคส 2 ฟลาโวนอยด์ ความเป็นพิษต่อไต กระชาย

INTRODUCTION

Diabetes mellitus (DM) is a group of metabolic disorder, which is more prevalent in elderly. The causes of T2DM are resulted from the defects in insulin secretion and/or insulin action. Approximately 2.8% of the population worldwide suffers from T2DM and it may reach 5.4% by the year 2025 (Wild, 2004). The prevalence of T2DM increases with age and it affects nearly 1 in 5 individuals over the age of 65 years. Blood glucose control is

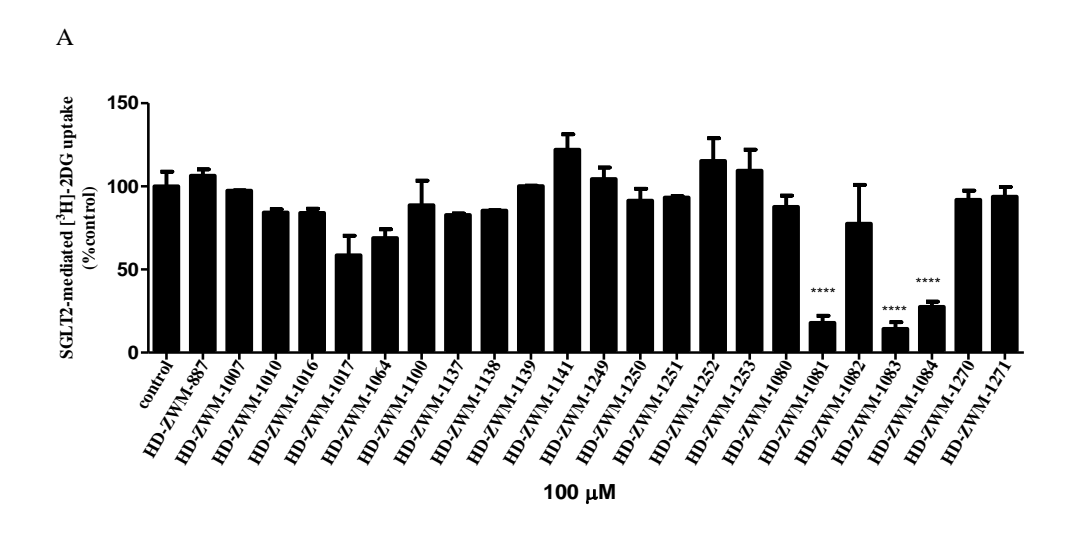
fundamental to diabetes management and is proven to reduce the risk of developing its complications. Therefore, antihyperglycemic agents are a key component of treatment strategies. A number of oral anti-diabetic agents are commercial available. However, adverse effects including hypoglycemia, weight gain and edema are frequently reported. A number of new antidiabetes drug classes have emerged over the past decade, the most recent being the sodium glucose co-transporter-2 (SGLT2) inhibitors. Inhibition of SGLT2 has generated the greatest pharmacological interest partly because SGLT2 reabsorbs the majority of glucose and also because it is expressed predominantly within the kidney and is, therefore, not expected to have off-target effects. A number of SGLT2 inhibitors have been developed based on the structure of phlorizin, a naturally occurring compound from the plant. Therefore, the natural products have high potential to show an inhibitory effect on SGLT2. Thailand and China possess a great diversity of natural materials; therefore, this research project will search for the potential compounds for treatment of type 2 diabetes from the natural sources of Thailand and China.

The scope of research work consists of three parts including 1) high-throughput screening for SGLT2 inhibitor and 2) investigation of the pharmacological effects of the potential compounds in a validated animal model of diabetes.

RESULTS

Screened for natural compounds inhibiting SGLT2 at renal proximal tubule

To obtain the natural compounds inhibiting SGLT2 activity, 134 natural compounds in the library which were tested for SGLT2 inhibitor. Natural compounds in the library can divide into 2 groups which are marine natural and plant compounds. The effect of natural compounds was screened by using glucose uptake assay. The human renal proximal tubule cell (HK-2 cell) was used as a model for in vitro study because this cell line highly express SGLT2 compared with SGLT1. HK-2 cells were seeded on 24 wells plate with 1:4 seeding ratio. The confluence cells were incubated with [³H]-2DG in present of 100 µM or µg/ml of natural compounds for 30 minutes. Accumulation of [³H]-2DG was measured to assess SGLT2 activity. Effect of 134 natural compounds comprising of 87 marine natural and 47 plant natural compounds on SGLT2 was determined. We found that 3 marines (HD-ZWM-1081, HD-ZWM-1083, HD-ZWM-1084) and *Kaempferia parviflora* extract (KPE), its active compound (DMF) and *Boesenbergia pandurata* extract (BPE), and its active compound (panduratin A) were found to inhibit SGLT2-mediated [³H]-2-DG uptake in screening experiment.



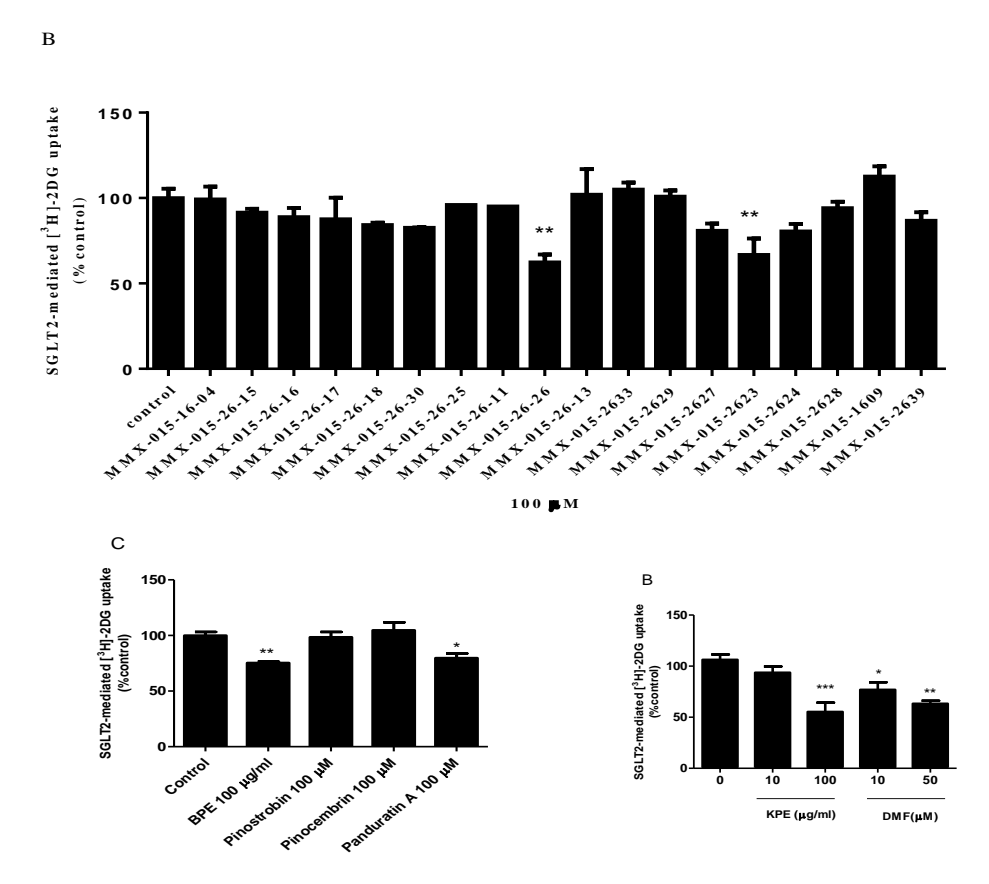


Figure 3.1 Screen for marine natural compounds inhibiting SGLT2-mediated [3 H]-2DG uptake in HK-2 cell. Data are shown as mean \pm SEM. One-way ANOVA *p<0.05, **p<0.01 compared to control.

Inhibitory potency of hit compounds on SGLT2-mediated glucose uptake in real proximal tubular cell.

To find inhibitory potency of hit compounds on SGLT2-meduated glucose uptake in human renal proximal tubular cell. Glucose uptake assay was performed using HK-2 cells.

The transport activity of SGLT2 was detected by measurement of $[^3H]$ -2DG accumulation. Cells were incubated with HD-ZWM-1081 (0-200 μ M), HD-ZWM-1083 (0-200 μ M), HD-ZWM-1084 (0-200 μ M), KPE (0-500 μ g/ml), BPE (0-200 μ g/ml), DMF, and panduratin A (0-200 μ M). As shownin Table 1, the IC $_{50}$ values of HD-ZWM-1081, HD-ZWM-1083, HD-ZWM-1084, KPE, and BPE were 41.73, 75.92, 208.1 μ M, 124, and 211.6 μ g/ml, respectively. Unfortunately, IC $_{50}$ of DMF and panduratin A could not be found because of low magnitude of inhibition. However, DMF at dose of 50-200 μ M significantly inhibited SGLT2-mediated $[^3H]$ -2DG uptake by ~20-30%. Inhibitory effect was not found in panduratin A treatment group.

Inhibitory potency of hit compounds on GLUT2-mediated glucose uptake in real proximal tubular cell.

Glucose reabsorption mechanism at human renal proximal tubule at S1 segment requires 2 steps of glucose transport. The first is to uptake glucose into cell by SGLT2 activity. Then glucose pass through blood circulation by GLUT2 (5). Moreover, in high glucose condition, high expression and translocation of GLUT2 to apical membrane were observed (86). So, inhibition of GLUT2 at renal proximal tubule may aid to reduce plasma glucose concentration in T2DM. To determine whether hit compounds inhibit GLUT2-mediated $\begin{bmatrix} ^3 \text{H} \end{bmatrix}$ -2DG uptake in human renal proximal tubular cell, glucose uptake assay was performed. Phlorizin at dose of 200 μ M was used to inhibit SGLT2 transport function. HK-2 cells were incubated with various doses of hit compounds. Cells were incubated with HD-ZWM-1081 (0-200 μ M), HD-ZWM-1083 (0-200 μ M), HD-ZWM-1084 (0-200 μ M), KPE (0-500 μ g/ml), BPE (0-200 μ g/ml), DMF, and panduratin A (0-200 μ M). As shown in figures 4.5. – 4.6, IC₅₀ of HD-ZWM-1081, HD-ZWM-1083, HD-ZWM-1084, KPE, and BPE were 42.58, 43.35, 384.1 μ M, 71.59, 190.9 μ g/ml, and 31.56 μ M, respectively. Panduratin A significantly inhibited GLUT2-mediated $\begin{bmatrix} ^3 \text{H} \end{bmatrix}$ -2DG uptake at doses of 50-200 μ M.

Table 3.1 IC_{50} of hit compounds in HK-2 cells

Companyoda	Half maximal inhibitory concentration (IC_{50})		
Compounds	SGLT2	GLUT2	
1. KPE (µg/ml)	124	71.59	
2. BPE (µg/ml)	211.6	190.9	
3. DMF (µM)	-	31.56	
4. Panduratin A (μM)	-	-	
5. HD-ZWM-1081 (μM)	41.73	42.58	
6. HD-ZWM-1083 (μM)	75.92	43.35	
7. HD-ZWM-1084 (μM)	208.1	384.1	

Cell viability of hit compounds

To test whether hit compounds direct inhibit transporter activity without causing toxicity, cell viability of 30 minutes' treatment of hit compounds were examined. Confluence HK-2 cells were treated with 0-200 µM HD-ZWM-1081, HD-ZWM-1083, HD-ZWM-1084, DMF, panduratin A or 0-200 µg/ml BPE or 0 – 500 µg/ml KPE for 30 minutes. As show in figures 4.7 - 4.8, HD-ZWM-1081, HD-ZWM-1083, and HD-ZWM-1084 caused cytotoxicity to cells after exposing for 30 minutes, fortunately, KPE, BPE, DMF, and panduratin A had no effect on cell viability. This indicated that reduction of SGLT2- or GLUT2-mediated [³H]-2DG uptake by HD-ZWM-1081, HD-ZWM-1083, and HD-ZWM-1084 was mediated by cytotoxicity and plant natural compounds (KPE, BPE, DMF, and panduratin A) direct inhibited SGLT2- or GLUT2-mediated [³H]-2DG uptake.

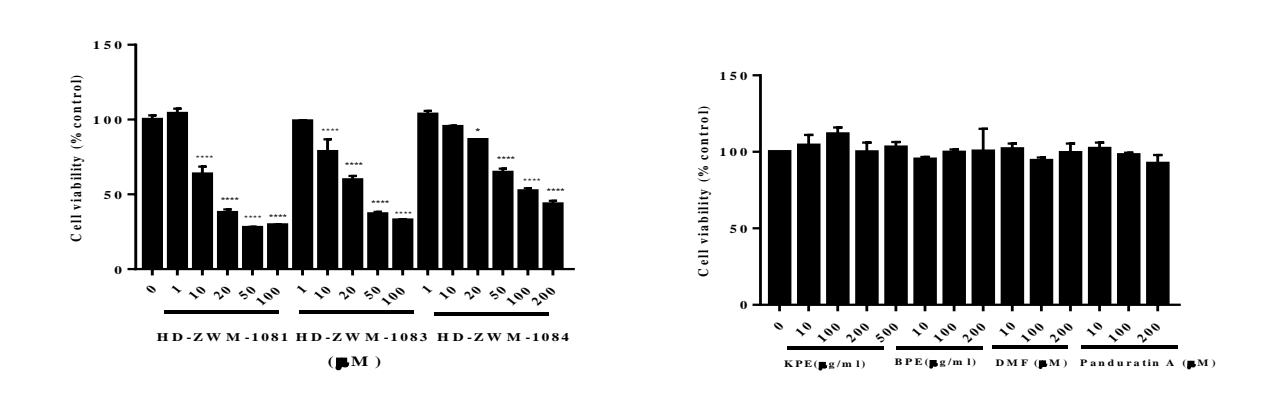


Figure 3.2 Effect of hit compounds on cell viability of HK-2 cells. Data are shown mean \pm SEM (****p<0.0001 compared with control).

Effects of hit compounds on SGLT1 and GLUT2 inhibition in enterocyte (Caco-2 cell)

To examine the selectivity of hit compounds in SGLT2 inhibition, effect of hit compounds on SGLT1 inhibition was examined in intestinal cell line (Caco-2 cell). Glucose uptake assay was performed, cytochalasin B was used to limited GLUT2 activity. KPE and BPE insignificant inhibited SGLT1 activity but not GLUT2 in Caco-2 cells.

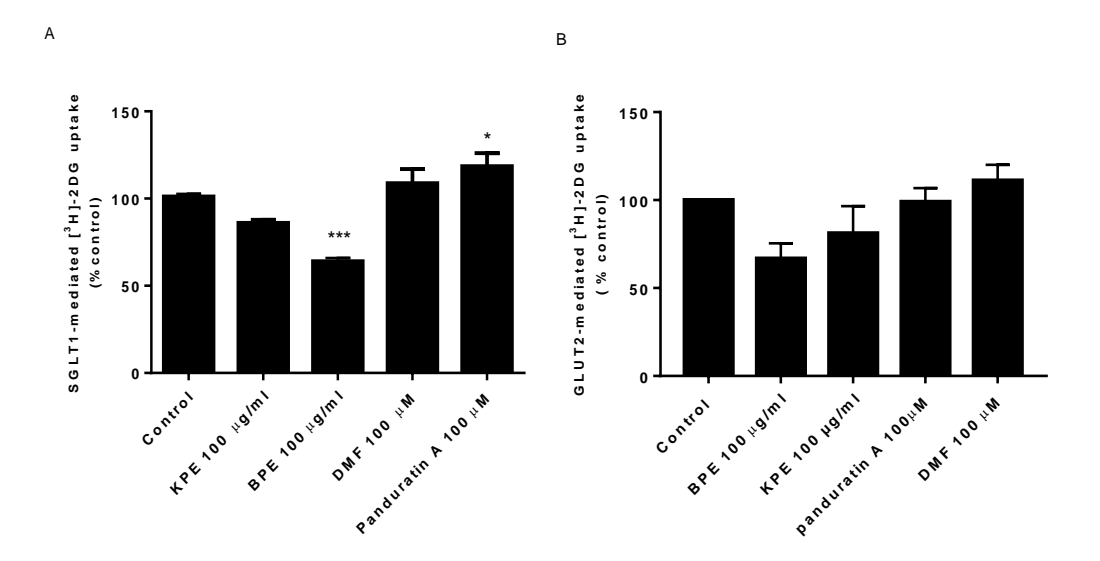
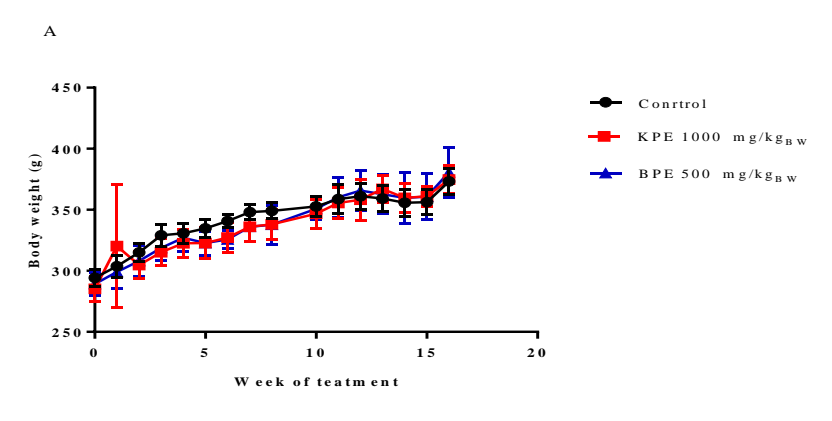


Figure 3.3 Effect of KPE, BPE, DMF, and panduratin A on SGLT1- and GLUTs-mediated [3 H]- 2DG uptake in enterocytes (Caco-2 cell). Results were analyzed by one-way ANOVA following Dunnett's multiple comparisons test. Data are shown as mean \pm SEM (compared to control; $^*p<0.05$, $^{***}p<0.001$).

Effect of hit compounds on bodyweight and hyperglycemia in type 2 diabetic rat.

The aim of this experiment is to investigate the anti-hyperglycemic effect of hit compounds in type 2 diabetic rat. Goto Kakiziki (GK) rat was chosen as diabetic model in this study. GK rat is characterized as lean type 2 diabetic rat model with progressive insulin resistance and deficiency. GK rats with non-fasting plasma glucose equal or more than 200 mg/dl were included in experiment. The GK rats were treated with vehicle, 100 mg/kg_{BW} KPE, and 100 mg/kg_{BW} BPE for 3 months. At the end of 3 months, rats were treated with vehicle, 1000 mg/kg_{BW} KPE, and 500 mg/kg_{BW} BPE for 1 month. Plasma glucose and body weight were measured weekly to observe the effect of hit compounds on antihyperglycemia or body weight. As show in figure 4.13, KPE and BPE had no effect on body weight. KPE and BPE significant reduced plasma glucose of GK rats compared to control (p< 0.0001).



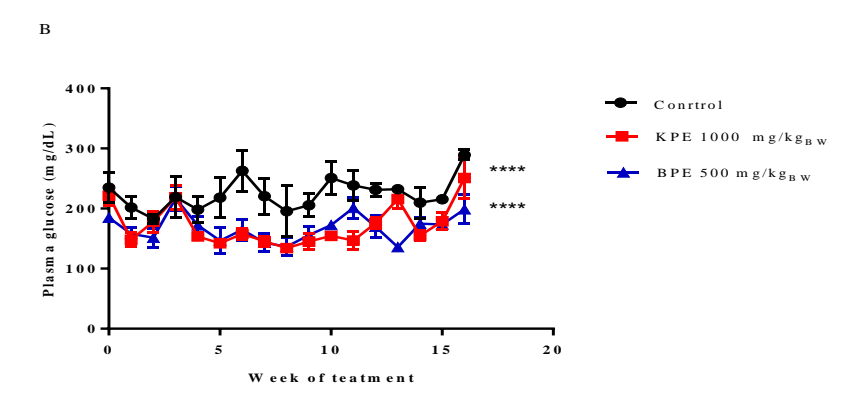


Figure 3.4 Effects of KPE and BPE on plasma glucose and affect body weight of GK rat. Data are shown in Mean \pm SEM. Results were analyzed by one-way ANOVA following Dunnett's multiple comparisons test. Data are shown as mean \pm SEM of 6-8 animals (****p<0.0001 compared with control).

Effect of panduratin A on bodyweight and hyperglycemia.

To determine whether panduratin A, a BPE component is the active compound reducing plasma glucose of GK rats, the effect of panduratin A on plasma glucose of GK rats was determined. Panduratin A did not reduce plasma glucose of GK rats (figure 4.15B). In addition, effect of panduratin A on body weight was examined, panduratin A reduced body weight but did not reduce plasma glucose (figure 3.5).

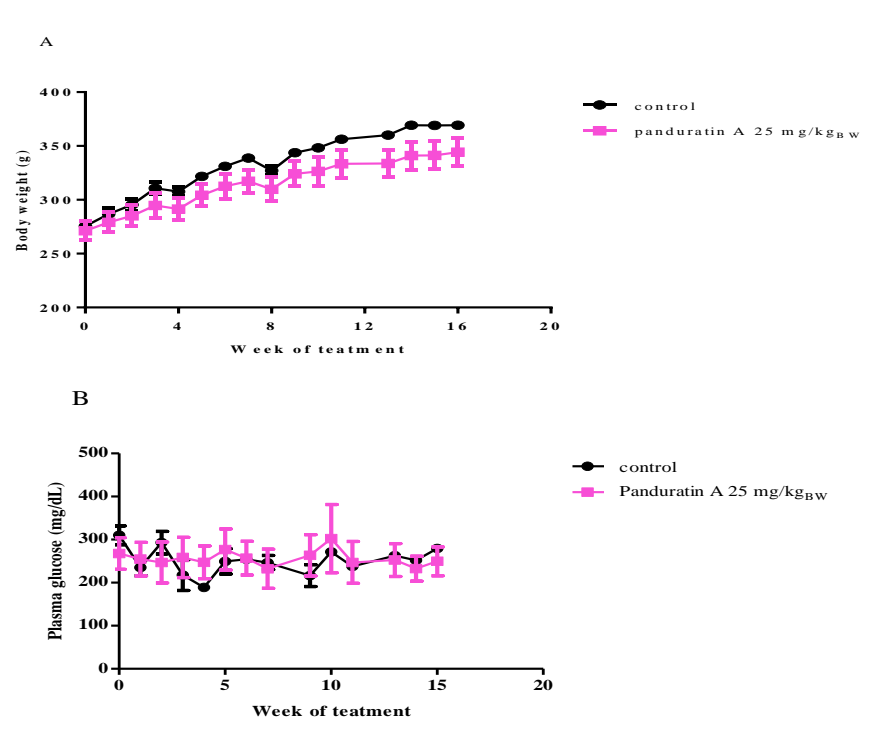


Figure 3.5 Effect of panduratin A on plasma glucose and body weight of GK rat. Data are shown in Mean \pm SEM. Data were analyzed by Unpaired t test.

Effect of hit compounds on insulin secretion

Insulin action is the major mechanism to defense rising in plasma glucose. Effect of KPE and BPE on insulin secretion was evaluated. OGTT was performed at the end of treatment (4 months). Rat sera were collected after glucose load 0 and 15 minutes. Plasma insulin level was assessed by insulin ELISA Kit. The result is shown in figure 4.20, the level of insulin in rats treated with KPE or BPE in both 0 and 15 minutes. This result indicated that treatment of KPE and BPE, did not affect plasma insulin level.

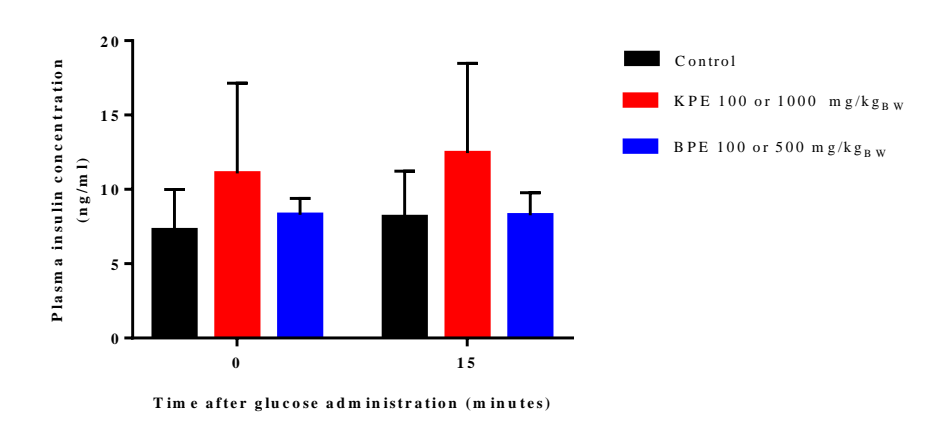


Figure 3.6 Effect of KPE and BPE on affect insulin secretion. Data are shown in mean ± SEM n=6-8. Result was analyzed by Two-way ANOVA followed by Tukey's multiple comparisons test.

Discussion and conclusion

From 134 natural compounds screening, KPE and BPE showed the inhibitory effect on SGLT2 in human renal proximal tubular cell. Interestingly, DMF and panduratin A had low effective effect. These results indicated that the extracts might contain other active compounds on SGLT2 inhibition. In addition, KPE and BPE also inhibited GLUT2 that expresses at basolateral membrane. KPE and BPE may reduce glucose reabsorption by blocking both SGLT2 and GLUT2 activity at apical and basolateral membrane of renal proximal tubule, respectively. The inhibitory effect of KPE and BPE was predominantly on SGLT2 and GLUT2 in renal cells compared with intestinal cells indicating these compounds might not interfere glucose absorption in small intestine and they might not produce osmotic diarrhea from non-absorbable glucose as found in non-specific SGLT2 inhibitor, phlorizin. Although, marine compounds showed the higher inhibitory potencies than that of plant natural compounds, they also produced cytotoxicity which might limit further study for drug development. In vivo, KPE and BPE at low dose and high dose showed the lowering effect on plasma glucose without changing plasma insulin. Interestingly, the bioactive compound of BPE, panduratin A, had no effect on plasma glucose. These results were

similar as found in *in vitro* data. Although, KPE and BPE showed the plasma glucose in diabetic rats, the mechanisms responsible are unknown. The further studies concerning the mechanisms are required.

Sub-project 4. Lipid lowering and anti-adiposity effects of naturally occurring compound

ABSTRACT

The incidence of obesity has substantially increased worldwide and has been received considerable attention as a major health hazard. It is common in aging population. The present study aimed to investigate lipid lowering effect of Curcuma comosa Roxb. (C. comosa) which contains phytoestrogen on adiposity and lipid metabolism in estrogendeprived rats. Adult female rats were ovariectomized (OVX) and received daily doses of either a phytoestrogen from C. comosa [(3R)-1,7-diphenyl-(4E,6E)-4,6-heptadien-3-ol; DPHD], C. comosa extract, or estrogen (17 β -estradiol; E2) for 12 weeks. Adipose tissue mass, serum levels of lipids and adipokines were determined. In addition, genes and proteins involved in lipid synthesis and fatty acid oxidation in visceral adipose tissue were analyzed. The results showed that ovariectomy for 12 weeks elevated level of serum lipids and increased visceral fat mass and adipocyte size. These alterations were accompanied with the up-regulation of lipogenic mRNA and protein expressions including LXR-lpha, SREBP1c and their downstream targets. OVX rats showed decrease in proteins involved in fatty acid oxidation including AMPK- α and PPAR- α in adipose tissue, as well as alteration of adipokines; leptin and adiponectin. Treatments with E2, DPHD or *C. comosa* extract in OVX rats prevented an increase in adiposity, down-regulated lipogenic genes and proteins with marked increases in the protein levels of AMPK- α and PPAR- α . These findings indicated that their lipid lowering effects were mediated via the suppression of lipid synthesis in concert with an increase in fatty acid oxidation and AMPK- α activity in adipose tissues, supporting the use of this plant for health promotion in the post-menopausal women.

In addition, DPHD also inhibited adipocyte differentiation of human bone marrow-derived mesenchymal stem cells (hBMSCs) by suppressing the expression of genes involved in adipogenesis through the activation of ER and Wnt/ β catenin signaling pathways. This finding suggests the potential role of DPHD in preventing bone marrow adiposity which is one of major factor that exacerbates osteoporosis in post-menopause.

Keywords: anti-adiposity, diarylheptanoid, phytoestrogen, ovariectomy, *Curcuma comosa*, adipocyte differentiation

บทคัดย่อ

อุบัติการของโรคอ้วนที่เพิ่มขึ้นอย่างชัดเจนทั่วโลก เป็นเรื่องที่ได้รับความสนใจอย่างมากเนื่องจากมี ผลกระทบเสียหายต่อสุขภาพ และโรคอ้วนพบมากในผู้สูงอายุ การวิจัยนี้มีวัตถุประสงค์เพื่อศึกษาฤทธิ์ของสาร จากธรรมชาติในลดไขมัน ได้ศึกษาฤทธิ์ของสารที่แยกได้จากว่านชักมดลูกซึ่งมีสมบัติเป็นไฟโตรเอสโตรเจน โดย ศึกษาผลต่อการสะสมไขมันในเซลล์ กระบวนการเมแทบอลิซึม และการทำหน้าที่ของเนื้อเยื่อไขมันในหนูที่ขาด ฮอร์โมนเอสโตรเจน ผลการศึกษาใช้หนูแรทที่ถูกตัดรังไข่ และได้รับการรักษาด้วยสาร phytoestrogen จาก C. comosa คือ (3R)-1,7-diphenyl-(4E,6E)-4,6-heptadien-3-ol; DPHD หรือสารสกัดของพืช หรือ ฮอร์โมนเอสโตรเจนเป็นเวลา 12 สัปดาห์ โดยศึกษาถึงปริมาณเนื้อเยื่อไขมัน ระดับไขมันในเลือด และฮอร์โมน นอกจากนี้ยังวิเคราะห์ถึงการแสดงออกของยีนและโปรตีน ที่เกี่ยวข้องกับกระบวนการ จากเซลล์ไขมัน สังเคราะห์ใขมัน และกระบวนการสลายไขมันของไขมันในช่องท้อง ยังได้วิเคราะห์ถึงการเปลี่ยนแปลงของเม ทาโบไลท์ของไขมันในเซรั่ม ผลการวิจัยพบว่าการตัดรังไข่เป็นเวลานาน 12 สัปดาห์ มีผลเพิ่มระดับไขมันใน ชีรั่มสูงขึ้น เพิ่มมวลและขนาดของเซลล์ไขมัน การเปลี่ยนแปลงดังกล่าวมีการเพิ่มของยีนและโปรตีนที่เกี่ยวข้อง กับการสังเคราะห์ใขมัน เช่น LXR-**α** และ SREBP-1c ในเนื้อเยื่อไขมัน อีกทั้งยังลดโปรตีนที่เกี่ยวข้องกับการ ออกซิเดชั่นของกรดไขมันได้แก่ AMPK- α และ PPAR- α และมีการเปลี่ยนแปลงของอะดิโพรไคน์ เช่น leptin และ adiponectin ที่หลั่งจากเนื้อเยื่อไขมันอีกด้วย การให้สารเอสโตรเจน (E2), DPHD หรือสารสกัด *C.* comosa แก่หนูที่ถูกตัดรังไข่สามารถป้องกันการเพิ่มขึ้นของมวลเนื้อเยื่อไขมัน รวมทั้งลดการแสดงออกของยืน และโปรตีนในกระบวนการสังเคราะห์ไขมัน เพิ่มระดับโปรตีน AMPK- α and PPAR- α ในกระบวนการออกซิ เดชั่นของกรดไขมัน ผลวิจัยแสดงให้เห็นว่าสาร DPHD และ สารสกัด C. comosa มีประสิทธิภาพดีเด่นในการ ออกฤทธิ์ลดการสะสมของเนื้อเยื่อไขมันโดยยับยั้งกระบวนการสังเคราะห์ไขมันและเพิ่มการสลายของกรด ไขมัน ซึ่งสนับสนุนการใช้สาร และ พืช C. comosaในการดูแลรักษาโรคที่เกี่ยวข้องกับการสะสมไขมัน ส่วนเกินในร่างกายในหญิงวัยหมดประจำเดือน

นอกจากนี้สาร DPHD ยังมีฤทธิ์ต้านการการจำแนกเซลล์ต้นกำเนิดของมนุษย์ในโพรงกระดูกไปเป็นเซลล์ ไขมัน โดยไปลดการแสดงออกของยีนที่เกี่ยวข้องกับการสร้างเซลล์ไขมัน ทำงานกระตุ้นวิถีสัญญาณในเซลล์ที่ เกี่ยวข้องกับตัวรับฮอร์โมนเอสโตรเจน และ Wnt/ $oldsymbol{eta}$ catenin ฤทธิ์ลดการสะสมไขมันในโพรงกระดูกนี้ สนับสนุน การใช้พืชและสารจากพืช C. comosa ในการดูแลรักษาโรคที่เกี่ยวข้องกับการสะสมไขมันส่วนเกินในร่างกาย และ โรคกระดูกพรุนในหญิงวัยหมดประจำเดือน

คำสำคัญ: ลดไขมัน ไดเอริลเฮปตานอย ไฟโตรเอสโตรเจน ตัดรังไข่ ว่านชักมดลูก พัฒนาการของเซลล์ไขมัน

1. INTRODUCTION

1.1 Statement and significance of the research problem, and objectives

Obesity is a disorder of energy balance caused by the energy intake exceeds the expenditure resulting in an excessive accumulation and expansion of adipose tissue. The increase of visceral adipose tissue, specifically in adipocyte size, contributes to a chronic state of low-grade inflammation affecting adipose tissue functionality. Dysfunction of adipose tissue has been reported to be a major cause of metabolic disorders including insulin resistance, type 2 diabetes, and cardiovascular diseases (Romeo, et al., 2012). The

prevalence of obesity in postmenopausal women has been reported to be higher compared to men of the same age (BaHammam, et al., 2016). Although many factors have been proposed to involve in the development of obesity in women (Vicennati, et al., 2009), aging and decline in estrogen level are the important contributing factors to increase the risk of obesity and metabolic diseases (D'Eon, et al., 2005).

The relationship between a systemic decline in estrogen level and an increase of adiposity has been observed in post-menopausal women (Lundholm, et al., 2004). Estrogen suppresses mRNA expression of genes involved in lipid synthesis including liver x receptor- α (Lxr- α) and its positive regulator, sterol regulatory element binding protein 1c (Srebp-1c) (Lundholm, et al., 2008). In addition, estrogen also regulates lipid metabolism by nongenomic activation of 5'AMP-activated protein kinase α (AMPK- α); a crucial metabolic sensor for energy regulation (D'Eon, et al., 2005).

Curcuma comosa Roxb. (C. comosa) a plant in Zingiberaceae family, is an indigenous medicinal herb that has traditionally been used for treatment of postpartum uterine bleeding and relieving unpleasant symptoms in menopausal women (Anonymous, 1967, Pongboonrod, 1976). C. comosa rhizome extract contains a number of diarylheptanoids (Suksamrarn, et al., 2008). A non-phenolic diarylheptanoid (3R)-1,7diphenyl-(4E, 6E)-4,6-heptadien-3-ol (DPHD) is identified as the major active constituent of C. comosa and possesses estrogenic-like activity (Winuthayanon, et al., 2009). In addition to the estrogenic-like activity, both C. comosa rhizome extract and DPHD exhibit several other pharmacological effects including lipid lowering effect in hypercholesterolemic animals (Charoenwanthanang, et al., 2011, Piyachaturawat, et al., 1999, Ratanachamnong, et al., 2012) and ovariectomized rats (Prasannarong, et al., 2012), anti-oxidant effect, antiinflammatory activity and protective effect on bone loss (Jantaratnotai, et al., 2006, Sodsai, et al., 2007, Weerachayaphorn, et al., 2011). C. comosa also improves lipid, glucose metabolisms, and insulin sensitivity in ovariectomy-induced dyslipidemia rats which show the impairment of insulin sensitivity (Prasannarong, et al., 2012). However, the mechanism underlying these systemic perturbations and the treatment effect of *C. comosa* are not clear. Adipose tissue which is the largest energy reservoir in the body, participating primarily in the energy homeostasis may be affected under this condition.

In the present study, we investigated the effect of DPHD and $C.\ comosa$ extract on lipid metabolism in adipose tissue of ovariectomy-induced estrogen-deprived rats. The expression levels of key transcription factors involved in lipid synthesis, their downstream targets, and 5'AMP-activated protein kinase α (AMPK- α) phosphorylation which is an integrating signaling regulator of lipid metabolism, were determined. We also investigated therapeutic potential of $C.\ comosa$ by determining changes of lipid profiles in the ovariectomized rat model of estrogen-deficiency-induced hyperlipidemia after treatment with different components of $C.\ comosa$ using an untargeted metabolomics approach.

Objectives:

- (1) To investigate the effect of DPHD and *Curcuma comosa* extract on adipose tissue mass and adipocyte size in OVX rats. The expression level of gene and protein involved in lipid synthesis and fatty acid oxidation in visceral adipose tissue was also determined.
- (2) To investigate the effect of DPHD from *Curcuma comosa* on the adipogenic differentiation of mesenchymal progenitors, human bone marrow-derived mesenchymal stem cells (hBMSCs)

2. Materials and methods

2.1. Plant materials and Preparation of C. comosa extract and DPHD

Curcuma comosa Roxb., a member of Zingiberaceae family, is commonly known as Wan chak motluk in Thai. They were collected from Kampangsaen District, Nakhon Pathom, Thailand and subjected to taxonomic identification by Soontornchainaksaeng and Jenjittikul (2010). The voucher herbarium specimen number SCMU-300 was deposited at the Department of Plant Science, Faculty of Science, Mahidol University, Thailand. *C. comosa* rhizomes extract and its phytoestrogen diarylheptanoid (3*R*)-1,7-diphenyl-(4*E*,6*E*)-4,6-heptadien-3-ol (DPHD, Fig 1) were prepared according to previously described (Suksamrarn, et al., 2008). The purity of DPHD was estimated to be >98% by HPLC.

2.2. Animals and treatments

Adult females Sprague-Dawley rats (8-weeks-old), weighing between 200-220 g, were used. The sample size in each experiment was determined using Minitab® statistical 18 software. Based on power analysis, six animals per group were required. The rats were randomly assigned to either sham-operated control (SHAM, n=6) or bilateral ovariectomy (OVX, n=24). Animals were allowed to recuperate for 7 days after surgery. Ovariectomized rats were divided into 4 groups of six animals each as follows: OVX rats receiving vehicle (OVX control); OVX rats receiving 17 β -estradiol (E2) at a dose of 10 µg/kg BW, s.c.(OVX+E2); OVX rats receiving DPHD 50 mg/kg BW, s.c. (OVX+DPHD); OVX rats receiving *C. comosa* extract 500 mg/kg BW, i.g. (OVX+extract). E2 and DPHD were initially dissolved in absolute ethanol and then diluted in olive oil to give a final injection volume of approximately 100-200 μ l. The extract was directly suspended in 1% carboxymethyl cellulose to the specified concentration for oral ingestion of not more than 1 ml. All treatments were given daily for 12 weeks as indicated. All animal procedures were approved by the Animal Care and Use Committee, Faculty of Science, Mahidol University (protocol no. MUSC 56-031-293).

2.3. Serum lipids and adipokine measurements

At the end of the treatment period, animals were fasted overnight (12 h). They were euthanized. Following adipose tissue dissection, whole blood was collected from the posterior vena cava. Serum levels of triglyceride (TG), total cholesterols, and low density lipoprotein cholesterol (LDL-c) were measured using automated enzymatic methods (Siemens Dimension RxL Max; Siemens Medical Solution Diagnostics, NY, USA). For adipokine measurements, serum was diluted to 100-fold and subjected to leptin, and adiponectin quantifications using adipokine enzyme-linked immunosorbent assay (ELISA) kit (R&D system, Minn, USA).

2.4. Adipose tissue mass and adipocyte morphometry

Visceral adipose tissue mass was determined by weighing fat pads dissected from specific depots which were retroperitoneal, periovarian and mesenteric fad pads. For adipocyte morphometry, fresh retroperitoneal adipose tissue was fixed with 10% neutral buffered formalin and process for routine staining of paraffin section with hematoxylin and eosin (H&E). Digital images were acquired randomly under Olympus BX51 microscope. Adiposoft, an automated software authorized by Center for Applied Medical Research (CIMA), University of Navarra, Spain, was used to measure adipocyte area at least 100-120 adipocytes/rat, which were represented as the percentage of total number adipocytes in different diameters (in µm).

2.5. Cell culture and differentiation

Cell lines used were human bone marrow derived-mesenchymal stem cells (MSCs) which were purchased from Lonza (Allendale, NJ, USA). They were isolated from normal person (non-diabetic), adult female human bone marrow, age22, by withdrawing marrow from the posterior iliac crest. Cells were cultured in Dulbecco's modified Eagle media (DMEM) with low glucose content (1g/L) containing 10 % fetal bovine serum (FBS) and antibiotics (100 U/ml penicillin and 100 μ g/ml streptomycin). They were incubated at 37°C under a humidified atmosphere containing 5% CO2.

2.6. Induction of cell differentiation

Adipogenic differentiation of human MSCs was induced by culturing in human adipogenic differentiation (HAD) medium. The medium consists of DMEM (high glucose) with 10% charcoal-stripped FBS, antibiotics, and inducing reagents; 10 µg/ml insulin, 0.5 mM 3-isobutyl-1 methyl xanthine (IBMX), 10 nM dexamethasone and 0.2 mM indomethacin. Briefly, human MSCs were seeded into 6 well-plates at a density of 1x106 cells per well. Two days after reaching confluence, the adipogenic differentiation medium was applied for culture

and the medium was replaced every 3 days until 14 days. During adipogenic differentiation, MSCs were treated with DPHD or 17 β -estradiol (E2). To investigate the involvement of estrogen receptor α (ER α), MSCs were pre-treated with 100 nM of ICI 182, 780, an ER α antagonist for 2 h before receiving DPHD or E2.

Osteogenic differentiation of human MSCs were induced by culturing in osteogenic differentiation (HOB) medium. The medium consists of DMEM (low glucose) without phenol red, 10% charcoal-stripped FBS, 5 mM β -glycerol phosphate, and 25 μ g/ml of ascorbic acid. Briefly, human MSCs were seeded into 6-well plates at a density of 1x106 cells per well. Two days after achieving confluence (day 0), HOB medium was applied for differentiation and they were maintained in osteogenic media for 21 days. The culture media was replaced every 3 days.

2.7. Real-time quantitative polymerase chain reaction (RT-qPCR) and Western blot analysis

Quantitative real-time PCR of each samples was done on the equal amount of cDNA using KAPA SYBR®FAST qPCR kit according to the manufacturer's instructions (KapaBiosystems) with the ABI PRISM 7500 Sequence Detection System and analysis software (Applied Biosystems). The target mRNA level was normalized by β -actin or GAPDH. The relative levels of transcript expression were quantified using the mathematical model described by Pfaffl, in which ratio = 2-(ρ Ct sample - ρ Ct control) when Δ Ct = Ct (vehicle) - Ct (treated sample), where E = efficiency of the primer set, calculated from the slope of a standard curve of log (ng of cDNA) versus the value for a sample that contains the target according to the formula E = 10-(1/slope) (Hewitt et al., 2005).

Western blot analysis was performed according to the previously described protocol and manufacturer's instruction (Bio-Rad Laboratories).

2.8. Whole genome Affymetrix GeneChip cRNA screening

Human MSCs were selectively induced to differentiate either to osteoblasts, or adipocytes. During differentiation, they were received 0.1 µM DPHD or 10 nM E2, as positive control. On day 7 of osteoblast and adipocyte differentiation, total RNA from MSCs was extracted and used as starting materials to obtain labeled cDNAs. Genome wide screening was performed using Affymetrix GeneChip® MG430A 2.0 Array (Affymetrix, USA) as previously described (Robinson, et al., 2010). Briefly, single stranded cDNA was synthesized by reverse transcription using the poly (A) RNA presented in the starting total RNA sample. Single stranded cDNA was then converted into double stranded cDNA and purified using the Affymetrix Cleanup Module. An in vitro transcription (IVT) reaction was then carried out overnight in the presence of biotinylated UTP and CTP to produce biotin-labeled cRNA from the double stranded cDNA. The resulting cRNA is fragmented in the presence of heat and

Mg+2, and hybridized to the DNA array on glass, the Hu 133.2 probe set of 54675 assays with 20 replicates per target. Targets include segments of most known genes, with two or more probes per target. Presence of transcripts and differences in gene expression between control and treatment were determined from the signal and variation of each assay replicate with statistical confidence as indicated. Analysis included determination of effect on common metabolic pathways by MetaCore (www.genego.com, Clarivate, Analytics, Philadelphia, PA, USA) comparing effect of DPHD, E2, and control against a library of 121 intracellular pathways.

2.9. Statistical analysis

Data were expressed as means and standard error of means (mean \pm SEM). They were analyzed by using the statistical software package, GraphPad Prism version 5.0. Data among groups were compared using one-way analysis of variance (ANOVA) followed by Tukey-Kramer post hoc test. Statistical significance was considered when p < 0.05.

3. **RESULTS**

Part I: To investigate the effect of *C. comosa* treatment on adipose tissue mass and adipocyte size of OVX rats. The expression level of gene and protein involved in lipid synthesis and fatty acid oxidation in visceral adipose tissue was also determined.

3.1. Body weight, uterine weight, serum glucose and insulin, and lipids.

Table 4.1 shows general characters of all experimental groups. Ovariectomy for 12 weeks markedly increased the body weight with a decrease in uterine weight as compared to those in SHAM control. However, E2 treatment restored the body weight, and uterine weight of the OVX rats to the level of SHAM control whereas C. comosa (DPHD and C. comosa extract) treatment restored the body weight with a slight increase in the uterine weight, but still far below that of SHAM control. Levels of serum lipids including total cholesterol, triglyceride, and LDL cholesterol were significantly increased in the OVX rats (p<0.05). Treatments with E2, DPHD, or C. comosa extract for 12 weeks essentially prevented the increases in body weight, and serum level of total cholesterol, and LDL cholesterol in the OVX rats, indicating lipid-lowering activities of DPHD and C. comosa extract. However, only C. comosa extract significantly decreased serum triglyceride level (p<0.05).

Fig. 4.1. Structure of a non-phenolic diarylheptanoid (3*R*)-1,7-diphenyl-(4*E*,6*E*)-4,6-heptadien-3-ol (DPHD) from *Curcuma comosa* Roxb.

Table 4.1. Effects of E2 and *C. comosa* on body weight, uterine weight and serum levels of lipids after 12-weeks of treatments.

PARAMETERS	SHAM	OVX control	OVX+E ₂	OVX+DPHD	OVX+extract
Body weight (g)	298.9 <u>+</u> 18.9	371.0 <u>+</u> 14.4**	286.7 <u>+</u> 11.4 ⁺⁺	297.3 <u>+</u> 13.8 ⁺⁺	285.4 <u>+</u> 14.0 ^{††}
Uterine weight (mg/kgBW)	2.42 <u>+</u> 0.04	0.31 <u>+</u> 0.07**	3.00 <u>+</u> 0.02 ^{††}	0.87 <u>+</u> 0.05	1.65 <u>+</u> 0.06 [†]
Cholesterol (mg/dL)	107.0 <u>+</u> 11.10	145.33 <u>+</u> 19.5 **	129.14 <u>+</u> 15.87 [†]	115.83 <u>+</u> 13.76 [†]	82 <u>+</u> 22.70 ^{††}
Triglyceride (mg/dL)	32.67 <u>+</u> 10.33	47.167 <u>+</u> 13.26 [*]	69.1.7 <u>+</u> 13.37	51.33 <u>+</u> 16.60	29 <u>+</u> 13.60 ^{††}
LDL-cholesterol (mg/dL)	13.33 <u>+</u> 1.21	22.83 <u>+</u> 4.36 **	14.14 <u>+</u> 2.34 ^{††}	12.43 <u>+</u> 2.15 ^{††}	11.14 <u>+</u> 3.48 ^{††}

Each value is mean \pm SEM obtained from 6 animals. Rats were assigned as sham operated control (SHAM), ovariectomized control (OVX control), OVX receiving E2 10 μ g /kg BW (OVX+E2); OVX receiving DPHD 50 mg /kg BW (OVX+DPHD); and OVX receiving *C. comosa* extract 500 mg /kg BW (OVX+extract). *p<0.05 and **p<0.01 (*vs.* SHAM); †p<0.05 and +p<0.01 (*vs.* OVX).

3.2. Adipose tissue mass and adipocyte sizes

OVX rats had a greater visceral adipose tissue mass (13.7 \pm 1.2 g; 126.0 \pm 10.9%) than SHAM control (10.7 \pm 1.1g; 100 \pm 10.7%) (Fig 3.2A). E2 was used as a positive control, the mass was significantly reduced to control level after treatment with E2 (95.4 \pm 5.4%), DPHD (96.6 \pm 3.8%), and *C. comosa* extract (91.7 \pm 3.5%). There was a similar trend to modulate the subcutaneouse adipose tissue mass by which ovariectomy caused an increase and the treatments decreased. However, there was no statistical significant compared to SHAM control ((P> 0.05) (Fig 3.2B). The increase of visceral adipose tissue mass in OVX rats was accompanied with an increase in the size of adipocytes (Fig3. 2C). As shown in Fig 3.2D, average adipocyte diameter significantly increased in OVX rats (128.4 \pm 53.12 μ m) compared to that in SHAM (40 \pm 14.72 μ m). Treatment with E2, DPHD or *C. comosa* extract reduced adipocyte diameter to the level comparable to that of SHAM. In Fig 3.2E, OVX rats had a greater number of adipocytes with larger cross-sectional area. The hypertrophy of adipocytes in OVX rats was a striking feature found in the visceral fat mass which was prevented by treatments with E2, DPHD or *C. comosa* extract.

The effect of *C. comosa* in preventing the hypertrophy of adipocytes and the increase in adipose tissue mass of OVX rats were further investigated. The mRNA expression of genes involved in lipid synthesis including liver x receptor- α (*Lxr-\alpha*), sterol regulatory element binding protein 1c (*Srebp-1c*), fatty acid synthase (*Fas*), stearoyl-CoA desaturase 1

(Scd-1), and acetyl-CoA carboxylase 1 (Acc-1) were dramatically increased in the hypertrophic adipocytes of OVX rats compared to those in SHAM control. Treatment of E2, DPHD or C. comosa extract markedly suppressed the expressions of these elevated lipogenic genes to the levels of control (SHAM) (Fig 3.3A). In corresponding to the expressions of lipogenic mRNAs, levels of proteins involved in lipid synthesis including LXR- α , SREBP-1c, FAS, and ACC-1 in adipose tissue of OVX rats were also increased and they were decreased by treatment with E2, DPHD or C. comosa extract (Fig4. 3B).

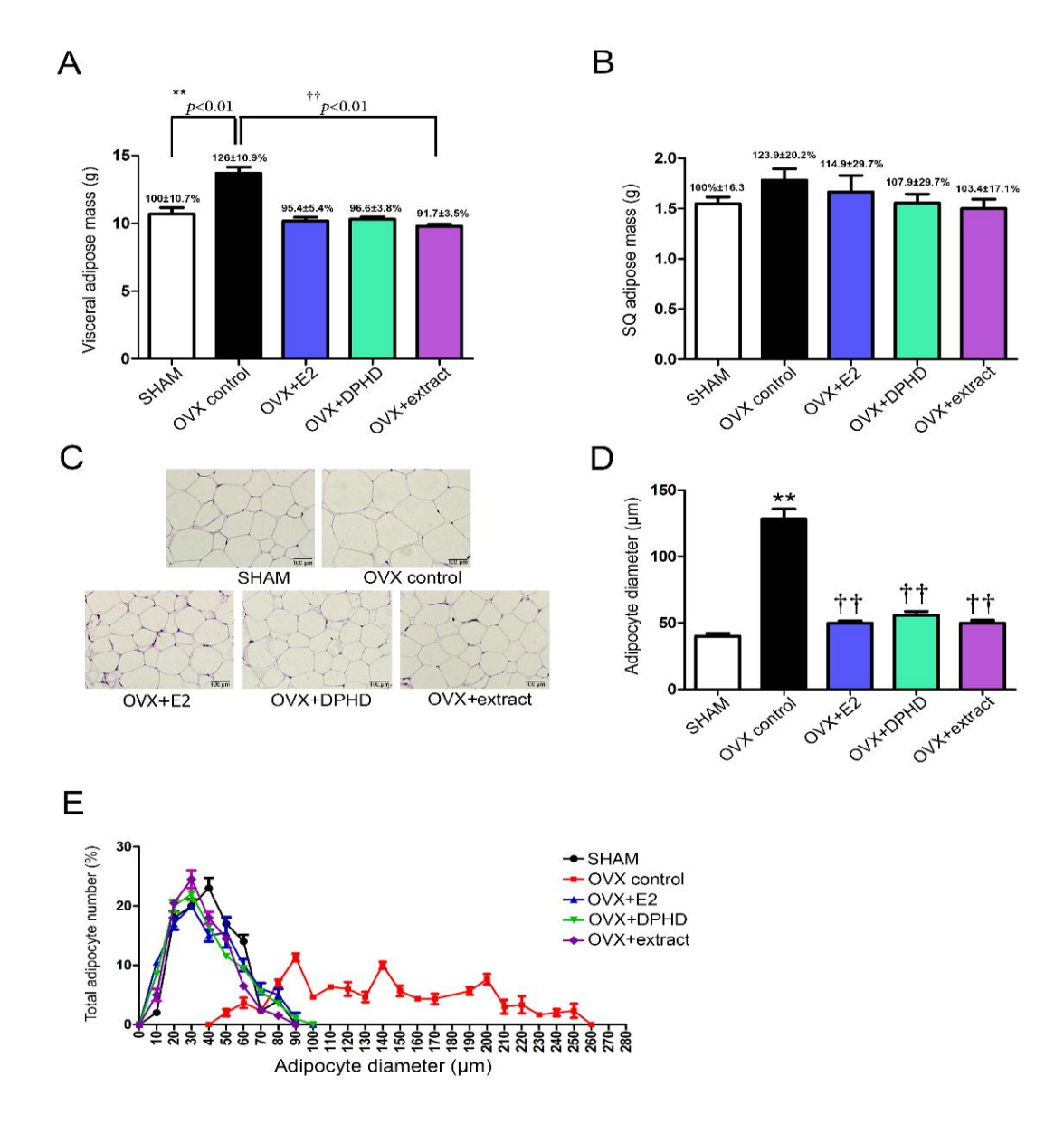
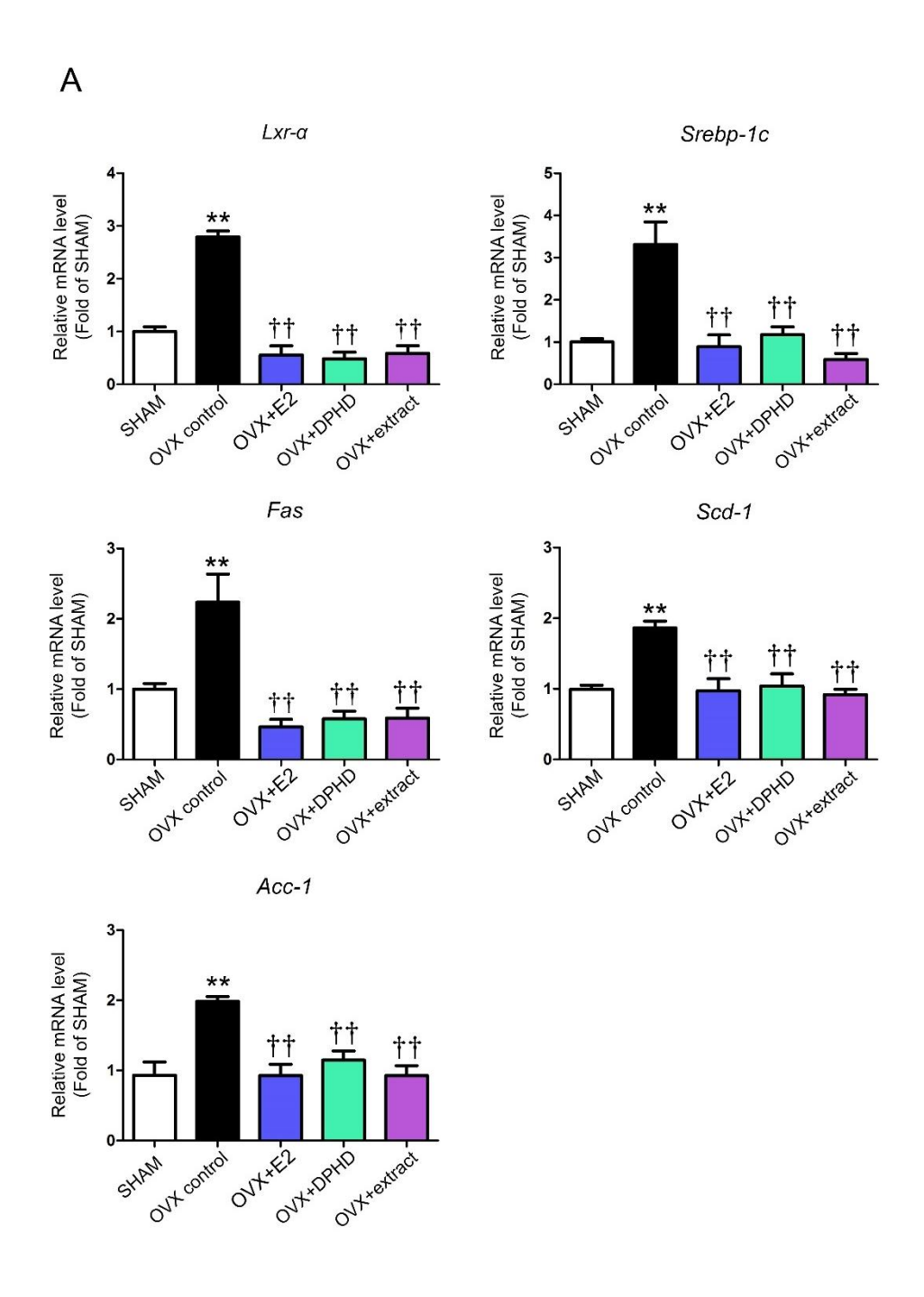
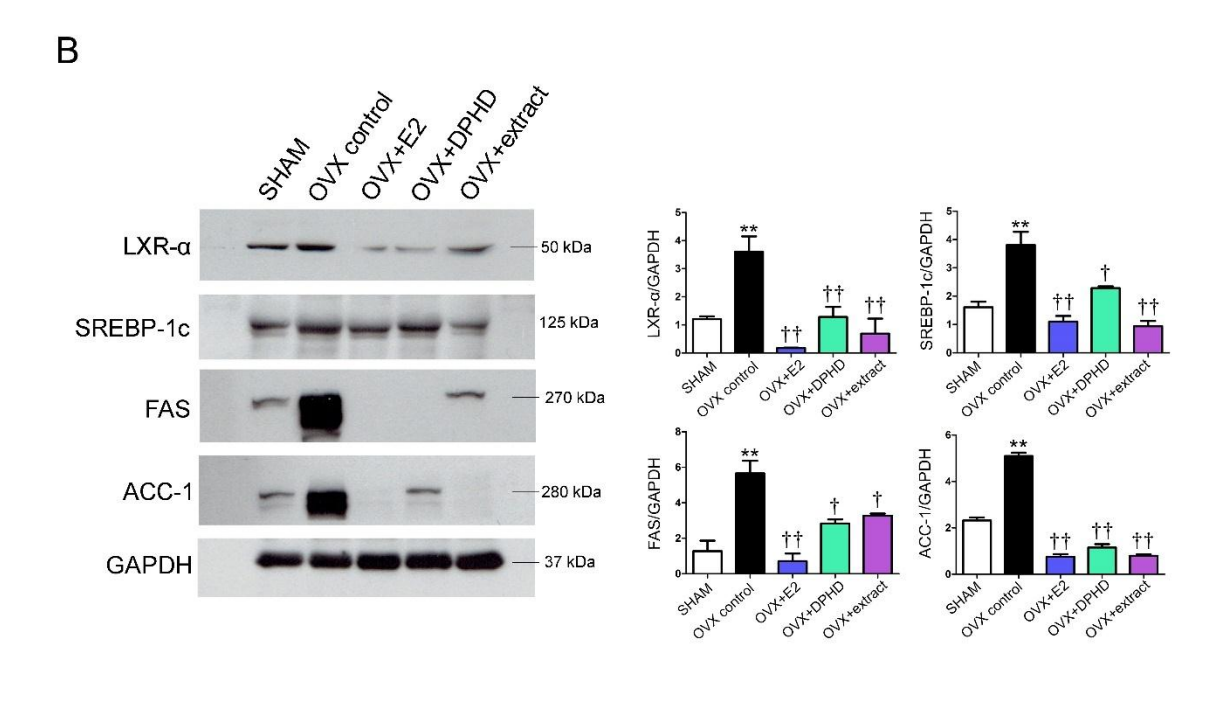


Fig. 4.2. Effects of treatments on adipose tissue masses from visceral (**A**); subcutaneous (**B**); and adipocyte size (**C**); average adipocyte diameter (**D**); and distribution of adipocyte size of visceral adipose tissue (**E**), in SHAM, OVX control, OVX+E2, OVX+DPHD and OVX+extract. Data are expressed as mean \pm SEM obtained from 6 animals. *p<0.05 and *p<0.01 (vs. SHAM); *p<0.05 and *p<0.01 (vs. OVX).

3.3. Expressions of genes and proteins involved in lipid synthesis and fatty acid oxidation in adipose tissue.





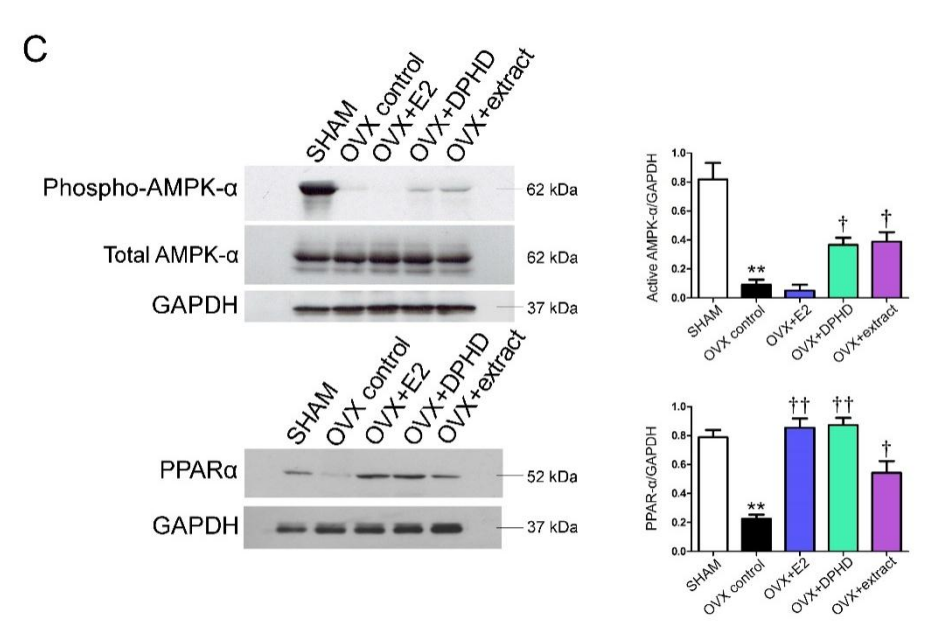


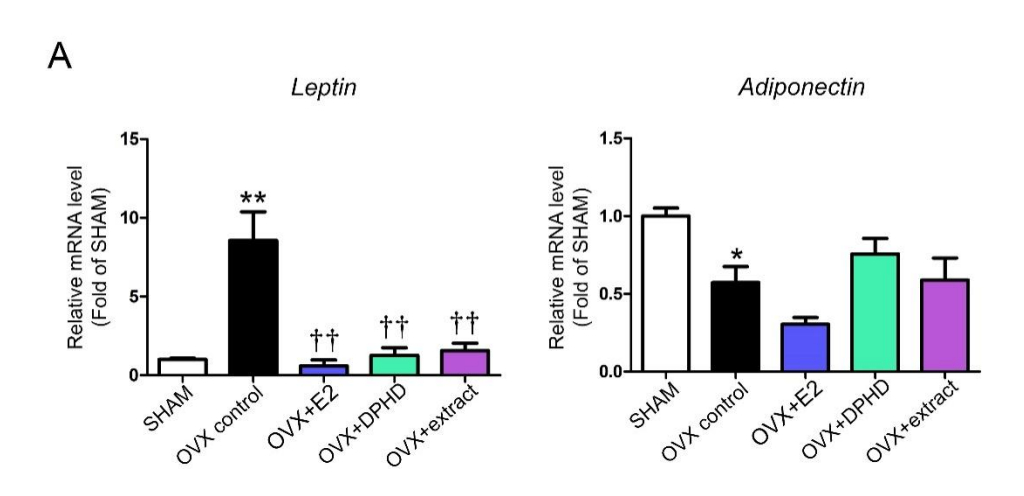
Fig. 4.3. Effects of treatments on the expressions of lipogenic mRNA: *Lxr-α*, *Srebp-1c*, *Fas*, *Scd-1* and *Acc-1*.(**A**); level of lipogenic proteins: LXR α , SREBP1c, FAS, ACC-1, and SCD-1 along with densitometric values of protein bands normalized by GAPDH (**B**); and level of proteins involved in fatty acid oxidation: AMPK- α and PPAR- α with densitometric values of protein bands normalized by GAPDH (**C**) in SHAM, OVX control, OVX+E2, OVX+DPHD and OVX+extract. Data are expressed as mean ± SEM from 6 animals. *p<0.05 and *p<0.01 (*vs.* SHAM); † p<0.05 and †† p<0.01 (*vs.* OVX)

The potential role of proteins involved in fatty acid oxidation including AMPK- α and PPAR- α in mediating the anti-adiposity of C. comosa treatments was also determined. In

Fig. 4.3C, level of phosphorylated AMPK- \mathbf{Q} (Threonine 172) protein, a marker of AMPK- \mathbf{Q} activation was significantly decreased in the adipose tissue of OVX rats in respect to SHAM control, whereas C. comosa and DPHD demonstrated marginal increases in the active form of AMPK- \mathbf{Q} . However, E2 treatment had no effect on AMPK- \mathbf{Q} activity in adipose tissue. The level of PPAR- \mathbf{Q} protein was also significantly decreased in OVX rats and it was significantly increased to the level of SHAM control after treatment with E2, DPHD or C. comosa extract.

3.4. Expression and secretion of adipocytokines

Hypertrophic adipocyte is often associated with adipokine dysregulation and insulin resistance (Jung and Choi, 2014). In OVX rats, the expression of *Leptin* mRNA in adipose tissue was highly upregulated whereas the expression of *Adiponectin* mRNA was downregulated. Treatment with E2 or *C. comosa* reduced the expression of *Leptin* mRNA to the level of SHAM control. On the other hand, DPHD or *C. comosa* extract failed to restore the level of *Adiponectin* mRNA whereas E2 treatment further decreased the expression of *Adiponectin* mRNA (Fig 4A). Concurrently, the circulating level of leptin was also increased in the OVX rats, but was decreased by treatment with E2 or *C. comosa*. On the contrary, the circulating level of adiponectin, which was decreased in the OVX rats, was restored only by DPHD (Fig 4.4B).



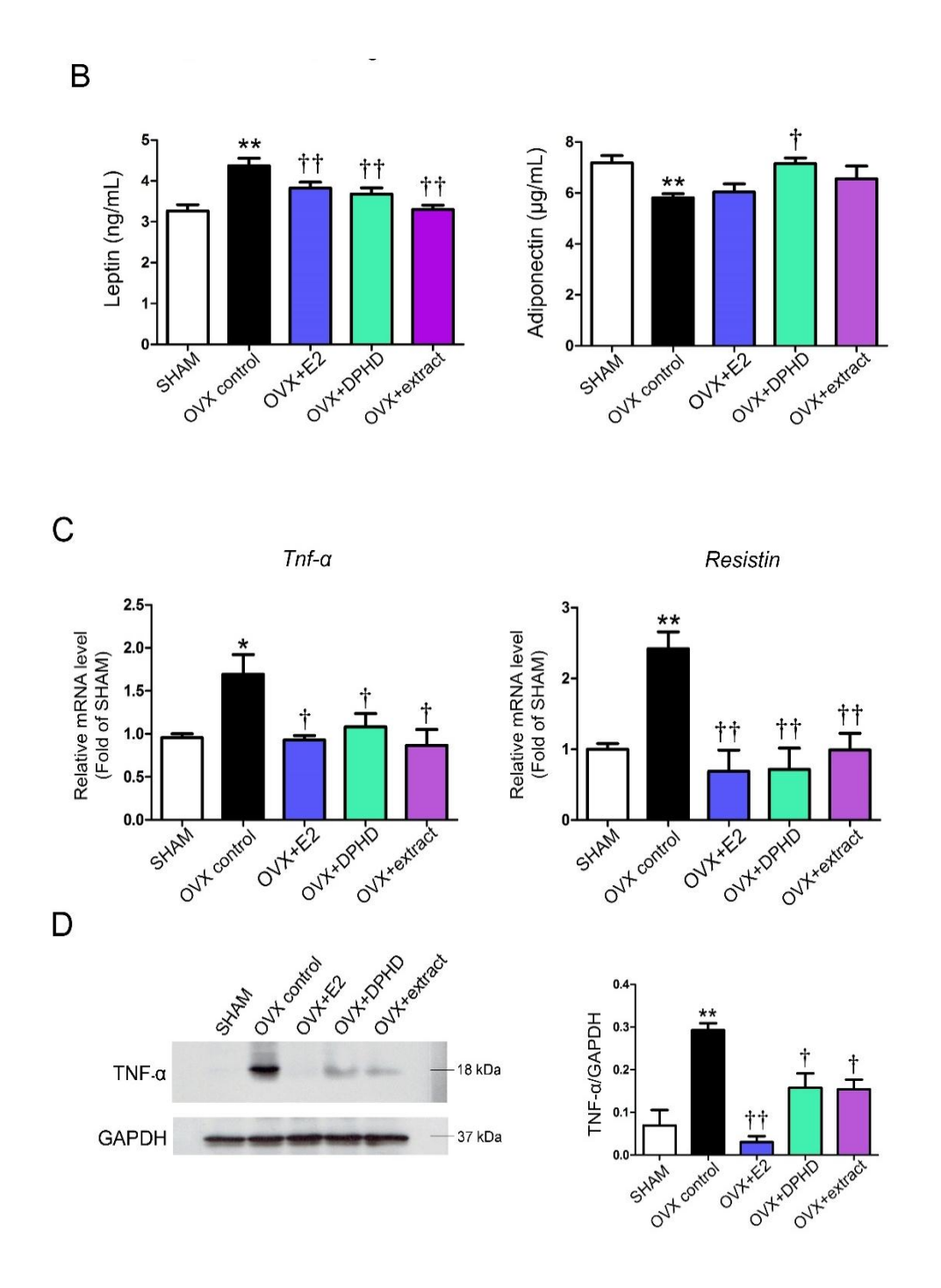


Fig. 4.4. Effects of treatments on the expressions of *Leptin* and *Adiponectin* mRNA determined by RT-qPCR (**A**); circulating leptin and adiponectin measured by ELISA (**B**); expression of *Tnf-α* and *Resistin* mRNA (**C**); and level of TNF- α protein along with densitometric values of protein bands normalized by GAPDH (**D**) in SHAM, OVX control, OVX+E2, OVX+DPHD and OVX+extract. Data are expressed as mean ± SEM of 6 animals. *p<0.05 and **p<0.01 (*vs.* SHAM); †p<0.05 and †*p<0.01 (*vs.* OVX).

Discussion and conclusion

The present study demonstrated the lipid lowering effect of C. comosa extract and its active phytoestrogen, DPHD, in estrogen-deficient rats. Both C. comosa extract and DPHD effectively prevented the gain of body weight, excessive visceral fat accumulation, enlargement of adipocyte, and metabolic disturbances in OVX rats similar to those by E2. In consistent with the reduced visceral fat mass, C. comosa down-regulated the expression of genes and proteins involved in lipid synthesis including LXR- \mathbf{Q} , SREBP-1c and their downstream targets. Moreover, they also increased proteins involved in fatty acid oxidation including AMPK- \mathbf{Q} and PPAR- \mathbf{Q} in adipose tissue of the OVX rats. Our data suggest that C. comosa reduced adiposity in OVX rats by inhibiting lipogenesis, in concert with promoting fatty acid oxidation and thereby improving adipokine secretion from adipose tissue. This is the first report showing the mechanism underlying lipid lowering effect of C. comosa.

Estrogen plays important roles in regulating energy and lipid homeostasis by both suppressing food intake and increasing energy expenditure (D'Eon, et al., 2005). Deficiency of estrogen is associated with increases in adiposity and risk of metabolic syndromes, particularly in postmenopausal women (Lundholm, et al., 2008). In the present study, ovariectomy markedly increased visceral adipose tissue mass. A similar trend was also seen in subcutaneous adipose tissue mass, although there was no statistically significant. Our finding is similar to the previous study reporting that ovariectomized (OVX) rats gain adipose tissue, specifically visceral adipose tissue with no significant change of subcutaneous adipose tissue (Clegg, et al., 2006). The marked increase in visceral adipose tissue mass was accompanied with up-regulation of key transcription factors responsible for lipid synthesis including LXR- α and SREBP-1c, which were suppressed by E2 or *C. comosa* treatments. The interplay between the LXR and ER ligand/receptor systems has been evidenced by the presence of ERE on LXR-lpha promoter (Han, et al., 2014). Decreased expressions of LXR-lpha and its positive regulator SREBP-1c found in E2 and C. comosa treatments might co-operatively suppress the de novo lipid synthesis which led to the reduction of adipose tissue mass. Our findings were consistent with the earlier report that E2 suppressed LXR-lpha- activated SREBP-1c expression (Han, et al., 2014). Although C. comosa contains a weak estrogenic-like activity as indicated by its weak uterotrophic effect (Table 4.1), it substantially suppresses the elevated expressions of LXR-lpha and lipogenic genes in OVX rats similar to those of estrogen (Fig. 4.3A).

C. comosa treatment also increased the level of proteins involved in fatty acid oxidation including AMPK- α , an important energy sensor in metabolic tissue, and PPAR- α , which was decreased in the OVX rats. Activation of AMPK- α inhibits lipid synthesis by suppressing the expression of Acc-1 mRNA and facilitating fatty acid oxidation in adipose tissue (Matejkova, et al., 2004, Sim and Hardie, 1988, Sullivan, et al., 1994). AMPK- α does not only influence lipid metabolism but also suppresses inflammation in adipose tissue (Viollet

and Andreelli, 2011). The activation of AMPK- α has been proposed to be a potential therapeutic target for the treatment of obesity and insulin resistance (Carling, et al., 2012). In this study, E2 and *C. comosa* treatments restored the level of PPAR α which acts synergistically with AMPK- α to increase fatty acid oxidation and suppress lipogenesis, contributing to the reduction of visceral adipose tissue mass.

C. comosa contains a weak estrogenic-like activity as indicated by its weak uterotrophic effect. The anti-lipogenic effect of *C. comosa* might, in part, be contributed by other pathways apart from estrogen signaling, particularly related to its anti-inflammatory activity. Recently, C. comosa has been shown to exhibit an anti-inflammatory activity in several experimental models. It suppresses the expression of tumor necrosis factor lpha (TNF**a**) in aortic rings of OVX rats (Intapad, et al., 2012). Similarly, *C. comosa* extract is also found to exert the anti-inflammatory effect in hypercholesterolemic rabbits by decreasing the expressions of pro-inflammatory cytokines; IL-1, MCP-1, and TNF- α (Charoenwanthanang, et al., 2011). In the present study, C. comosa also reduced the expression of Tnf- α and Resistin genes which are associated with the inflammatory response. On the other hand, it also increased levels of adiponectin and AMPK-lpha which are anti-inflammatory factors. The improvement of lipid metabolism by C. comosa treatments was essentially related to the reduced adipose tissue mass which is likely contributed by its anti-inflammatory activity. In addition, the alterations in adipose tissues in the present study may account for the underlying systemic perturbations in the estrogen deficiency condition and after receiving the DPHD and C. comosa treatments in the previous metabolomic study (Vinayavekhin, et al., 2016). More importantly, DPHD gave rise to the same outcome as C. comosa extract, indicating that most of the modulating effects observed in C. comosa extract might be mainly responsible by DPHD.

In conclusion, we report herein for the first time the lipid lowering effect of *C. comosa* extract and its major active compound, DPHD, on adipose tissue in OVX rats. These compounds suppressed lipogenesis in concert with the improvement of fatty acid oxidation, which promoted metabolically healthy adipocytes with normal adipokine secretion. This study provides insight information for the development of *C. comosa* and DPHD as a dietary supplement for treatments of metabolic complications related with estrogen deficiency-induced adipose tissues accumulation.

Graphical abstract Lean with functional Obesity with adipose OVX adipose tissue tissue dysfunction Ovariectomy Lipogenesis Fatty acid Leptin oxidation Adiponectin Resistin Leptin TNF-a Adiponectin PPAR-a LXR-a AMPK-a OVX + C. comosa DPHD Adipocyte Stimulation Macrophage Inhibition Preadipocyte Leptin Adiponectin Resistin Curcuma comosa TNF-a

Figure 4.5 Schematic diagram showing the anti-adiposity activities of *C. comosa* treatments in visceral adipose tissue of OVX rats. The *C. comosa* extract as well as DPHD, its major active compound, suppresses lipogenesis in concert with the improvement of fatty acid oxidation in adipose tissue in OVX rats. They promote metabolically healthy adipocytes with normal adipokine secretion.

Part II: Inhibition of Adipogenic Differentiation of Human Bone Marrow Derived Mesenchymal Stem Cells by DPHD, a Phytoestrogen from *Curcuma comosa*

Adipocytes in bone marrow share a common precursor with osteoblast, so called mesenchymal stem cells (MSCs). In aging, a number of MSCs in the bone marrow, which are multipotent stem cells are decreased. In addition, they lose their ability to differentiate into osteoblasts but tend to differentiate into adipocytes, causing bone loss. Thus, any compound that has an ability to increase MSC pool and promote differentiation of osteoblasts with an inhibition on adipogenic differentiation may be the attractive therapeutic agent for the treatment of osteoporosis in aging and postmenopausal women.

DPHD, a phytoestrogen from *C. comosa* has previously been demonstrated to have a positive osteogenic effect in committed MC3T3-E1 pre-osteoblast (Bhukhai, et al., 2012) and in human osteoblasts (Tantikanlayaporn, et al., 2013). DPHD also provides adipogenic effect in 3T3–L1 pre-adipocytes (Unpublished data). However, its effect on the differentiation of uncommitted MSCs has not been investigated. The present study was designed to investigate the effect of DPHD on mesenchymal stem cell differentiation. As the differentiation of MSCs into mature adipocytes takes approximately 14 days whereas differentiation toward mature osteoblast requires additional 7 days, the experiments were conducted for 14 and 21 days.

Results and Conclusion

DPHD treatment suppressed differentiation of MSCs into adipocytes while promoted differentiation into osteoblasts. In Fig. 4.6, after incubation in human adipogenic differentiation (HAD) medium for 7 days, MSCs differentiate into mature adipocytes, which was manifested by an increase in intracellular lipid droplet to 3.01± 0.4 compared to noninduced MSCs (assigned as 1). E2, which was used as a positive control, significantly reduced lipid accumulation. Similar to E2, treatment with DPHD at concentrations of 0.1, 1, and 10 µM during early period of differentiation (first 7 day of induction) also reduced the intracellular lipid accumulation to 2.5±0.2, 2.4±0.2, and 2.1±0.5, respectively. The intracellular lipid is stored in the form of triglycerides in adipocytes that are detected by the Oil Red O staining and triglyceride colorimetric assay. In addition to the morphological changes and lipid accumulations in the differentiated adipocytes, adipogenic genes and proteins were examined as markers of the differentiated cells. In Figure 4.7, levels of lipogenic proteins including PPARV and FABP4 were markedly increased in HAD control compared to non-induced MSCs. DPHD inhibited adipocyte differentiation by suppressing the expression of adipogenic genes and protein including PPARV, LPL and FABP4, thereby decreasing intracellular triglyceride accumulation. PPAR $oldsymbol{V}$ is the key transcription factor that induces and enhances the expression of adipocyte-specific genes (Farmer 2005). The suppression of PPARV expression by DPHD treatment led to inhibition of adipogenic gene expression including LPL and FABP4, and subsequently inhibited adipogenesis (Figure 4.10). As adipocytes and osteoblasts share a common progenitor cell, the differentiation of MSCs to adipocytes essentially suppresses their differentiation toward osteoblast and vice versa.

DPHD enhanced differentiation of MSCs into osteoblast by increasing the mRNA expression of osteogenic transcription factors including RUNX2 and OSX (encoded osterix), which are early and late osteoblast differentiation markers, respectively (Figure 4.8-4.9). Runx2 and osterix positively regulate osteogenic differentiation of MSCs. Accordingly, the expression of genes and proteins involved in anti-adipogenic and osteogenic effects of DPHD in MSCs were correlated with gene profiling obtained from wide genome expression screening (Fig.4.10). Surprisingly, DPHD partially restored the levels of cell proliferation factors during adipogenic differentiation. However, it suppressed the expression of genes encoding adipogenic transcription factor, PPAR γ and its target genes, and many lipogenic proteins, thereby inhibiting adipocyte differentiation and maturation. The anti-adipogenic activity of DPHD in MSCs was similar to that of estrogen. Furthermore, the anti-adipogenic effect of DPHD was likely to be mediated through the cross-talk between estrogen receptor (ER) signaling and Wnt/ β -catenin signaling pathway.

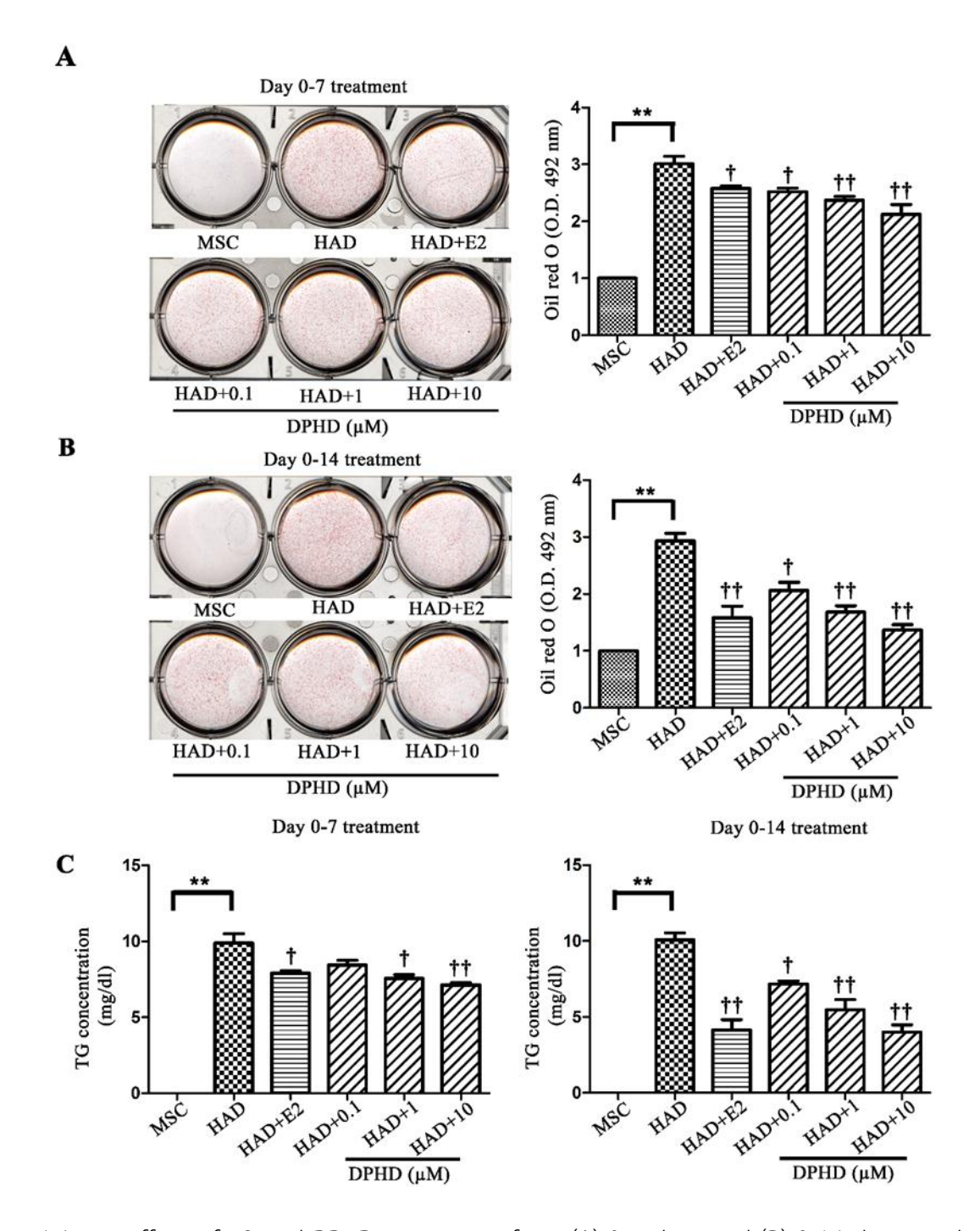
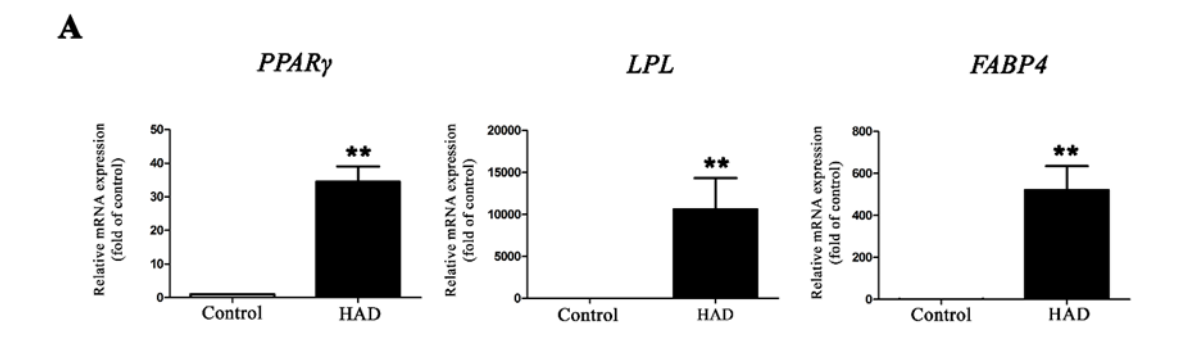


Figure 4.6 Effect of E2 and DPHD treatments from (A) 0-7 days and (B) 0-14 days on the accumulation of intracellular lipid by Oil red O staining, and (C) the intracellular triglyceride concentrations determined by triglyceride colorimetric assay on day 7 and 14 of adipogenic induction, respectively. Data are expressed as means \pm SEM obtained from 3 independent experiments. *p < 0.05 and **p < 0.01 (vs. MSC) and †p < 0.05 and †p < 0.01 (vs. HAD)



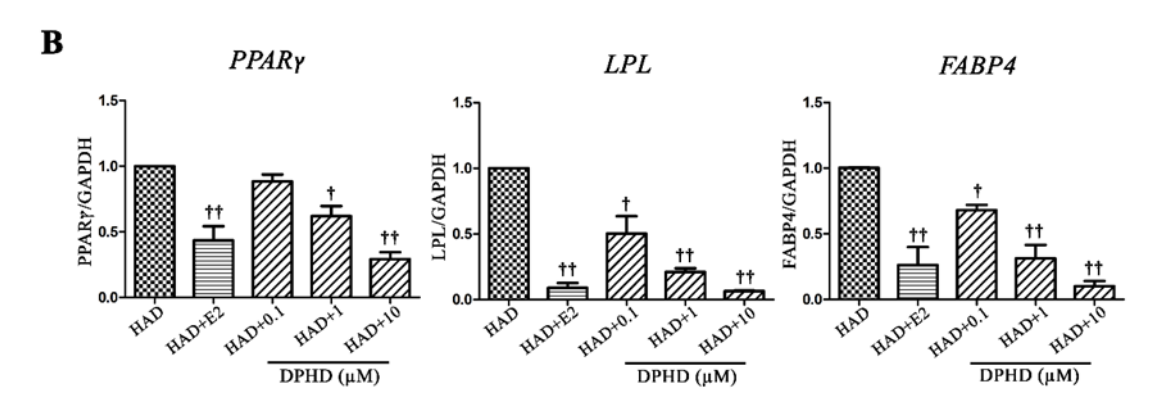


Figure 4.7 (A)The expression of adipogenic mRNAs: LPL, PPAR γ , and FABP4 after incubating with human adipogenic differentiation (HAD) media for 7 days compared to control, non-induced MSCs and (B) the effect of treatments on the expression of adipogenic mRNA (LPL, PPAR γ , and FABP4) compared to that of HAD control for 7 days. Data are expressed as mean \pm SEM obtained from 3 independent experiments. *p < 0.05 and **p < 0.01 (vs. MSC) and †p < 0.05 and †p < 0.01 (vs. HAD)

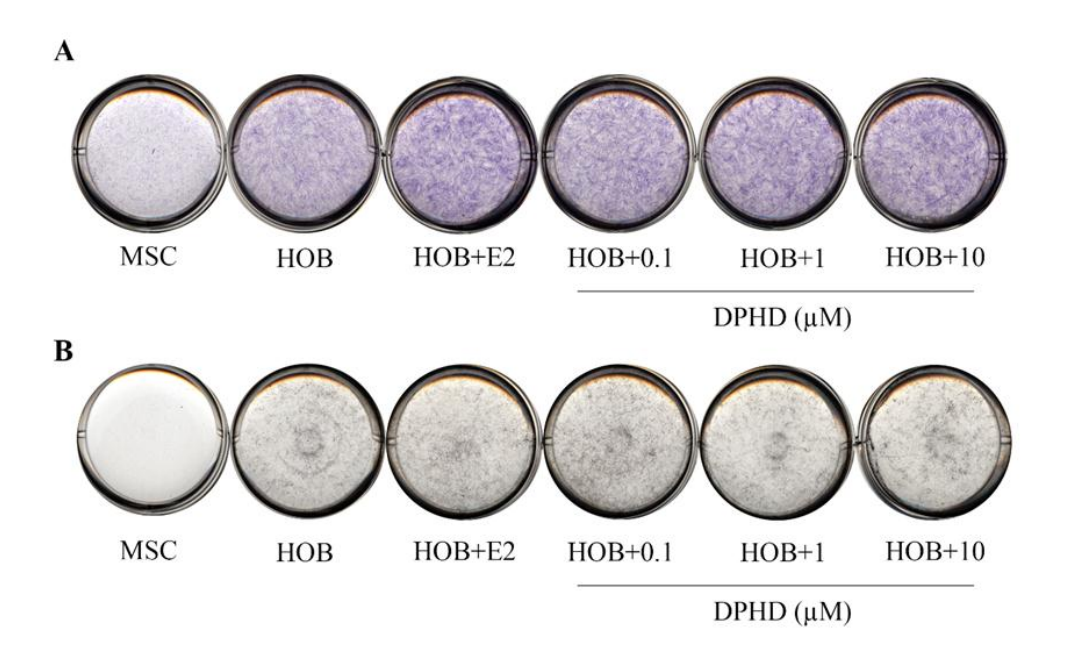


Figure. 4.8 Effect of treatments on (A) alkaline phosphatase activity determined by phosphatase staining and (B) calcium deposition determined by Von kosha staining in MSCs on day 21 of osteogenic induction.

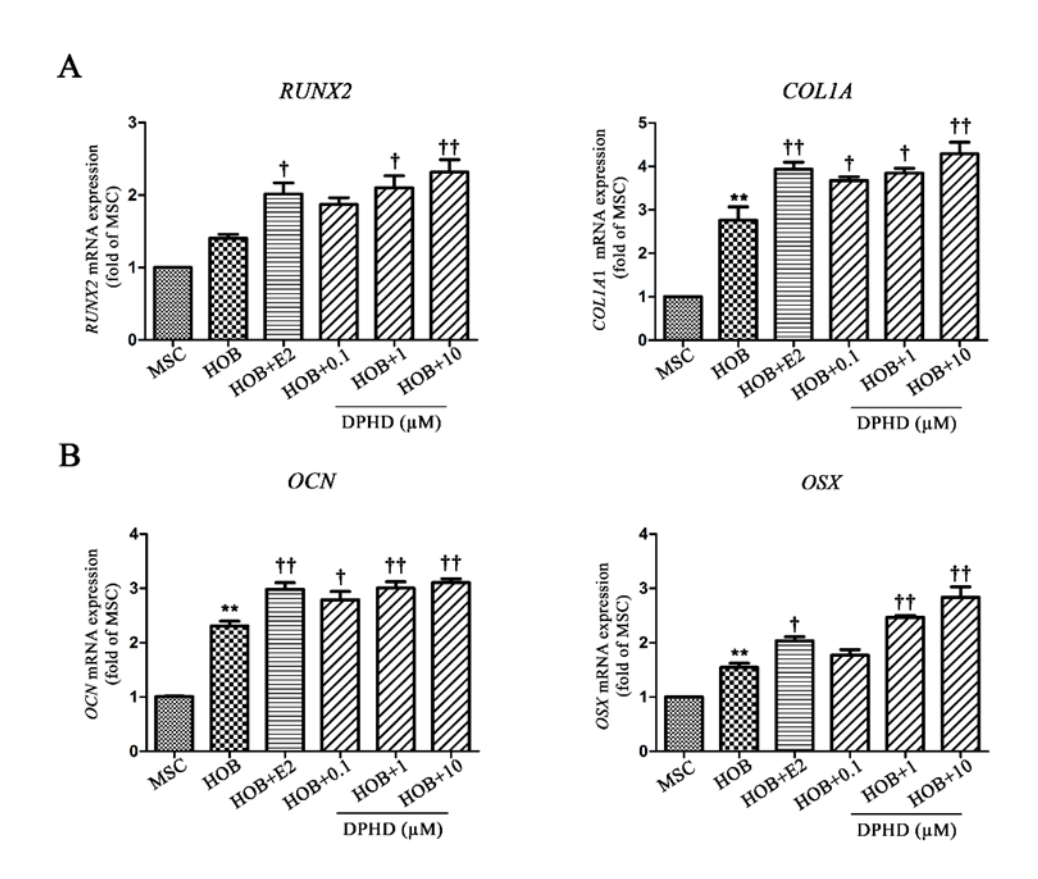


Fig. 4.9. Effect of E2 and DPHD treatments on the mRNA expression of osteogenic mRNA markers: (A) early markers at day-7: RUNX2 and COL1A1 and (B) late markers at day-21: OCN and OSX during osteogenic induction by real-time PCR. Each value is expressed as mean \pm SEM obtained from 3 independent experiments. *p < 0.05 and **p < 0.01 (vs. MSC) and †p < 0.05 and †p < 0.01 (vs. HOB).

In the present study, DPHD enhanced differentiation of MSCs into osteoblast by increasing the mRNA expression of osteogenic transcription factors including RUNX2 and OSX (encoded osterix), which are early and late osteoblast differentiation markers, respectively.. Runx2 and osterix positively regulate osteogenic differentiation of MSCs. This osteogenic effect of DPHD observed in MSCs was consistent the previous studies in which DPHD stimulates osteoblast differentiation of mouse osteoblast, and human preosteoblast (Bhukhai, Suksen et al. 2012), thereby promoting bone formation. Moreover, DPHD exerts a bone sparing effect in ovariectomy-induced trabecular bone loss and prevents deterioration

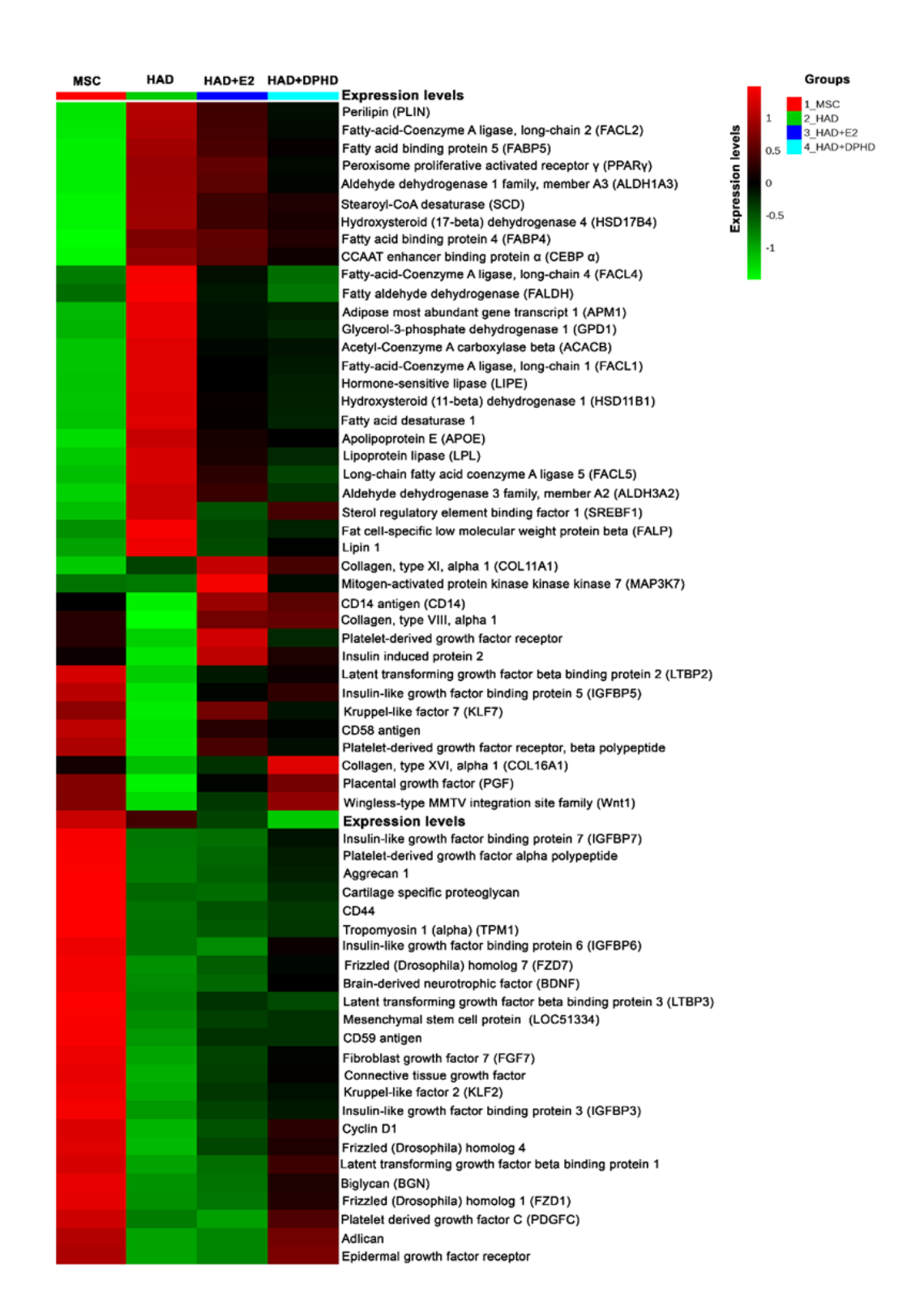


Figure 4. 10 Hierarchical clustering analysis of gene expression profile of the 63 candidate genes in non-induced MSCs, HAD induction (HAD control), HAD+E2, and HAD+DPHD (25 genes were decreased, and 38 genes were increased by treatments compared to HAD control) selected as relevant by Metabolyst

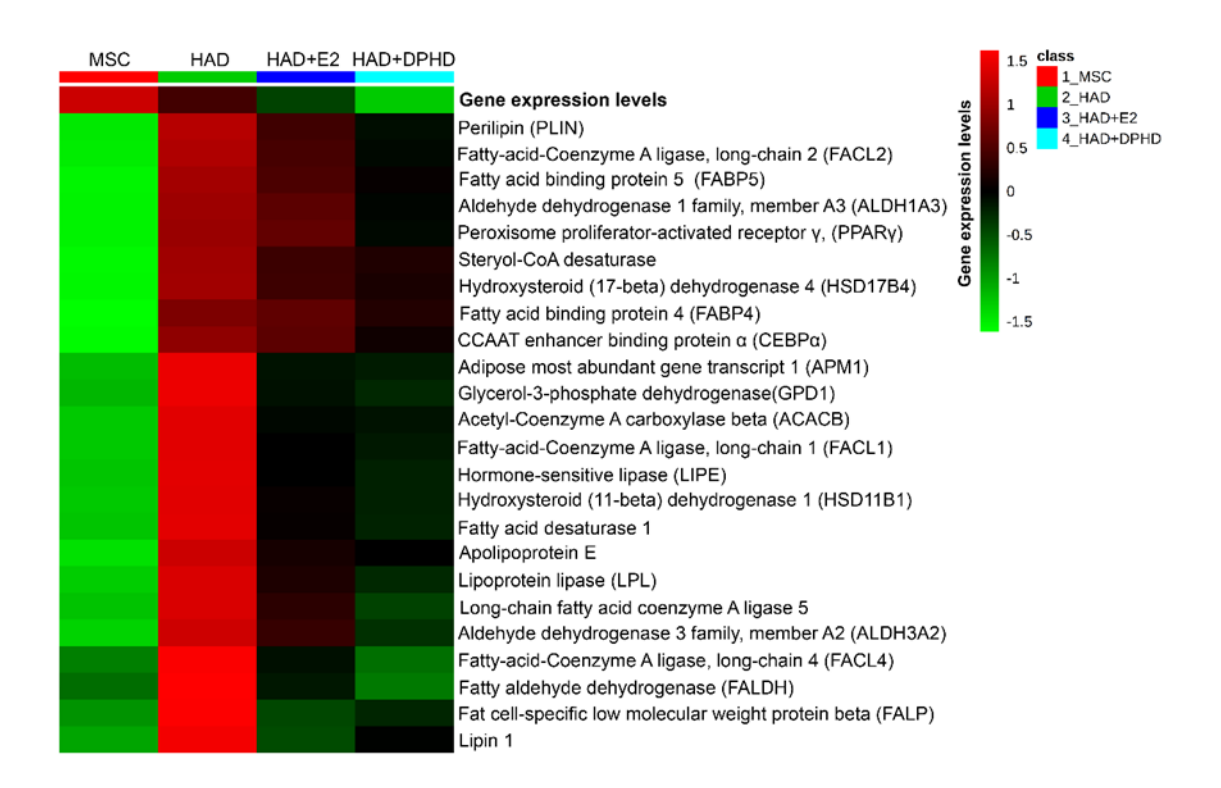


Figure 4.11. Hierarchical clustering analysis of 24 lipogenic genes in non-induced MSCs, HAD induction (HAD control), HAD+E2, and HAD+DPHD on day-7 of adipogenic differentiation selected as relevant by Metabolyst

of bone microarchitecture (Tantikanlayaporn, Wichit et al. 2013). Accordingly, the expression of genes and proteins involved in anti-adipogenic and osteogenic effects of DPHD in MSCs were correlated with gene profiling obtained from wide genome expression screening (Fig.4.10). Surprisingly, DPHD partially restored the levels of cell proliferation factors during adipogenic differentiation. However, it suppressed the expression of genes encoding adipogenic transcription factor, PPARY and its target genes, and many lipogenic proteins, thereby inhibiting adipocyte differentiation and maturation. The anti-adipogenic activity of DPHD in MSCs was similar to that of estrogen. Furthermore, the anti-adipogenic effect of DPHD was likely to be mediated through the cross-talk between estrogen receptor (ER) signaling and Wnt/eta-catenin signaling pathway. This is the first reported showing the antiadiposity effect of C. comosa extract and its isolated compound DPHD in visceral adipose tissue of the OVX rats, which is the major cause of metabolic diseases. DPHD also increased proliferation of progenitor cells, human bone marrow-derived mesenchymal stem cells, and exerted the anti-adipogenic effect. Meanwhile, it suppressed bone marrow adiposity which is associated with osteoporosis in postmenopausal. This study provides insight health beneficial information for the development of *C. comosa* and DPHD as a dietary supplement to alleviate metabolic complications related to excessive adipose tissues accumulation in the body including insulin resistance and osteoporosis.

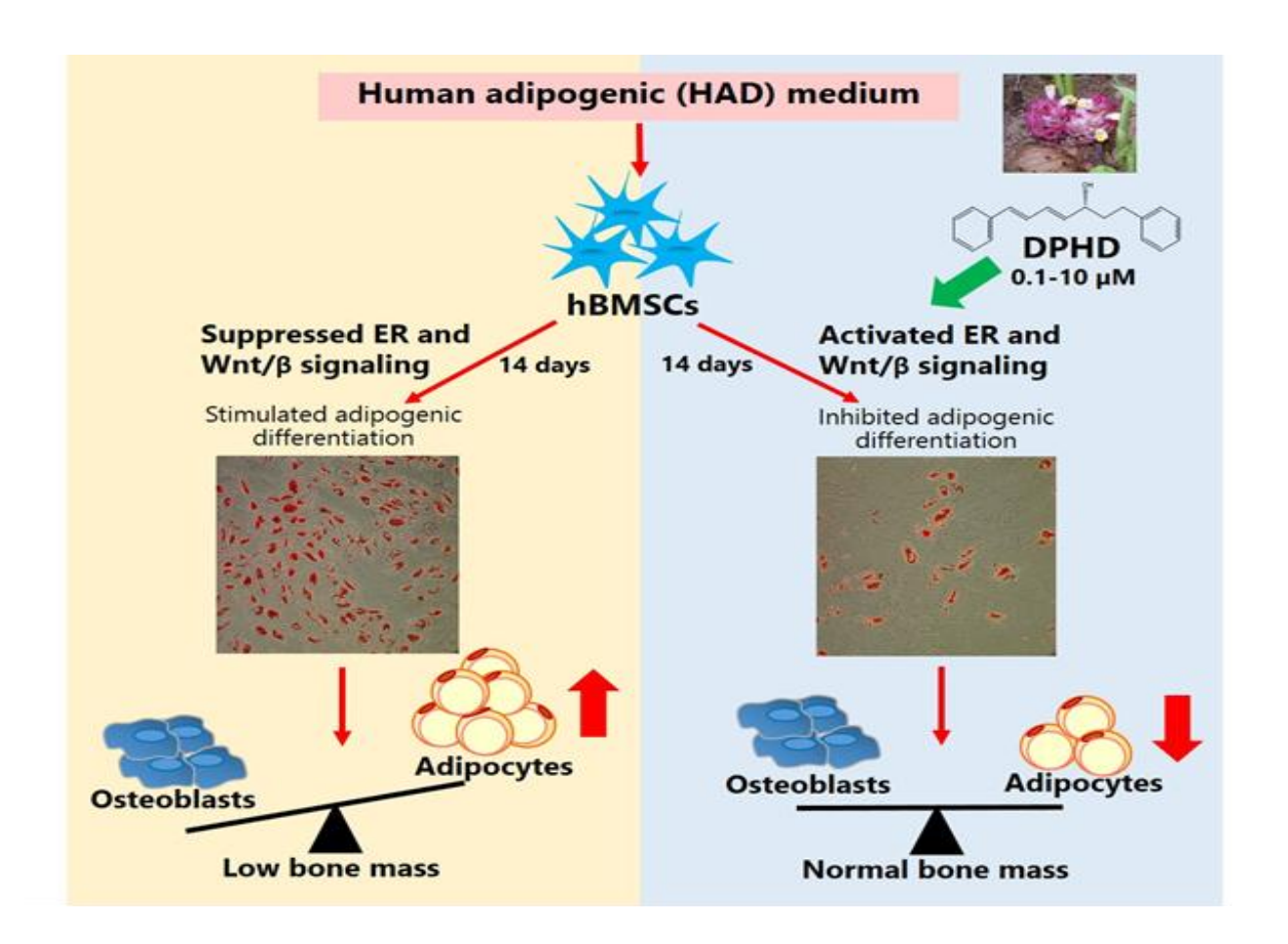


Figure 4.12. Schematic diagram showing the suppressing activities of DPHD from *C. comosa* on the differentiation of MSCs into adipocytes while promoted differentiation into osteoblasts. It indicates health beneficial effect of DPHD to reduce bone loss in aging population.

References

- 1. Anonymous, 1967. Pramuan Sapakun Ya Thai, Part 3, Wat Prachetupon (Wat Poh), Bangkok, Thailand
- 2. BaHammam, A.S., S.R. Pandi-Perumal, A. Piper, S.A. Bahammam, A.S. Almeneessier, A.H. Olaish, et al. 2016. Journal of sleep research 25: 445-453.
- 3. Bhukhai, K., K. Suksen, N. Bhummaphan, K. Janjorn, N. Thongon, D. Tantikanlayaporn, P. Piyachaturawat, A. Suksamrarn and A. Chairoungdua (2012). "A Phytoestrogen Diarylheptanoid Mediates Estrogen Receptor/Akt/Glycogen Synthase Kinase 3 β Protein-dependent Activation of the Wnt/ β -Catenin Signaling Pathway." The Journal of Biological Chemistry 287(43): 36168-36178.
- 4. Carling, D., C. Thornton, A. Woods and Matthew J. Sanders. 2012. Biochemical Journal 445: 11-27.

- 5. Charoenwanthanang, P., S. Lawanprasert, L. Phivthong-Ngam, P. Piyachaturawat, Y. Sanvarinda and S. Porntadavity. 2011. J Ethnopharmacol 134: 608-613.
- 6. Clegg, D.J., L.M. Brown, S.C. Woods and S.C. Benoit. 2006. Diabetes 55: 978-987.
- 7. D'Eon, T.M., S.C. Souza, M. Aronovitz, M.S. Obin, S.K. Fried and A.S. Greenberg. 2005. J Biol Chem 280: 35983-35991.
- 8. Farmer, S. R. (2005). "Regulation of PPARgamma activity during adipogenesis." Int J Obes (Lond) 29 Suppl 1: S13-16.
- 9. Han, S.I., Y. Komatsu, A. Murayama, K.R. Steffensen, Y. Nakagawa, Y. Nakajima, et al. 2014. Hepatology 59: 1791-1802.
- 10. Henneman, P., F.G. Schaap, P.C.N. Rensen, K.W.v. Dijk and A.H.M. Smelt. 2008. Journal of Internal Medicine 263: 107-108.
- 11. Ingvartsen, K.L. and Y.R. Boisclair. 2001. Domestic Animal Endocrinology 21: 215-250.
- 12. Intapad, S., V. Saengsirisuwan, M. Prasannarong, A. Chuncharunee, W. Suvitayawat, R. Chokchaisiri, et al. 2012. J Agric Food Chem 60: 758-764.
- 13. Jantaratnotai, N., P. Utaisincharoen, P. Piyachaturawat, S. Chongthammakun and Y. Sanvarinda. 2006. Life Sci 78: 571-577.
- 14. Jung, U.J. and M.-S. Choi. 2014. International Journal of Molecular Sciences 15: 6184-6223.
- 15. Kafkas, S., T. Dost, H. Ozkayran, C. Yenisey, P. Tuncyurek and M. Birincioglu. 2012. Effect of estrogen therapy on adipocytokines in ovariectomized-aged rats. J Obstet Gynaecol Res 38: 231-238.
- 16. Lundholm, L., S. Moverare, K.R. Steffensen, M. Nilsson, M. Otsuki, C. Ohlsson, et al. 2004. J Mol Endocrinol 32: 879-892.
- 17. Lundholm, L., H. Zang, A.L. Hirschberg, J.A. Gustafsson, P. Arner and K. Dahlman-Wright. 2008. Fertil Steril 90: 44-48.
- 18. Matejkova, O., K.J. Mustard, J. Sponarova, P. Flachs, M. Rossmeisl, I. Miksik, et al. 2004. FEBS Lett 569: 245-248..
- 19. Piyachaturawat, P., J. Charoenpiboonsin, C. Toskulkao and A. Suksamrarn. 1999. J Ethnopharmacol 66.
- 20. Pongboonrod, S., 1976. Mai Thed, Muang Thai. Kasembanakit Press, Bangkok, Thailand.
- 21. Prasannarong, M., V. Saengsirisuwan, P. Piyachaturawat and A. Suksamrarn. 2012. BMC Complementary and Alternative Medicine 12: 28.
- 22. Ratanachamnong, P., U. Matsathit, Y. Sanvarinda, P. Piyachaturawat and L. Phivthong-Ngam. 2012. International Journal of Pharmacology 8: 234-242.
- 23. Romeo, G.R., J. Lee and S.E. Shoelson. 2012. Arterioscler Thromb Vasc Biol 32: 1771-1776.
- 24. Sim, A.T. and D.G. Hardie. 1988. FEBS Lett 233: 294-298.

- 25. Sodsai, A., P. Piyachaturawat, S. Sophasan, A. Suksamrarn and M. Vongsakul. 2007. Int Immunopharmacol 7.
- 26. Soontornchainaksaeng, P. and T. Jenjittikul. 2010. Journal of Natural Medicines 64: 370-377.
- 27. Suksamrarn, A., M. Ponglikitmongkol, K. Wongkrajang, A. Chindaduang, S. Kittidanairak, A. Jankam, et al. 2008. Bioorg Med Chem 16: 6891-6902.
- 28. Sullivan, J.E., K.J. Brocklehurst, A.E. Marley, F. Carey, D. Carling and R.K. Beri. 1994. FEBS Lett 353: 33-36.
- 29. Tantikanlayaporn, D., P. Wichit, J. Weerachayaphorn, A. Chairoungdua, A. Chuncharunee, A. Suksamrarn, et al. 2013. PLOS ONE 8: e78739.
- 30. Trayhurn, P. 2007. Adipocyte biology. Obes Rev 8 Suppl 1: 41-44.
- 31. Vicennati, V., F. Pasqui, C. Cavazza, U. Pagotto and R. Pasquali. 2009. Stress-related development of obesity and cortisol in women. Obesity (Silver Spring) 17: 1678-1683.
- 32. Vinayavekhin, N., J. Sueajai, N. Chaihad, R. Panrak, R. Chokchaisiri, P. Sangvanich, et al. 2016. J Ethnopharmacol 192: 273-282.
- 33. Viollet, B. and F. Andreelli. 2011. Handb Exp Pharmacol: 303-330.
- 34. Weerachayaphorn, J., A. Chuncharunee, C. Mahagita, B. Lewchalermwongse, A. Suksamrarn and P. Piyachaturawat. 2011. J Ethnopharmacol 137.
- 35. Winuthayanon, W., K. Suksen, C. Boonchird, A. Chuncharunee, M. Ponglikitmongkol, A. Suksamrarn, et al. 2009. J Agric Food Chem 57: 840-845.
- 36. Yadav, A., M.A. Kataria, V. Saini and A. Yadav. 2013. Clin Chim Acta 417: 80-84.
- 37. Yamauchi, T., J. Kamon, Y. Minokoshi, Y. Ito, H. Waki, S. Uchida, et al. 2002. Nat Med 8: 1288-1295.

Sub-project 5: Neuroprotective effects of compounds

ABSTRACT

Alzheimer's disease (AD) and Parkinson's disease (PD) are the most two common neurodegenerative diseases related with aging. The cause of these two diseases are still unknown and treatment is unavailable. Oxidative stress occurred form free radical accumulation increased with age and consequences of metabolic disorders are believed to be a major cause of damage and death of neurons. Therefore, preventing oxidative stress could be a strategy preventing neurodegeneration. In this project, in collaboration with chemist from Thailand and China, we have tested several natural product derived compounds and modified compounds for their ability to prevent neurons from damages and death caused by both oxidative stress and factors known to induce neurodegeneration. We found that several plant-derived compounds showed high scavenging property and can protect neurons from oxidative stress induced cell damage and death. Interestingly, modification of a known anti-oxidant compound also yielded compounds with better activities. Among these, linking Alpha-lipoic acid (ALA) with an anti-ischemic drug 3-nbutylphthalide (NBP) produced compounds that contain significantly greater neuroprotective effect. Together the results from this study shade light to several possible compounds that can be further developed into novel therapeutic agents for treatment of neurodegenerative diseases.

Keywords: Neurodegenerative diseases, Alzheimer's disease, Parkinson disease, modified natural compounds, neuroprotection, antioxidant

บทคัดย่อ

โรคอัลไซเมอร์และโรคพาร์กินสันเป็นโรคความเสื่อมของสมองที่พบบ่อยที่สุดในผู้สูงอายุ สาเหตุของ โรคดังกล่าวยังไม่เป็นที่ทราบดีและปัจจุบันยังไม่มีวิธีรักษาให้หายขาด อย่างไรก็ตาม ปัจจุบันเป็นที่ทราบดีว่า ภาวะเครียดที่เกิดจากอ๊อกซิเดชันเกิดจากการสะสมของอนุมูลอิสระที่เพิ่มมากขึ้นตามอายุ และจากโรคที่ เกี่ยวกับเมตาบอลิก เป็นสาเหตุสำคัญของการเสื่อมและตายของเซลล์ประสาท ดังนั้น การป้องกันไม่ให้เซลล์ ประสาทถูกทำลายจากภาวะเครียดที่เกิดจากอ๊อกซิเดชันเป็นวิธีการป้องกันความเสื่อมของสมองที่สำคัญ งานวิจัยในโครงการนี้ ได้มีความร่วมมือกับนักวิจัยด้านเคมีจากประเทศจีน โดยได้พัฒนาโมเดลเพื่อทดสอบฤทธิ์ ของสารที่ได้จากธรรมชาติ สารสังเคราะห์ชนิดใหม่ ตลอดจนสารที่ดัดแปลงโครงสร้างทางเคมี ในการป้องกัน เซลล์ประสาทจากการถูกทำลายด้วยภาวะเครียดที่เกิดจากอ๊อกซิเดชัน ด้วยสภาวะที่เหนี่ยวนำให้เกิดโรคอัลไซ เมอร์และโรคพาร์กินสัน ผลการทดลองพบว่าสารจากพืชสมุนไพรหลายชนิดมีฤทธิ์ต้านอนุมูลอิสระ และ สามารถปกป้องเซลล์ประสาทจากสภาวะดังกล่าวได้อย่างมีประสิทธิภาพ ยกตัวอย่างเช่น การดัดแปลง โครงสร้างของกรดแอลฟาลิโปอิกที่นำมาเชื่อมต่อกับ NBP ซึ่งเป็นยาที่ปัจจุบันใช้เป็นยารักษาภาวะสมองขาด เลือด มีประสิทธิภาพในการป้องกันการทำลายของเซลล์ประสาทได้ดีมากเมื่อเทียบกับสารเดี่ยว ๆ นอกจากนี้ โครงการวิจัยยังได้ค้นพบโมเดลของเซลล์ประสาทแบบใหม่ เพื่อนำไปใช้ในการวิเคราะห์ผลของสารต่อการ

ปกป้องเซลล์ประสาทได้ในอนาคต ผลงานวิจัยจากโครงการนี้เป็นข้อมูลสำคัญที่จะนำไปสู่การพัฒนายาใหม่ สำหรับการป้องกันและรักษาโรคความเสื่อมของสมองได้ในอนาคต

คำสำคัญ: โรคความเสื่อมของสมอง โรคอัลไซเมอร์ โรคพาร์กินสัน สารธรรมชาติดัดแปลง การปกป้องเซลล์ ประสาท ฤทธิ์ต้านอนุมูลอิสระ

Introduction

Neurodegenerative diseases such as Alzheimer's disease (AD) and Parkinson's disease (PD) are progressive and irreversible damage of the nervous system. The pathogenesis of these diseases is still unclear but several evidences suggest that oxidative stress, resulted from accumulation of free radicals and decreasing function of endogenous anti-oxidant system, is one of major causes of the degeneration [1-4]. The free radicals oxidize cellular components such as lipids, proteins, and DNA leading to neuronal damage and death. Mitochondrial electron transport chain generates reactive oxygen species (ROS) which toxic to neuron. The ROS that are generated by mitochondrial respiration, including hydrogen peroxide (H_2O_2), hydroxyl radical (OH), superoxide anion (O^{2-})[5, 6] are potent inducers of oxidative damage and mediators of ageing. Moreover, ROS particularly active in neurons as the excitatory amino acid and neurotransmitters serve as source of oxidative stress. In addition, neurons are post-mitotic cells and therefore, they are particularly sensitive to free radicals leading to neuronal dysfunction, neuronal cell death and eventually neurodegenerative diseases [7]. Currently there is no treatment for these diseases once they occur, therefore protecting neurons from such damages is the best way to prevent these neurodegenerative diseases.

Natural products from plants and marine microbes are sources of various biological active compounds. Several of these compounds demonstrated potent anti-oxidation activity. As oxidative stress in a major course of neurodegeneration, compounds derived from these natural products might be able to protect neurons from damages and death caused by oxidative stress or other related factor. Alpha-lipoic acid (ALA) is a naturally occurring compound that has been shown to exert antioxidant and anti-inflammatory properties. Several studies showed that ALA elicits neuroprotective effects both *in vitro* and *in vivo* models [8-16]. Synergistic protective effect has been observed if ALA is combined with other drugs in several different animal models of pathology [17-23].

In this study, a clinical anti-ischemic and neuroprotective drug 3-n-butylphthalide (NBP) [24] was conjugated with lipoic acid by an amide bond and determined its neuroprotective activities against oxidative stress-induced neuronal cell damage.

Results

Part I Determine neuroprotective effects of marine microbes derived compounds

1.1 Screening for neuroprotective effects of marine microbes derived compounds against hyper-phosphorylated Tau-induced neurodegeneration

First, we tested for safety dose of the compounds derived from marine microbes to identify which concentrations are safe to use in neuronal cells (SH-SY-5Y). Most of the compounds are very safe in neuronal cells as shown in the table below. Then we test whether the compounds can prevent neuronal death induced by Okadeic acid, a toxin used to induce hyper-phosphorylated Tau, which mimics pathological cause of neuronal death found in Alzheimer's disease. However, none of these compounds could protect neurons from hyper-phosphorylated Tau-induced neurodegeneration.

Table 5.1. Cytotoxicity and neuroprotective test for marine microbes-derived compounds

No.	Sample No.	IC50 (uM)	Neuroprotective effect
1	HD-ZWM-1085	1.539e+010	-
2	HD-ZWM-1087	>50	No
3	HD-ZWM-1089	>50	No
4	HD-ZWM-1090	>50	No
5	HD-ZWM-1091	>50	No
6	HD-ZWM-1092	6.179e+029	-
7	HD-ZWM-1164	>50	No
8	HD-ZWM-1166	4.504	-
9	HD-ZWM-1167	14.50	-
10	HD-ZWM-1170	6.807	-
11	HD-ZWM-1171	>50	No
12	HD-ZWM-1172	>50	No
13	HD-ZWM-1186	8.661	-
14	HD-ZWM-1273	0.06643	-
15	HD-ZWM-1274	>50	No
16	HD-ZWM-1281	>50	No
17	HD-ZWM-1289	>50	No
18	HD-ZWM-1290	>50	No

No.	Sample No.	IC50 (uM)	Neuroprotective effect
19	LWL-1	>50	No
20	LWL-2	>50	No
21	LWL-3	>50	No
22	LWL-4	>50	No
23	LWL-5	>50	No
24	LWL-6	>50	No
25	LWL-7	>50	No
26	LWL-8	>50	No
27	LWL-9	>50	No
28	LWL-10	>50	No

Part II Determine neuroprotective effects of plant-derived compounds

2.1 Screening for neuroprotective effects of plant-derived compounds against oxidative stress induced neurodegeneration

2.1.1 Determine scavenging effect of plant-derived compounds

First, we screen for plant-derived compounds with ability to scavenge the free radicals using in vitro DPPH assay. Several of these compounds showed very high ability to scavenge the free radical. Among these compounds, the MUC 971, 972 and 978 elicit strongest effects. We therefore select these compounds for further investigation.

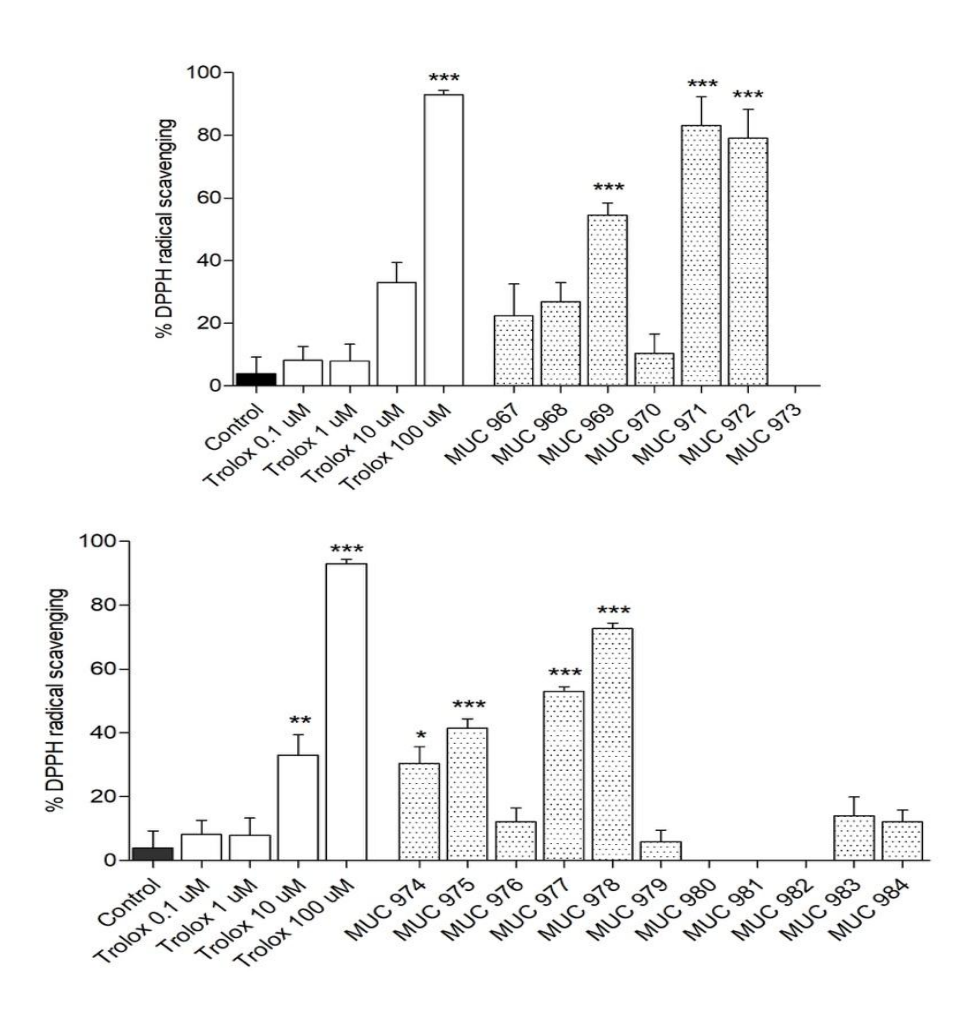


Figure 5.1. Graph showing scavenging effect of compounds from *Zingiber mekongense* (A) and *Gardenia sessiliflora* (B). Trolox was used as a positive control. Several compounds significantly decreased DPPH free radical. Data show as mean \pm S.E.M., n=3. *P < 0.05, **P < 0.01 and ***P < 0.001 versus control group (ANOVA).

2.1.2 Determine safety of the plant-derived compounds on neuronal cells

Next, we performed cytotoxicity test of the selected compounds derived from plant to identify their safe concentration that can be used in neuronal cells. Most of the compounds are quite safe to neuronal cells as shown in Figure 5.2.

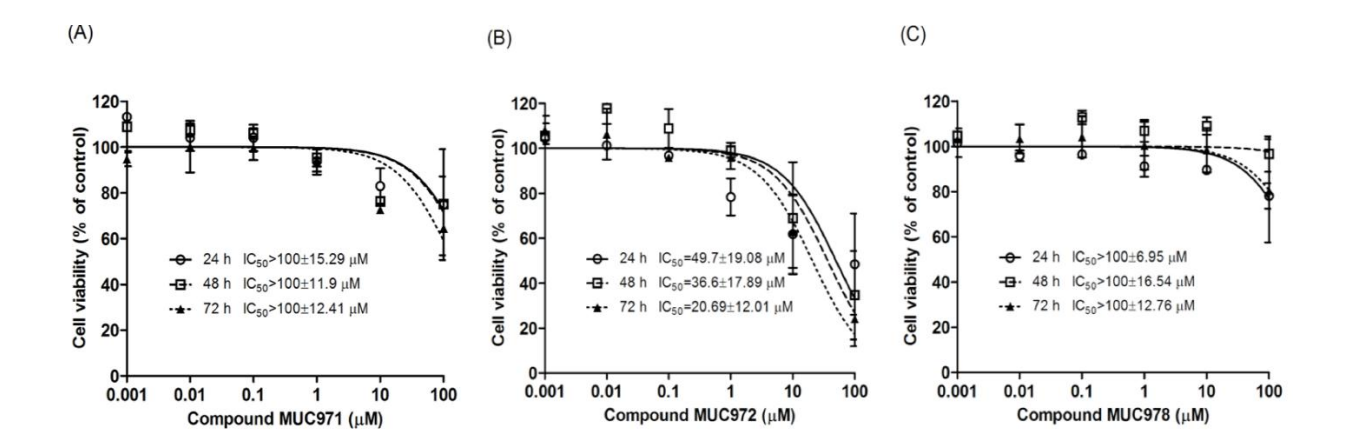


Figure 5.2. Graph showing cytotoxicity test of MUC971, 972 and 978. All of these compounds are quite safe with IC50 > 50 uM for MUC972 and >100 uM for MUC 971 and 978.

2.1.3 Plant derived compounds prevent neuronal death against oxidative stress

To determine whether the selected plant derived compounds can protect neurons against oxidative stress, CAD cells were pretreated with MUC 971, 972 and 978 (10 uM) for 24h before being exposed to $\rm H_2O_2$ for 12 h. Cell viability was assessed by MTT assay. We observed increased in cell viability in the presence of MUC 971, 972 and 978, with the strongest activity in MUC 978 (Figure 5.3).

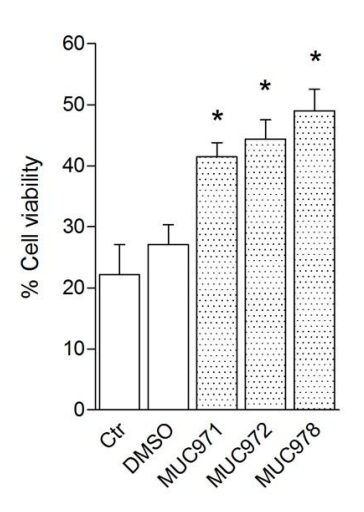


Figure 5.3. Graph showing neuroprotective effect of MUC971, 972 and 978. The pretreated compounds increased cell viability of neuronal cells exposed to H_2O_2 . Data are mean \pm SEM from three independent experiments. *p < 0.05, *p < 0.01, and ***p < 0.001 compared with H_2O_2 -treated group.

1.2.4 Plant derived compounds prevent neuronal growth cone damage against oxidative stress

Next, we selected MUC978 and determined whether it could protect primary neurons from damages induced by oxidative stress by using cortical neurons. One of the most sensitive structure in the neurons is the growth cone, a cytoskeletal enriched structure at the tip of the axons, which plays several crucial roles including neurite formation, axon guidance and neuronal branching [28]. Damages of growth cone therefore lead to neuronal dysfunction and eventually neuronal death. Growth cone is very dynamic and sensitive to the oxidative stress [29, 30]. In the present of H_2O_2 the growth cone of the cortical neurons shrank with disruption of both microtubules and actin filament (Figure 4). Interestingly, when the primary neurons were pretreated with MUC978 the growth cone structure was well preserved after H_2O_2 exposure.

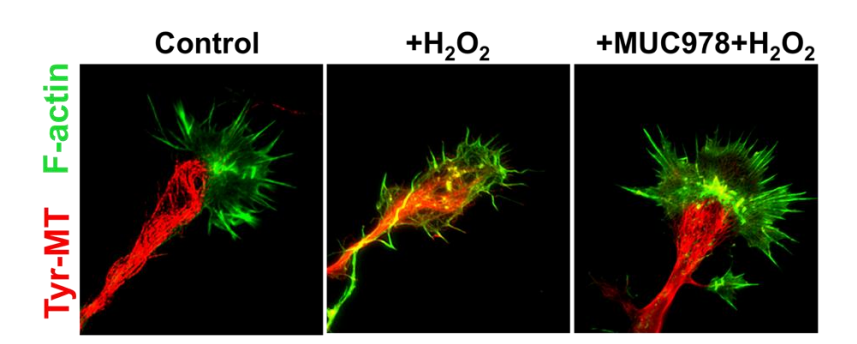


Figure. 5.4 Representative images of the growth cone of cortical neurons before and after exposure to H_2O_2 in the absence or presence of MUC978. The cells were pretreated with vehicle control (DMSO) or MUC978 (10 uM) for 24 hours prior to exposure to H_2O_2 . The cells were fixed and immunostained with tyrosinated tubulin antibody for dynamic microtubules (red) and Phalloidin for F-actin (green).

Part III Determine neuroprotective effects of modified compounds

3.1 Screening for neuroprotective effects of modified compounds against oxidative stress-induced neurodegeneration

3.1.1 Determine safety of the modified compounds on neuronal cells

First, we test for safety of the modified known compounds including lipoic acid and organoseleniums derivatives. These compounds are synthesized and modified by our Chinese collaborators. All of these compounds are safe with neuronal cells.

Table 5.3. Cytotoxicity test for modified compounds in neuronal cells.

IC ₅₀ (μM) 72 hours exposure							
Lipoic acid derivatives							
dlx-13	>50						
dlx-15	>50						
dlx-18	>50						
dlx-23	>50						
dlx-zj-10	>50						
R-(+)lipoic acid	>50						
DL-lipoic acid	>50						
Organoseleniums							
YBXL	>50						
LJ-YBDJY	>50						
LJ-YBJJY	>50						
LZ-YBJ1	>50						
LZ-YBL1	>50						
LJ-YC1	>50						
LZ-YBL2	>50						
LZ-YBG2(H)	>50						
LJ-YBBD	>50						
LJ-YBBYA	>50						

3.1.2 Determine the neuroprotective effect of modified compounds against neuronal cell death induced by oxidative stress

After we identify safe concentration range of the modified compounds for neuronal cells we tested these compounds for their ability to protect the neurons against oxidative stress induced cell death. We pretreated the cells with the compounds for 24 h before exposing with H2O2. Interestingly, several of these compounds could significantly protect the neuronal death compared to untreated cells.

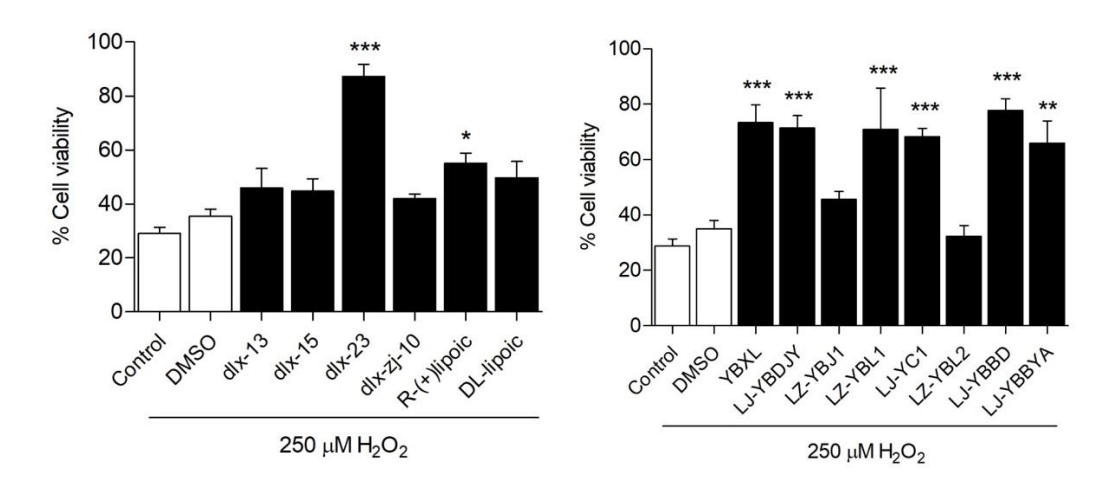
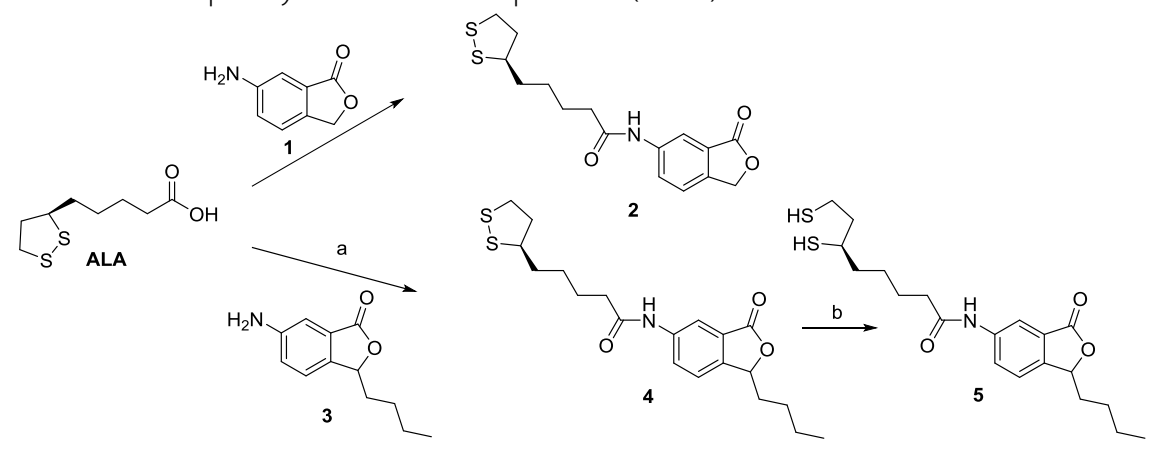


Figure 5.5. Effects of ALA (A) and Organoselenium (B) derivatives on H_2O_2 -induced CAD cells death. **(A)** The cells were treated with the maximum concentration that are safe to use in neuronal cells before being exposed to H_2O_2 for 12 hours **(B)**. The values are presented as percentages of control. Data are means \pm SEM from three independent experiments. *p < 0.05, *p < 0.01, and ***p < 0.001 compared with H_2O_2 -treated group.

3.1.3 Structural modification of Alpha-lipoic acid ALA

Among the modified compounds, the Dlx23 showed the best activity. Therefore, we decided to further investigate the Dlx23 for its effect and underlying mechanism. This compound is the ALA derivative, which was synthesized by the Chinese collaborator. Briefly, ALA was coupled with compound 1 [25] to provide the conjugated compound 2. Coupling of ALA and 6-amino-3-n-butylphthalide 3 [26] produced another conjugated compound 4 which was subsequently reduced to compound 5 (Dlx23).



Reagents and condition:
(a) EDC•HCI / DMAP / DCM / rt / overnight; (b) NaBH₄/MeOH/NaOH/H₂O.

Figure 5.6 Structure and synthetic route of ALA derivatives

3.1.4 ALA derivative elicits stronger free radical scavenging property than the parent compound

Next, we investigated whether neuroprotective effect of dlx-23 is elicited via its anti-oxidant activity. To examine anti-oxidant activity of ALA modified compounds the *in vitro* DPPH assay was used. Consistent with its neuroprotective effect, dlx-23 exerted antioxidant activity by scavenging DPPH radical *in vitro* (Figure 5.7).

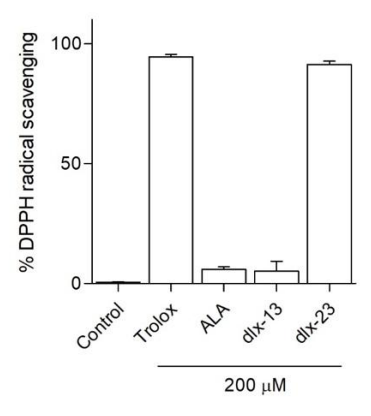
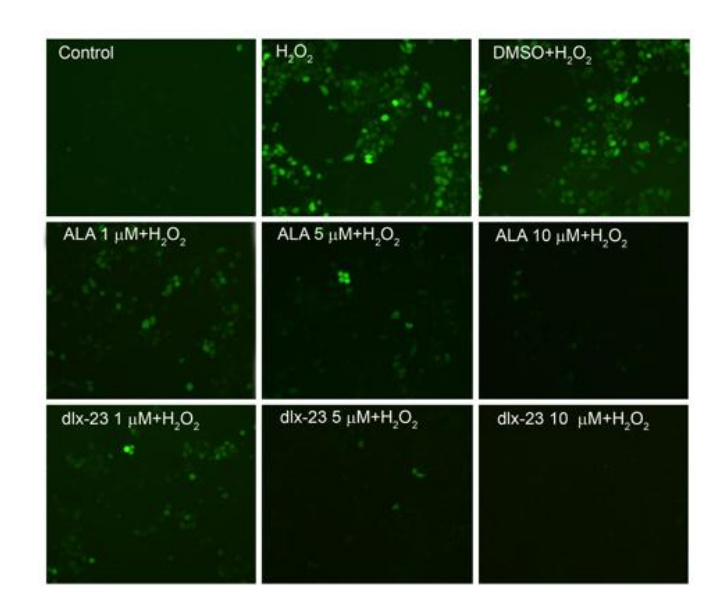


Figure 5.7. DPPH scavenging activity. Percentage of DPPH radical scavenging was calculated against control group. Data are means \pm SEM from three independent experiments.

3.1.5 ALA derivative elicits higher anti-oxidant property

We further determined the ability of dlx-23 to prevent intracellular ROS accumulation. Intracellular ROS in CAD cells was significantly increased after treated with H_2O_2 for 3 hours. Pretreatment with dlx-23 significantly reduced the ROS production induced by H_2O_2 in CAD cells. This anti-oxidant effect was stronger compared to ALA at the same concentrations (Figure 5.8).



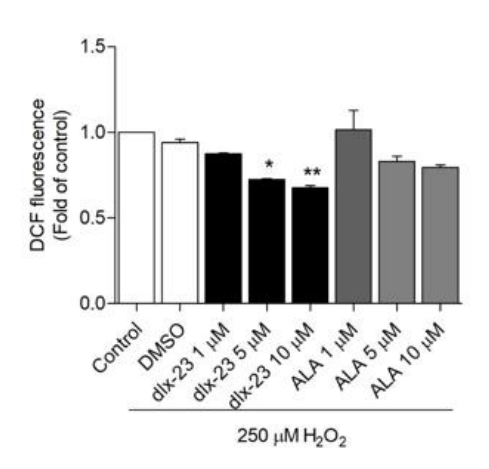


Figure 5.8. Effects of dlx-23 on H_2O_2 -induced intracellular ROS accumulation. CAD cells were pretreated with dlx-23 or ALA at 1, 5, 10 uM for 24 hours before exposed to H_2O_2 for 3 hours. The DCF fluorescence signal was observed under florescence microscope.

Decreasing of GSH levels correlates with increasing oxidative stress. In this study, we further examined the effect of dlx-23 on intracellular GSH levels. As shown in Figure 9A, the cells exposed to 250 mM $\rm H_2O_2$ for 1 hour were slightly reduced intracellular GSH levels. Cells pretreated with vitamin C (a positive control) increased GSH levels in a concentration dependent manner. Although ALA maintains GSH levels, it was not significantly increased than those treated with $\rm H_2O_2$ alone. Pretreatment with dlx-23 efficiently maintains intracellular GSH at 5 mM and strongly increased the levels at 10 mM (lower concentration than that of vitamin C). Dlx-23 itself increases GSH expression in the cells at concentration of 10 mM (Fig. 5.9B). This result suggests greater effect of dlx-23 on intracellular GSH levels compared to its parent, ALA, and a well-known antioxidant, vitamin C.

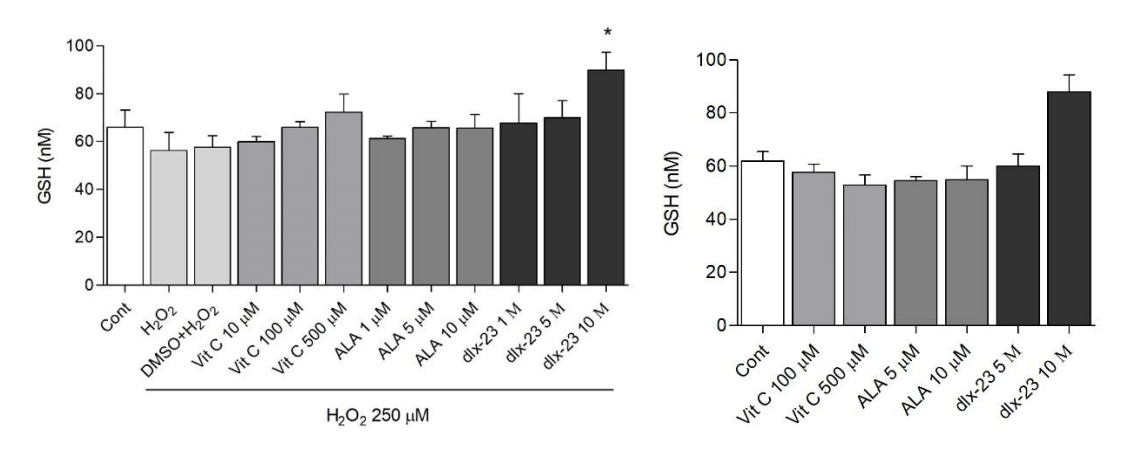
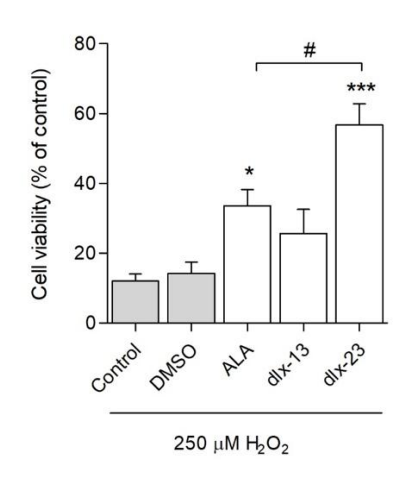


Figure 5.9. The effect of dlx-23 on intracellular GSH levels. (A) The cells were pretreated with indicated concentration of compounds for 24 hours before exposed to 250 mM H_2O_2 for 1 hour. (B) The intracellular GSH levels after the cells exposed to the compounds alone for 24 hours.

3.1.6 ALA derivative prevents neuronal death against oxidative stress

To determine the neuroprotective effect of ALA derivative compounds against oxidative stress-induced cell death, H_2O_2 was used to generate free radical in the CAD cells, a CNS catecholaminergic cell line. The cells were pretreated with different concentration of the compounds or DMSO as a vehicle control before being exposed to H_2O_2 . Cell viability was then determined by MTT assay. Exposure to 250 uM of H_2O_2 for 12 hours decreased the cell viability compared to control. Pretreatment with 10 uM of dlx-23 prior to H_2O_2 exposure significantly increased the cell viability (Fig. 5.10). We then further investigated different concentration of dlx-23 and found that its neuroprotective effect was a concentration-dependent manner (Figure 5.10B). These results suggest that compound 5 (dlx-23) exerts a stronger neuroprotective effect against H_2O_2 -induced cell death compared to its parent compound (ALA).



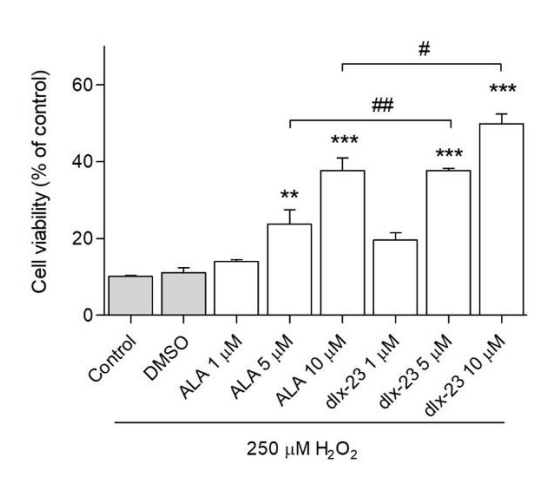


Figure 5.10. Effects of ALA derivatives on H_2O_2 -induced CAD cells death. **(A)** The cells were treated with maximum concentration with no toxic effect of compounds before exposed to H_2O_2 for 12 hours **(A)**. Comparison of the effect of dlx-23 and ALA was showed a concentration dependent manner (1, 5, 10 uM) at 12 hours **(B)** The values are presented as percentages of control. Data are mean \pm SEM from three independent experiments. *p < 0.05, *p < 0.01, and ***p < 0.001 compared with H_2O_2 -treated group.

3.1.7 ALA derivative prevents neuronal growth cone damage against oxidative stress

As mentioned earlier, growth cone is one of the most sensitive structure in the neurons. We therefore ask whether the ALA derivative dlx23 could prevent growth cone damage induced by oxidative stress. Interestingly, when the primary neurons were pretreated with the dlx23 the growth cone structure was well preserved after H_2O_2 exposure suggesting that the dlx23 can protect the primary neurons from H_2O_2 induced growth cone damages.

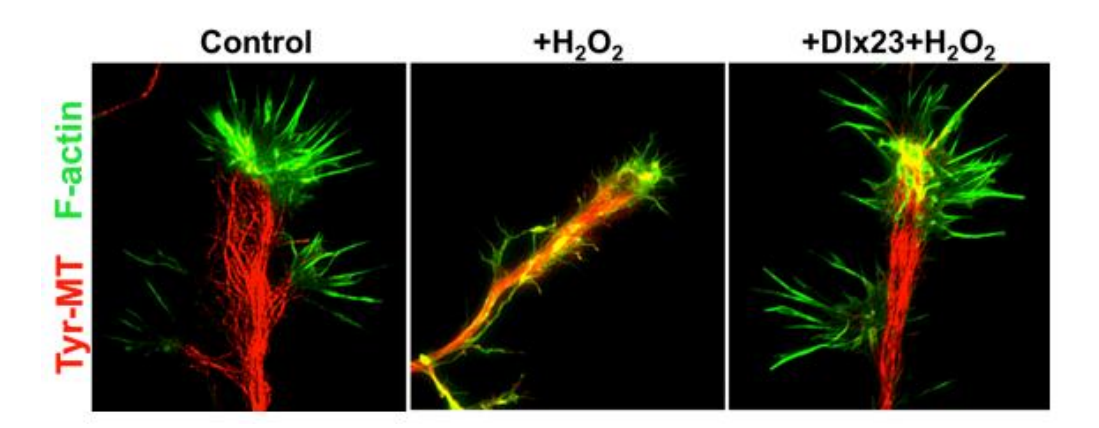


Figure 5.11. Representative images of the growth cone of cortical neurons before and after exposure to H_2O_2 in the absence or presence of dlx-23. The cells were pretreated with vehicle control (DMSO) or dlx-23 (10 uM) for 24 hours prior to exposure to H_2O_2 . The cells were fixed and immunostained with tyrosinated tubulin antibody for dynamic microtubules (red) and Phalloidin for F-actin (green).

3.2 The neuroprotective effects of modified compounds against toxin-induced Parkinson's disease

3.2.1 6-OHDA induce cell death as a cell model of Parkinson's disease

The toxicity of 6-OHDA was investigated by pre-treating cells with the fresh medium for 24 hours, similarly to pre-treatment condition, prior to 6-OHDA exposure for 24 hours. 6-OHDA was found to significantly decrease cell viability and this toxicity was dose dependent. A significant toxic effect was observed in groups that received 6-OHDA at 50, 75, 100, 150, and 200µM by 75.89±1.59%, 51.17±3.5%, 36.39±3.52%, 21.99±1.69%, and 23.55±0.46% cell viability relative to control. Therefore, the cells exposed to 75µM 6-OHDA was selected to induce toxicity and evaluate protection of ALA or its derivative against the toxicity of 6-OHDA

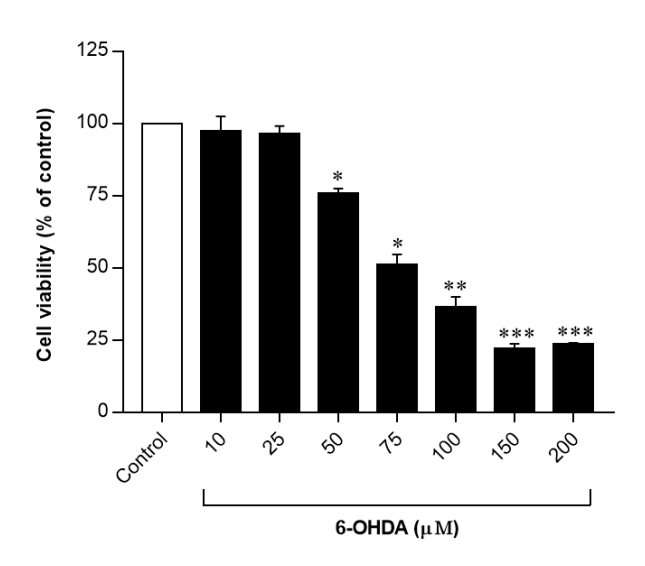


Figure 5.12. Effect of 6-OHDA on cell viability. The cells were treated with fresh media for 24 hours, followed by incubation with the different concentration of 6-OHDA (10, 25, 50, 75, 100, 150, and 200 μ M) for 24 hours. After treatment, MTT assay was performed to investigate viable cell. Data are percentage to control group and are mean \pm SEM of three independent experiment. *P<0.05, **P<0.01 and ***P<0.001 versus control group (One-way ANOVA followed by Tukey's test).

3.2.2 Neuroprotective effect of ALA hybrid compound against 6-OHDA induce cell death in a cell model of Parkinson's disease

To investigate the neuroprotective effects of ALA and its derivative (dlx23) on 6-OHDA-induced cell death, SH-SY5Y cells were pretreated with either ALA or its derivative at 1, 5, 10, and 25µM for 24 hours prior to exposure to 75µM 6-OHDA for a further 24 hours. The viability of cells incubated with 75µM 6-OHDA for 24 h was 45.43±2.3% of the control value, and the viability significantly increased to 59.1± 2.36%, 68.83±0.46%, and 66.79±1.38% when cells were pretreated with ALA at 5, 10, and 25µM, respectively. Pretreatment with 10, and 25µM of ALA derivative for 24 hours showed protective effects against the damage caused by 6-OHDA to 83.01±2.38%, and 82.06±3.59%, respectively. The results showed that both ALA and its derivative dose-dependently protect cells from 6-OHDA-induced decreases in cell viability. However, the protective effect of the ALA derivative was significantly greater than ALA at 10, and 25µM.

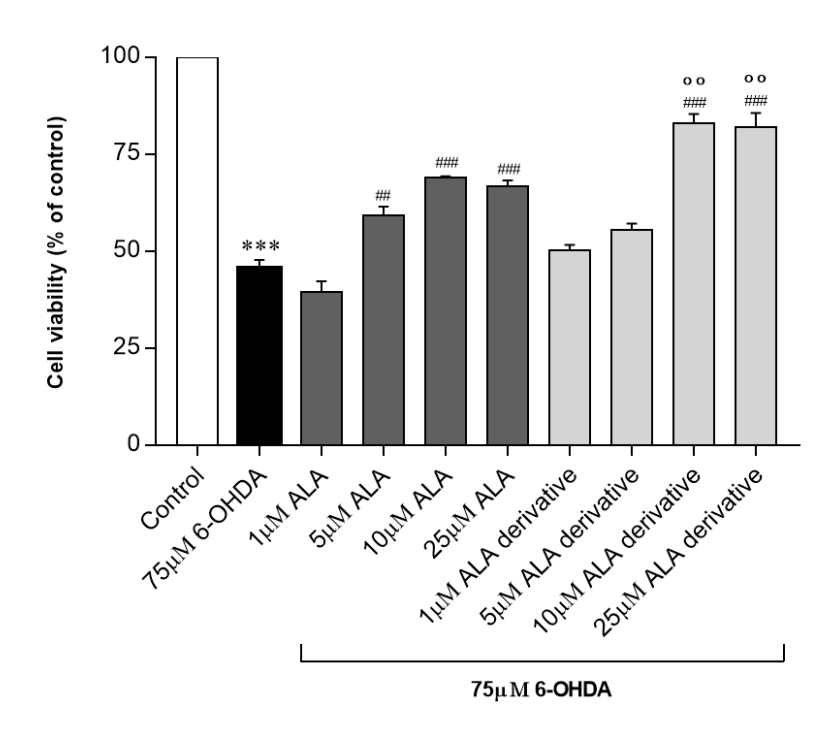


Figure 5.13. Neuroprotective effect of ALA and its derivative. The cells were pretreated with either ALA or its derivative at the indicated concentration for 24 hours and then further incubated for 24 hours with 75 μ M 6-OHDA. Viability of cells was assessed by MTT assay. Data are expressed as percentages of control group and presented as mean \pm SEM of three independent experiment. ***P<0.001 versus control group, **P<0.01 and ***P<0.001 versus 6-OHDA-treated group, **OP<0.01 versus ALA-treated group (One-way ANOVA followed by Tukey's test).

Conclusion

This study found neuroprotective effects in several compounds including compounds derived from plant as well as modified compounds. Some of these compounds demonstrate strong anti-oxidant activity and protect neuronal death and damage from oxidative stress. Several modified compounds also elicit the ability to protein neuronal death from both oxidative stress and factors known to induce neurodegeneration. Together the results from this study shade light to several possible compounds that can be further developed into novel therapeutic agents for treatment of neurodegenerative diseases.

References:

- [1]. Barnham, K.J., C.L. Masters and A.I. Bush, Neurodegenerative diseases and oxidative stress. Nat Rev Drug Discov, 2004. 3(3): p. 205-14.
- [2]. Chen, X., C. Guo and J. Kong, Oxidative stress in neurodegenerative diseases. Neural Regen Res, 2012. 7(5): p. 376-85.
- [3]. Giasson, B.I., et al., Oxidative damage linked to neurodegeneration by selective alpha-

- synuclein nitration in synucleinopathy lesions. Science, 2000. 290(5493): p. 985-9.
- [4]. Melo, A., et al., Oxidative stress in neurodegenerative diseases: mechanisms and therapeutic perspectives. Oxid Med Cell Longev, 2011. 2011: p. 467180.
- [5]. Giorgio, M., et al., Hydrogen peroxide: a metabolic by-product or a common mediator of ageing signals? Nat Rev Mol Cell Biol, 2007. 8(9): p. 722-8.
- [6]. Park, W.H., The effects of exogenous H2O2 on cell death, reactive oxygen species and glutathione levels in calf pulmonary artery and human umbilical vein endothelial cells. Int J Mol Med, 2013. 31(2): p. 471-6.
- [7]. Mattson, M.P. and T. Magnus, Ageing and neuronal vulnerability. Nat Rev Neurosci, 2006. 7(4): p. 278-94.
- [8]. Gruzman, A., et al., Synthesis and characterization of new and potent alpha-lipoic acid derivatives. Bioorg Med Chem, 2004. 12(5): p. 1183-90.
- [9]. Holmquist, L., et al., Lipoic acid as a novel treatment for Alzheimer's disease and related dementias. Pharmacol Ther, 2007. 113(1): p. 154-64.
- [10]. Connell, B.J., et al., UPEI-400, a conjugate of lipoic acid and scopoletin, mediates neuroprotection in a rat model of ischemia/reperfusion. Food Chem Toxicol, 2017. 100: p. 175-182.
- [11]. Connell, B.J., et al., Lipoic acid protects against reperfusion injury in the early stages of cerebral ischemia. Brain Res, 2011. 1375: p. 128-36.
- [12]. Richard, M.J., et al., Cellular mechanisms by which lipoic acid confers protection during the early stages of cerebral ischemia: a possible role for calcium. Neurosci Res, 2011. 69(4): p. 299-307.
- [13]. Clark, W.M., et al., Efficacy of antioxidant therapies in transient focal ischemia in mice. Stroke, 2001. 32(4): p. 1000-4.
- [14]. Panigrahi, M., et al., alpha-Lipoic acid protects against reperfusion injury following cerebral ischemia in rats. Brain Res, 1996. 717(1-2): p. 184-8.
- [15]. Wolz, P. and J. Krieglstein, Neuroprotective effects of alpha-lipoic acid and its enantiomers demonstrated in rodent models of focal cerebral ischemia. Neuropharmacology, 1996. 35(3): p. 369-75.
- [16]. Cao, X. and J.W. Phillis, The free radical scavenger, alpha-lipoic acid, protects against cerebral ischemia-reperfusion injury in gerbils. Free Radic Res, 1995. 23(4): p. 365-70.
- [17]. Mukherjee, R., et al., A combination of melatonin and alpha lipoic acid has greater cardioprotective effect than either of them singly against cadmium-induced oxidative damage. Cardiovasc Toxicol, 2011. 11(1): p. 78-88.
- [18]. Bano, M. and D.K. Bhatt, Ameliorative effect of a combination of vitamin E, vitamin C, alpha-lipoic acid and stilbene resveratrol on lindane induced toxicity in mice olfactory lobe and cerebrum. Indian J Exp Biol, 2010. 48(2): p. 150-8.
- [19]. Nagesh, B.G., A. Kumar and R.L. Singh, Chronic pretreatment with acetyl-L-carnitine and

- +/-DL-alpha-lipoic acid protects against acute glutamate-induced neurotoxicity in rat brain by altering mitochondrial function. Neurotox Res, 2011. 19(2): p. 319-29.
- [20]. Garcia-Estrada, J., et al., An alpha-lipoic acid-vitamin E mixture reduces post-embolism lipid peroxidation, cerebral infarction, and neurological deficit in rats. Neurosci Res, 2003. 47(2): p. 219-24.
- [21]. Sola, S., et al., Irbesartan and lipoic acid improve endothelial function and reduce markers of inflammation in the metabolic syndrome: results of the Irbesartan and Lipoic Acid in Endothelial Dysfunction (ISLAND) study. Circulation, 2005. 111(3): p. 343-8.
- [22]. Shotton, H.R., S. Broadbent and J. Lincoln, Prevention and partial reversal of diabetes-induced changes in enteric nerves of the rat ileum by combined treatment with alphalipoic acid and evening primrose oil. Auton Neurosci, 2004. 111(1): p. 57-65.
- [23]. Gonzalez-Perez, O., et al., Beneficial effects of alpha-lipoic acid plus vitamin E on neurological deficit, reactive gliosis and neuronal remodeling in the penumbra of the ischemic rat brain. Neurosci Lett, 2002. 321(1-2): p. 100-4.
- [24]. Abdoulaye, I.A. and Y.J. Guo, A Review of Recent Advances in Neuroprotective Potential of 3-N-Butylphthalide and Its Derivatives. Biomed Res Int, 2016. 2016: p. 5012341.
- [25]. Wang, Z., et al., Neuroprotective effects of benzyloxy substituted small molecule monoamine oxidase B inhibitors in Parkinson's disease. Bioorg Med Chem, 2016. 24(22): p. 5929-5940.
- [26]. Qiang, X., et al., DL-3-n-butylphthalide-Edaravone hybrids as novel dual inhibitors of amyloid-beta aggregation and monoamine oxidases with high antioxidant potency for Alzheimer's therapy. Bioorg Med Chem Lett, 2017. 27(4): p. 718-722.
- [27]. Saah, M., et al., Design, synthesis, and pharmacokinetic evaluation of a chemical delivery system for drug targeting to lung tissue. J Pharm Sci, 1996. 85(5): p. 496-504.
- [28]. Lowery, L.A. and D. Van Vactor, The trip of the tip: understanding the growth cone machinery. Nat Rev Mol Cell Biol, 2009. 10(5): p. 332-43.
- [29]. Kuhn, T.B., Oxygen radicals elicit paralysis and collapse of spinal cord neuron growth cones upon exposure to proinflammatory cytokines. Biomed Res Int, 2014. 2014: p. 191767.
- [30]. Shanmugam, G., et al., A biphasic effect of TNF-alpha in regulation of the Keap1/Nrf2 pathway in cardiomyocytes. Redox Biol, 2016. 9: p. 77-89.
- [31]. Vattanarongkup, J., et al., Protective Effects of a Diarylheptanoid from Curcuma comosa Against Hydrogen Peroxide-Induced Astroglial Cell Death. Planta Med, 2016. 82(17): p. 1456-1462.

Sub-project 6: Targeted drug delivery systems (TDDS) for anticancer activities

ABSTRACT

Andrographolide diphenylsilyl-8,17-epoxy analogue, namely 19-tert-butyl andrographolide, or 3A.1, has been reported to be a potential anticancer agent for several cancer types. Due to its poor aqueous solubility, 3A.1 was incorporated within pH-sensitive amphiphilic chitosan derivatives (N-naphthyl-N,O-succinyl chitosan (NSCS), N-octyl-N-Osuccinyl chitosan (OSCS) and N-benzyl-N,O-succinyl chitosan (BSCS). These 3A.1-loaded nanoparticles were nano-sized (<200 nm) and spherical in shape with a negative surface charge. 3A.1-loaded nanoparticles were produced by dropping method. 40% initial 3A.1loaded NSCS exhibited the highest entrapment efficiency. The release of 3A.1 from these nanoparticles displayed a delayed release pattern. Under acidic conditions (pH 1.2) there was no free drug release. After the pH was adjusted to 6.8, a high cumulative 3A.1 release was obtained. In vitro anticancer activity against colorectal cancer cell HT-29 indicated that the 3A.1-loaded nanoparticles had significantly lower IC50 than the free drug and promoted apoptosis. In addition, in vitro wound healing migration assay on head and neck cancer cell (HN-22) revealed that free 3A.1 and the 3A.1-loaded nanoparticles inhibited cell motility compared to untreated cells. Moreover, we synthesized folic acid conjugated NSCS (F-NSC) for active targeting. The result of anticancer activity against HT-29, which are overexpressed folate receptors on cell surface, clearly showed that 3A.1-loaded F-NSC had greater potency than unconjugated NSCS nanoparticles and also more accumulation into cancer cells through folate receptor-mediated endocytosis. These pH-sensitive amphiphilic chitosan nanoparticles decorated with folate may be promising nanocarriers for oral anti-cancer drug delivery to the targeted colon cancer sites.

Keywords: Anticancer, Andrographolide analogue, nanocarrier decorated with folate

บทคัดย่อ

แอนโดรกราโฟไลด์สกัดได้จากฟ้าทะลายโจร มีการเพิ่มฤทธิ์ให้ดีมากขึ้นโดยการเตรียมให้อยู่ในรูป อนุพันธ์ต่างๆ หนึ่งในอนุพันธ์ของสารกึ่งสังเคราะห์มีชื่อทางเคมี 19-tert-butyldiphenylsilyl-8,17-epoxy andrographolide หรือ 3A.1 มีฤทธิ์ต้านเซลล์มะเร็งที่ดีมากและใช้ได้กับเซลล์มะเร็งหลายชนิด 3A.1 จึงเป็น สารที่มีศักยภาพต่อการนำไปใช้เป็นยาเคมีบำบัดตัวใหม่ได้ อย่างไรก็ตามปัญหาหลักของสารนี้ คือ การละลาย น้ำที่ต่ำมาก ดังนั้นในการศึกษานี้จึงสังเคราะห์อนุพันธ์ไคโตซานที่ไวต่อการเปลี่ยนแปลงพีเอช N-naphthyl-N,O-succinyl chitosan (เอ็นเอสซีเอส), N-octyl-N,O-succinyl chitosan (โอเอสซีเอส) และ N-benzyl-N,O-succinyl chitosan (บีเอสซีเอส) และเตรียมพอลิเมอริกไมเซลล์สำหรับนำส่งยา 3A.1 โดยบรรจุยาในพอ

ลิเมอริกไมเซลล์ ด้วยวิธีทางกายภาพ ศึกษาผลของวิธีการเตรียม ชนิดของพอลิเมอร์และปริมาณตัวยาเริ่มต้น ต่อประสิทธิภาพในการบรรจยาและความสามารถในการบรรจยา นอกจากนี้ศึกษาขนาดอนภาค รปร่าง และ การปลดปล่อยยา พบว่าวิธีการหยดสามารถบรรจุยาได้มากกว่าวิธีอื่น และพอลิเมอริกไมเซลล์ที่เตรียมจากเอ็น เอสซีเอสและปริมาณตัวยาเริ่มต้นต่อพอลิเมอร์ร้อยละ 40 โดยน้ำหนัก มีความสามารถในการบรรจยามากกว่า การใช้อนุพันธ์ชนิดอื่น ขนาดอนุภาคเล็กกว่า 200 นาโนเมตร และมีรูปร่างกลม การศึกษาการปลดปล่อยยา 3A.1 ในตัวกลางที่จำลองสภาวะทางเดินอาหารเป็นเวลา 8 ชั่วโมง พบว่าไม่มีการปลดปล่อย 3A.1 ในสภาวะ จำลองกระเพาะอาหารพีเอช 1.2 และเมื่อปรับพีเอชของตัวกลางให้จำลองสภาวะลำไส้เล็กพีเอช 6.8 พบว่า การปลดปล่อย 3A.1 เพิ่มขึ้นอย่างมาก ทั้งนี้เนื่องจากผลของการแตกตัวเป็นไอออนของส่วนหมู่กรดซักซินิก การทดสอบความเป็นพิษต่อเซลล์เอชที-29 พบว่า 3A.1 ที่บรรจุในพอลิเมอริกไมเซลล์มีค่าความเป็นพิษต่อ เซลล์สูงกว่ายาอิสระโดยเพิ่มการตายแบบอะพอพโทซิส การศึกษาการเคลื่อนที่ของเซลล์มะเร็งชนิดเอ็นเอช-22 พบว่าทั้ง 3A.1 อิสระและที่บรรจุในพอลิเมอริกไมเซลล์สามารถยับยั้งการเคลื่อนที่ของเซลล์ได้ นอกจากนี้การ นำโฟลิกมาควบคู่กับเอ็นเอสซีเอส (F-NSC) เพื่อเพิ่มความจำเพาะกับเซลล์มะเร็งลำไส้ใหญ่เอชที-29 ซึ่งที่ผิว เซลล์มีตัวรับโพเลตสูง พบว่าสามารถเพิ่มประสิทธิภาพของระบบนำส่งได้ดีกว่าชนิดไม่มีโฟลิก ผลที่ได้แสดงให้ พอลิเมอริกไมเซลล์เอ็นเอสซีเอสควบคู่กับโฟลิกมีศักยภาพในการเพิ่มการละลายยา ควบคุมการ ปลดปล่อยและนำส่งยาไปบริเวณเป้าหมายที่เป็นมะเร็งลำไส้ใหญ่โดยการรับประทาน

Keywords: ยาต้านมะเร็ง ระบบนำส่งควบคู่กับโฟลิก อนุพันธ์แอนโดรกราโฟไลด์

I. INTRODUCTION

1.2 Statement and significance of the research problem

Drug delivery systems (DDS) are processes or methods of pharmaceutical compounds' administration for an improved therapeutic effect in humans or animals body. DDS improve therapeutic efficacy through control of rate, time and place of drug release. There are commonly used routes of drug delivery including parenteral delivery, oral delivery, transdermal delivery, mucosal delivery (e.g. pulmonary, ocular, sublingual). administration is the most widely used route of drug delivery due to its convenience in terms of self-administration, pain free and high patient compliance, especially in the case of chronic therapies. However, some properties of drugs are not suitable for oral route due to side effects, rapid metabolism, and poor solubility. The low solubility of drug, that is classified in Biopharmaceutical Classification System (BCS) class II and class IV, is a crucial obstacle due to low absorption in the gastrointestinal (GI) tract. Accordingly, the low solubility leads to low bioavailability (Li et al., 2009; Lu and Park, 2013). More than 40% of new chemical entities (NCEs) developed in pharmaceutical industry are practically insoluble in water (Kalepu, 2013). The techniques used for solubility enhancement of drug include particle size reduction, cosolvents, solid dispersions, complexation (Kumar, 2011). Recently, scientists have challenged to generate novel carriers of oral drug delivery for obtaining higher levels in bioavailability such as polymeric micelles, microemulsions, nanoparticles.

Polymeric micelles as a nano-sized carrier which is prepared through self-assembly of amphiphilic copolymers in an aqueous solution when a concentration of polymer is above the critical micelle concentration (CMC) value. The inner core is hydrophobic segment which entraps hydrophobic drugs while the outer hydrophilic shell stabilizes interface between the hydrophobic core and aqueous solution, protects the hydrophobic drugs from the environmental stimuli (e.g. gastric pH, enzyme, temperature)and decreases adverse effect of drugs on healthy cells and tissues (Ghaemy, 2014). Polymeric micelles bring some advantages for oral drug delivery such as encapsulating drug into inner core to avoid destruction in the GI tract, increasing efficient solubilization, releasing them in spatially controlled manner, which could enhance drug absorption (Kedar, 2010). Some widely used techniques for drug-incorporated polymeric micelles preparation and the efficacy of drug loading depends on the applied tools. They include techniques of chemical conjugation, physical entrapment, electrostatic and other methods. Physical entrapment is the simplest and the most convenient method and can be implemented via dialysis, O/W emulsion, dropping and evaporation. The hydrophobic drugs can be incorporated into the micelles inner core by hydrophobic interaction between entrapped drug molecules and the hydrophobic inner-core-forming polymer (Murthy, 2015). The hydrophobic interactions also work as a driving force for micelle formation such as hydrophobic force, electrostatic force, ¶-¶ interaction and hydrogen bonding. Physical entrapment was selected to use in some studied such as dexamethasone-entrapped into PEGylated poly-4-(vinylpyridine) micelles by dialysis, O/W emulsion or evaporation (Miller, 2013), doxorubicin-loaded polyphosphazenes with poly(N-isopropylacrylamide-co-N,N-dimethylacryl amide) polymeric micelles by dialysis or O/W emulsion method (Qui, 2009), and preparation the polymeric micelles of methoxy poly(ethyleneoxide)-block-poly (&C-caprolactone) (MePEO-b-PCL) containing cyclosporine A by co-solvent evaporation (Aliabadi, 2007). However, the polymeric micelles preparation with high drug loads remains challenging because different techniques may affect the efficacy of drug loading (Kim, 2010).

As it is known, pH levels in the GI tract vary from 1-3 in the stomach to 6-7.5 in the small intestine and the variation of pH has been utilized to control drug release from carriers (Xu, 2013). In oral administration, pH-sensitive polymeric micelle-based carrier can be made to improve the stability of micelles in the stomach and attain a controlled release in the intestine which improves oral bioavailability. The poly(acrylic acid) (PAA) and poly (methacrylic acid) (PMAA)are generally used as pH-responsive polymers in pH-sensitive polymeric micelles in some studies. These polymers have pendant carboxyl groups with pK_a values of about 4-6 in the chain. For example, pH-responsive amphiphilic poly (acrylic acid-b-DL-lactide) (PAAc-b-PDLLA) was developed to incorporate prednisone acetate (Xue, 2009). This formulation of polymeric micelles showed minimizing drug release at pH 1.4 and burst release at pH 7.4. The pendant carboxyl groups in PAA moieties preserve collapsed states

and are protonated in the low pH environment of the stomach; however, PAA swells in the intestines, ionizes, and releases protons (Sant, 2004). Yang et al. (2011, 2012) developed self-assembled, pH-sensitive micelles from amphiphilic copolymer brushes (e.g., poly(methyl methacrylate-co-methacrylic acid)-b-poly(poly(ethylene glycol) methyl ether monomethacrylate) [P(MMA-co-MAA)-b-PPEGMA] and poly(lactide)-b-poly (metha-crylic acid)-b-poly(poly(ethylene glycol) methyl ether monomethacrylate) (PLA-b-MAA-b-PPEGMA) containing ibuprofen and nifedipine, respectively). They found that the drug release rates increased by modifying the MAA blocks.

Chitosan, is produced by Mucorales and other fungi, but on the whole it is manufactured by the deacetylation of chitin isolated from by-products of the marine fisheries. It is soluble in aqueous acidic solutions (pH < 6.0) (Muzzarelli et al., 2003; Muzzarelli et al., 2012), however, it cannot form polymeric micelles in water. Chitosan derivatives have been widely utilized in pharmaceutical applications since, they are biodegradable and less expensive (Bonferoni et al., 2014). Presently, chitosan derivatives in the form of polymeric micelles have been investigated for drug delivery. Several modified chitosans, for example *N*-lauryl-carboxymethyl-chitosan, N-phthaloylchitosan-g-mPEG, N-octyl-O-sulfate chitosan and N,N-dimethylhexadecylcarboxy methyl chitosan (DCMCs) have been utilized for the polymeric micelles preparation (Lia, 2014).

Many people are suffering from cancer which is an important lethal disease (Siegal, 2017). Colorectal cancer (CRC) is malignant tumors of colon and rectum with high mortality and morbidity in human beings. The statistics show that mortality rates from CRC have declined over the past decades as a result of better screening devices and more effective treatments. Unfortunately, in many cases, CRC patients are first diagnosed in the advanced stages making it hard to cure these patients. Therefore, early detection and optimal treatment such as surgery, radiotherapy, and chemotherapy, or combination therapy, should be able to improve patients' quality of life, and increase survival time with a higher cure rate. Chemotherapy is still the principal option for the treatment of advanced CRC or metastasis stage which cannot be treated by surgery alone (DiPiro, 2016). However, the clinical use of conventional chemotherapy is extremely restricted due to its low therapeutic efficacy, non-specific biodistribution, undesirable side effects, and high drug resistance, which may be the cause of treatment failure. It is therefore necessary to develop effective novel nanocarriers containing anticancer drugs with high potency against CRC, but low toxicity to normal tissues (Cisterna, 2016).

In recent years, plant-derived anticancer compounds have been developed to treat many types of cancer (Demain, 2011). Andrographolide (AG, Figure 1a) is a major active phytoconstituent derived from *Andrographispaniculata* Nees (Acanthaceae). It is widely used as a traditional herbal medicine in many countries such as India, China, and Southeast Asian countries, including Thailand (Hossain, 2014). This herb appears officially in the Thai Herbal

Pharmacopeia for the treatment of common colds and diarrhea. This natural compound has been revealed to demonstrate numerous pharmacological activities such as antibacterial and anti-inflammatory properties, and as an immune stimulant. Interestingly, many publications have confirmed that AG exhibits anticancer activity against various cancer cell lines but its anticancer potency is low (Shi, 2009; Varma,2011; Aromdee, 2012). In order to improve its cytotoxic activity and obtain a potential anticancer compound, many researchers have attempted to modify the AG into various AG analogs (Nanduri, 2004; Sirion, 2012; Preet, 2014). One of them, a novel semi-synthetic AG analog, 19-tert-butyldiphenylsilyl-8,17-epoxy andrographolide (3A.1, Figure 1b) has recently been reported to demonstrate potent in vitrogrowth suppression of cancer cells including hepatocellular carcinoma, cervical carcinoma, cholangiocarcinoma, and colorectal carcinoma. However, the poor aqueous solubility (<1 μ g/mL) of 3A.1 remains one of the main problems that limits the effective use of the analog in cancer therapy (Nateewattana,2014).

Figure 6.1 (a) Chemical structure of andrographolide(b) andrographolide analog (3A.1)

In order to improve the aqueous solubility and therapeutic efficacy of the 3A.1, nanosized drug delivery system should be employed. Previous study revealed that curcumin can be loaded into amphiphilic N-benzyl-N,O-succinyl chitosan (BSCS) via dialysis method to increase solubility of curcumin. The BSCS consists of hydrophobic benzyl group and hydrophilic succinyl group that can form self-aggregation micelles in water during dialysis. Curcumin-loaded BSCS micelles show small particle size, highly negative charge, high water solubility, strong cytotoxicity to cervical cancer cells and high amount of drug release in physiological pH 5.5-7.4 (Sajomsang et al., 2014). To the best of our knowledge, there is no report in the literature about the drug delivery system used for 3A.1 analog. Therefore, this study aims to develop 3A.1-loaded pH-sensitive, amphiphilic self-assembled nanoparticles based on the amphiphilic CS graft copolymer for colorectal cancer treatment. Due to the properties of these self-assembled nanoparticles, they could improve the solubility of 3A.1 by

entrapping the drug into the hydrophobic inner core, while the hydrophilic shells are compatible with aqueous medium and help increase colloidal stability. The effects of preparation methods and hydrophobic cores on the drug loading were investigated. The surface morphology, size, charge, and drug release characteristics were also examined. Most importantly, the anticancer efficiency, apoptosis induction and antimigratory activity were also assessed.

Moreover, by coupling specific tumor-homing ligands such as folic acid to the surface of nanoparticles, an active targeting of anticancer drug to cancer cells overexpressed specific receptors for enhancing cellular uptake and minimizing side effects. Some tumor cells within solid tumors would overexpress folate receptor (e.g. breast, ovary, lung, brain, colorectal cancers), which can specifically recognize the folate molecule (oxidized form of folic acid). Thus, the targeting of folate-modified polymeric nanoparticles to these tumors is a promising strategy for active targeting treatment (Bahrami, 2015). Here, by coupling folate to the NSC nanoparticles (Fol-NSC) was developed and loaded optimal drug amount into polymeric micelles. The physicochemical characteristics were evaluated. Finally, *in vitro* antitumor activities of drug-loaded Fol-NSC nanoparticles against HT-29 colorectal cancer cells were also investigated, compared with drug-loaded NSC nanoparticles (unmodified nanoparticles).

1.3 Objectives of this research

- 1. To synthesize pH responsive amphiphilic chitosan derivatives and formulate polymeric micelles for the 3A.1 drug delivery
- 2. To investigate the influence of the physical entrapment methods, type of amphiphilic chitosan derivatives, type and amount of drugs on entrapment efficiency, loading capacity and particle size of 3A.1-loaded polymeric micelles
- 3. To evaluate the drug release, anticancer efficiency, apoptosis induction and antimigratory activity of the 3A.1-loaded polymeric micelles
- 4. To compare anticancer activity of 3A.1-loaded polymeric micelles as passive targeting and 3A.1-loadedfolate-modified surface of polymeric micelles as active targeting.

1.4 The research of hypothesis

- 1. The amphiphilic chitosan derivatives can be synthesized and used to formulate 3A.1-loaded polymeric micelles.
- 2. The physical entrapment methods, type of amphiphilic chitosan derivatives, type and amount of drugs influence on the characteristics of polymeric micelles (i.e. particle size, size distribution, entrapment efficiency, loading capacity and stability).
 - 3. Polymeric micelles can be used for the 3A.1 delivery to the targeted tumor site.

MATERIALS AND METHODS

Materials

Equipments

Methods

- 1. Synthesis of pH sensitive amphiphilic chitosan derivatives
- 2. Characterization of pH sensitive amphiphilic chitosan derivatives
 - 2.1 Proton nuclear magnetic resonance (¹H NMR)
 - 2.2 Attenuated total reflection Fourier Transform Infrared Spectroscopy (ATR-FTIR)
- 3. Characterization of polymeric micelles
 - 3.1 Critical micelle concentration (CMC)
 - 3.2 *In vitro* cytotoxicity
- 4. Drugs-loaded polymeric micelles
 - 4.1 Physicalentrapmentmethods
 - 4.1.1 Dialysis method
 - 4.1.2 O/W emulsion method
 - 4.1.3 Dropping method
 - 4.1.4 Evaporation method
 - 4.2 Entrapmentefficiency
 - 4.3 Characterizations of drugs-loadedpolymeric micelles
 - 4.3.1 Particle size, PDI and zeta potential
 - 4.3.2 Morphology
 - 4.3.3 Drug loading content
 - 4.3.4 The stability of drug-loaded micelles
- 5. In vitro releases study
- 6. In vitro cytotoxicity
- 7. Induction of cell apoptosis
- 8. In vitro cell migration
- 9. Short-term physical stability studies
- 10. Statistical analysis

Materials

- 1. Acetonitrile HPLC grade (RCI Labscan Limited, Bangkok, Thailand)
- 2. Annexin-V FITC apoptosis kit (BD bioscience, USA)
- 3. Benzaldehyde (Sigma Aldrich[®], St. Louis, MO, USA)
- 4. Chitosan (Degree of deacetylation; DDA 96%, MW 10-13 kDa) (OilZac Technologies Co., Ltd., Bangkok, Thailand)
- 5. Dimethyl sulfoxide (Fisher Scientific, UK Limited, UK)
- 6. Dulbecco's modified Eagle's medium (DMEM) (GIBCO[®], Grand Island, NY, USA)

- 7. Fetal bovine serum (FBS) (GIBCO[®], Grand Island, NY, USA)
- 8. Human colorectal adenocarcinoma cells (HT-29) cell line (Rockville, MD, USA)
- 9. N,N-dimethylformamide (DMF, 99.8%) (BrightchemSdnBhd, Malaysia)
- 10. 2-Naphthaldehyde (Sigma Aldrich[®], St. Louis, MO, USA)
- 11. Octaldehyde (Sigma Aldrich[®], St. Louis, MO, USA)
- 12. Oral squamous cell carcinoma (HN-22) was procured from the Faculty of Dentistry, Naresuan University.
- 13. Penicillin-streptomycin (GIBCO[®], Grand Island, NY, USA)
- 14. Semi-synthetic andrographolide analog (3A.1) was kindly provided by the Faculty of Science, Burapha University.
- 15. Succinic anhydride (Sigma Aldrich[®], St. Louis, MO, USA)
- 16. Sodium borohydride (Sigma Aldrich[®], St. Louis, MO, USA)
- 17. Trypsin-EDTA (0.25 %) solution (GIBCO®, Grand Island, NY, USA)
- 18. 3-(4,5-Dimethythiazol-2-yl)-2,5-diphenyl-tetrazolium bromide (MTT) (Sigma Aldrich®, St. Louis, MO, USA)
- 19.19-tert-butyldiphenylsilyl-8,17-epoxy andrographolide (3A.1)

Equipments

- 1. Analytical balance (Sartorious CP224S; Scientific Promotion Co., Ltd., Bangkok, Thailand)
- 2. Atomic-force microscope (AFM) (SPA400, Seiko, Japan)
- 3. Bruker AVANCE 500 spectrometer (Bruker, Switzerland)
- 4. CO₂ incubator (Heraeus HERA Cell 240, Heraeus Holding GmbH., Germany)
- 5. Dialysis bag (CelluSep® (6000–8000 MWCO) Membrane Filtration Products, USA)
- 6. Franz diffusion cells
- 7. Freeze-dryer (Model: Freezone 2.5, LABCONCO, USA)
- 8. Freezer/Refrigerator -20 °C, -80 °C, 5°C
- 9. Hot air oven (WTB Binder, Germany)
- 10. High performance liquid chromatography (HPLC) instrument (Agilent 1100
- 11. series, Agilent Technologies, USA)
- 12. HPLC column (Eclipse XDB-C18, 5 µm, 15 cm x 4.6 mm) (Santa Clara, CA, USA)
- 13. High voltage power supply (Model: Gamma High Voltage Research, USA)
- 14. Incubated shaker (Model: KBLee 1001, Daiki sciences, Bio-Active, Bangkok, Thailand)
- 15. Laminar air flow (BIO-II-A, Telstar Life Science Solutions, Spain)
- 16. Magnetic stirrer (Framo, Germany) and magnetic bar
- 17. Micropipette 0.1-2.5 μ L, 2–20 μ L, 20–200 μ L, 100–1000 μ L, 1–5 mL, and micropipettetip
- 18. Microcentrifuge (Microfuge 16[®], Model: A46473, Beckman Coulter Inc., Germany)

- 19. Microcentifuge tube (Eppendorf®, Corning Incorporated, NY, USA)
- 20. Microplate reader (Universal Microplate Analyzer, Model AOPUS01 and AI53601, Packard BioScience, CT, USA)
- 21. Nicolet 6700 spectrometer (Thermo Company, USA)
- 22. Nylon membrane filter (diameter 47 mm, pore size 0.45 µm)
- 23. pH meter (Horiba compact pH meter B-212, Japan)
- 24. Probe-type sonicator (model CV 244, Sonics VibraCellTM, USA)
- 25. Sonicator bath
- 26. Sonicator probe-type (CV 244, Sonics VibraCellTM, Newtown, CT, USA)
- 27. Transmission Electron Microscopy (TEM) (Philips® Model TECNAI 20, Holland)
- 28. Vortex mixer (VX100, Model: Labnet, NJ, USA)
- 29. Water bath (HETOFRIG CB60; Heto High Technology of Scandinevia, Birkerod, Denmark)
- 30. Well-plate (96 Well plate) (Corning Incorporated, NY, USA)
- 31. ZetasizerNano ZS (Malvern Instruments, Malvern, UK)

Methods

1. Synthesis of amphiphilic chitosan derivatives

The amphiphilic chitosan derivatives, i.e. N-naphthyl-N,O-succinyl chitosan (NSCS), Noctyl-N,O-succinyl chitosan (OSCS) and N-benzyl-N,O-succinyl chitosan (BSCS), were synthesized by reductive N-amination and N,O-succinylation. Two grams of chitosan was dissolved in 150 mL of 1% (v/v) aqueous acetic acid. Then, 100 mL of ethanol was added to the solution. 2-Naphthaldehyde, octanaldehyde or benzaldehyde (2.0 meg/GlcN) was added, and the reaction mixture was stirred at room temperature for 24 h. At this point, the pH of the solution was adjusted to 5 by adding 1 M NaOH, and 2.0 g of NaBH₄ (52.9 mmol) was added to the reaction mixture and stirred at room temperature for 24 h. The precipitate was collected by filtration, washed several times with ethanol, before being dried under a vacuum at room temperature to obtain the N-naphthyl chitosan (NCS), N-octyl chitosan (OCS) or N-benzyl chitosan (BCS). The N,O-succinylation was conducted using succinic anhydride. Briefly, 1.0 g of NCS, OCS or BCS was dispersed in 40 mL of N,Ndimethylformamide (DMF)/dimethyl sulfoxide (DMSO), (1:1 v/v), and 3.0 g of succinic anhydride (5.0 meg/GlcN) was added. The reaction was heated at 100°C under nitrogen atmosphere for 24 h. Next, the reaction mixture was cooled to room temperature and filtered to remove undissolved NCS, OCS or BCS. The clear solution was dialyzed with distilled water for 3 days to remove excess succinic anhydride and DMF/DMSO. powdered NSCS, OSCS or BSCS were then obtained by lyophilization. The number average molecular weights (M_n) of chitosan derivatives were evaluated based on the theoretical molecular weight increase of the derivatives and the degree of substitution.

2. Characterization of pH sensitive amphiphilic chitosan derivatives

2.1 Proton nuclear magnetic resonance (¹H NMR)

The 1 H-NMR spectra of chitosan and its derivatives were measured on a Bruker AVANCE 500 spectrometer (Bruker, Switzerland) using D_2O/CD_3COOD (99:1 v/v) solution and DMSO-d6, respectively, at 10 mg/mL polymer concentrations. All measurements were performed at 300 K, using the pulsed accumulation of 64 scans and an LB parameter of 0.30 Hz. Tetramethylsilane was used as an internal standard.

2.2Attenuated total reflection Fourier Transform Infrared Spectroscopy (ATR-FTIR)

ATR-FTIR spectra were collected on a Nicolet 6700 spectrometer (Thermo Company, USA) using a single-bounce ATR-FTIR Smart Orbit accessory with a diamond internal reflection element (IRE) at ambient temperature (25°C). All spectra were taken from 400-4000 cm⁻¹. Typically, 32 scans at a resolution of 4 cm⁻¹were accumulated by using rapid-scan software in OMNIC 7.0 to obtain a single spectrum.

3. Characterization of polymeric micelles

3.1 Critical micelle concentration (CMC)

The CMC of graft copolymers in aqueous medium was determined using fluorescence spectroscopy with pyrene employed as a fluorescent probe. An aliquot (10 μ L) of 1 mM pyrene solution in acetone was added to each vial of a series of aqueous polymer solutions (4 mL, 0.5-3.9×10⁻³ mg/mL). The final concentration of pyrene in each sample solution was 2.5×10⁻⁶ M. The mixtures were sonicated for 15 min, heated at 50°C for 2 h, and then kept in the dark at room temperature overnight to equilibrate. Fluorescence spectra were recorded at an excitation wavelength of 335 nm, and the emission spectra were monitored over a range of 350-500 nm. The change in the intensity ratio of the first and third vibration bands (I₁/I₃) at 373 nm (I₁) and 382 nm (I₃) in the emission spectra was used to investigate the shift in graft copolymer hydrophobic microdomains. The CMC was calculated after fitting the semi-log plot of the intensity ratio I₁/I₃ vs. the concentration.

3.2 *In vitro* cytotoxicity

The cytotoxicity of blank polymeric micelles was evaluated using an MTT cytotoxicity assay. The Caco-2 cells and HT-29 cells were cultured until 60–70% confluency in Dulbecco's modified Eagle's medium (DMEM) at pH 7.4 supplemented with 10% fetal bovine serum (FBS), 2 mM L-glutamine, 1% non-essential amino acid solution and 0.1% penicillin-streptomycin solution in a humidified atmosphere (5% CO₂, 95% air, 37°C). The cells were seeded into each well of 96-well plates and preincubated for 24 h at a seeding density of 10,000 cells/well. Then, the cells were treated with blank polymeric micelles at various

concentrations. After treatment, the solution was removed, fresh medium was added. Then, the mixture was incubated with MTT solution (final concentration 1 mg/mL) for 4 h at 37°C. The culture medium was removed, and the formazan crystals formed in the living cells were solubilized in 100 µL DMSO. Relative cell viability was calculated based on the absorbance at 550 nm using a microplate reader (Universal Microplate Analyzer, AOPUS01 and AI53601, Packard BioScience, CT, USA). The viability of non-treated control cells was arbitrarily defined as 100%.

4. Drugs-loaded polymeric micelles

4.1 Physical entrapment methods

4.1.1 Dialysis method

Overall, 5 mg of the amphiphilic copolymers (NSCS, OSCS and BSCS) and hydrophobic drugs (3A1) were dissolved in 2 mL of DMSO in a glass bottom container. Then, the mixture was stirred at room temperature until completely dissolved and transferred to dialysis bag (molecular weight cut-off, MWCO 6000-8000). The deionized water was replaced every 4 h for 24 h. The solution was centrifuged at 1000 rpm for 5 min. Then, the supernatant was filtered through a 0.45-µm membrane filter and collected.

4.1.2 O/W emulsion method

The copolymers (NSCS, OSCS and BSCS) were prepared as for dialysis method. Then, drug was dissolved in DCM and was injected under constant stirring into 2 mL of blank polymeric micelles solution. Then, DCM was evaporated by overnight stirring at room temperature. The solution was centrifuged at 1000 rpm for 5 min. Then, the supernatant was filtered through a 0.45-µm membrane filter and collected.

4.1.3 Dropping method

Five milligrams of copolymer and drugs were dissolved in 0.5 mL DMSO. The solution was slowly dropped into stirred water, and the mixed solution was stirred overnight. The final ratio of DMSO: water was 1:5. The mixture was then placed in a dialysis bag and dialyzed against deionized water overnight. The solution was centrifuged at 1000 rpm for 5 min. Then, the supernatant was filtered through a 0.45-µm membrane filter and collected.

4.1.4 Evaporation method

Five milligrams of copolymer and drug were dissolved in DMF in a glass bottom container. The solution was mixed with acetone (1/3 of DMF) and stirred at room temperature under nitrogen gas flow until the solvent completely evaporated. Then, 3 mL of deionized water was added, and the solution was sonicated using a probe-type sonicator in a cycle with a sonication time of 5 min and a standby time of 5 min for 20 min. The solution was centrifuged at 1000 rpm for 5 min. Then, the supernatant was filtered through a 0.45-µm membrane filter and collected.

4.2 Entrapment efficiency

The drug-loaded polymeric micelles of each method were dissolved in a mixture solution of DMSO: H_2O (9:1). The amount of drug loaded into the polymeric micelles was determined using the high performance liquid chromatography (HPLC) (Agilent 1100 Series HPLC System, Agilent Technologies, USA) equipped with Eclipse XDB-C18 column (particle size 5 μ m, 15 cm \times 4.6 mm) and DAD detector at 219 nm. The injection volume was 20 μ L. The isocratic elution was carried out with a mobile phase made of water and methanol (20:80, v/v), and a flow rate of 1.0 mL/min. Standard solutions with different drug concentrations were used to generate the calibrate curve. The entrapment efficiency and loading capacity were calculated with the following Eqs. (1) and (2), respectively.

Entrapment efficiency (%) =
$$(C_1/C_2) \times 100$$
(Eq.1)

where C_1 is the amount of drug in polymeric micelles and C_2 is the initial of amount drug used for preparation

Loading capacity
$$(\mu g/mg) = L_1/L_2$$
 (Eq.2)

where L_1 is the amount of drug in micelles and L_2 is the amount of graft copolymer used for preparation.

4.3 Characterizations of drugs-loaded polymeric micelles

4.3.1 Particle size

The micelle samples were diluted with distilled water prior to measure. The mean particle size and size distribution of the polymeric micelles with and without drugs were determined in triplicate at 25°C using the dynamic light scattering (DLS) (Malvern, Worcestershire, UK).

4.3.2 Morphology

Surface morphologies of the blank and 3A.1-loaded nanoparticles (unmodified and folate-modified NPs) were examined using a transmission electron microscopy (TEM) (Philips® Model TECNAI 20,Holland) at an accelerating voltage of 80 kV. The nanoparticle solutions were negatively stained with 1% uranyl acetate solution and dropped onto a formvar-coated copper grid before the observation.

4.3.3 The stability of drug-loaded micelles

The stability of drug-loaded micelles was determined by gel permeation chromatography (GPC) as described previously (Opanasopit et al., 2004). GPC was carried out using an Agilent HPLC system (Agilent 1100 series, USA) equipped with a Shodex $^{\circledR}$ GFC SB804 HQ column at 40°C. Drug-loaded polymeric micelles freshly prepared solutions (50 μ L), were passed through a 0.45- μ m membrane filter and then injected into the column

and eluted with deionized water at a flow rate of 1 mL/min. Detection was performed by refractive index (RI) and UV detector.

5. In vitro releases study

In this study, 3A.1-loaded nanoparticles (unmodified and folate-modified NPs at 40 wt% of 3A.1 to polymer) prepared using the dropping method were selected for the release study. Briefly, 3A.1-loaded nanoparticles and drug suspension (the drug powder dispersed in deionized water) containing equal quantity of 3A.1 (40 μ g) were added to microcentrifuge tubes containing release medium. A simulated gastric fluid (SGF± standard deviation) at pH 1.2 was used as the medium for the first 2 h, followed by a simulated intestinal fluid (SIF) at pH 6.8 for 6 h and a simulated colonic fluid (SCF) at pH 7.4 for the further 4 h. The release study was conducted at 37 ± 0.5 °C in a shaking incubator at a speed of 150 rpm. The samples were collected at predetermined time intervals and filtered prior to the content determination. The release study was done in triplicate.

6. *In vitro* **cytotoxicity**

The anticancer activity of the 3A.1 free drug and 3A.1-loaded nanoparticles (unmodified and folate-modified NPs) on HT-29 cells (human colorectal cancer cells) was evaluated by MTT assay (Mosmann,1983). Briefly, HT-29 cells (1×10⁴ cells/well) were seeded in 96-well plates with DMEM supplemented with 10% FBS at pH 7.4 and cultured at 37 °C in a humidified 5% CO₂ incubator. After incubation for 24 h, the cells were treated with various concentrations (0.1 to 16.0 µg/mL) of the 3A.1-loaded nanoparticles (NSCS, OSCS, and BSCS; Fol-NSCS) and 3A.1 free drug, and further incubated for 36 h. After treatment, the medium was withdrawn and the cells were covered with fresh medium containing 0.5 mg/mL of MTT for 4 h. After that, the medium was taken out and the formazan crystals generated in the surviving cells were liquefied by adding 100 μ L of DMSO, after which the optical density (OD) of each well was analyzed using a microplate reader (Universal Microplate Analyzer, Model AOPUS01and Al53601, Packard BioScience, CT, USA) at 550 nm. The percentage of cell viability was determined using the equation: Cell viability (%) OD(treated)/OD(untreated)×100. Moreover, half-maximal inhibitory concentration (IC50) values were assessed using GraphPad Prism version 5.01 (GraphPad Inc., USA). In a similar procedure, the cytotoxicity of the blank nanoparticles was also evaluated.

7. Induction of cell apoptosis

An apoptosis assay was carried out using a flow cytometer (BD, FACSC Canto, Becton Dickinson, CA, USA) with FITC-conjugated Annexin V/propidium iodide (PI) (BD Bioscience) costaining (Reabroi, 2018). Briefly, HT-29 cells were sowed in 6-well plates and incubated in a

humidified 5% CO $_2$ incubator at 37 °C until 60–70% confluence. The cells were treated with 3A.1-loaded nanoparticles (NSCS, OSCS, BSCS, Fol-NSCS) and 3A.1 free drug in fresh medium (the final drug concentration was fixed at 3.5 μ g/mL) at 37 °C for 24 h. After treatment, the cells were collected by adding EDTA solution as cell detachment agent and subsequently washed with medium. Then, the cells were gently pipetted to detach the cells. The treated cells were tainted with Annexin V-FITC and PI in the dark for 15 min at ambient temperature, and immediately subjected to flow cytometry analysis. The data were evaluated using FACS diva software (BD Bioscience, USA). Both early apoptotic (Annexin V+/PI–) and late apoptotic (Annexin V+/PI+) cells were embraced in the cell apoptosis evaluation. The untreated HT-29 cells were used as negative control and the HT-29 cells treated with 2% Triton X-100 was used as positive control (Jain, 2017).

8. In vitro cell migration

The effect of 3A.1-loaded nanoparticles and free 3A.1 on HN-22 (human oral squamous cancer) cell motility was performed using scratch wound healing assay as previously explained (Grada, 2017; Wongprayoon, 2018). Briefly, HN-22 cells were grown in 6-well culture plates with DMEM containing 10% FBS at pH 7.4 to achieve confluent monolayer. A monolayer of the cell in each well were gently scratched with a sterile 200- μ L pipette tip to make three straight lines/well and rectangular cell-free spaces. Then, the culture medium was discarded and washed twice with PBS (pH 7.4) to remove debris and scratched cells. After that, the 3A.1-loaded nanoparticles (NSCS, OSCS, and BSCS) and free 3A.1 dispersed in fresh medium (3.0 μ g/mL) were placed into each well and cultured at 37 °C under a humidified 5% CO2 incubator for 24 h. Culture medium without drug and DMSO were used as control. After scraping at 0, 12, 18, and 24 h, the images (5 images/well)of the wound were captured at × 40 magnification using inverted microscope (Nikon T-DH, Japan). The wound gap and wound area were quantified using JMicroVision version 1.2.7 and calculated to determine the cell migration rate and percentage of wound closure. The antimigratory activity was assessed in triplicate.

9. Short-term physical stability studies

The stability of the 3A.1-loaded polymeric nanoparticles (NSCS, OSCS, and BSCS) was determined according to ICH guideline section Q1A R2. The nanoparticles samples were stored in glass bottles at 5 ± 3 °C, 60 ± 5 %RH (long-term condition) and at 25 ± 2 °C, 60 ± 5 %RH (accelerated condition) for 6 months. The particle size, zeta potential, and content of 3A.1 remaining in the drug-loaded nanoparticles were evaluated after storage for 0, 30, 60, 120, and 180 days. All data were measured in triplicate.

10. Statistical Analysis

All experiments were accomplished in triplicate. Data were presented as mean ±

standard deviation (SD). The statistical significance of differences was assessed using one-way analysis of variance (ANOVA) followed by a LSD post hoc test (SPSS version 16.0 for Window, SPSS Inc., USA). The statistical significance of differences was noted when the p value <0.05 for all statistical tests.

RESULTS AND DISCUSSION

1. Synthesis and characterizations of pH sensitive amphiphilic chitosan derivatives

The synthesis of the amphiphilic chitosan derivatives i.e. NSCS, OSCS and BSCS, was carried out by reductive N-amination and N,O-succinylation (Sajomsang et al., 2014) as shown in Figure 2. Overall, the N-alkyl or N-aryl chitosan were formed from the corresponding Schiff base intermediates before the reduction using sodium borohydride. The homogenous N,O-succinylation of NCS, OCS and BCS was carried out by using succinic anhydride in the mixture of solvents consisting of DMF and DMSO at 100°C. The successful synthesis of all amphiphilicchitosan derivatives was confirmed by ¹H NMR, ATR-FTIR and elemental analysis. The series of amphiphilicchitosan derivatives with different N-hydrophobic substituents were obtained as shown in Table 1. The degree of substitution (DS), defined as the number of N-hydrophobic groups, and the degree of N,O-succinylation (DSS), defined as the number of N,O-succinyl groups per hundred glucosamine units of chitosan, were determined by elemental analysis. The DS and DSS were calculated by comparing the C/N molar ratios obtained from the elemental analyses using Eqs. (3) and (4), respectively (Huo et al., 2012).

DS of hydrophobic group (%) =
$$\frac{(C/N)_{ACS} - (C/N)_{CS}}{x} \times 100$$
 (Eq.3)

DSS of succinylgroup(%) =
$$\frac{(C/N)_{scs} - (C/N)_{ACS}}{4} \times 100$$
 (Eq.4)

where $(C/N)_{ACS}$ represents the C/N ratio of amphiphilicchitosan derivatives, $(C/N)_{CS}$ represents the C/N ratio of chitosan, $(C/N)_{SCS}$ represents the C/N ratio of succinylatedamphiphilicchitosanderivatives, and X represents the number of carbon atoms on the hydrophobic moieties of the chitosan backbone, which are 11, 8, and 7 for naphthyl, octyl, and benzyl substituents, respectively.

Both aliphatic and aromatic aldehydes at 2-fold molar ratios relative to the glucosamine (GlcN) residues of chitosan were used to study the DS. By varying the hydrophobic substituents on the chitosan backbone, the impact of the steric and electronic factors on this procedure could be elucidated. As shown in Table 1, the N-benzylation of

chitosan by benzaldehyde had a higher DS than the N-naphthylation and N-octylation by 2naphaldehyde and octanaldehyde, respectively, at similar molar ratios ofaldehyde to GlcN. The DS order of N-hydrophobically modified chitosan was N-benzyl (0.69) > N-naphthyl (0.52) > N-octyl (0.47).This indicated that octanaldehyde was less reactive than benzaldehyde and 2-naphaldehyde. This could beattributed to the relative stability of the Schiff base intermediate and steric hindrance effect. In the case of benzaldehyde and 2naphaldehyde, the Schiff bases were stabilized by resonance with the aromatic ring, while the Schiff base of octanaldehyde with chitosan could not be stabilized by the resonance effect. Compared with 2-naphaldehyde, benzaldehyde showed lower steric hindrance, leading to a higher DS. Moreover, the hydrophobic moieties (i.e., the naphthyl, octyl, and benzyl groups) effectively substituted onto the primary amino groups, while the succinyl groups were added to both the primary amino and hydroxyl groups on the chitosanbackbone. The M_n of all chitosanderivatives could be calculated based on the increase of theoretical molecular weight of the derivatives due to the DS of the hydrophobic groups and the DSS of the succinyl groups. The M_n of chitosanwas determined to be 7,633 g/mol (47 repeating units) by GPC. The DS values of NCS, OCS, and BCS were calculated to be 0.54 (approximately 25 repeating units), 0.47 (approximately 22 repeating units), and 0.69 (approximately 32 repeating units), while the DSS values were 0.52 (approximately 24 repeating units), 1.13 (approximately 53 repeating units), and 1.07 (approximately 50 repeating units), respectively (Table 1). According to the DS and DSS, the hydrophobic/hydrophilic ratios on the chitosanbackbone were 1.04, 0.42, and 0.65 for NSCS, OSCS, and BSCS, respectively.

Figure 2 Synthesis scheme showing the formation of amphiphilic chitosan derivatives.

Sample	%C	%Н	%N	C/N	DS ^a	DS ^b	DSS ^c	M _n (g/mol)
CS	44.3	7.87	8.38	5.28	-	-	-	7633 ^d
NCS	66.79	11.29	5.97	11.18	0.52	0.54	-	10907 ^e
OCS	49.49	12.68	5.47	9.04	0.37	0.47	ı	10046 ^e
BCS	65.48	11.76	6.45	10.15	0.65	0.69	ı	10467 ^e
NSCS	54.97	10.41	4.14	13.27	ı	0.54	0.52	13351 ^e
OSCS	49.17	11.28	3.61	13.59	ı	0.47	1.13	15321 ^e
BSCS	56.89	9.97	3.93	14.44	-	0.69	1.07	15462 ^e

Table.6.1 Elemental analysis data for chitosan(CS) and its amphiphilic derivatives

1.1 ¹H NMR characteristics

The ¹H-NMR spectrum of chitosan, NCS, OCS, BCS, NSCS, OSCS and BSCS are shown in Figure 3 and 4, respectively. In comparison with the ¹H NMR spectra of chitosan that contains no aromatic protons, the ¹H NMR NCS spectra and BC exhibited broad multiple protons at ranging from 7.42 to 7.89 ppm and at 7.32 ppm due to the presence of the naphthyl and benzyl groups, respectively. The OCS showed the proton signals at 0.82 ppm and 1.21 ppm due to the methyl and methylene protons of long chain hydrocarbon (Figure 4.2). Moreover, the proton signal at 2.45 ppm in NSCS, OSCS and BSCS represented the methylene protons of the succinyl moiety on the chitosan backbone (Figure 4) (Lim, 2013; Sajomsang, 2014). Based on the ¹H-NMR spectra, the DS values of NCS, OCS, and BCS were calculated using Eqs. (5)–(7), respectively. The DS values were 0.52, 0.37, and 0.65 for NCS, OCS, and BCS, respectively.

$$DS = \left(\frac{INap/7}{IH2 - H6/6}\right) \tag{Eq.5}$$

whereINap represents the total area (integration) of the N-naphthyl protons, and IH2–H6 represents the peak area of protons C2–C6 on the chitosan backbone.

$$DS = \left(\frac{IMe/3}{IH2-H6/6}\right) \tag{Eq.6}$$

^a The degree of *N*-substitution (DS) determined by ¹H-NMR

^b The degree of *N*-substitution (DS) determined by elemental analysis

^c The degree of *N,O*-succinylation (DSS) determined by elemental analysis

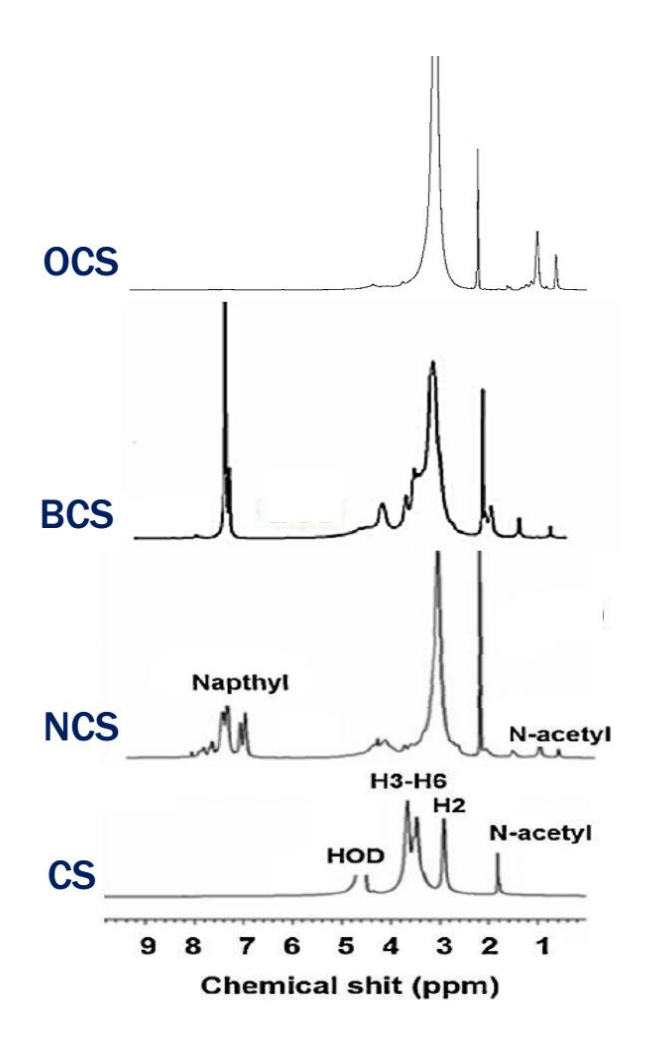
^d Measured by GPC ^e Determined by elemental analysis

whereIMe represents the total area (integration) of N-methyl protons of the octyl group, and IH2–H6 represents the peak area of protons C2–C6 on the chitosan backbone.

$$DS = \left(\frac{IAr/5}{IH2-H6/6}\right) \tag{Eq.7}$$

whereIAr represents the total area (integration) of N-benzyl protons, and IH2–H6 represents the peak area of protons C2–C6 on the chitosan backbone.

It is important to note that DS value determined by ¹H-NMR method is less than elemental analysis method (Table 1), particularly in case of OCS. This difference was due to the limitation of solubility in ¹H-NMR solvent. Moreover, the methylene protons of the succinyl groups overlapped with the solvent, DMSO-d6. Therefore, the DSS was determined using elemental analysis instead of ¹HNMR spectroscopy. These results from ATR-FTIR and ¹H-NMR spectra were discussed to indicate the successful introduction of both functionalities onto the chitosan backbone.



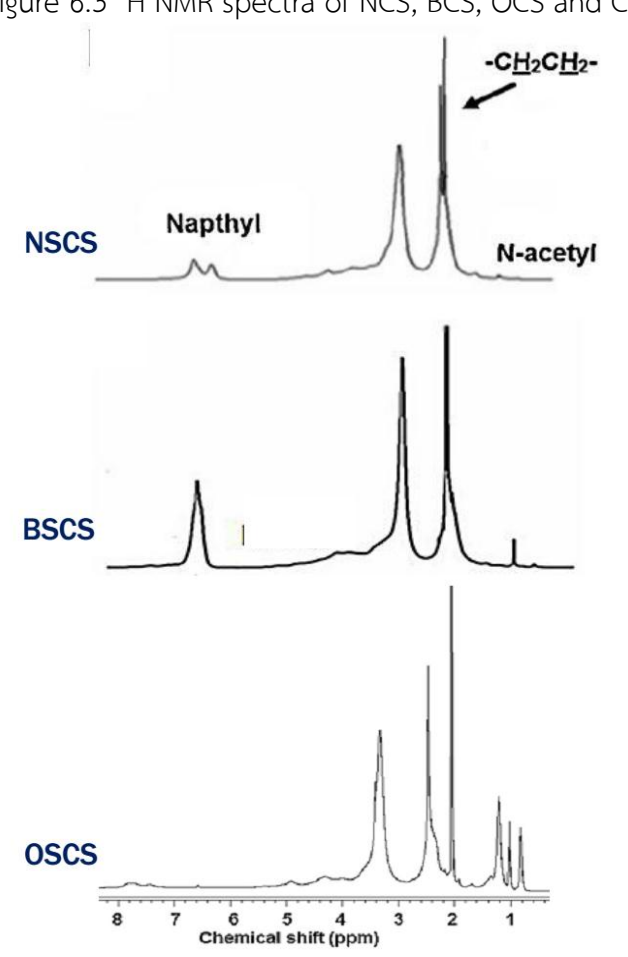


Figure 6.3 ¹H NMR spectra of NCS, BCS, OCS and CS

Figure 6.4 ¹H NMR spectra of NSCS, BSCS and OSCS

1.2 ATR-FTIR characteristics

The ATR-FTIR spectra of CS, NCS, OCS, BCS, NSCS, OSCS and BSCS are shown in Figure 6.5. The ATR-FTIR spectra of NCS, OCS and BCS were similar to that of CS and showed the additional absorption bands of functional groups (i.e., naphthyl, benzyl and octyl). The characteristic bands at 1632, 1490, 817 and 746 cm⁻¹ (NCS spectrum) and at 1600, 1494, 743 and 695 cm⁻¹(BCS spectrum) were assigned to C=C stretching, C-H deformation (out of plane) for naphthyl and benzyl groups, respectively (Lim et al., 2013; Sajomsang et al., 2008) while the OCS spectrum had the strong absorption bands for C-H stretching of octyl groups at 2923 and 2856 cm⁻¹(Figure 5a). After *N,O*-succinylation process, the NSCS, OSCS and BSCS spectra exhibited the characteristic bands for C=O streching of the succinic acid moiety at 1704 cm⁻¹ (NSCS spectrum), 1714 cm⁻¹ (OSCS spectrum) and 1715 cm⁻¹ (BSCS spectrum) (Figure 6.5b).

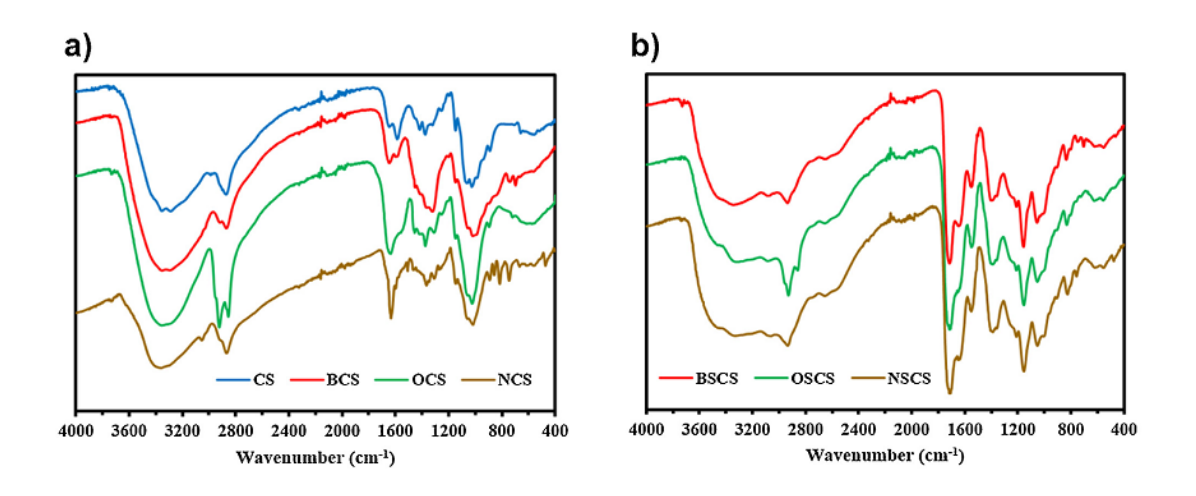


Figure 6.5(a) ATR-FTIR spectra of CS, BCS, OCS and NCS; (b) BSCS, OSCS and

NSCS

2. Blank polymeric micelles

2.1 Critical micelle concentration (CMC)

The fluorescence assay was conducted to determine the concentration of NSCS, OSCS and BSCS polymer for micellization at the first taken place. Briefly, the hydrophobic pyrene probe was added to aqueous polymer solutions of increasing concentration and pyrene fluorescence spectra were recorded for all solutions. The change in the intensity ratio of the first and third vibration bands (I_1/I_3) at 373 nm (I_1) and 382 nm (I_3) in the emission spectra was used to investigate the shift in graft copolymer hydrophobic microdomains. The plots of the intensity ratio I_1/I_3 versus the concentration of polymer solutions of NSCS, OSCS and BSCS are shown in Figure 6 and the CMC value was determined for each copolymer solution from the intersection of two straight lines. When the concentration reached the CMC, the I_1/I_3 ratio dramatically decreased. The CMC for NSCS, OSCS and BSCS was 0.0678, 0.0855 and 0.0575 mg/mL, respectively, and was lower than the CMC value of low molecular weight surfactants (Jiang et al., 2006). There is a covalent linkage in individual molecules within the hydrophobic core in polymeric micelles. This linkage prevents dynamic exchange of monomers between free solution and the micellar pseudo-phase which confers rigidity and stability to the polymeric micelles (Murthy, 2015).

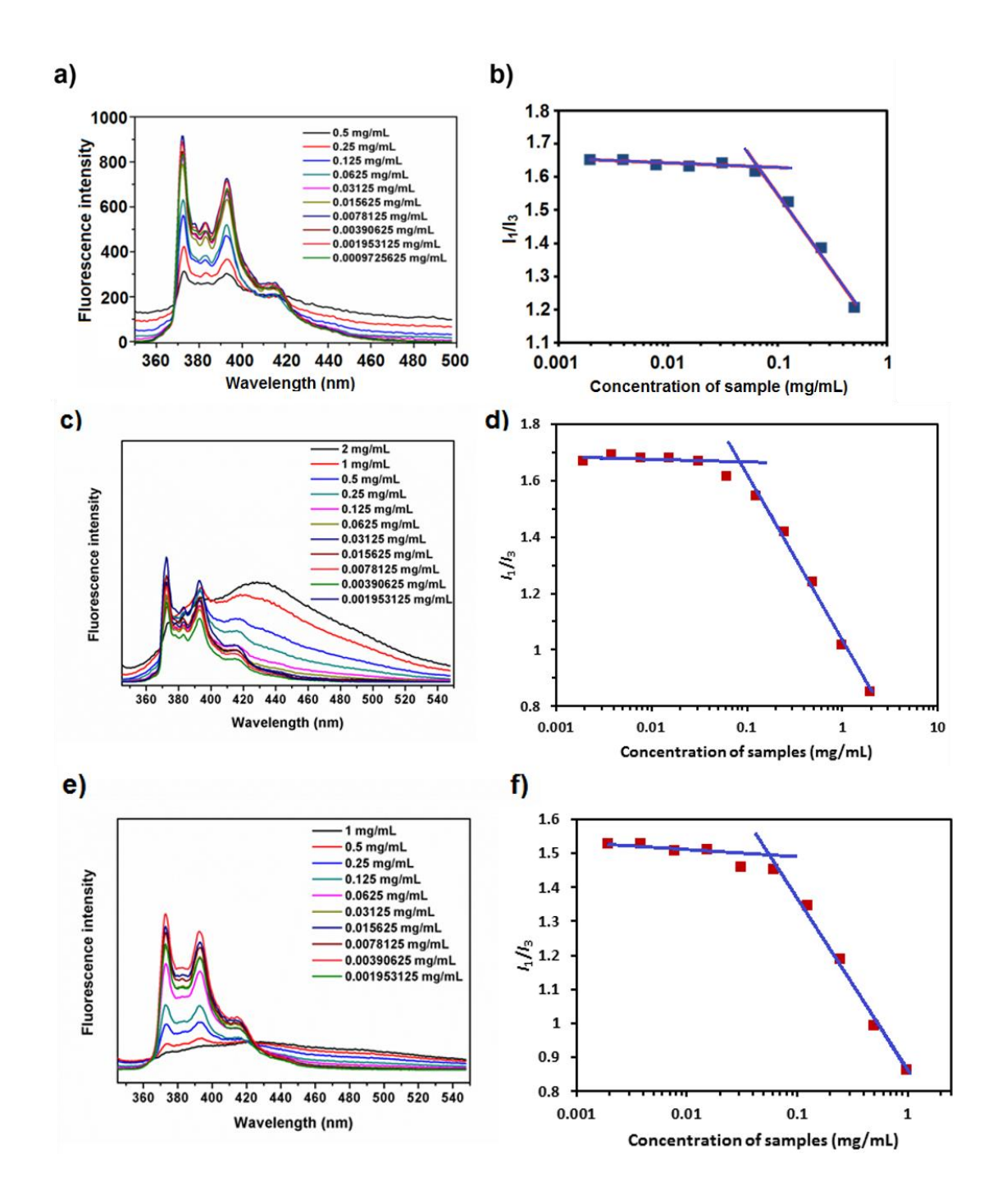


Figure 6.6 Fluorescence emission spectra of pyrene in water in the presence of NSCS (a), BSCS (c), and OSCS (e) polymeric micelles; a plot of the change in the intensity ratio (I1/I3) from excitation spectra of pyrene in water at various concentrations of NSCS (b), BSCS (d), and OSCS (f).

2.2 *In vitro* cytotoxicity

As a major requirement, the polymer used to prepare the polymeric micelles should be non-toxic. Although chitosan is generally considered as a biodegradable and safe polymer, some case studies identified the toxic effects of chitosan derivatives (Ngawhirunpat et al., 2009). The Caco-2 cells, represented functional similarities to intestinal epithelium, are commonly used in vitro model for studies cytotoxicity or prediction of intestinal drug absorption. HT-29 cells, originally derived from a human colon cancer, were selected as model for the study of colon cancer. Thus, the cytotoxicity of blank NSCS, OSCS and BSCS micelles was determined using MTT assay, which is based on the reduction of MTT by the mitochondrial dehydrogenase of intact cells to a purple formazan product (Calvello et al., 2016), performed with Caco-2 cells and HT-29 cells. The viability of Caco-2 cells treated with the various concentrations of all blank polymeric micelles is shown in Figure 6.7. The half maximal inhibitory concentration (IC₅₀) value of the NSCS, OSCS and BSCS polymeric micelles for Caco-2 cells was 3.08 ± 0.15 , 2.95 ± 0.06 and 3.23 ± 0.08 mg/mL, respectively. No significant differences in the cytotoxicity were observed among the polymeric micelles in the Caco-2 cells. In a previous research, Chae et al. (2005) described low molecular weight chitosan (3.8-13 kDa; DDA 87-92%) at concentrations lower than 5 mg/mL revealed cell viability of Caco-2 cell > 80% after treating sample for 2 h. These results showed that all self-assembled polymeric micelles had low cytotoxicity in Caco-2 cells, indicating the excellent biocompatibility of the constituent polymers. As shown in Figure 6.8, blank NSCS, OSCS and BSCS micelles showed minimal cytotoxicity under concentration up to 0.5 mg/mL. The result indicated that blank micelles may be regarded as a safe drug carrier.

1. Preparation and Characterization of the 3A.1-Loaded Polymeric Nanoparticles

The blank nanoparticles and hydrophobic 3A.1-loaded nanoparticles based on the three types of amphiphilic chitosan graft copolymer (NSCS, OSCS, and BSCS) were prepared using different physical encapsulation techniques including dialysis, O/W emulsion, and dropping. These chitosan graft copolymers could generate core-shell structural nanoparticles which encapsulated the 3A.1 in the hydrophobic inner core by a self-assembly process.

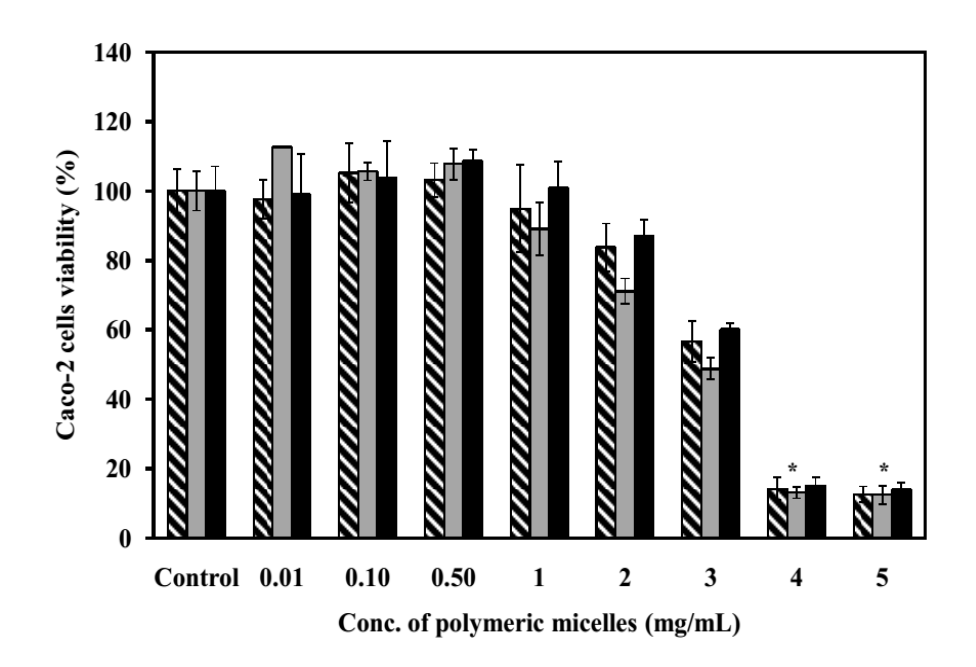


Figure 6.7 The percent cell viability in Caco-2 cells at varying concentrations of polymeric micelles; (★) NSCS, (■) OSCS, (■) BSCS. Each value represents the mean ± SD of five wells. * Statistically significant (p <0.05).

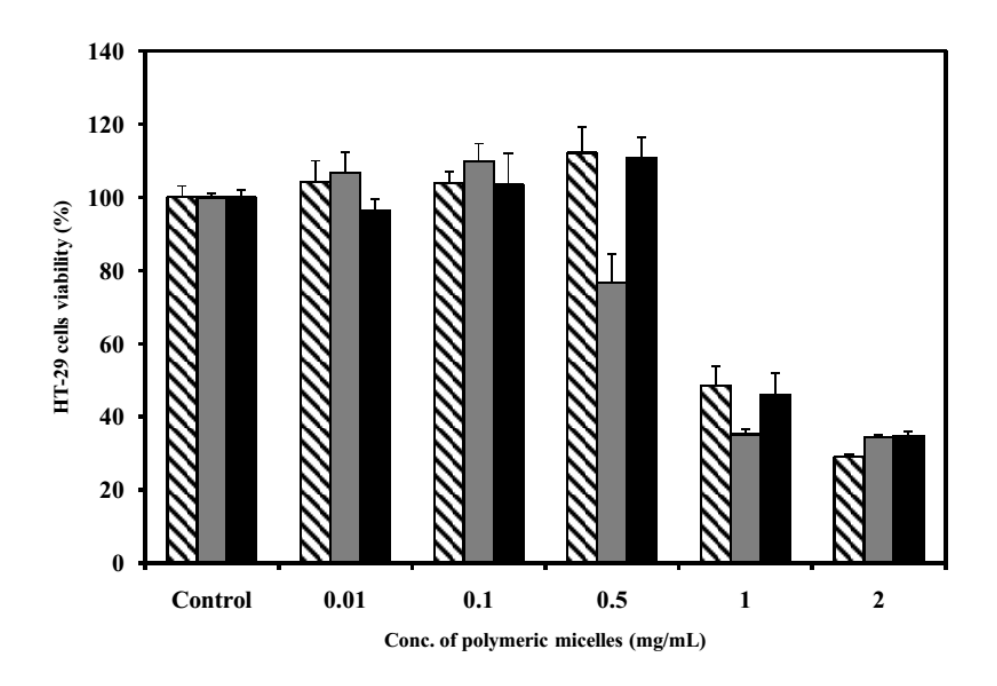


Figure 6.8 The present cell viability in HT-29 cells at varying concentrations of polymeric micelles; (**X**) NSCS, (■) OSCS, (■) BSCS. Each value represents the mean ± SD of five wells.

3.1 Effects of physical entrapment methods

The effects of different physical entrapment methods on the physicochemical properties of the nanoparticles loaded with 3A.1 were investigated at a fixed initial ratio of 20 wt% drug to polymer. The parameters which were considered when selecting the optimal drug-loading method were particle size, zeta potential, entrapment efficiency (%EE), and drug-loading capacity (LC). All the data are listed in Table 6.2. Among the three drug-loading methods with different grafted hydrophobic moieties, the nanoparticles formed by the dropping method exhibited the smallest particle size with the diameter ranging from 90.33 to 165.63 nm, while the zeta potential values showed a highly negative surface charge (– 24.97 to – 28.40 mV). On the other hand, the 3A.1-loaded nanoparticles prepared by O/W emulsion method were found to be the biggest, with the lowest values of drug-loading content. The %EE and LC of 3A.1-loaded nanoparticles prepared by dropping method were 72.59 \pm 8.61 to 80.13 \pm 5.01% and 145.17 \pm 17.21 to 160.27 \pm 10.03 μ g/mg, respectively. These high values of drug content indicated that this method could efficiently entrap the hydrophobic 3A.1 anticancer drug within the cores of the nanoparticles. Therefore, the dropping method was selected to formulate 3A.1-loaded nanoparticles for further studies.

Table 6.2 The physicochemical properties of 3A.1-loaded nanoparticles with 20% initial drug added (NSCS, OSCS, and BSCS) prepared using three physical entrapment methods

Chitosan derivatives	Method	Particle size (nm)	Zeta potential (mV)	Entrapment efficiency (%)	Loading capacity (µg/mg)
NSC	Dialysis	136.07 ± 1.43	(-) 25.10 ± 0.22	66.70 ± 2.57	133.39 ± 5.13
	O/W emulsion	105.03 ± 1.28	(-) 24.90 ± 1.34	7.86 ± 1.89	15.72 ± 3.78
	Dropping	90.33 ± 2.28	(-) 24.97 ± 1.11	72.59 ± 8.61	145.17 ± 17.21
OSC	Dialysis	287.00 ± 3.81	(-) 29.60 ± 0.33	62.88 ± 1.58	125.77 ± 3.17
	O/W emulsion	249.50 ± 8.78	(-) 25.80 ± 0.29	14.34 ± 1.29	28.67 ± 2.59
	Dropping	165.63 ± 9.80	(-) 26.67 ± 0.82	80.13 ± 5.01	160.27 ± 10.03
BSC	Dialysis	242.67 ± 2.23	(-) 26.77 ± 0.46	65.31 ± 1.89	130.62 ± 3.77
	O/W emulsion	160.60 ± 0.50	(-) 32.37 ± 1.54	12.34 ± 1.97	24.68 ± 3.95
	Dropping	131.63 ± 1.05	(-) 28.40 ± 0.68	73.06 ± 2.38	146.13 ± 4.76

3.2 Effects of initial 3A.1 and hydrophobic cores

The effects of the initial drug amount (5–40 wt% drug to polymer) and hydrophobic functionalities on the physicochemical properties of the amphiphilic nanoparticles were studied. The 3A.1-loaded nanoparticles were prepared by dropping method. The particle size, size distribution, and surface charge of the nanoparticles were determined by dynamic light scattering (DLS), as shown in Table 3. It was found that an

increase in the initial drug amounts resulted in an increase in the mean particle sizes (75.23 to 170.67 nm), which were bigger than those of the blank nanoparticles (66.26 to 132.33 nm). This might be due to the high amount of the drug molecule entrapped inside the nanoparticles. However, it should be noted that some aggregations occurred as the initial drug amount (wt% to polymer ratio) was increased to 80% (data not shown). At the initial drug-to-polymer ratio of 40%, the mean particle sizes of the 3A.1-loaded follows: NSCS $(102.53 \pm 0.60 \text{ nm}) < BSC$ nanoparticles were ranked as $(153.97 \pm 1.20 \text{ nm}) < OSCS (170.67 \pm 1.72 \text{ nm})$. The 3A.1-loaded NSCS nanoparticles exhibited the smallest particle size compared with other nanoparticles. In addition, the polydispersity indices (PDI) of all nanoparticles were lower than 0.3, indicating that the particle size distribution of these nanoparticles was narrow. The surface charges were also negative (-22.23 ± 5.27 to -32.07 ± 3.07 mV) which may be resulted from the appearance of negatively charged succinyl moieties on the nanoparticles that reduce nanoparticles aggregation, stabilize the nanoparticles in an aqueous medium, and display pH sensitivity feature. The morphology of the blank and drug-loaded nanoparticles was examined using a transmission electron microscope (TEM), and the resulting images are illustrated in Figure 9. In comparison with the blank nanoparticles, the TEM images of 3A.1-loaded nanoparticles (NSCS, OSCS, and BSCS) with 40 wt% initial drug added were spherical in shape, with a smooth surface and uniform size. Their mean sizes were in the nanometer range (approximately 40 to 90 nm in diameter). Notably, the mean particle sizes of the nanoparticles shown in the TEM images were smaller than those from the DLS technique. This is because the nanoparticles analyzed using TEM were performed in a dry state. On the other hand, those analyzed by DLS were carried out in an aqueous solution. These nanoparticles with a uniform size of not more than 200 nm could penetrate through the leaky vasculature of tumors and accumulate in tumor tissues via passive tumor targeting (You, 2016).

For characterization of Fol-NSCS nanoparticles, the results were expressed in Table 4. The surface modified polymeric nanoparticles were able to form nano-sized micelles in aqueous solution with folate molecule as targeting ligand, hydrophilic CS shells and hydrophobic naphthyl cores. The average diameters of 40% 3A.1 loaded Fol-NSCS nanoparticles (189.47 ± 2.90 nm) were bigger than unmodified NSC nanoparticles due to the steric structure of folic acid that was linked to succinic acid on CS structure.Both PDI value and zeta potential value of Fol-NSCS nanoparticles were similar with unmodified NSCS nanoparticles, which have narrow size distribution and optimal negative surface charge. In addition, TEM observation (Figure 10) also showed the Fol-NSCS nanomicelles dispersed in shape with nano-size.

Table 6.3 The physicochemical properties of 20% initial 3A.1-loaded micelles (NSCS, OSCS and BSCS) prepared using three physical entrapment methods. Each value represents the mean ± standard deviation from three independent experiments.

3A.1 to			oscs			BSCS			
polyme r (%)	Size (nm)	PDI	Zeta potential (mV)	Size (nm)	PDI	Zeta potential (mV)	Size (nm)	PDI	Zeta potential (mV)
0	66.2 ± 1.2	0.300	(-) 30.5±1.9	132.33 ± 6.6	0.131	(-)17.6± 1.5	111.1 ± 1.05	0.160	(-) 29.3± 0.3
5	75.2 ± 1.3	0.164	(-) 26.7±0.9	150.43 ± 6.7	0.181	(-) 29.2±3.4	112.2 ± 0.67	0.138	(-) 26.2± 0.6
10	82.1 ± 3.5	0.185	(-) 28.8±2.3	161.81 ± 5.2	0.194	(-) 27.0±0.2	127.1± 2.32	0.185	(-) 27.3± 1.5
20	90.3 ± 2.2	0.255	(-) 24.9±1.1	165.63 ± 9.8	0.185	(-) 26.6±0.8	131.6 ± 1.05	0.208	(-) 28.4± 0.6
40	102.5 ± 0.6	0.162	(-) 22.2±5.2	170.67 ± 1.7	0.192	(-) 32.0±3.0	153.9 ± 1.20	0.195	(-) 26.0± 0.4

Table 6.4 The physicochemical properties of blank and 40% initial 3A.1-loaded micelles and folate-conjugated micelles. Data represent the mean \pm standard deviation (n=3).

Sample	Particle size (nm)	PDI	Zeta potential (mV)	Entrapment efficiency (%)	Loading capacity (µg/mg)
Blank NSCS micelles	85.26 ± 1.21	0.383	(-) 23.03 ± 1.11	-	- (p-3,3)
Blank Fol-NSCS micelles	343.80 ± 43.73	0.494	(-) 28.50 ± 1.15	-	-
3A.1-loaded NSCS micelles	110.17 ± 1.13	0.170	(-) 26.17 ± 1.44	90.84 ± 7.43	363.35 ± 29.74
3A.1-loaded Fol-NSCS micelles	189.47 ± 2.90	0.174	(-) 31.67 ± 0.39	68.44 ± 3.72	273.75 ± 14.91

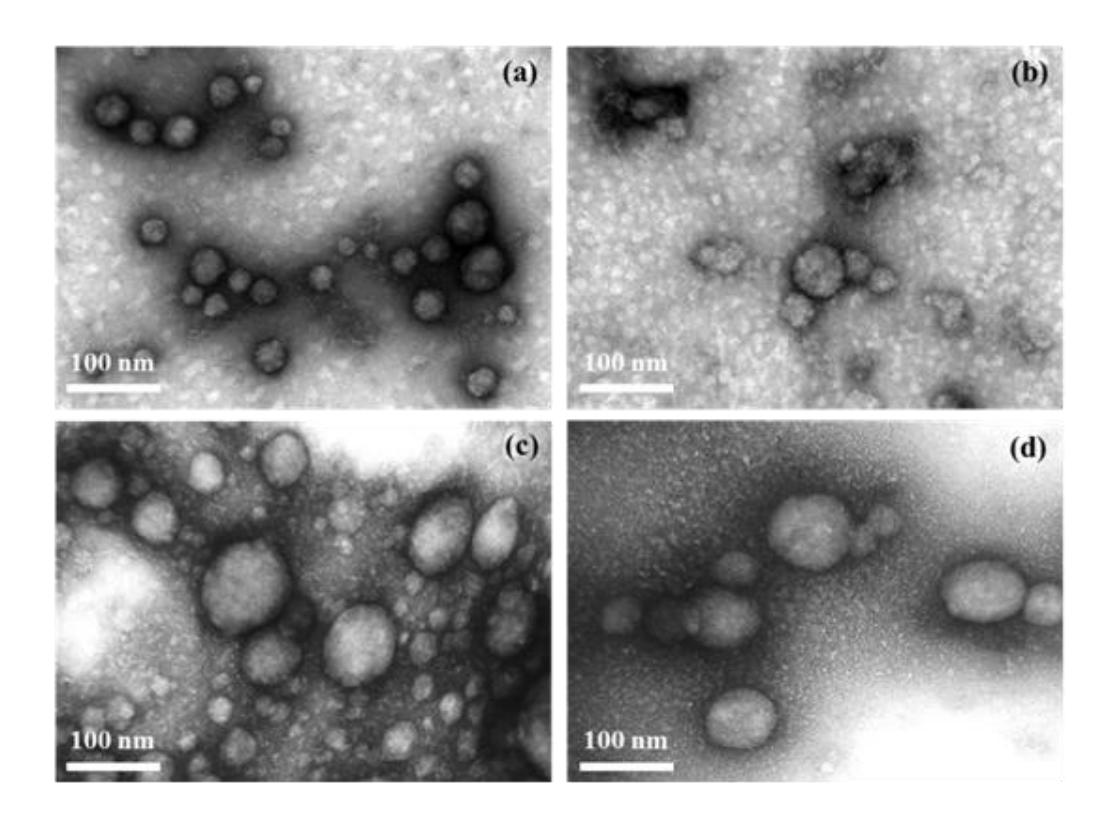


Figure 6.9 TEM images of nanoparticles prepared by dropping method: (a) blank NSCS nanoparticles, (b) 3A.1-loaded NSCS nanoparticles, (c) 3A.1-loaded OSCS nanoparticles and (d) 3A.1-loaded BSCS nanoparticles.

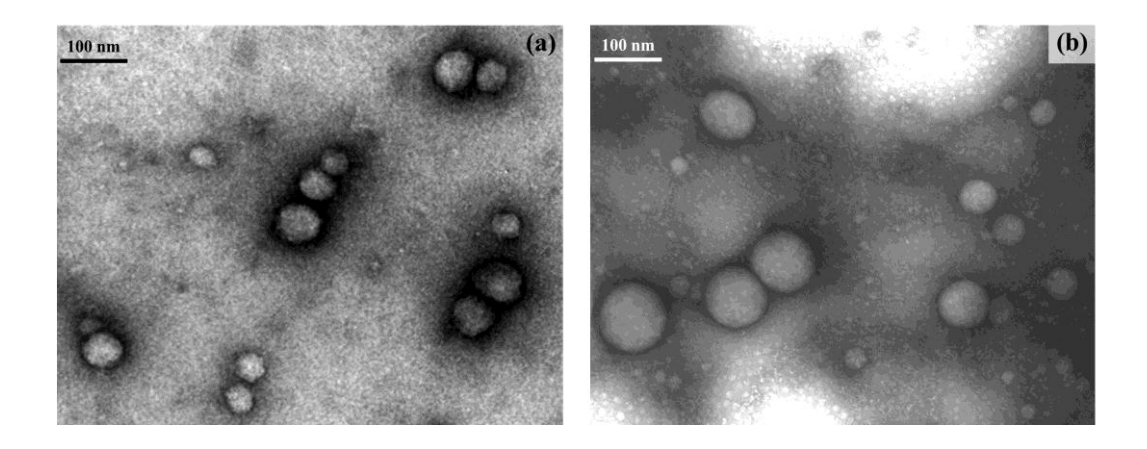


Figure 6.10 TEM images of nanoparticles prepared by dropping method: (a) 3A.1-loaded NSCS nanoparticles (b) 3A.1-loaded folate-conjugated NSCS nanoparticles.

A quantitative analysis of the drug content incorporated in the hydrophobic core of the nanoparticles was undertaken using HPLC. The effects of the initial drug amounts (5–40 wt% to polymer weight ratio) and the different grafted hydrophobic moieties (naphthyl,

octhyl, and benzyl groups) on the %EE and LC are presented in Figure 6.3. The x-axis represents the initial drug amount added to the nanoparticle formulations, and the y-axis represents the drug content in the nanoparticles in terms of %EE (Figure 11a) and LC (Figure 11b). The results revealed that the initial drug amount directly correlated with the drug loading content. An increase in the initial drug amount resulted in an increase in LC due to the hydrophobic interactions between the hydrophobic naphthyl, octhyl, and benzyl groups with the hydrophobic drug. Moreover, the NSCS nanoparticles with 40 wt% initial drug concentration demonstrated the highest value of LC compared with the other nanoparticles. These high levels of entrapped drug can be explained by the hydrophobic ¶-¶ interactions between the hydrophobic moieties of the polymer and the aromatic rings of the drug. These were an important factor when entrapping the drug into the nanoparticles, therefore, the NSC nanoparticles which presented naphthyl groups (double aromatic rings) on the CS backbone created strong ¶-¶ interactions which were greater than the BSC (benzyl group; single aromatic ring) and OSC (octhyl group; aliphatic hydrocarbon chain) alternatives. These results were in agreement with the previously investigated incorporation behavior of camptothecin by varying the degrees of the hydrophobicity of the nanoparticle inner cores (Opanasopit, 2004). Overall, these CS graft copolymers are beneficial when designing drug delivery systems due to their highly efficient drug encapsulation and capability of increasing drug solubility.

For drug loading content of Fol-NSCS nanoparticles, the 3A.1 hydrophobic anticancer agent was physically loaded into Fol-conjugated NSC nanoparticles by dropping method. Drug loading was performed at 40% feed weight to polymer ratio, while the results were shown in Table 6.4. Compared with unmodified NSCS nanoparticles, the conjugation of folate on NSCS nanoparticles could affect the %EE and LC. The %EE of Fol-NSCS nanoparticles were decrease to 68.44 \pm 3.72 % while LC were also decrease to 273.75 \pm 14.91 μ g/mg, indicating that Fol-NSC nanoparticles still had high drug loading content, probably due to good hydrophobic interaction.

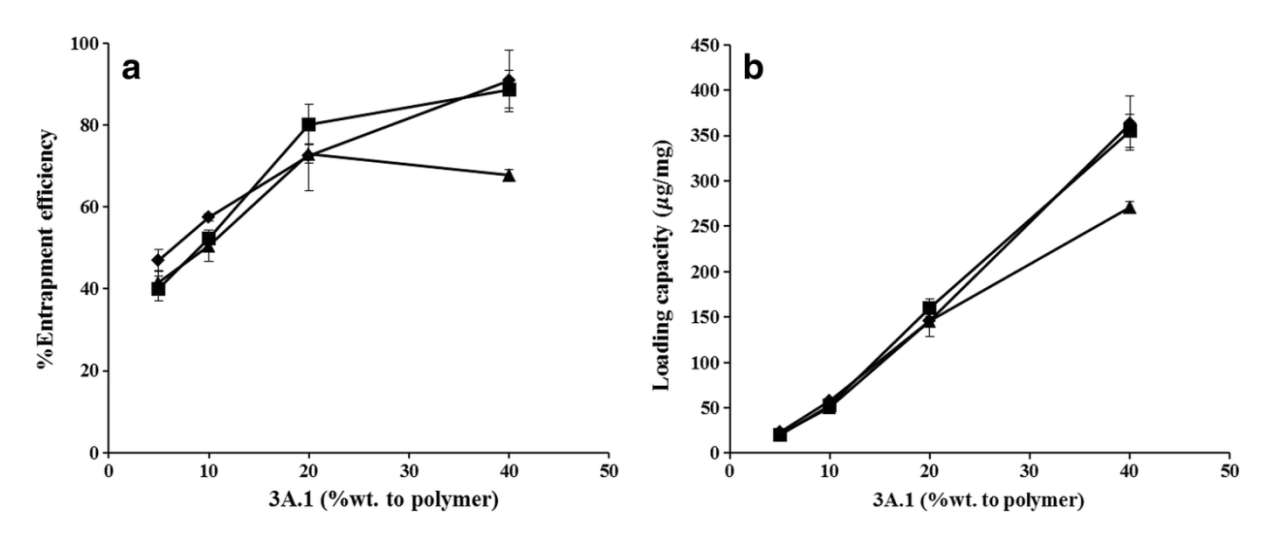


Figure 6.11 Effects of the initial drug loading ratio (5–40 wt% to polymer) on a the entrapment efficiency and b loading capacity of 3A.1-loaded nanoparticles prepared by dropping method; filled diamonds, NSCS; filled squares, OSCS; and filled triangles, BSCS. Data are expressed as the mean ± standard deviation (n=3)

2. In vitro release

The *in vitro* release behaviors of the 3A.1 from the 3A.1-loaded nanoparticles (NSCS, OSCS, and BSCS) with 40 wt% initial drug added were examined at 37 °C in three stages with different pH imitated the condition in GI tract. A plot of the cumulative drug release from the 3A.1 free drug and 3A.1-loaded nanoparticles as a function of time is shown in Figure 12. In SGF (pH 1.2), there was no apparent amount of drug released from any 3A.1-loaded nanoparticles. When the release medium was changed to SIF (pH 6.8) for 6 h, the 3A.1 was considerably released from the 3A.1-loaded nanoparticles which significant difference in the release amounts was observed from the nanoparticles prepared from different CS derivatives, indicating that the release rate depended on the hydrophobic functionalities of the polymer. The percentages of drug release from these nanoparticles after 4 h were as follows: NSCS $(84.10 \pm 2.43\%) > BSCS$ $(63.41 \pm 2.95) > OSCS$ $(52.03 \pm 3.33\%)$. On the other hand, none of the 3A.1 free drug could be released through the simulated GI tract (SGF, SIF and SCF). This might be due to the poor aqueous solubility of 3A.1 in all types and pH values of release medium (< 1 μ g/mL).

Generally, the pK_a value of succinic acid is approximately 4.21 at 25 °C. In the gastric fluid (pH 1.2), the succinyl groups grafted onto the CS polymer were unionized, resulting in a tight arrangement of the polymer core-shell structure and protection of 3A.1 from the acidic environment. When the nanoparticles were exposed to the alkaline environment in SIF (pH 6.8) and SCF (pH 7.4), the succinyl groups grafted onto the CS polymer showed high ionization and created a negative charge, leading to lose compaction of the nanoparticle structures and promotion of the release of 3A.1 from the inner cores of the nanoparticles. In addition, the different hydrophobic moieties influenced the drug release in SIF and SCF. The extent of drug release reduced as follows: NSC nanoparticles > BSC nanoparticles > OSC nanoparticles (p < 0.05). These results suggested that not only the $\P-\P$ interactions restrict water penetration but also other factors such as hydrophobicity, mobility/rigidity, hydrogen bonding, and steric factors, influencing the difference in drug release (Yokoyama, 2014). Hence, many drug release studies have inferred that these pH-sensitive nanoparticles could enhance the solubility of 3A.1 in SIF and SCF mediums, and different inner cores could influence the degrees of drug release. OSCS could retain 3A.1 within the inner core of the nanoparticles greater than the nanoparticles prepared from NSCS and BSCS. Therefore, it can be assumed that the 3A.1-loaded nanoparticles (NSCS, OSCS, and BSCS) exhibited delayed release profiles useful for improving the bioavailability of 3A.1 for oral intestine/colon drug delivery.

The release behavior of 3A.1 from Fol-NSCS nanoparticles were investigated with the same condition compared with unmodified NSCS nanoparticles (Figure 13). This folate-conjugated NSCS still possessed pH-sensitive property with specific drug release at intestinal/colon sites. At time intervals (4-12 h), the Fol-NSCS nanoparticles showed an obviously lower release of 3A.1 than the unmodified NSCS nanoparticles. For example, about 52% and 80% of loaded 3A.1 could be release from Fol-NSCS nanoparticles and NSCS nanoparticles, respectively after 12 h. The lower content of drug release might be explained that conjugation of folic acid on NSCS polymer could enhance the strong hydrophobic interaction between the hydrophobic domain of polymer and drug. Therefore, Fol-NSCS nanoparticles for delayed release is helpful for site-specific release and decreasing drug leakage form nanoparticles before drug-loaded nanoparticles reach to target cells.

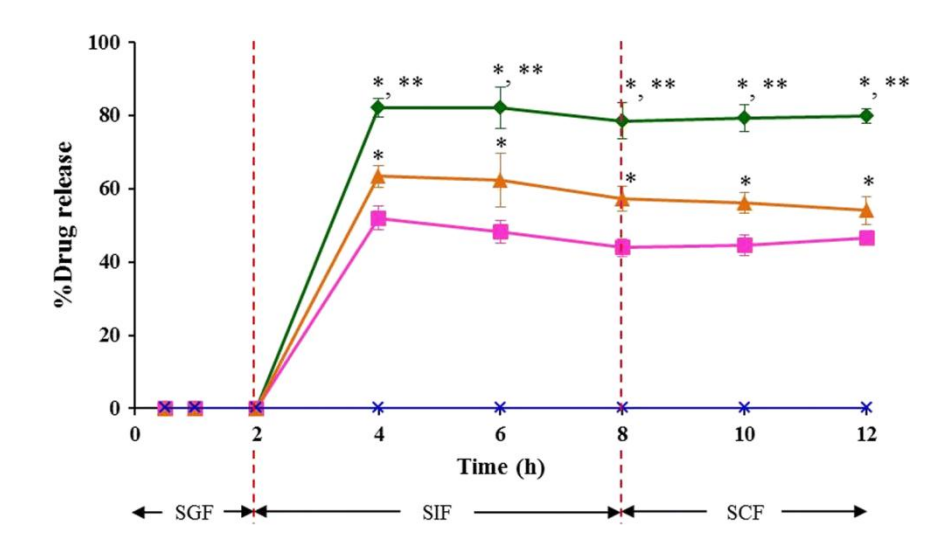


Figure 6.12 Release profiles of free 3A.1 and 3A.1-loaded nanoparticles (error marks) prepared by dropping method; filled diamonds, NSCS; filled squares, OSCS; and filled triangles, BSCS in simulated gastric fluid (SGF; pH 1.2, 0-2 h), simulated intestinal fluid (SIF; pH 6.8, 2-8 h) followed by simulated colonic fluid (SCF; pH 7.4, 8-12 h) (n=3).



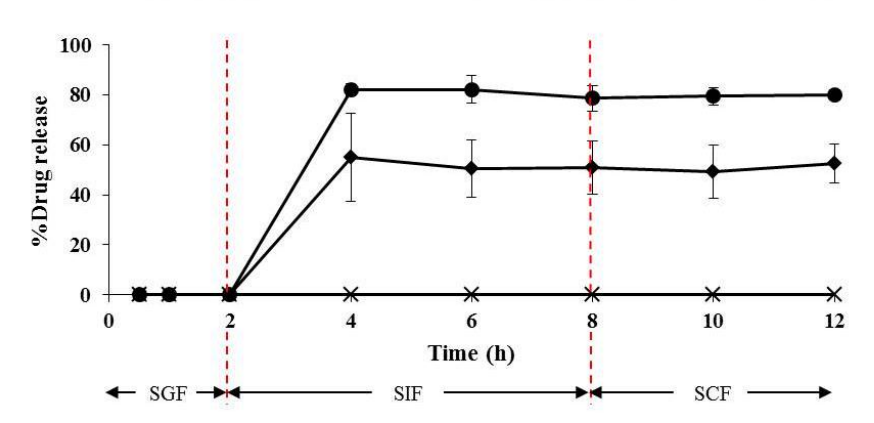


Figure 6.13 Release profiles of free 3A.1, 3A.1-loaded NSC nanoparticles and 3A.1-loaded Fol-NSC nanoparticles in SGF, SIF followed by SCF at 37 °C. Data represent the average values from triplicate experiments.

3. In vitro anticancer activity

The anticancer activity of 3A.1 free drug and 3A.1-loaded NSCS, OSCS and BSCS nanoparticles against human colorectal cancer (HT-29) cells was assessed using an MTT assay. The finding indicated that the %cell viability was dose-dependent. The half-maximal inhibitory concentration (IC50) was determined from the %cell viability-drug concentration relationship. The IC50 values of the 3A.1-loaded NSCS, OSCS and BSCS nanoparticles were 1.024 ± 0.071 , 0.693 ± 0.099 , and 0.538 ± 0.025 μ g/mL, respectively, which are significantly lower than that of the free drug (3.816 \pm 0.376 μ g/mL; p < 0.05) (Figure 14). Cell viability of the blank nanoparticles remained at more than 80% even at high polymer concentrations up to 500 μ g/mL. No significant differences in the cytotoxicity were noticed between the blank nanoparticles prepared from different CS derivatives. These results clearly indicated that all the blank nanoparticles demonstrated minimal cytotoxicity in HT-29 cells, and the cytotoxicity was due to the presence of 3A.1.

To compare antitumor activities of non-conjugated and folated-conjugated NSC nanoparticles against HT-29 cell, which over-expressed folate receptors on cell surface (Bahrami, 2015), it is interesting that Fol-NSC nanoparticles exhibited obviously higher cytotoxicity than the non-conjugated nanoparticles. This lower IC $_{50}$ value (0.412 \pm 0.048 μ g/mL) that was improved sharply by 2.5-fold compared to non-conjugated nanoparticles was attributed to the enhance cellular drug uptake via folate-receptor mediated endocytosis. The over-expressed folatereceptor on HT-29 cell facilitate the effective recognition of the folate ligand on surface of nanoparticles, leading to an increased cellular cytotoxicity. Therefore, conjugation of folic acid on nanoparticles has benefit to more deliver drug into cancer cell through active tumor targeting.

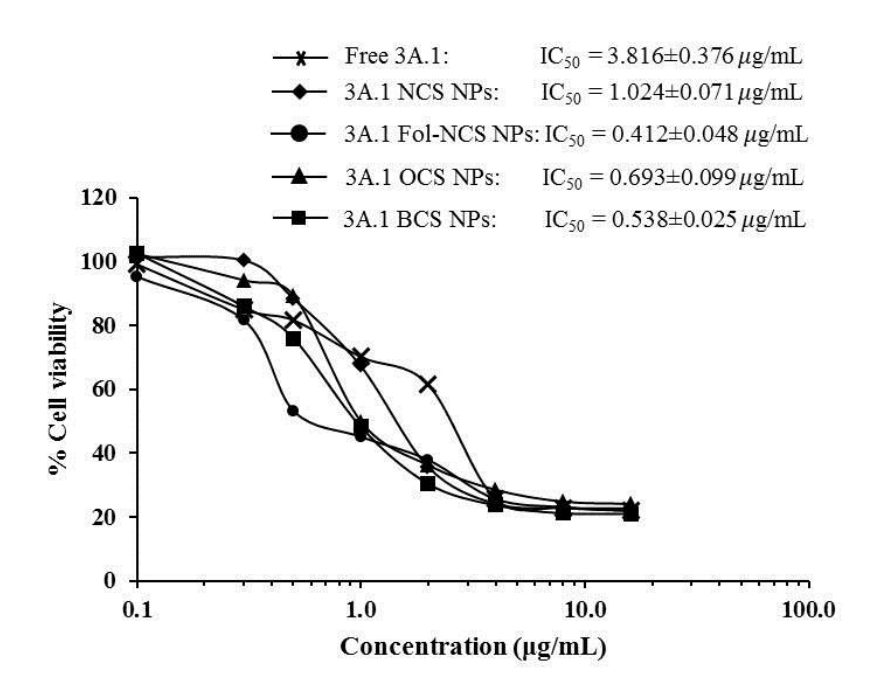


Figure 6.14 The percentage of cell viability (y-axis) of HT-29 cells after being exposed to various concentration drug-loaded nanoparticles or free 3A.1 (x-axis) and the IC₅₀ values

4. Induction of cell apoptosis

To confirm that this drug can induce apoptosis in HT-29 colorectal cancer cells, a costaining assay (annexin V-FITC and PI) was used to quantitatively analyze the degree of cell death, especially cell apoptosis, by flow cytometry analysis (Figure 15a). In this part, the cell apoptosis rate was calculated by the inclusion of the percentage of early apoptosis (Q4; annexin V-FITC+/PI-) and the percentage of late apoptosis (Q2; annexin V-FITC+/PI+) (Figure 15b). After incubation with the free drug and different formulations of 3A.1-loaded nanoparticles containing equivalent drug concentrations (at IC₅₀ of the free drug) for 24 h, the cell apoptosis rates of the drug-loaded NSCS, OSCS, and BSCS nanoparticles were 45.20 ± 3.27 , 41.60 ± 2.45 , and $40.50 \pm 2.04\%$, respectively, which were significantly greater than those of the free drug (33.10 \pm 2.45%) and Triton X (9.50 \pm 1.63%). This degree of cell apoptosis is in concordance with the results of the in vitro anticancer activity. In addition, the percentage of cell necrosis of the cells treated with the drug-loaded nanoparticles was lower than that treated with free drug at this stage. This might be a beneficial property of the nanoparticles for growth suppression of cancer cells. Thus, 3A.1-loaded NSC, OSC, and BSC nanoparticles induced intense apoptosis in HT-29 colorectal cancer cells. Moreover, it should be noticed that Fol-NSCS nanoparticles had significantly higher cell apoptosis than unmodified NSCS nanoparticles due to the increase of drug into cell internalization via

receptor-mediated endocytosis. This result was in accordance with the *in vitro* anticancer activity.

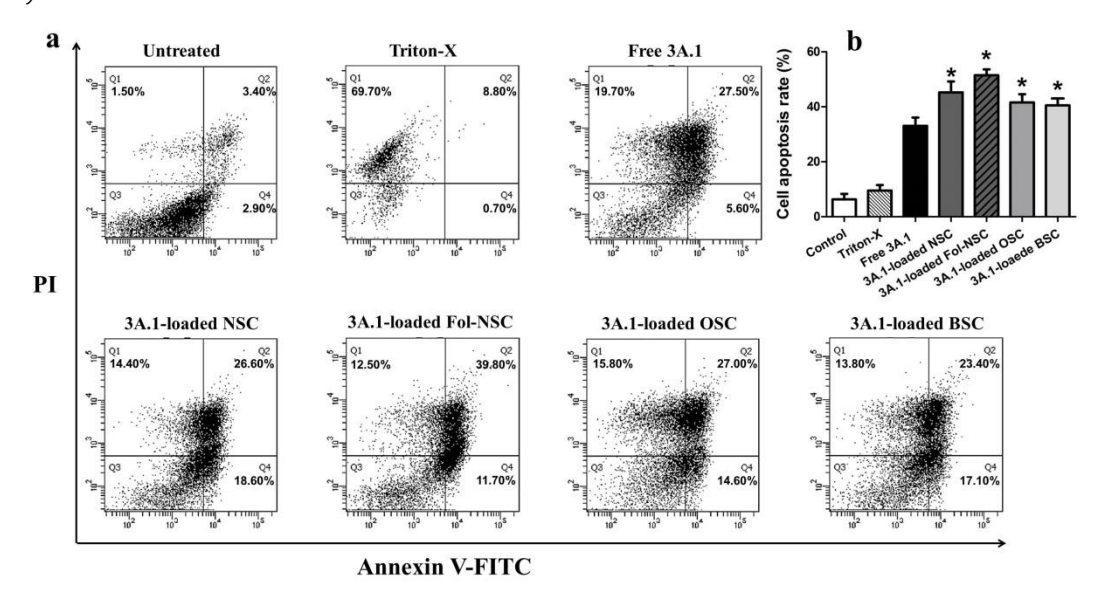


Figure 6.15 3A.1-loaded nanoparticles induced HT-29 cancer cell apoptosis examined by flow cytometry; **a** the cells treated with 3A.1-loaded nanoparticles, free 3A.1 (at the equivalent concentration), and Triton X for 24 h which are presented in four quadrants (Q) with dot plot. The number of the late apoptotic cells, early apoptotic cells, and living cells are displayed on Q2, Q4, and Q3, respectively, **b** percentage of cell apoptosis rate of the cells after treated with 3A.1-loaded nanoparticles, free 3A.1, and Triton X. Astersik, statistically significant difference from free 3A.1 group.

5. In vitro antimigratory activity

The scratch would migration assay was selected to assess the antimigratory effect of free 3A.1 and 3A.1-loaded nanoparticles on human oral cancer (HN-22) cells because of simple and cost-effective procedure. The wound gap images of cells after being treated with the 3A.1-loaded nanoparticles and free drug are shown in Figure 16a. After 24-h treatment, the scratch areas of untreated cell monolayer were almost fully closed, whereas both free 3A.1 and 3A.1-loaded nanoparticles tended to reduce the cell motility. In addition, the cell migration rate and %wound closure are illustrated in Figure 16b, c. respectively. The results found that free 3A.1 has significant slower cell migration rate than that of untreated cells and it also decrease %wound closure compared with untreated cell, indicating that 3A.1 could suppress cell motility. Moreover, both cell migration rate and %wound closure of 3A.1-loaded nanoparticles were not significant different to the free drug at the same concentration. From these results, it could be concluded that free 3A.1 might be one of the antimigration compounds and loading 3A.1 into the nanoparticles did

not affect its antimigratory activity. Therefore, 3A.1-loaded nanoparticles could be a potential carrier to reduce metastasis of oral cancer.

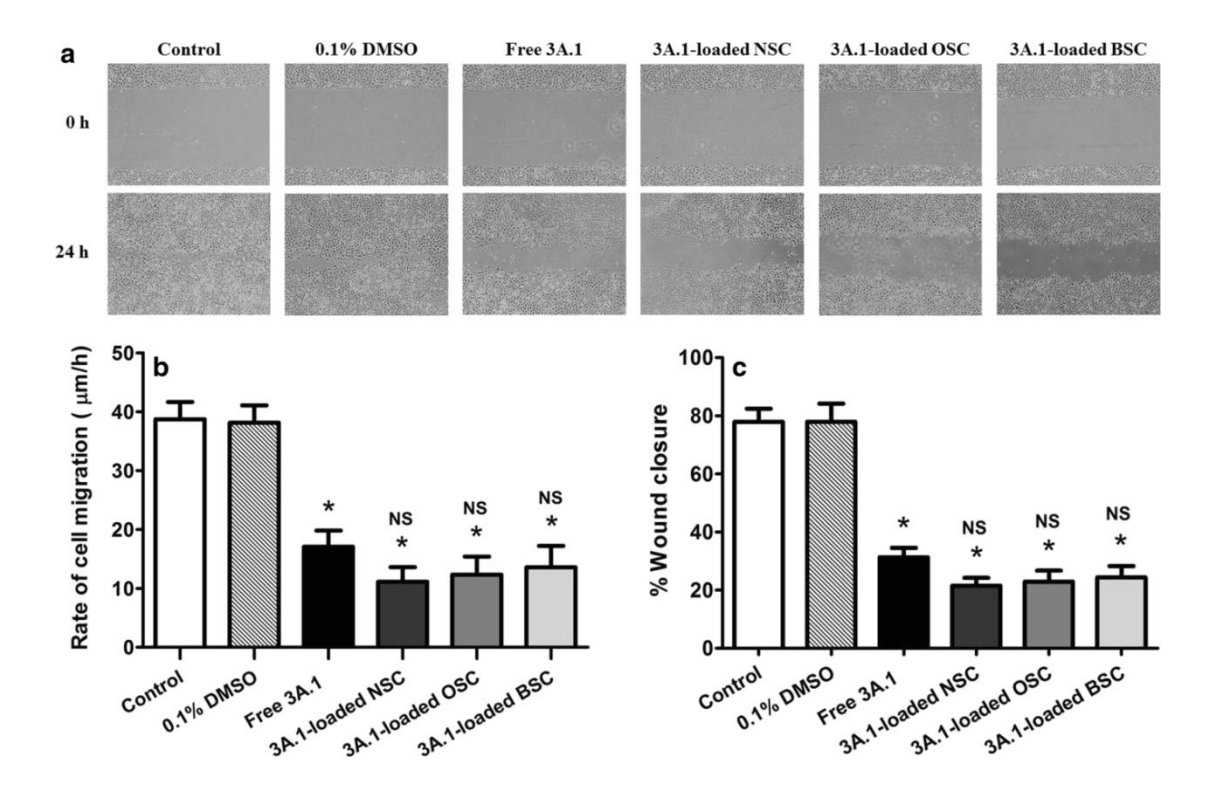


Figure 6.16 The antimigration of free 3A.1 and 3A.1-loaded nanoparticles prepared by dropping method on HN-22 cells presented as the value of **a** wound images taken by a microscope (x 40 magnification) at 0 and 24 h **b** cell migration rate and **c** %wound closure after 24-h treatment exposure. Asterisk, statistically significant difference from untreated control group; NS, not significantly different from free 3A.1 group.

6. Short-Term Stability

One of the main stability concerns regarding polymeric nanoparticles is particle aggregation. The physical stability of 3A.1-loaded nanoparticles (NSCS, OSCS, and BSCS) were examined under two conditions, an accelerated environment (25 ± 2 °C, 60 ± 5 %RH) and a long-term environment (5 ± 3 °C, 60 ± 5 %RH), for 180 days. The physical stability of the 3A.1-loaded nanoparticles was studied and the data, including particle size, PDI and percentage of drug remaining, is presented in Figure 17. The results indicated that the particle sizes of the nanoparticles stored at 5 ± 3 °C, 60 ± 5 %RH were smaller than those stored at 25 ± 2 °C, 60 ± 5 %RH over 180 days, the surface charges of the nanoparticles were not altered which a highly negative zeta potential value of approximately – 30 mV

was remained. Interestingly, the mean particle size of these nanoparticles in both conditions still remained lower than 200 nm without nanoparticle aggregation. These results might suggest that the high negative charge of these nanoparticles helped to stabilize the nanoparticles in the aqueous solution through electrostatic repulsion. After storage at the long-term condition for 6 months, the total contents of 3A.1 in the NSCS, OSCS, and BSCS nanoparticles were 93.65, 87.22, and 85.67%, respectively. However, under the accelerated condition the drug content was found to be 81.64, 68.27, and 53.62%, respectively. The 3A.1-loaded nanoparticles kept under accelerated condition exhibited faster degradation than those stored under long-term condition. The 3A.1-loaded BSCS nanoparticles demonstrated poor stability, whereas the NSC nanoparticles showed better stability with the high values of %drug remaining after 6 months when stored under longterm condition. These results explained that naphthyl groups had stronger hydrophobic interaction between the hydrophobic groups of polymer and the hydrophobic drug than the benzyl groups do result in higher drug protection capability and decrease in drug leakage from the NSCS nanoparticles. Our data suggested that the nanoparticles should be stored in a refrigerator to maintain the particle size, zeta-potential, and the amount of drug remaining in the nanoparticles.

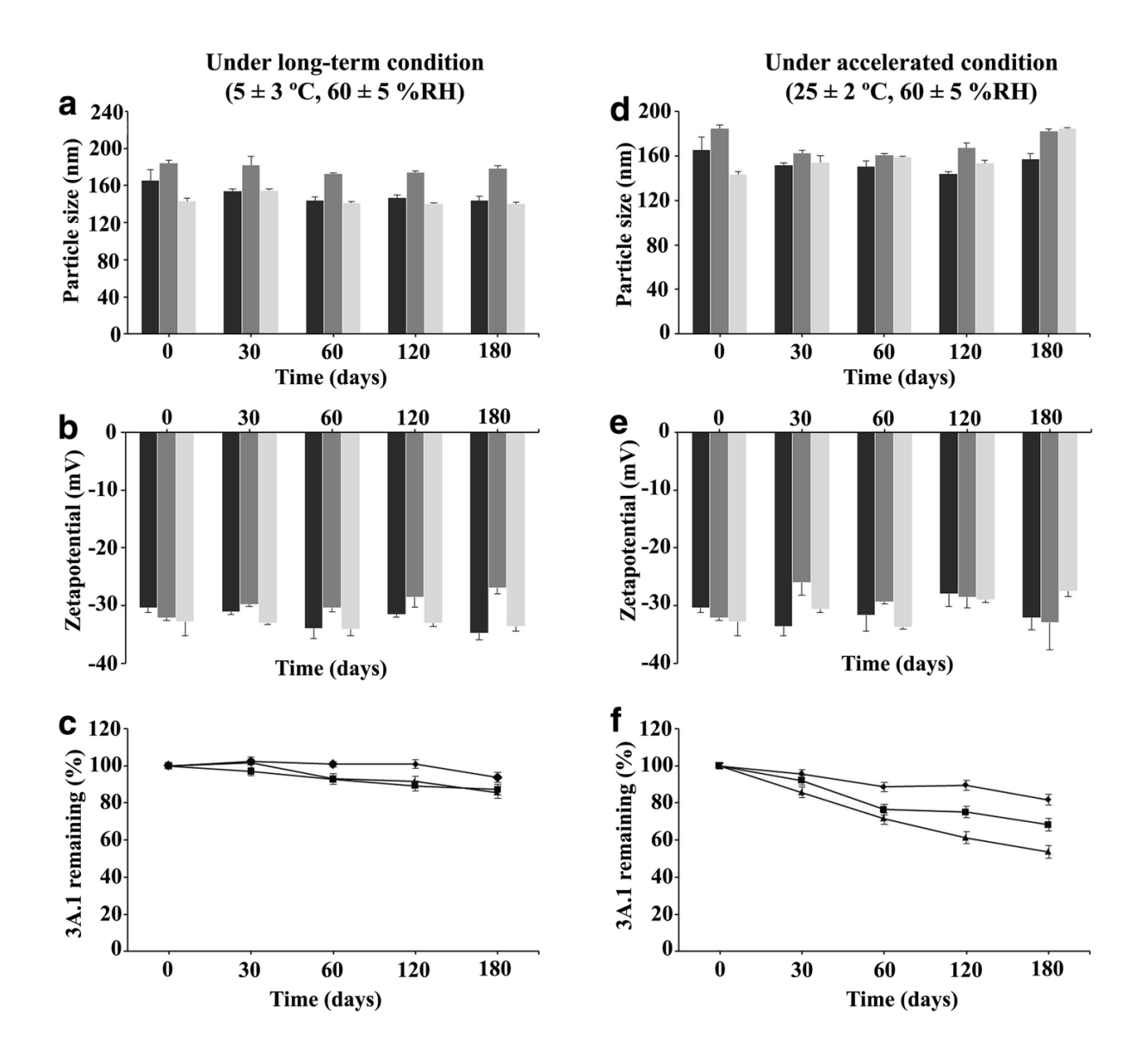


Figure 6.17 The short-term stability of 3A.1-loaded nanoparticles stored under long-term condition (left) compared with under accelerated condition (right) for 6 months; $\bf a$, $\bf d$ particle size of NSCS nanoparticles (black-filled bars), OSCS nanoparticles (dark-gray-filled bars), and BSCS nanoparticles (light-gray-filled bars); $\bf b$, $\bf e$ zeta-potential of NSCS nanoparticles (black-filled bars), OSCS nanoparticles (dark-gray-filled bars), and BSCS nanoparticles (light-gray-filled bars); $\bf c$, $\bf f$ the amount of 3A.1 remaining in NSCS (filled diamonds), OSCS (filled squares), and BSCS (filled triangles) nanoparticles. All data are presented as the mean $\bf t$ standard deviation (n = 3)

IV. CONCLUSION

In the present study, pH sensitive amphiphilic chitosan derivatives, i.e. N-naphthyl-N,O-succinyl chitosan (NSCS), N-octyl-N,O-succinyl chitosan (OSCS) and N-benzyl-N,Osuccinyl chitosan (BSCS) were synthesized and prepared as polymeric micelles to improve the solubility of poorly water soluble drug and to control the drug release. Semi-synthetic andrographolide (3A.1) was selected as a hydrophobic drug for colorectal cancer treatment. The influence of the physical entrapment methods, type of amphiphilic chitosan derivatives, amount of drugs on entrapment efficiency, loading capacity, particle size and stability of drugs-loaded polymeric micelles were evaluated. In addition, the in vitro cytotoxicity and their release behavior were investigated. The results showed that 3A.1 was successfully incorporated into self-assembled polymeric nanoparticles based on amphiphilic chitosan derivatives (NSCS, OSCS, and BSCS). These nanoparticles were formed by self-assembly in an aqueous solution and their hydrophobic part helped to solubilize the hydrophobic drug within the nanoparticles. The 3A.1-loaded NSCS nanoparticles with 40 wt% drug added prepared by a dropping method revealed the highest drug loading capacity, favorable properties (spherical shape, nanometer-size, negative surface charge) and good physical stability in a refrigerator. The release behavior of the 3A.1 depended on the pH of the medium, and high drug amounts were specifically released at intestinal/colon sites. Importantly, the 3A.1-loaded nanoparticles clearly showed great anticancer activity against colorectal cancer HT-29 cells and potent apoptotic induction, compared with free 3A.1. Moreover, the 3A.1-loaded nanoparticles also inhibited cell migration of oral cancer HN-22 cells. Therefore, these 3A.1-loaded pH-sensitive polymeric nanoparticles could be promising nanocarriers of the hydrophobic anticancer agent 3A.1 for oral intestine/colon drug delivery. Furthermore, compared with the non-conjugated polymers, the folateconjugated NSCS polymers showed much more anticancer activity and highly potent apoptotic induction, suggesting that the folate-conjugated were active-targeting drug nanocarriers for colon tumor therapy via folate mediation.

V. REFERENCES

- Aliabadi H.M. et al.Encapsulation of hydrophobic drugs in polymeric micelles through cosolvent evaporation: The effect of solvent composition on micellar properties and drug loading.Int J Pharm. 2007 Feb 1;329(1-2):158-65.
- Aromdee C. Modifications of andrographolide to increase some biological activities: a patent review (2006-2011). Expert OpinTher Pat. 2012;22:169–80.
- Bahrami B, Mohammadnia-Afrouzi M, Bakhshaei P, Yazdani Y, Ghalamfarsa G, Yousefi M, et al. Folate-conjugated nanoparticles as a potent therapeutic approach in targeted

- cancer therapy. Tumor Biol. 2015;36:5727-5742.
- Bonferoni, M.C. et al. Ionic polymeric micelles based on chitosan and fatty acids and intended for wound healing. Comparison of linoleic and oleic acid.Eur J Pharm Biopharm. 2014 May;87(1):101-6.
- Calvello, R. et al. Bovine and soybean milk bioactive compounds: Effects on inflammatory response of human intestinal Caco-2 cells. Food Chem. 2016 Nov 1;210:276-85.
- Chae SY, Jang MK, Nah JW. Influence of molecular weight on oral absorption of water soluble chitosans. J Control Release. 2005 Feb 2;102(2):383-94.
- Cisterna BA, Kamaly N, Choi WI, Tavakkoli A, Farokhzad OC, Vilos C. Targeted nanoparticles for colorectal cancer. Nanomedicine (London). 2016;11:2443–56.
- Demain AL, Vaishnav P. Natural products for cancer chemotherapy. MicrobBiotechnol. 2011;4:687–99.
- DiPiro JT, Talbert RL, Yee GC, Matzke GR, Wells BG, Posey LM. Pharmacotherapy: a pathophysiologic approach. In: Holle LM, Clement JM, Davis LE, editors. Colorectal cancer. 10th ed. New York: McGraw-Hill Education; 2016.
- Ghaemy M, Ziaei S, AlizadehR. Synthesis of pH-sensitive amphiphilicpentablock copolymers via combination of ring-opening and atom transfer radical polymerization for drug delivery. EurPolym J. 2014; 58 (September): 103-114.
- Grada A, Otero-Vinas M, Prieto-Castrillo F, Obagi Z, Falanga V. Research techniques made simple: analysis of collective cell migration using the wound healing assay. J InvestigDermatol. 2017;137:e11–6.
- Hossain MS, Urbi Z, Sule A, Rahman KMH. *Andrographispaniculata* (Burm. F.) Wall. exNees: a review of ethnobotany, phytochemistry, and pharmacology. Sci World J. 2014;2014:1–28.
- Jain A, Barve A, Zhao Z, Jin W, Cheng K. Comparison of avidin, neutravidin, and streptavidin as nanocarriers for efficient siRNA delivery. Mol Pharm. 2017;14:1517–27.
- Jiang, G.B. et al. (2006). "Novel polymer micelles prepared from chitosan grafted hydrophobic palmitoyl groups for drug delivery." Molecular Pharmaceutics 3, 2 (January): 152-160.
- Kalepu S, Manthina M, Padavala V. Oral lipid-based drug delivery systems—an overview." ActaPharmaceuticaSinica B.2013;3: 361-372.
- Kedar U. et al. Advances in polymeric micelles for drug delivery and tumor targeting-review article.Nanomedicine: Nanotechnology, Biology and Medicine2010;6 (December): 714-729.
- Kim S. et al. Overcoming the barriers in micellar drug delivery: loading efficiency, in vivo stability, and micelle-cell interactionExpert Opin Drug Deliv. 2010 Jan;7(1):49-62.
- Kumar A. et al. Review on solubility enhancement techniques for hydrophobic drugs. Int J Compre Pharm. 2011; 3: 1-7.

- Li, Y. et al. pH-Responsive composite based on prednisone-block copolymer micelle intercalated inorganic layered matrix: Structure and in vitro drug release.

 ChemEngJ.200;151: 359-366.
- Lia W. et al. Amphiphilic chitosan derivative-based core—shell micelles: Synthesis, characterisation and properties for sustained release of Vitamin D3. Food Chem. 2014; 152:307-15.
- Lim, E. et al. Chitosan based intelligent theragnosisnanocomposites enable pH-sensitive drug release with MR-guided imaging for cancer therapyNanoscale Res Lett. 2013 Nov 8;8(1):467.
- Lu Y, Park K.Polymeric micelles and alternative nanonized delivery vehicles for poorly soluble drugs.Int J Pharm. 2013 Aug 30;453(1):198-214
- Miller, T. et al. Drug loading of polymeric micelles. Pharm Res. 2013;30:584-595.
- Mosmann T. Rapid colorimetric assay for cellular growth and survival: application to proliferation and cytotoxicity assays. J Immunol Methods. 1983;65:55–63.
- Murthy, RSR. Polymeric micelles in targeted drug delivery. In Targeted drug delivery: Concepts and design, 501-540. Edited by Padma V. Devarajan and Sanyog Jain. USA: Springer. 2015.
- MuzzarelliC. et al. Alkaline chitosan solutions. Carbohyd Res. 2003;338, 21: 2247-2255.
- Muzzarelli RAA. et al Current views on fungal chitin/chitosan, human chitinases, food preservation, glucans, pectins and inulin: A tribute to Henri Braconnot, precursor of the carbohydrate polymers science, on the chitin bicentennial. Carbohyd Polym. 2012; 87:995-1012.
- Nanduri S, et al. Synthesis and structure-activity relationships of andrographolide analogues as novel cytotoxic agents. Bioorg Med ChemLett. 2004;14:4711–7.
- Nateewattana J, Dutta S, Reabroi S, Saeeng R, Kasemsook S, Chairoungdua A, *et al.* Induction of apoptosis in cholangiocarcinoma by an andrographolide analogue is mediated through topoisomerase II alpha inhibition. Eur J Pharmacol. 2014;723:148–55.
- Ngawhirunpat T. et al. Incorporation methods for cholic acid chitosan-g-mPEG self-assembly micellar system containing camptothecin.Colloids Surf B Biointerfaces. 2009 Nov 1;74 (1):253-9
- Opanasopit P. et al. Block copolymer design for camptothecin incorporation into polymeric micelles for passive tumor targeting. Pharm Res. 2004 Nov;21(11):2001-8.
- Preet R, Chakraborty B, Siddharth S, Mohapatra P, Das D, Satapathy SR, *et al.* Synthesis and biological evaluation of andrographolide analogues as anti-cancer agents. Eur J Med Chem. 2014;85:95–106.
- Qiu LY, Wu XL, Jin Y.Doxorubicin-Loaded Polymeric Micelles Based on Amphiphilic Polyphosphazenes with Poly(N-isopropylacrylamide-co-N,N dimethylacrylamide)

- and Ethyl Glycinate as Side Groups: Synthesis, Preparation and In Vitro Evaluation. Pharm Res. 2009 Apr;26(4):946-57.
- Reabroi S, Chairoungdua A, Saeeng R, Kasemsuk T, Saengsawang W, Zhu W, et al. A silyl andrographolide analogue suppresses Wnt/ β -catenin signaling pathway in colon cancer. Biomed Pharmacother. 2018;101:414–21.
- Sajomsang W. et al. Synthesis and anticervical cancer activity of novel pH responsive micelles for oral curcumin delivery. Int J Pharm. 2014 Dec 30;477(1-2):261-72
- Sant VP, Smith D, Leroux JC. Novel pH-sensitive supramolecular assemblies for oral delivery of poorly water soluble drugs: preparation and characterization. J Control Release. 2004 Jun 18;97(2):301-12.
- Shi MD, Lin HH, Chiang TA, Tsai LY, Tsai SM, Lee YC, et al. Andrographolide could inhibit human colorectal carcinoma Lovo cells migration and invasion via down-regulation of MMP-7 expression. Chem Biol Interact. 2009;180:344–52.
- Siegal RL, Miller MD, Jemal A. Cancer statistics, 2017.CA Cancer J Clin. 2017;67:7–30.
- Sirion U, Kasemsook S, Suksen K, Piyachaturawat P, Suksamrarn A, Saeeng R. New substituted C-19-andrographolide analogues with potent cytotoxic activities. Bioorg Med ChemLett. 2012;22:49–52.
- Varma A, Padh H, Shrivastava N. Andrographolide: a new plant-derived antineoplastic entity on horizon. Evid Based Complement Alternat Med. 2011;2011:1–10.
- Wongprayoon P, Charoensuksai P. Cytotoxic and anti-migratory activities from hydroalcoholic extract of *Euphorbia lactea* Haw. against HN22 cell line. Thai Bull Pharm Sci. 2018:13(1):69–7.
- Xu W, Ling P, Zhang T. Polymeric micelles, a promising drug delivery systemtoenhance bioavailability of poorly water-soluble drugs. J Drug Deliv. 2013;2013:340315.
- Xue Y-N.et al. Synthesis and self-assembly of amphiphilic poly (acrylic acid-b-DL-lactide) to form micelles for pH-responsive drug delivery.Polymer2009;50: 3706-3713.
- Yang YQ, Zheng LS, Guo XD, Qian Y, Zhang LJ.pH-sensitive micelles self-assembled from amphiphilic copolymer brush for delivery of poorly water-soluble drugs. Biomacro molecules. 2011 Jan 10;12(1):116-22
- Yang YQ, Lin WJ, Zhao B, Wen XF, Guo XD, Zhang LJ. Synthesis and physicochemical characterization of amphiphilic triblock copolymer brush containing pH-sensitive linkage for oral drug delivery. Langmuir. 2012 May 29;28(21):8251-9.
- Yokoyama M. Polymeric micelles as drug carriers: their lights and shadows. J Drug Target. 2014;22:576–83.
- You X, Kang Y, Hollett G, Chen X, Zhao W, Gu Z, et al. Polymeric nanoparticles for coloncancer therapy: overview and perspectives. J Mater Chem B. 2016;4:7779–92.

กิจกรรมที่ได้วางแผนและได้ดำเนินการตลอดโครงการ

Objectives	Output
1. สกัดแยกสารจากพืช และ marine microbes ดัดแปลงโครงสร้าง และ สังเคราะห์สาร เพื่อเป็น compound library ใช้ในการนำไปทดสอบฤทธิ์	1. ได้สกัดแยกสาร ดัดแปลงโครงสร้างและสังเคราะห์สารไว้ใช้เป็น compound library 725 สารจากพืชไทย และจาก marine microbes และพืชของจีนประมาณ 300 ตัว ให้โครงการย่อยทำการ ทดสอบฤทธิ์ชีวภาพต่างๆ
2. ทดสอบฤทธิ์ และกลไกการออก ฤทธิ์ต้านมะเร็ง (anti-cancer effects and mechanisms)	1. พบสารมีฤทธิ์ยับยั้งการแบ่งตัว เพิ่มจำนวนของเซลล์ชนิดต่างๆ 2. ได้ศึกษากลไกการออกฤทธิ์เชิงลึกของสารบางตัวในการต้านมะเร็ง กระเพาะ ลำไส้ใหญ่ และทวารหนัก 3. นำส่งสารที่ทราบกลไกการออกฤทธิ์เชิงลึกบางตัวให้กลุ่มวิจัยพัฒนา ระบบส่งยาดำเนินการต่อไป สารที่ไม่เป็นพิษต่อเซลล์ ได้นำไปศึกษา ฤทธิอื่นๆ
3. ศึกษาค้นหาฤทธิ์ต้านเบาหวาน (Anti-diabetes type 2) และฤทธิ์ลด ความเป็นพิษของยาต้านมะเร็ง cisplatin	 ค้นพบสารที่มีฤทธิ์ยับยั้งการขนส่งกลูโคสในเซลล์ไตมนุษย์ สารบริสุทธิ์จากนักวิจัยไทย จำนวน 7 ตัว สารบริสุทธิ์จากกวิจัยจีน จำนวน 4 ตัว สารสกัดจากนักวิจัยไทยจำนวน 2 สารสกัด มีผลดีเด่นในการลด ระดับน้ำตาลในเลือดของหนูเบาหวาน ค้นพบสารบริสุทธิ์จากนักวิจัยไทย มีฤทธิ์ลดความเป็นต่อเซลล์ไต ของยาต้านมะเร็ง cisplatin จำนวน 1 ตัว
4. ศึกษาฤทธิ์ของสารต่อการสร้าง และ การเมทาโบลิสมของเนื้อเยื่อไขมันใน สัตว์ทดลอง และศึกษาฤทธิ์ของยาต่อ การจำแนกตนเองของเซลล์ต้นกำเนิดมี เซนไคม์จากไขกระดูกมนุษย์ (human bone marrow-derived mesenchymal stem cells, MSCs)	1. พบฤทธิ์ดีเด่นของสาร DPHD ต่อการ metabolism ในเนื้อเยื่อไขมัน และการออกฤทธิ์ป้องกันพยาธิสภาพในสัตว์ทดลองที่ตัดรังไข่เป็น เวลานาน ซึ่งเป็นแบบจำลองของสตรีวัยหมดประจำเดือน มีภาวะ ผิดปกติของไขมันในเลือด 2. พบกลไกการทำงานของสาร และสารสกัดจากพืช มีศักยภาพดีเด่นใน การลดการสร้างไขมันและเร่งการใช้ไขมัน ลดการสะสมไขมันของ ร่างกาย กระตุ้นการหลั่งอะดิโพไคน์ ช่วยเพิ่มความไวของเนื้อเยื่อในการ ตอบสนองต่อฮอร์โมน insulin เพื่อลดภาวะดื้อต่อฮอร์โมน insulin 3. พบว่าสาร DPHD มีฤทธิ์ยับยั้งการจำแนกตนเองของเซลล์ต้นกำเนิดมี เซนไคม์จากไขกระดูกมนุษย์ไปเป็นเซลล์ไขมัน โดยยับยั้งการแสดงออก ของยีนที่จำเป็นต่อกระบวนการสร้างเซลล์ไขมัน
5 ตรวจสอบฤทธิ์ของสารบริสุทธิ์ที่แยก ได้จากพืชต่อการป้องกัน การเสื่อมของ เซลล์ประสาท	พบฤทธิ์ของสารอนุพันธ์ของ lipoic acid ต่อการป้องกันการเสื่อมและ การตายของเซลล์ประสาทจากอนุมูลอิสระและปกป้อง microtubules และ actin filament ใน growth cone จากเซลล์ประสาทไม่ให้ถูก ทำลายด้วย oxidative stress

Objectives	Output
6. พัฒนาระบบนำส่งยารูปแบบลิโพโซม	 การเตรียมตำรับลิโพโซม การตรวจสอบสมบัติทางเคมีฟิสิกส์ของตำรับลิโพโซม การวิเคราะห์หาปริมาณยาที่กักเก็บในตำรับลิโพโซม การศึกษาการปลดปล่อยยาในหลอดทดลอง (In vitro drug release) ได้พัฒนาระบบส่งยาของสารต้านมะเร็งลำไส้ที่ศึกษากลไกการทำงาน แล้ว ให้ไปยังเป้าหมาย ลดความเป็นพิษต่อเซลล์ข้างเคียง

ผลผลิตที่ได้รับจากงานวิจัย (Output-Outcome) (IRN580W0004)

- ก. ผลงานวิจัยได้รับการตีพิมพ์ในวารสารระดับนานาชาติ จำนวน 37 ชิ้น
 (โครงการเครือข่ายวิจัยการค้นหาและพัฒนายาจากสารธรรมชาติ)
 - 1. Vinayavekhin N, Sueajai J, Chaihad N, Panrak R, Chokchaisiri R, Sangvanich P, Suksamrarn A, Piyachaturawat P*. Serum lipidomics analysis of ovariectomized rats under *Curcuma comosa* treatment. **J Ethnopharmacol**. 2016 Jul 19; 192: 273-282.
 - 2. Thongnuanjan P1, Soodvilai S, Chatsudthipong V, Soodvilai S*. Fenofibrate reduces cisplatin-induced apoptosis of renal proximal tubular cells via inhibition of JNK and p38 pathways. J Toxicol Sci. 2016;41(3): 339-49.
 - 3. Boonmuen N, Thongon N, Chairoungdua A, Suksen K, Pompimon W, Tuchinda P, Reutrakul V, Piyachaturawat P*. 5-Acetyl goniothalamin suppresses proliferation of breast cancer cells via Wnt/ β -catenin signaling. Eur J Pharmacol. 2016 Sep 16; 791: 455-464.
 - 4. Soodvilai S, Soodvilai S, Chatsudthipong V, Ngawhirunpat T, Rojanarata T, Opanasopit P*. Interaction of pharmaceutical excipients with organic cation transporters. Int J Pharm. 2017 Jan 25; 520(1-2):14-20.doi: 10.1016/j.ijpharm.2017.01.042.
 - 5. Thongon N, Boonmuen N, Suksen K, Wichit P, Chairoungdua A, Tuchinda P, Suksamrarn A, Winuthayanon W, Piyachaturawat P*. Selective Estrogen Receptor Modulator (SERM)-like activities of Diarylheptanoid, a Phytoestrogen from *Curcuma comosa*, in Breast Cancer Cells, Pre-Osteoblast Cells, and Rat Uterine Tissues. J Agric Food Chem. 2017 May 3; 65(17):3490-3496.
 - 6. Chen Lingling, Zhu Tonghan, Zhu Guoliang, Liu Yunlong, Wang Cong, Piyachaturawat Pawinee, Chairoungdua Arthit, Zhu Weiming*. Bioactive Natural Products from the Marine-Derived Penicillium brevicompactum OUCMDZ-4920. **Chinese J. Organic Chem**. 2017 Oct 25; 37(10): 2752-2762,

- 7. Monger A, Boonmuen N, Suksen K, Saeeng R, Kasemsuk T, Piyachaturawat P, Saengsawang W, Chairoungdua A*. Inhibition of Topoisomerase II**Q** and Induction of Apoptosis in Gastric Cancer Cells by 19-Triisopropyl Andrographolide. **Asian Pac J Cancer Prev**. 2017 Oct 26;18 (10):2845-2851.
- 8. Thipboonchoo N, Soodvilai S*. Effects of *Kaempferia parviflora* extract on glucose transporters in human renal proximal tubular cells. **J Physiol Biomed Sci** 2017; 30(2)
- 9. Sutjarit N, Sueajai J, Boonmuen N, Sornkaew N, Suksamrarn A, Tuchinda P, Zhu W, Weerachayaphorn J, Piyachaturawat P*. *Curcuma comosa* reduces visceral adipose tissue and improves dyslipidemia in ovariectomized rats. **J Ethnopharmacol**. 2017 Dec 20; 215:167-175.
- 10. Zhu T, Lu Z, Fan J, Wang L, Zhu G, Wang Y, Li X, Hong K, Piyachaturawat P, Chairoungdua A, Zhu W. Ophiobolins from the Mangrove Fungus *Aspergillus ustus*. J Nat Prod. 2018 Jan 26;81(1):2-9
- 11. Reabroi S, Chairoungdua A, Saeeng R, Kasemsuk T, Saengsawang W, Zhu, W, Piyachaturawat P*. A silyl andrographolide analogue suppresses Wnt/ β -catenin signaling pathway in colon cancer. Biomed. Pharmacoltherapy. 2018 Mar 1; 101:414-421.
- 12. Reabroi S, Saeeng R, Boonmuen N, Kasemsuk T, Saengsawang W, Suksen K, Zhu W, Piyachaturawat P, Chairoungdua A*, The anti-cancer activity of an andrographolide analogue functions through a GSK-3 β -independent Wnt/ β -catenin signaling pathway in colorectal cancer cells. Sci. Report 2018 May 21; 8(1):7924.
- 13. Wang C, Monger A, Wang L, Fu P, Piyachaturawat P, Chairoungdua A, Zhu W*. Precursor-Directed Generation of Indolocarbazoles with Topoisomerase II**Ω** Inhibitory Activity. **Marine Drugs**. 2018 May 17; 16 (5). pii: E168. doi: 10.3390/md16050168.
- 14. Apisornopas J, Silalai P, Kasemsuk T, Athipornchai A, Sirion U, Suksen K, Piyachaturawat P, Suksamrarn A, Saeeng R*. Synthetic analogues of durantoside I from *Citharexylum spinosum* L. and their cytotoxic activity. **Bioorg Med Chem Lett.** 2018 May 15; 28(9):1558-1561.
- 15. Kitdumrongthum S, Metheetrairut C, Charoensawan V, Ounjai P, Janpipatkul K, Panvongsa W, Weerachayaphorn J, Piyachaturawat P, Chairoungdua A*. Dysregulated microRNA expression profiles in cholangiocarcinoma cell-derived exosomes. **Life Sci**. 2018, 210; 65–75. pii: S0024-3205(18)30520-4.
- 16. Rangsimawong W, Wattanasri P, Tonglairoum P, Akkaramongkolporn P, Rojanarata T, Ngawhirunpat T, Opanasopit P*. Development of Microemulsions and Microemulgels for Enhancing Transdermal Delivery of *Kaempferia parviflora* Extract. **Pharm Sci Tech.** 2018 Jul; 19(5):2058-2067
- 17. Kansom T, Sajomsang W, Saeeng R, Charoensuksai P, Opanasopit P, Tonglairoum P*. Apoptosis Induction and Antimigratory Activity of Andrographolide Analog (3A.1)-Incorporated Self-Assembled Nanoparticles in Cancer Cells. **Pharm Sci Tech.** 2018

- 18. Wang L, Han X, Zhu G, Wang Y, Chairoungdua A, Piyachaturawat P, Zhu W*. Polyketides from the Endophytic Fungus *Cladosporium* sp. Isolated from the Mangrove Plant *Excoecaria agallocha*. **Front Chem**. 2018 Aug 14; 6: 344.
- 19. Fan Y, Wang C, Wang L, Chairoungdua A, Piyachaturawat P, Fu P, Zhu W*. New Ansamycins from the Deep-Sea-Derived Bacterium *Ochrobactrum* sp. OUCMDZ-2164. **Mar Drugs**. 2018 Aug 15; 16(8). pii: E282. doi: 10.3390/md16080282.
- 20. Limjiasahapong, S., Tuchinda P*., Reutrakul, V., Pohmakotr, M., Akkarawongsapat, R., Limthongkul, J., Napaswad, C., Nuntasaen, N., Anti-HIV-1 activities and chemical constituents from leaves and twigs of *Santisukia pagetii* (Bignoniaceae) **Natural Product Communications**. 2018:13: 1149-1452.
- 21. Dong-Dong Luo, Kai Peng, Jia-Yu Yang, Pawinee Piyachaturawat, Witchuda Saengsawang, Lei Ao, Wan-Zhou Zhao, Yu Tang. Sheng-Biao Wan. Structural modification of oridonin via DAST induced rearrangement. **RSC Adv.**, 2018, 8, 29548
- 22. Yaqin Fan, Yi Wang, Peng Fu, Arthit Chairoungdua, Pawinee Piyachaturawat, Weiming Zhu*. Secopaxilline A, an indole-diterpenoid derivative from an aciduric Penicillium fungus, its identification and semisynthesis. **Org. Chem. Front**. 2018, 5(19): 2835–2839.
- 23. Kansom T, Dumkliang E, Patrojanasophon P, Sajomsang W, Saeeng R, Weiming Zhu, Opanasopit P*, Folate-Functionalized Amphiphilic Chitosan Polymeric Micelles Containing Andrographolide Analogue (3A.1) for Colorectal Cancer. Key Engineering Materials ISSN: 1662-9795, Vol. 819, pp 15-20 doi:10.4028/www.scientific.net/KEM.819.15 © 2019
- 24. Kansom T, Saeeng R, Ngawhirunpat T, Rojanarata T, Tonglairoum P, Opanasopit P, Charoensuksai P. Effect of Semi-synthetic Andrographolide Analogue-loaded Polymeric Micelles on HN22 Cell Migration. Walailak J Sci & Tech 2020; 17(2): 88-95.
- 25. Uppakara K, Jamornwan S, Duan LX, Yue KR, Sunrat C, Dent EW, Wan SB, Saengsawang W. Novel **α**-Lipoic Acid/3-n-Butylphthalide Conjugate Enhances Protective Effects against Oxidative Stress and 6-OHDA Induced Neuronal Damage. ACS Chem Neurosci. 2020 Jun 3; 11(11):1634-1642. doi: 10.1021/acschemneuro.0c00105.
- 26. Chuaicharoen P, Charaslertrangsi T, Chuncharunee A, Suksamrarn A, Piyachaturawat P*. Non-Phenolic Diarylheptanoid from Curcuma comosa Protects Against Thioacetamide-Induced Acute Hepatotoxicity in Mice. **Pharmaceutical Sciences Asia 2020;** 47 (1), 74-85. DOI:10.29090/psa.2020.01.019.0004
- **27.** Kitdumrongthuma S, Reabroi S, Suksen S, Tuchinda P, Munyoob B, Mahalapbutr P, Rungrotmongkol T, Ounjai P, Chairoungdua A*. Inhibition of topoisomerase II**Q** and induction of DNA damage in cholangiocarcinoma cells by altholactone and its halogenated benzoate derivatives. **Biomed. Pharmacotherapy.** 127 (2020) 110149

- 28. Soodvilai S, Meetam P, Siangjong L, Chokchaisiri R, Suksamrarn A, Soodvilai S*. Germacrone Reduces Cisplatin-Induced Toxicity of Renal Proximal Tubular Cells via Inhibition of Organic Cation Transporter. **Biol. Pharm. Bull.** (2020), 43 (11): 1693–1698.
- **29.** Chatsirisupachai K, Kitdumrongthum S, Panvongsa W, Janpipatkul K, Worakitchanon W, Lertjintanakit S, Wongtrakoongate P, Chairoungdua A*. Expression and roles of system L amino acid transporters in human embryonal carcinoma cells. **Andrology**. 2020 Nov; 8 (6):1844-1858. doi: 10.1111/andr.12880
- 30. Sutjarit N, Thongon N, Weerachayaphorn J, Piyachaturawat P, Suksamrarn A, Suksen K, Dionysios J Papachristou, and Harry C. Blair*. Inhibition of Adipogenic Differentiation of Human Bone Marrow-Derived Mesenchymal Stem Cells by a Phytoestrogen Diarylheptanoid from *Curcuma comosa*. J Agric Food Chem. 2020 Sep 16; 68(37): 9993-10002. doi: 10.1021/acs.jafc.0c04063.
- 31. Tantikanlayaporn D, Wichit P, Suksen K, Suksamrarn A, Piyachaturawat P. Andrographolide modulates OPG/RANKL axis to promote osteoblastic differentiation in MC3T3-E1 cells and protects bone loss during estrogen deficiency in rats. **Biomed Pharmacotherapy**. 2020 Nov; 131:110763. doi: 10.1016/j.biopha.2020.110763.
- 32. Kansom T, Saeeng R, Ngawhirunpat T, Rojanarata T, Tonglairoum P, Opanasopit P, Charoensuksai P, Effect of Semi-synthetic Andrographolide Analogue-loaded Polymeric Micelles on HN22 Cell Migration. **Walailak J Sci & Tech** 2020; 17(2): 88-95.
- 33. Janpipatkul K, Trachu N, Watcharenwong P, Panvongsa W, Worakitchanon W, Metheetrairut C, Oranratnachai S, Reungwetwattana T, Chairoungdua A. Exosomal microRNAs as potential biomarkers for osimertinib resistance of non-small cell lung cancer patients. **Cancer Biomark**. 2021; 31: 281-294. doi: 10.3233/CBM-203075.
- 34. Thongnuanjan P, Soodvilai S, Fongsupa S, Chabang N, Vivithanaporn P, Tuchinda P, Soodvilai S. Protective effect of panduratin A on cisplatin-induced apoptosis of human renal proximal tubular cells and acute kidney injury in mice. **Biol Pharm Bull** (2021), 44: 1-9.
- 35. Khongkla E, Uppakara K, Boonmuen N, Bhukhai K, Saengsawang W. A Novel Methodology Using Dexamethasone to Induce Neuronal Differentiation in the CNS-Derived Catecholaminergic CAD Cells. **Cellular and Molecular Neurobiology**. 2021 (May) https://doi.org/10.1007/s10571-021-01109-z
- 36. Suksen K, Janpipatkul K, Reabroi S, Anantachoke N, Reutrakul V, Chairoungdua A, Thongon N, Bhukhai K. Gambogic Acid Inhibits Wnt/β-catenin Signaling and Induces ER Stress-Mediated Apoptosis in Human Cholangiocarcinoma. Asian Pacifc Journal of Cancer Prevention 2021, 22 (6): 1913-1920. DOI:10.31557/
- 37. Worakajit N, Thongnuanjan P, Chabang N, Soodvilai S, Tuchida P, Soodvilai S. Pinostrobin attenuates colistin-induced apoptosis of human renal proximal tubular cells. **Pharmaceutical Sciences Asia** (2021) (In Press).

ผลงานวิจัยที่ตีพิมพ์อื่นๆ บทความสืบเนื่องจากการประชม (Proceeding)

- (1) Sirima Soodvilai, Warayuth Sajomsang, Sunhapas Soodvilai, Praneet Opanasopit, เรื่อง Inhibitory mechanism of chitosan derivatives on transport function of organic cation transporter1 เพื่อนำเสนอผลงานวิจัยในการประชุมวิชาการนานาชาติของเภสัชสมาคม ในเดือน พฤษจิกายน 2559 กรุงเทพ
- (2) Teeratas Kansom, Rungnapha Saeeng, Pawinee Piyachaturawat, Theerasak Rojanarata, Tanasait Ngawhirunpat and Praneet Opanasopit. "Preparation and Characterization of Semi-synthetic andrographolide analogue-loaded Liposomes for Cancer Therapy" Seoul International Conference on Engineering and Applied Science (SICEAS), 7-9 Feb 2017, Marriott Seoul Times Square, Seoul, South Korea.
- (3) Pawinee Piyachaturawat, Antiproliferative and Anticancer Mechanisms of Styryl Lactones through Inhibition of Wnt/ $oldsymbol{eta}$ -catenin Signaling.The 6th China-Thailand Joint Workshop on Natural Products and Drug Discovery 16 20 October, 2016 Aonang Cliff Beach Resort, Krabi, Thailand (Oral presentation)
- (4) Wei-Ming Zhu, Marine Natural Products Sourced from Actinobacteria, The 6th China-Thailand Joint Workshop on Natural Products and Drug Discovery 16 – 20 October, 2016 Aonang Cliff Beach Resort, Krabi, Thailand (Oral presentation)
- (5) Praneet Opanasopit, Water Soluble Chitosan Derivatives for Applications as Drug/Gene Carriers *by* The 6th China-Thailand Joint Workshop on Natural Products and Drug Discovery 16 20 October, 2016 Aonang Cliff Beach Resort, Krabi, Thailand (Oral presentation)
- (6) Patoomratana Tuchinda, Halogenated Benzoate Derivatives of Altholactone with Cytotoxic Activity, The 6th China-Thailand Joint Workshop on Natural Products and Drug Discovery 16 20 October, 2016 Aonang Cliff Beach Resort, Krabi, Thailand (Poster presentation)
- (7) Arthit Chairoungdua, Induction of Cholangiocarcinoma Cell Death through Topoisomerase II Ω Inhibition by Altholactone and Halogenated Benzoate Derivatives, The 6th China-Thailand Joint Workshop on Natural Products and Drug Discovery 16 – 20 October, 2016 Aonang Cliff Beach Resort, Krabi, Thailand (Poster presentation)

- (8) Sunhapas Soodvilai, Inhibitory Effect of Compounds Isolated from *Kaempferia* parviflora on Transport Function of Human Renal Sodium Glucose Co-transporter, The 6th China-Thailand Joint Workshop on Natural Products and Drug Discovery 16 20 October, 2016 Aonang Cliff Beach Resort, Krabi, Thailand (Poster presentation)
- (9) Witchuda Saengsawang, *Phyllanthus taxodiifolius* Beille extract disrupted cytoskeletal dynamics of cancer cells. The 6th China-Thailand Joint Workshop on Natural Products and Drug Discovery 16 20 October, 2016 Aonang Cliff Beach Resort, Krabi, Thailand (Poster presentation)
- (10) Sirima Soodvilai, Sunhapas Soodvilai, Varanuj Chatsudthipong and Praneet Opanasopit. Effect of pharmaceutical excipients on organic cation transporter 2 activity. FAPA Congress 2016. November 9-13, 2016. BITEC Bangna, Bangkok, Thailand.
- (11) Teeratas Kansom, Warayuth Sajomsang, Rungnapha Saeeng, Pawinee Piyachaturawat, and Praneet Opanasopit. Preparation and characterization of semi-synthetic andrographolide analogue-loaded amphiphilic chitosans micelles for cancer therapy. FAPA Congress 2016. November 9-13, 2016. BITEC Bangna, Bangkok, Thailand.
- (12) Sirima Soodvilai, Warayuth Sajomsang, Sunhapas Soodvilai, Praneet Opanasopit, Inhibitory mechanism of chitosan derivatives on transport function of organic cation transporter 1. 32nd International annual meeting in Pharmaceutical Sciences, March 10 - 11, 2016 at Faculty of Pharmaceutical Sciences, Chulalongkorn University, Bangkok, Thailand.
- (13) Teeratas Kansom, Kritsanaporn Tansathien, Warayuth Sajomsang, Rungnapha Saeeng, Pawinee Piyachaturawat, Praneet Opanasopit. "Preparation of semi-synthetic andrographolide analogue-loaded polymeric micelles" The International Conference of Pharmaceutical Sciences and Medicines 2017 (ICPAM 2017)"Integrating of pharmaceutical sciences and health cares for aging society"16 Jun 2017, Burapha University, Thailand.
- (14) TeeratasKansom, RungnaphaSaeeng, PawineePiyachaturawat, TheerasakRojanarata, TanasaitNgawhirunpat and PraneetOpanasopit. "Preparation and Characterization of Semi-synthetic andrographolide analogue-loaded Liposomes for Cancer Therapy"

- Seoul International Conference on Engineering and Applied Science (SICEAS), 7-9 Feb 2017, Marriott Seoul Times Square, Seoul, South Korea.
- (15) Teeratas Kansom, Warayuth Sajomsang, Rungnapha Saeeng, Pawinee Piyachaturawat, Tanasait Ngawhirunpat, Theerasak Rojanarata, Praneet Opanasopit. Preparation and evaluation of semi-synthetic andrographolide analogue-loaded amphiphilic chitosan micelles for colorectal cancer therapy. The 1st international Conference on Natural Medicine: From Local Wisdom to International Research, 5-6 August 2017 SukosonHotel, Bangkok, Thailand.
- (16) Teeratas Kansom, Rungnapha Saeeng, Tanasait ngawhirunpat, Theerasak Rojanarata, Prasopchai Tonglairoum, Praneet Opanasopit, and Purin Charoensuksai. Effect of semi-synthetic andrographolide analogue-loaded polymeric micelles on HN22 cell migration. The 10th Walailak Research National Conference, 27-28 March 2018, Walailak University Thailand. (Poster presentation)
- (17) Praneet Opanasopit, Teeratas Kansom, Rungnapha Saeeng, Prasopchai Tonglairoum, Theerasak Rojanarata, Tanasait Ngawhiranpat. Fabrication of andrographolide analogue-loaded nanocarriers for cancer treatment. 43rd FEBS Congress 2018 Prague Congress Centre, Prague, Czech Republic.
- (18) Jaturon Kwanthongdee, Witchuda Saengsawang and Patoomratana Tuchinda. *Phyllanthus taxodiifolius* Beille extract disrupted microtubule dynamics in glioma cells. Experimetal Biology meeting, Chicago, IL, USA. (Poster presentation)
- (19) Somrudee reabroid et.al., An andrographolide analogue suppresses the proliferation and Wnt/ β -catenin signaling pathway in colorectal cancer cells. The 45th Physiology Society of Thailand Annual Meeting 2017, 6-8 December 2017, Khonkaen University
- (20) Nareerat Sujarit et al., Modulating effect of Wan-Chak motluk in adipose tissues of ovariectomized (OVX) rats. The 45th Physiology Society of Thailand Annual Meeting 2017, 6-8 December 2017, Khonkaen University Thailand

นักศึกษาระดับปริญญาเอกร่วมโครงการด้วยทุนของ

- ✓ โครงการ IRN จำนวน 2 ทุน จบการศึกษาได้แก่
- 1. นายเกียรติดำรงค์ จันทร์พิพัฒน์กุล ภายใต้การดูแลของ รศ.ดร.อาทิตย์ ไชยร้องเดื่อ
- 2. นางสาวเพ็ญใจ ทองนวลจันทร์ ภายใต้การดูแลของ รศ.ดร. สัณหภาส สุดวิลัย

🗹 โครงการอื่นๆที่ร่วมโครงการละจบการศึกษา 9 คน จบการศึกษาได้แก่

ก.. โครงการ คปก.

- นักศึกษา คปก. ชื่อ ชื่อ น.ส.นิตยา บุญหมื่น และ น.ส. สมฤดี เรียบร้อย หลักสูตรสรีรวิทยา
- นักศึกษา คปก. ชื่อ น.ส.ศรัญญา กิจดำรงธรรม นักศึกษาหลักสูตรพิษวิทยา
- นักศึกษา คปก .ชื่อ นางศิริมา สุดวิลัย นักศึกษาหลักสูตรเทคโนโลยีเภสัชกรรม
- นักศึกษา คปก. ชื่อ นางศิริมา สุดวิลัย นักศึกษาหลักสูตรเทคโนโลยีเภสัชกรรม
- นักศึกษาคปก. ชื่อ นายธีรทัศน์ กันโสม นักศึกษาหลักสูตรเทคโนโลยีเภสัชกรรม

ข. โครงการพัฒนากำลังคนด้านวิทยาศาสตร์

- 1. นางสาวนรีรัตน์ สุจริต นักศึกษาปริญญาเอก หลักสุตรพิษวิทยา
- 2. นางสาวขวัญชนก อุปการะ นักศึกษาปริญญาเอก หลักสูตรพิษวิทยา
- 3. นายเอกพจน์ คงกล้า นักศึกษาปริญญาเอก หลักสูตรสรีรวิทยา

ค. โครงการศรีตรั้งทอง

1. นายจาตุรนต์ ขวัญทองดี นักศึกษาปริญญาเอก หลักสูตรสรีรวิทยา

สรุปผลการดำเนินงานของโครงการโดยย่อ (หากพบอุปสรรคในการดำเนินงาน กรุณาระบุว่ามีอะไรบ้าง และได้แก้ไขอย่างไร)

การดำเนินงานของโครงการเป็นไปตามที่ได้วางแผนไว้ ไม่มีอุปสรรคใดๆ โดยได้มีความร่วมมืออย่าง ใกล้ชิดกับนักวิจัยในโครงการทั้งในสถาบันและต่างสถาบันในประเทศ และได้มีความร่วมมือกับนักวิจัยใน ต่างประเทศ ทั้งในสาธารณรัฐประชาชนจีน และประเทศสหรัฐอเมริกา ความร่วมมือในด้านงานวิจัยเป็นการ ทำงานที่เสริมกัน ความร่วมมือกับนักวิจัยจีนที่เป็นนักเคมีเป็นกลัก ทีมนักวิจัยไทยได้ทำการทดสอบฤทธิ์ทาง เภสัชวิทยาและวิจัยต่อยอดสารจีน ได้พบฤทธิ์ที่น่าสนใจของสารที่พัฒนาโดยนักเคมีชาวจีนหลายชนิด ผลงาน ดังกล่าวได้รับการเผยแพร่ทั้งในรูปแบบของการตีพิมพ์ในวารสารวิชาการนานาชาติ และการนำเสนอผลงานใน ที่ประชุมวิชาการ นอกจากนี้นักวิจัยหลักแต่ละท่านของโครงการ ยังมีความร่วมมืออยู่แล้วกับนักวิจัยใน ประเทศสหรัฐอเมริกา ได้เข้ามามีส่วนร่วมในโครงการ ได้มาเยี่ยมเยียน ได้สร้างความร่วมมือทั้งการวิจัยให้ เข้มแข็งและพัฒนาบุคคลากร ได้ส่งนักศึกษาและอาจารย์ไปปฏิบัติงานวิจัยในห้องปฏิบัติการในต่างประเทศ ระยะสั้นเพื่อต่อยอดงานวิจัยที่ใช้เครื่องมือสมัยใหม่ ดังที่ได้ระบุไว้ในรายละเอียดในส่วนที่ 1

โครงการได้มีการจัดกิจกรรมเพื่อพัฒนาเครือข่ายอย่างสม่ำเสมอมาต่อเนื่อง โดยได้จัดให้มีการประชุม หารือเกี่ยวกับงานวิจัยร่วมกับนักวิจัยในโครงการทั้งในสถาบันและต่างสถาบันเป็นประจำ และมีการจัดสัมมนา วิชาการเพื่อให้นักวิจัยและนักศึกษาในกลุ่มวิจัยนำเสนอผลงาน แลกเปลี่ยนความรู้ และหารือเกี่ยวกับความ ร่วมมือในงานวิจัย อีกทั้งยังมีการจัดสัมมนาพิเศษให้แก่นักวิจัยในทีมวิจัยรวมทั้งผู้ที่สนใจทั่วไป โดยได้เชิญ นักวิจัยในเครือข่ายที่ได้เดินทางมาเจรจาธุรกิจเป็นวิทยากรให้สัมมนาพิเศษ วิทยากรที่มาล้วนเป็นผู้เชี่ยวชาญ ในสาขาของตนเองทั้งจากประเทศจีน และประเทศสหรัฐอเมริกา นอกจากนี้คณะวิจัยจีนได้เดินทางมาประเทศ ไทย และนักวิจัยไทยได้มีโอกาสเดินทางไปประเทศจีน เพื่อประชุมปรึกษาหารือวางแผนงานวิจัยร่วมกัน และ ทำความรู้จักกับสถาบัน กลุ่มสมาชิก และนำเสนอความก้าวหน้าของงานวิจัยในโครงการ

การสร้างเครือข่ายของกลุ่มนักวิจัยในประเทศของโครงการ มีแนวคิดที่จะพัฒนาสารที่ได้ไปเป็น ผลิตภัณฑ์ให่ผู้บริโภคในอนาคต โดยดำเนินการวิจัยในแนวทางของ Modern drug discovery and development เป็นเครือข่ายของผู้วิจัยที่มีความเชี่ยวชาญแตกต่างกัน รับช่วงการทำงานต่อเนื่องกัน โดยใน โครงการนี้ได้ศึกษาวิจัยพัฒนาสารที่มีประสิทธิภาพดีเด่นเป็นยาต้านมะเร็ง โดยนักเคมีได้ปรับปรุงโครงสร้าง สาร จนทดสอบฤทธิ์ได้ว่าดีเด่น ได้ศึกษากลไกการออกฤทธิ์ต่อเป้าหมายจำเพาะในเซลล์มะเร็ง ได้พัฒนาระบบ นำส่งยาไปยังเป้าหมาย นับว่ามี readiness ทาง technology ที่ใกล้จะสมบูรณ์

ปัจจุบัน มีผลงานตีพิมพ์ในวารสารนานาชาติ 37 เรื่องมากกว่าเป้าหมาย

4. ความเห็นและข้อเสนอแนะ

ระเบียบและเกณฑ์ต่างๆที่สกว.มีอยู่ในปัจจุบันดีอยู่แล้ว โดยเฉพาะระเบียบการตีพิมพ์ผลงานทำให้ นักวิจัยตื่นตัวอยู่ตลอดเวลาถึงความก้าวหน้า นวัตกรรม และความสมบูรณ์ของาน

ลงนาม.....

ศาสตราจารย์ภาวิณีปิยะจตุรวัฒน์) หัวหน้าเครือข่ายวิจัยผู้รับทุน วันที่ 19 กรกฎาคม 2564

Monday